HIGH SPEED ELECTRODEPOSITION USING

FLUIDISED BEDS

by

MICHAEL JOHN PAUL McBURNEY

B.Sc. (Wales) M. Met. (Sheffield)

This thesis is submitted in fulfilment of the regulations for the degree of Doctor of Philosophy at the Loughborough University of Technology

September 1978

Supervisor: Dr. D. R. Gabe

Department of Materials Technology

SYNOPSIS

The relevant literature, relating to electrochemical cells, mass transfer, fluidised beds and mass transfer in fluidised beds, has been reviewed.

Extensive experimental data for the cathodic reduction of copper from acid $CuSO_4$ electrolytes, in fluidised beds of copper powder, demonstrated the effectiveness of the cell at removing copper from the electrolytes.

For a given bed weight the cell only acted efficiently below 25% bed expansion. Above this the operation of the cell changed to that of acting as a turbulent promoter for the feeder electrode.

Two modes of cell operation were investigated. The electrolyte flow was either parallel or perpendicular to current flow. Of the two, electrolyte flow perpendicular to current flow was more effective overall, as it was more amenable to scale-up of the cell. When electrolyte flow and current flow were parallel particles in the bed had to be within a radius of one centimetre for the cell to act efficiently.

Potential gradients within the bed caused many problems and prevented limiting currents from being observed because of secondary reactions increasing the total current from the bed.

Preferential polarization of the bed during potentiodynamic sweeps of the cathode caused reactions to occur at low 'apparent' overvoltages. This was more noticeable in concentrated electrolytes or when larger beds were used.

A reassessment of mass transfer data obtained previously (73,76) in an inert fluidised bed gave the following correlation;

$$St_I = 0.38.Re^{-0.54}.Sc^{-0.77}$$

A similar reassessment of mass transfer data obtained previously (73,76) for laminar flow of electrolyte through an annulus and with a Reynolds number and Stanton number based on the length of the sample rather than on the equivalent diameter yielded;

$$Sh = 2.25.Re^{0.32}.Sc^{0.33}$$

ACKNOWLEDGEMENTS

I am indebted to Professor A. Argent at the Department of Metallurgy in Sheffield and Professor I. Menzies at the department of Materials Technology in Loughborough for the opportunity to undertake research in their departments and for the provision of laboratory facilities. Sincere thanks are due to Dr. D.R. Gabe for his very patient supervision and guidance throughout this project.

I wish to express my appreciation to the technical and clerical staff, to the academic staff, and to my colleagues for for their friendship and constructive discussions and suggestions.

The award of an S.R.C. Research studentship for the duration of this project is also gratefully acknowledged.

Finally, I wish to thank my family, for their love patience and encouragement, without which this work would never have been possible.

CONTENTS

1. INTRODUCTION

1.1 History of Electrochemistry.

The developments in electrochemistry have followed very closely on developments in electricity and, although galvanic effects between metals were noted earlier, they could not be associated with electrical energy as such. The early discoveries really began with Galvani in 1791 upon noticing that a recently dissected frog suddenly underwent muscular convulsions when lightly touched by a scalpel. Further to Galvani's work Michael Faraday deduced his laws of electrolysis after showing that a definite quantity of electric charge deposited a given mass of metal. Meanwhile in 1839 Sir William Grove produced the first fuel cell. In this instance hydrogen and oxygen were forced across electrodes where they underwent spontaneous combustion producing both electrical energy and water. A third landmark in electrochemistry occurred at the beginning of this century when Tafel realised the relationship between current density and overpotential at an electrode,

$$\eta = a \pm b \log i$$

where a and b are constants for the reaction and i is current density.

From the beginning of this century to the late nineteen fifties electrochemistry stagnated to a considerable extent and a major factor in this stagnation was the dominence of thermodynamic theory over kinetic practise. Thermodynamics had made great advances in the nineteenth century and unfortunately

the treatment of the electrochemical cell as given by Nernst only considered reactions occurring at or close to equilibrium. With the Nernst theory available it was easier for scientists to 'travel the thermodynamic road' than to labour over problems of reaction kinetics, and ideas concerning the rate limiting steps of a reaction were often disregarded. As a result of the considerable utilisation of thermodynamics in electrochemistry scientists did not seriously consider the effects of electrode kinetics until twenty years ago.

1.2 More Recent Developments.

In the last fifteen years a number of ideas have been put forward to reduce kinetically-limiting factors occurring in electrochemical reactions. The most important of these has been the use of agitation as a means of reducing the diffusion control of a reaction. Techniques of gas bubbling, stirring, and electrode movement have all been used to eliminate or reduce solution inertia. The approach used into the type of agitation required is clearly dependent upon the application of the product; so for instance in electrowinning the quality of the product is of less importance than in electroforming. In comparison to agitation the effects of increased temperature and solution concentration are relatively small.

Apart from reaction limitations imposed by the solution, the electrode itself plays an important role since the quantity

of reaction (as opposed to the rate) is directly proportional to the electrode area available. A technological requirement therefore in electrowinning has been the production of a large surface area electrode. Again , in the application of metal recovery where large electrodes are needed to deal with the vast throughput of solution, it has been suggested(1) that the most useful methods of producing high speed reactions will be realised by electrodes used in a highly agitated medium, or electrodes having a very large surface area. Such electrodes are exemplified by the rotating cylinder and the fluidised bed. The rotating cylinder has been considered previously(2), and shows quite well the beneficial effects that can be achieved on reaction rates by the use of a turbulent solution. The conducting fluidised bed combines the advantages achieved by turbulence with a large surface area, making it an ideal electrode for the removal of elements from solutions of low concentration.

Since the introduction of the conducting fluidised bed in 1966(89) work on it has been reported both of an empirical(3) and theoretical(106) nature, and because of its large surface area possible applications in fuel cell development; metal recovery systems;and reactor design have been formulated. Meanwhile fluidised bed systems containing inert particles have been investigated empirically(70) and , more recently , in terms of mass transport behaviour, to optimise operational conditions.

The two types of fluidised bed electrode exhibit widely different attractions to the industrialist. The inert bed has the advantage of containing particles which remain of constant size, allowing the electrolyte, moving around the particles, to attain and maintain a stable flow condition. This makes it an electrode suitable for adaptation to the production of high quality deposition. The main advantage of the conducting fluidised bed over other electrodes is its large surface area to volume ratio, and it is ideally suited to situations where low current densities make other methods of electrolysis unviable.

This thesis is concerned with the application of a fluidised bed of conducting particles, incorporating quite low flow rates($\lesssim 5cm^2/sec$), capable of producing high currents(>1 Amp) from low concentration solutions (e.g. 10^{-3}Molar). It reports the findings of experimental investigations into the effect of fluidised bed parameters on deposition rates and electrodeposit structure. The electrode has been compared with other electrode systems which may provide industrial competition in those areas where it has application and the consequences of this competition has been discussed.

2. THE CELL IN INDUSTRY.

2.1 Introduction.

Since electrochemical cells were first used in industry it has become apparent that the only processes which survive are those which do not suffer from a large mass transport problem. Recently a plethora of new cells have evolved as fundemental principles have been explored. Many of these cells have been developed for their own sake rather than to satisfy a need or the shortcomings of other cells and some cells which have been regarded as failures in the past have been rediscovered. Today there are new cells incorporating the rotating disc(horizontal and vertical), the rotating cylinder, the slurry electrode, the packed bed and the fluidised bed. These new cells have been introduced to increase mass transport in electrochemical systems.

Most employers of electrochemical cells require maximum current density and efficiency at minimum operating voltages; they also want the corrosion of the cell and the cell capital cost to be a minimum. The most fundemental requirement however is that of simplicity in design and construction. This one factor alone is the reason why many cells have not proved as industrially successful as they might.

The choice for using an electrochemical process for the refining or extraction of a metal is purely an economic one. In the practise of metal production other methods using hydrogen

and carbon are often used and very few metals are produced solely by electrolysis.

Electrodeposition occurs from a solution containing an appropriate metal ion in a suitable solvent and it is important that the solvent does not react with the metal. It is this question of solvent reactivity that restricts water as a solvating agent to those elements less reactive than tungsten and molybdenum. Organic solvents,which have been used to produce reactive elements, have met with little industrial success either because of the power costs involved and the reaction sensitivity to impurities, or because of the hazardous nature of the solvent. There is a renewed interest in the deposition of elements from molten salts. but again the power costs will prove prohibitive for all but the most specialised of applications. Only the elements of group IA, IIA, and aluminium are solely electrowon (table 1).

The problems of power do not arise to the same extent in electrorefining and finishing and thus the anodization of aluminium is quite cheap and the electrorefining of copper is standard practise. Electrochemical cells are also used to polish metals (a form of anodic oxidation). In this instance the metal is made the anode of the cell and polishing occurs when the rate of diffusion of oxide away from the metal is less than the rate of oxidation of the metal itself. Increase in electrical

resistance occurs at the anode, the current drops, and a stable oxide forms on the surface with the underlying irregularities being slowly removed.

Apart from in the electrodeposition and oxidation of metals,electrolytic processes are sometimes used in the production of other elements and compounds. Halogens such as fluorine and chlorine have been produced from halide melts(4), and hydrogen fluoride has been used in the fluorination of many compounds (table 2). In the Chlor-Alkali industry the decomposition of hydrochloric acid is in direct competition with non-electrochemical processes and the production of sodium hydroxide by the electrolysis of brine (with chlorine as a useful by-product) is one of the oldest, and perhaps one of the most important of all industrial electrochemical processes. Where cheap power is available hydrogen and oxygen have been produced by the electrolysis of water and in this case D_2O (heavy water) is a by-product. The technology of paint electrodeposition is expanding and is beginning to find applications; particularly in the coating of steels (6). Perhaps the most outstanding example of an electrochemical cell is the battery,which has been available in one form or another for over a hundred years.

The electrochemical cell is obviously important in a number of different industries and each industry has its own problems.Sometimes a cell is specially made to fit a process and occassionally a process is adapted for a particular kind of cell. Today the number of different kinds of cell which are in

use is quite large and to provide an outline to this subject a number of different cells are discussed briefly in the following sections.

2.2 Planar Electrodes

Until twenty years ago the planar electrode was the only electrode of any type to be widely used in industry. (Under the heading of planar electrodes are also those electrodes which are not truely planar but have been bent into some other shape e.g. the cylindrical electrode). In most cases the mass transfer properties of these electrodes depend upon the condition of the electrode surface and mass transfer can be approximately apportioned to the surface area available(Levich(7)). In the case of diffusion controlled reactions Levich has shown that the relationship is not quite so simple but also depends upon whether the roughness extends into the diffusion layer.

2.2.1 Widely Spaced Electrodes.

These cells are still used industrially but not on a wide scale. One of their main uses, although not metallurgical, is in the reduction of pyridine on lead anodes(8). The only aid to mass transport is by the natural convection in the cell and by solution stirring when gas evolves at the electrodes.

2.2.2 Parallel Plate Cells: gas stirred.

This particular type of electrode is frequently used

in many electrofinishing processes, with air generally being injected into the bottom of the cell. According to Schreiber (9) and Farnstein(15) this cell has not become established because bubbles of injected air tend to decrease the effective plating areas by sitting on the electrode surface. Garbutt(10) has also pointed out that the air often causes foaming at the top of the cell leading to many operational difficulties. Ibl (11) has shown that the energy required to pump air into these cells is independent of cell height and thus as the cell height increases the pumping energy per unit of electrode actually decreases. (This holds only whilst the electrolyte pressure head is insignificant with respect to the pressure drop across the air inlet).

Recent experiments carried out by King(12) to determine diffusion layer thichnesses in these systems have produced diffusion layer values greater than 0.005 cms and Beck(13), and not quite so recently, Tobias (14) have shown how the cell voltage varies with the rate of gas bubbling.

2.2.3 Parallel Plates (pumped flow).

These cells are often the standard by which all other cells are judged. Kuhn(16) differentiates between those cells which are open topped and those cells operating under rather higher pressure drops. Copper refining cells belong to the former of these two groups and performance has been quoted, again by Kuhn(17), as being better under low flow rates and laminar flow than where forced flow regimes operate. In this latter group are the capilliary cells of Beck(18) which suffer

a severe disadvantage in having to maintain electrode gaps to very high tolerences(0.02cms), as well as operating under pressure. Eisenberg(19) has given a comprehensive treatment of parallel plate electrodes and has pointed out the fact that in the majority of cases flow is laminar. For rectangular channels having a width:plate separation of the order of 3 - 165 and for Reynolds numbers upto 2800,two types of flow regime can exist(20). Initially there is undeveloped flow caused by the entrance of the cell, The length of this region is given by the equation

$$l_{ent} = 0.04hU/\nu \qquad = 0.04N_{Re}$$

where h is the thickness of the electrolyte, ν is the kinematic viscosity of the electrolyte, and U is thc flow velocity of the electrolyte(21). N_{Re} is the Reynolds number based on channel width. In this region the limiting current density is given by

$$i_L = 0.66nFDC_b(\nu/D)^{0.33}(y/l)^{0.5}$$

where L is the downstream region over which i_L is measured Once the flow has become fully developed the limiting current may be obtained from the equation given by Leveque(22),

$$i_l = 1.62FC_bU(uh/\nu)^{-0.66}(h/L)^{-0.33}(\nu/D)^{-0.66}$$

Ibl has shown that i_L decreases as the plate length increases and this effect can only be overcome by increasing the flow regime. As Eisenberg points out(19) a tenfold increase in the flow requires almost a thousandfold increase in the pumping energy due to the power dependences of flow and pumping energy $(U^{0.33}P^{1.0})$.

Many other parallel plate electrodes exist. Cells based on two concentric rings have been used in the electrolysis of sea water(16) and cells similar in form have been hydrodynamically analysed(23). A variation on the ring cell is the Engelhard cell which is electrically split half-way along its length, one half acting as the anode and the other half acting as the cathode; the inner tube acts as a floating bipole.

2.2.4 Parallel Plate with Turbulence Promoters.

These cells can operate either as open top or closed top systems and turbulence may be introduced in a variety of ways. Le Goff(24) has suggested the use of glass beads which can be fluidised or left static around the electrode. Surfleet (25) has constructed planar cells interleaved with Netlon mesh (mesh size 2cms square) and claims thirty per cent efficiency from solutions of 100 p.p.m. at a current density of $5mA/cm^2$. Although not a parallel plate electrode, I.C.I. have patented a mesh electrode where the expanded metal acts as its own turbulence promoter(26). It has been quoted as giving currents equivalent to 2000 Amps, in a cell 25 - 50 cm^3 in which six individual cells were connected. At such large currents, however, heat dissipation must become a limiting factor.

2.3 The Rotating Disc Electrode.

This particular cell has received universal usage in laboratories because it maintains an even viscous boundary layer over its whole surface. A rigorous hydrodynamic treatment

is available(7) and the limiting current density in laminar flow is given by,

$$i_L = 0.62nFDC_b D^{0.66}\nu^{-0.166}\omega^{0.5} \quad ,$$

where ω is the angular velocity. Such is the use that is made of this electrode that Adams is able to cite more than one hundred references relating to its application (27).

2.4 Modern Electrodes.

2.4.1 The Rotating Cylinder Electrode.

This is a recent innovation to the electrochemistry department and was devised because of its ability to produce turbulent flow at low rotation speeds. Taylor(28) and Flower(29) have found that when the inner cylinder rotates then the flow between the cylinders is generally turbulent even when the rotation speed is low. If the inner to outer diameter ratio is small and the outer cylinder is rotated, Taylor(28) has found that laminar flow exists at higher Reynolds numbers. Ibl has found that these cells give good limiting current (11) values at quite low metal concentrations; 19mA/cm^2 in 0.01M solution. Kuhn (16) cannot forsee any large scale industrial application for these cells because of the limiting parameter of cell size:rotation speed ratio. Mass transfer data for the rotating cylinder in turbulent flow has been presented by a number of authors(11,30,31,32) and Arvia and Carozza(33) have produced a dimensionless group correlation of the form:

$$St = 0.079Re^{-0.30}.Sc^{-0.644}$$

One form of the rotating cylinder is made under the name 'Eco-Cell'(66).

2.4.2 The Packed Bed and the Porous Electrode.

The packed bed is another electrode system which has recently become popular. Colquhoun-Lee(34) has studied these electrodes and surveyed their hydrodynamic properties at low flow rates. At higher rates of flow, Houghton(35) has produced quite a detailed account of the removal of antimony using lead shot as the cathode. The effect of flow and bead size on the current efficiency is discussed. Armstrong et alia(36) were perhaps the first to suggest that increasing the bed size brings diminishing returns in metal removal, because of the corresponding increase in resistance in the bed.

A few industrially used packed beds may be cited, such as the Nalco process for the production of tetra-alkyl lead compounds(37) and a patent was taken out by Bayer(38) in 1956 for the use of lead scrap in such an electrode. With the recent advances in powder metallurgy, a number of firms have now proposed the replacement of atomised powders by powders produced by cathodic deposition. Atomised powders are often useful because of their sphericity, particularly in packed bed and fluidised bed media. Chu and Hills have discussed the extraction of copper from dilute solutions using a graphite particle bed(39) and have found the current efficiency to be near 100%. They also studied the stripping of the same copper from the bed; they

found that the process was not diffusion controlled, but was. dependent upon the bed potential. Using high bed potentials the copper could be dissolved from the bed in a few seconds with 95% efficiency. They concluded that this cell could be used successfully as a metal ion concentrator and might even be able to replace ion exchange columns.

As an alternative to packed bed electrodes, which are made up of a large number of individual particles, there is the porous bed which does not suffer from particle to particle. contact resistance. Bennion and Newman have studied these electrodes with a view to using them as concentration cells: perhaps in electrowinning or metal recovery(40). A preliminary economic analysis for the recovery of copper suggested that the value of metal recovered would more than pay for capital installation and running costs, even for quite small cells. The authors believe that this electrode could be used for other metal recovery, e.g. gold, silver, mercury, lead and cadmium.

One disadvantage of the porous electrode is that paths to and from reaction sites may be quite tortuous, causing large pH fluctuations in the pores with corresponding problems of hydroxide formation and removal. One method of overcoming this particular type of problem has been suggested by Nanis(41), who used a conventional plate cell but foamed the electrolyte around the electrodes. The effect of the foam was to cover the electrode in a very thin surface film, allowing easy access to and from the elctrodes by gases and waste products.

2.4.3 The Extended Mesh Electrode.

This has recently been developed to the pilot plant stage by I.C.I. and Du Pont(64, , 63) and results have shown that for an ideal waste product such as acidified copper sulphate, it is less costly to use this electrode for copper removal from concentrations of 10 p.p.m. or less than ion exchange methods. It is pointed out that under actual conditions of waste treatment where many cations are present, then the same may not be true. The cell is made from expanded metal mesh and, as electrolyte is pumped past the electrode , turbulence is created by the electrode shape and mass transfer to the electrode is enhanced. Surfleet and Crowle(1) have shown that the current efficency of the cell drops dramatically above currents of 20mA/cm^2: e.g. the current efficiency of the cell is 58% at 11mA/cm^2 and only 10% at 110mA/cm^2, for concentrations of Cu^{2+} of 100 -300mg/1, for flow through solution of 3l/min. High current densities, required to keep capital costs down, may be equated with high running costs because of the poor efficiency of the process.

2.4 4 The Swiss Roll Electrode.

This electrode consists of two continuous metal strips which act as anode and cathode, which are separated by an expanded membrane or separator. The anode, separator and cathode are wound together in layers and a swiss roll type of effect is produced. This electrode has some good design properties in that electrolyte can be forced through the electrode at high speed, where the separator causes turbulence of the electrolyte, creating high mass transfer

rates and because the anode and cathode are so close together the cell resistance is small. This electrode is fairly effective at removing metal from solution(65),giving a 57% efficiency during the reduction of copper from 10^{-3}M solution to 5 p.p.m. The electrode operates on a batch basis,with removal of metal from the electrode being achieved by chemical stripping. At the moment,anodic stripping is not very effective and tends to preferentially corrode parts of the anode. The electrode has been used on a small scale for the removal of other ions,such as Ag and Hg. In the former case it is capable of reducing the silver content of a solution to less than 0.1 p.p.m.,but mercury to only 2p.p.m.,because the mercury can leave the electrode in the form of very fine droplets which are difficult to filter out and thus reoxidise in the solution($Hg^0 + Hg^{2+} \quad 2Hg^+$). In rinse waters containing cyanides,e.g. zinc, the zinc can be reduced to 1 p.p.m. and at the same time the cyanide oxidised by oxygen evolved at the anode. Although current efficiencies are apparently not very good (65) the total running costs are more favourable than those achieved in the oxidation of cyanides by sodium hypochlorite, comparison of costs coming out at £1.36/Kg compared to £1.98/Kg.

The swiss roll electrode has not yet been built on a large scale and yet it is already competing with present forms of effluent treatment in terms of cost for a cell treating 200 gallons of water a day; and with scale-up of the cell, overhead costs should be reduced, possibly making this method cost effective.

2.4.5 Fluidised Bed Electrodes.

Two types of fluidised bed are available :those using inert particles and those using conducting particles. The inert bed enhances mass transfer by increasing turbulence in the electrolyte and thus decreasing the diffusion layer in the electrode vicinity. Using this electrode, uniform deposits are obtained over the cathode and currents 4 to 5 times greater than those in stagnant solution are achieved.Further details of this electrode are given in section five..

The conducting bed makes use of its large surface area to produce very large currents from solutions containing even very small concentrations of metals. In conjunction with this the hydrodynamic path through the bed provides the forced convection necessary to realise such currents. The concept of a conducting fluidised bed is not a new one, however a recent patent was necessary to set off a wave of interest in this type of electrode(2).

Two main types of conducting bed configuration have been considered(43):-

(1) The plane-parallel configuration.

(2) The side-by-side configuration.

In the plane-parallel configuration electrolyte passes up through a porous support, upon which the bed rests, and passes out through the top of the cell. A feeder electrode is situated in the bed to provide electrical contact with the particles

and current flow and electrolyte flow are parallel to each other but perpendicular to the feeder electrode(fig. 1). The counter electrode is situated above the bed and requires a large surface area to stop the bed from limiting.

The side-by-side configuration differs from the plane-parallel configuration in a number of ways. Firstly,the anode and cathode are at the same level and separated from each other by a membrane(fig. 2). This membrane plays a dual role by both supporting the bed and separating the anolyte and catholyte. Secondly electrolyte flow and current flow are perpendicular to each other,which is useful as it makes the electrode more amenable to scale-up. Further details of this electrode are given in chapter five.

In this section,a number of cells that are used or have been considered by the electrochemical industry have been discussed. Modern cells have evolved as the underlying theories of mass transfer have become more widely accepted. Cells have been created which reduce mass transfer problems either by causing turbulence in the cell and thus reducing diffusion limitations, or by having very large surface areas. The theories that have led to the discovery of these problems are discussed in the next section.

3. MASS TRANSFER AND DIFFUSION CONTROL IN LIQUIDS.

3.1 Introduction.

When a system contains two or more components and the concentration of the components varies throughout the system, there is a tendency for each component to diffuse in a direction that will reduce or eliminate its own concentration variations. In a fluid which is either stationary or in laminar flow, reduction of these concentration gradients occurs by molecular diffusion of the component species because of differences in density and temperature of the fluid. This type of diffusion is called natural convection. It is a slow process with diffusion rates of the order of 10^{-2} cm^2/sec. In contrast to natural convection there is the bulk movement of fluid by eddies produced in turbulent flow. This latter type of convection is called forced convection and can produce diffusion rates a thousand times, higher than those occurring in natural convection.

Natural convection is a spontaneous process and as such requires no major external energy source. Forced convection requires a large amount of energy to keep it in operation. The advantages of this energy expenditure usually manifest itself in a shorter reaction time. The amount of energy used to create turbulence is usually a balance between a reduction in the reaction time and the cost of the energy expended in providing the extra agitation.

3.2 Development of the Mass Transfer Theory in Liquids.(laminar flow)

The research which led to the distinction between the

two types of convective flow started in the 19th century with Shchukarev(44) who compared the dissolution rates of solids immersed in liquids. Following this Nernst(45) put forward the hypothesis that all such liquids are covered by a thin static layer of liquid which is unaffected even by the most vigorous stirring. He termed this layer the diffusion layer, and stated that mass transfer across this layer was only by molecular diffusion. This diffusion layer thickness is much greater than the double layer(re: the capacitance layer set up when a metal is immersed in solution), but, as far as it is generally necessary to consider electrode processes, it is close enough to the electrode for its concentration at its boundary to be considered the same as that at the electrode surface.

3.2.1 The Nernst Film Theory.

Nernst suggested that when a current removes ions from the vicinity of an electrode the concentration of ions in that area decreases. A concentration gradient is set up between ions near the electrode and similar ions in the bulk solution. To establish this gradient, diffusion of the ions towards the electrode from the bulk solution occurs, until the number of ions being replenished by the bulk solution equals the number of ions being removed by the electrode. A steady state is reached and this state will have been determined primarily by the rate of diffusion of the ions.

Provided that there is sufficient support electrolyte to prevent ion migration, then Nernst showed that the diffusion current and thus the diffusion current density(current/area),

may be determined from the use of Fick's laws. Thus,

$$J = - D(dc/dx)$$

where J is the unit flux,per unit area, per unit time; D is the diffusion coefficient of the ion in question; and dc/dx is the concentration gradient in the electrode vicinity (where x is the direction of diffusion and is normal to the electrode).

By expressing the valency, n, of the ions, in moles and the concentration of the fluid in moles per litre, the current density i may be expressed as,

$$i = nFJ = - nFD(dc/dx)$$

where F is the Faraday. From Ficks second law,

$$(dc/dt) = D(d^2c/dx^2) = 0 \ ,$$

thus dc/dx = k, where k is a constant and t is time. In other words, the concentration gradient is constant throughout the diffusion layer(fig. 3). If C_s represents the concentration of ions at the electrode surface and C_b the bulk concentration , , then,

$$dc/dx = (C_b - C_s)/\delta \ .$$

The concentration of ions at the electrode is a function of the current density and if the current density is increased until C_s = 0,i.e. the ions are removed as soon as they reach the electrode, then the limiting current density i_L is obtained,

$$i_l = nFCDC_b/\delta \ .$$

This was the simple mass transfer theory put forward by Nernst and it has since received many criticisms:

(1) The formation of this diffusion layer requires laminar flow and therefore under conditions where turbulent flow prevails the situation becomes much more complex than this theory suggests.

(2) Neither the thickness of the diffusion layer nor its dependence upon diffusion velocity can be calculated directly and although it has been shown that it is a function of the fluid velocity(46)

$$1/U^m \propto \delta ,$$

values of m have varied between 0.5 and 1.0, giving a range of values between 10^{-2} - 10^{-4}cms. Some work by Fage and Townsend(47) has in fact shown that motion of the electrolyte at distances of only 10^{-5}cms. from the electrode has been observed. Thus it is no longer valid to say that the electrolyte is static in the Nernst diffusion layer, and the equation for the concentration profile no longer has a sound basis.

3.2.2 The Levich Hydrodynamic Film Theory.

The conditions at the surface of an electrode have been treated more recently by Levich(48). As his simplest model Levich took a planar electrode with liquid flowing past and parallel to it. At the surface of the electrode the liquid has a velocity of zero and this velocity increases normal to the electrode until the velocity in the main stream of the solution is attained(fig. 5). (This contrasts with the Nernst theory where the velocity of fluid changes its bulk velocity to zero at the outer limit of the diffusion layer(fig. 4)). This layer of thick-

ness δ_u, is known as the Prandtl boundary layer, and its thickness is dependent upon the laminar flow velocity relative to the solid surface and upon the kinematic viscosity of the liquid. For a planar electrode, δ_u is given by

$$\delta_u = \sqrt{\frac{\nu . x}{U}} \quad .$$

Momentum gradients in the solution are much greater than concentration gradients(fig. 6), i.e. $\delta \ll \delta_u$, because δ_u is a function of viscosity whereas δ is a function of the diffusion coefficient. Kinematic viscosity is of the order of 10^{-2}cms/sec, whereas diffusion coefficients are in the range of 10^{-5}cms/sec. A much greater concentration gradient is therefore required by diffusion than by velocity if transfer of velocity and momentum are to proceed at the same rate. Levich has shown that(48),

$$\frac{\delta}{\delta_u} = k\left(\frac{D}{\nu}\right)^{0.33} \quad .$$

and knowing that $\delta_u = (\nu . x/u)^{0.5}$, δ can be obtained.

$$\delta = kD^{0.33}U^{-0.5}x^{0.5}\nu^{0.166}$$

The current density may also be calculated from known values of δ,

$$i = nFD(C_b - C_s)/\delta \quad ,$$

and therefore

$$i_L = nFD^{0.66}\nu^{0.166}x^{-0.5}U^{0.5}C_b \quad ,$$

which is somewhat different from the equation obtained by Nernst.

The main differences between the Nernst theory and the Levich theory may be summarised as follows:

(1) The Levich theory predicts that liquid is mobile in the diffusion layer δ.

(2) δ is dependent upon the stirring rate of the solution and the diffusion coefficient of the ion. Consequently ions with high diffusion coefficients reach the electrode from further distances in the same time as others with lower coefficients.

Using similar techniques to those outlined above, the concentration diffusion layer for a rotating disc has been determined:

$$\delta = 1.62D^{0.66}\nu^{0.166}\omega^{-0.5} \qquad \text{Levich (48)}$$

$$\delta = 1.75D^{0.66}\nu^{0.166}\omega^{-0.5} \qquad \text{Vielstich(49)}$$

$$i = 0.62nFD^{0.66}\omega^{0.33}\nu^{-0.166} \qquad \text{Levich (48)}$$

$$i = 0.57nFD^{0.66}\omega^{0.33}\nu^{-0.166} \qquad \text{Vielstich(49)}$$

3.3 Mass Transfer(turbulent flow).

The theories of mass transfer discussed so far are only relevant for laminar flow. Under turbulent conditions mass transfer becomes much more complicated and the theories put forward so far to explain turbulent behaviour have not yet been put through any rigorous mathematical treatment.

The first theory depicting mass transfer in turbulent flow was suggested by Prandtl and Taylor(50). They suggested that in liquids two distinct flow regimes exist. In the main stream of the liquid flow is turbulent, however as the electrode surface is approached this flow changes and a viscous sublayer is encountered. In the turbulent layer all transport is achieved by eddy currents whereas in the sublayer, flow becomes laminar and

transport by molecular diffusion prevails. At the boundary of the two layers transport changes from one type of control to the other. The results of this theory lead to an equation of the form,

$$i = C_b UD/\nu ,$$

but this equation has not been confirmed by experiment. Von Karman(51) criticised the ideas of Prandtl on the grounds that a sharply defined boundary between laminar and turbulent flow was unlikely. He therefore modified Prandtl's theory replacing the sharply defined boundary by a buffer zone. In this zone the turbulent to laminar transition occurred and all eddy currents were removed. Levich and Landau(48) disagreed with the idea that all eddies could be removed by the time this viscous sublayer is entered. They suggested that turbulence could exist right up to the electrode itself, but that the closer to the surface the turbulence was after entering the sublayer the less important it became as a controlling parameter. The four layer theory supported by Levich and Landau is summarised below:(fig.7)

Layer 1. The main turbulent stream. In this region the electrolyte concentration is constant.

Layer 2. The turbulent boundary layer. In this layer the average velocity of the stream and the electrolyte concentration decrease slowly. Transport is still by eddy currents.

Layer 3 Viscous sublayer. Here turbulent eddies become very small. Momentum is transported more by

molecular viscosity than by eddy currents, however, since diffusion coefficients are less than 1/1000th of the kinematic viscosity, mass transfer is still predominantly caused by eddy currents.

Layer 4 The diffusion sublayer.

The results of Levich and Landau led to the prediction that

$$J = D^{0.75} U . C_b / \nu^{0.75}$$

and experimental findings by Adams support this result(52). The main difference between the Prandtl theory and the Levich theory for mass transport is in the power dependence of the diffusion coefficient ($D^{1.0}$ and $D^{0.75}$). The lower power for the diffusion coefficient in the Levich model has a definite importance. The smaller diffusion coefficient means that eddy currents predominate closer to the electrode over molecular diffusion in the mass transfer process.(Turbulent motion is more effective than molecular diffusion in the transfer of mass and this increased effectiveness compensates for the reductin in D).

In all the models discussed, although turbulence is found to be very important, the rate limiting transfer step is still controlled by molecular diffusion through a diffusion layer.

3.4 Other Models of Mass Transfer.

3 4.1 The Penetration Theory.

Apart from film theories, other theories have been

proposed to explain the diffusion of species in liquids. Such a model is the penetration theory put forward by Higbie(53) to explain mass transfer in the liquid phase during gas absorption. It has been applied by Danckwerts(54) to turbulent flow when the diffusing component only penetrates a short distance into the phase of interest, because of its own rapid disappearance through chemical reaction or short contact time.

Higbie considered mass to be transfered by turbulent eddies which exist upto the electrode surface. Packets of solute elements are transported to the surface where the contents of the package discharge by unsteady state molecular transport.(Transient processes, in which the concentration at a given point varies with time, are referred to as unsteady state or time dependent processes; this variation in concentration is associated with a variation in the mass flux.) The packets are then replaced by new packets from the bulk solution. Using these concepts, Higbie produced an expression for the mass transfer coefficient, K_m,

$$K_m = 2.D^{0.5}\pi^{-0.5}\Theta^{-0.5},$$

where Θ is the residence time of each packet at the surface of the solid. Danckwerts(54) modified the Higbie theory because he considered it unlikely that each packet would have the same residence time. He suggested that the rate of surface removal was constant only for a given degree of turbulence and was equal to a surface renewal factor, S. This gave a solution

for K_m as

$$K_m = D^{0.5}.S^{0.5}$$

It may be noted that both the above theories show a dependence on the diffusion coefficient to a power 0.5. Toor and Marchello say that the penetration concept of Danckwerts is valid only when(55) the surface removal is rapid. Where a long residence time exists a steady state concentration gradient is set up, as predicted by the Nernst film theory. Where the ratio of viscous coefficient to diffusion coefficient is low, i.e. at low Schmidt numbers (ν/D = Sc), a concentration gradient is rapidly set up, so that unless there is rapid removal of the packets they behave similarly to packets which have been at the surface a long time. At high Schmidt numbers the time necessary to set up a concentration gradient increases so that the surface renewal rate need not be rapid, and when conditions are such that both new and old packets are on the surface the transfer characteristics are intermediate between the film and penetration models.

The same criticisms levelled at the Nernst film theory may be levelled at these penetration theories. No relationship exists between S and the hydrodynamic and the geometric factors of the system; such relationships must be determined experimentally. The penetration theory has been developed primarily for the absorption of a gas by a liquid surface(54) and is found to agree well with experimental findings.

3.5 Electrode Systems used in the study of Mass Transfer.

Numerous studies relating to mass transfer in electrochemical systems may be found in the literature for both laminar and turbulent flow. Robinson(2) has tabulated available transfer data for the rotating disc, concentric rotating cylinders, and concentric circular annuli electrodes as well as for square-section pipes, and for flow over vertical and horizontal plates. These have been reproduced in Table 4. The rotating disc electrode appears to be the most practical elctrode for which a rigid hydrodynamic treatment is available(48). The extensive use made of this electrode has been demonstrated by Adams(27), who has reported more than one hundred sources where it has been applied in electrochemical application.

Illustration of some of the theory of mass transfer in liquids, which has been discussed in this section, can be provided by looking at one of the cells which has been developed since these mass transfer problems have become more widely understood. The next section gives an introduction to fluidisation and the fluidised bed electrode and this is followed by a section on mass transfer in fluidised beds.

4. THE FLUIDISED BED AND SOME FLUIDISATION CHARACTERISTICS .

4.1 Introduction.

If a bed of solid particles is supported on a horizontal porous plate in a vertical tube and gas or liquid is forced to flow upwards through the plate and the bed, a pressure drop will occur across the depth of the bed. As the flow of the fluid is increased, so also will the pressure drop increase until, at some point, the pressure difference will be sufficient to support the weight of particles in the bed. The bed is now defined as being incipiently fluidised. Any further increase in fluid velocity will be counteracted by an expansion of the bed and the pressure drop will remain constant. A fluidised bed will exist.

The fluidised bed derives its name from exhibiting many of the characteristics of a fluid and, as such, frequently behaves in a fluid manner. Thus the application of vibrations results in the formation of waves and ripples at the top of the bed; it only slightly impedes the immersion of solids; and if the apparatus containing a fluidised bed is tilted then the upper surface of the bed remains horizontal. As with most electrodes the fluidised bed has its advantages and disadvantages. Some of its more useful properties as well as some of its limitations are outlined below:

(1) Fluidised beds always cause a high degree of mixing throughout the system, therefore there are no large temperature gradients

in the bed. This is highly advantageous when highly endothermic or exothermic reactions are involved and also in catalytic reactions where a close temperature control is required.

(2) Because fluidised beds behave like pseudo-liquids they can be designed for continuous processing and the ready addition or withdrawal of solids from the system is possible.

(3) Fluidised beds contain a large number of particles and therefore have a large area to volume ratio. This can be made use of very effectively in electrochemical systems where the rate of reaction is kinetically hindered. In such situations, large currents (surface reaction rates) achieved by the fluidised bed counteract the overall low current density.

Even though there are a number of uses for fluidised beds in chemical and physical processes, there are many difficulties. These difficulties may extend from lack of data on the behaviour a system under various processing conditions, to problems inherent in the process itself. For instance:

(1) Often during a fluidised operation the particles of the bed undergo a size reduction by attrition, which changes the fluidising properties of the bed. In a plant process, continuous supervision and adjustment of flow rates up through the bed may therefore be necessary to ensure constant conditions in the bed.

(2) Some reactions proceed along a path where a suitable temperature gradient is necessary. Equilibration of temperature in such systems would not be suitable.

(3) Many gas/solid reactions are accompanied by the formation of liquid and gas by-products. These products are not suitable for fluidised systems. (This is a great restriction where hydrocarbon synthesis is concerned).

(4) In fluidised operation, equipment erosion is serious. Special, and therefore expensive, designs are required to reduce wear in reactors. Extra difficulties are encountered because of the bed's inherent nature in having to operate at above ambient pressure.

4.2 Fluidised Systems. - some basic concepts.

The upward flow of fluid through a bed of particles gives rise to a fixed bed at low flow rates. At higher velocities the particles become freely supported in the fluid and the bed becomes fluidised. At very high velocities there is entrainment of the particles in the fluid stream.

If the flow rate is increased above that necessary for incipient fluidisation, either the bed will expand or excess fluid will pass through the bed in the form of bubbles. When the bed expands, a single phase system associated with liquid/solid fluidised systems occurs, whereas when bubbles are formed a two phase system more associated with gas/solid systems occurs. Occasionally liquid/solid systems do enter this latter class, but this generally only happens when there is a large difference between the solid and liquid densities(56). Single phase fluidisation is known as particulate fluidisation and the two -

phase fluidisation is called aggregative fluidisation. One example of where aggregative fluidisation occurs in liquid/solid systems has been given by Kwauk and Wilhelm(57), who have shown that a bed of lead shot behaves aggregatively when fluidised by water. These workers suggested that the type of system's fluidisation could be characterised by the ratio of inertial forces to gravitational forces. These forces may be expressed dimensionlessly using the Froude number, Fr. ($Fr = u^2/d_p \cdot g$). Kwauk's criterion predicts particulate fluidisation for $Fr < 1$ and aggregative fluidisation for $Fr > 1$. This relationship between Froude number and fluidisation is empirical and is only correct in a general sense. Harrison and co-workers(58) considered that the ratio of maximum bubble size to particle diameter, d_m/d_p, is a better maxim and that when

$d_m/d_p \ll 1$ particulate fluidisation occurs;

$d_m/d_p > 10$ aggregative fluidisation occurs.

In the region $1 < d_m/d_p < 10$ there is an intermediate zone where the type of fluidisation cannot easily be determined. What Harrison suggests is that all systems behave aggregatively unless the maximum stable bubble size is of the same order as the particle diameter, in which case the behaviour is particulate and,

$d_m/d_p = k.Fr$, where k is a constant

4.2.1 The Pressure Drop - Velocity Relationship.

The relationship between the pressure drop and the fluid

flow velocity in a fluidised system has been explained by Richardson et alia(59), who states that when the flow velocity is increased until the pressure drop occurring equals the buoyant weight of the particles, then any further increase in the flow velocity will cause a corresponding increase in the bed height with the particles rearranging themselves to give minimum resistance to flow. Further velocity increases will cause continued expansion of the bed until eventually all the particles physically separate from each other and move freely in the fluid. At the point where the particles lose contact with each other the bed is said to be incipiently fluidised. The fluid velocity is called the minimum fluidising velocity, U_{mf}, and the pressure drop through the bed is a maximum. Above this velocity the bed continues to expand but the pressure drop remains constant. Reversing the process,with reduction in the flow velocity, causes the bed height to decrease and the pressure drop to remain constant until the point of incipient fluidisation is reached. Further velocity reduction below this point causes a decrease in the pressure drop in the bed.Experimental results have shown that the curve for decreasing velocity, versus pressure drop is usually lower than that for increasing velocity because it is found that, in the absence of vibration, the bed voidage remains approximately at ϵ_{mf}, corresponding to a bed at incipient fluidisation(fig 9).

4.2.2 Deviations from Ideal Behaviour.

Very few systems have such properties that they describe

almost perfect fluidisation and systems often suffer from:

(1) Slugging — where complete layers of particles are lifted up the tube by the fluid until the fluid 'bursts' allowing particles to fall back on the bed.

(2) Channelling — this is the result of preferential flow of fluid through certain parts of the bed causing some areas of the bed to fluidise whilst some of the bed remains static.(fig. 10)

Storrow et alia(60) have related the fluid velocity for slugging, U_s, in gas/solid systems, to the velocity for minimum fluidisation U_{mf} and the bed height L_h,

$$U_s = 6.8\ U_{mf}^{0.6}/L_h^{0.8}$$

(U_{mf} in the equation is also a function of the particle diameter).

When channelling occurs, then as the flow rate increases the channelling becomes more wide spread until eventually the whole bed becomes fluidised. The main causes of channelling are a) a large particle size distribution, b) low sphericity of the particles, c) poor design factors such as preferential flow through the porous plate beneath the bed.

4.3 The Pressure Drop Relationship - A quantitative treatment.

A quantative approach to the pressure drop relationships of fixed beds has been given by Ergun(61). Ergun has shown that for fixed beds , where the fluid is in laminar flow, then a form of the Carmen-Kozeny equation holds for pressure drop such that:

$$\frac{\Delta P}{L} = \frac{150\ U.\mu.(1-\epsilon)^2}{d_p^2 .\ \epsilon^3} \qquad \text{for } Re<10\ (Re = U.d_p/\nu)\ ,$$

where L is the height of the bed, μ is the viscosity, ϵ is the bed porosity, and ΔP is the pressure drop across the bed. For fixed beds in turbulent flow

$$\frac{\Delta P}{L} = \frac{1.75\,\rho_f . U^2 (1-\epsilon)}{d_p . \epsilon^3} \quad , \qquad \text{for } Re > 1000$$

where ρ_f is the fluid density. For intermediate Reynolds numbers Ergun showed that a summation of the two equations fitted experimental data giving an equation

$$\frac{\Delta p}{L} = \frac{150 . U . \mu (1-\epsilon)^2}{d_p . \epsilon^3} + \frac{1.75 . \rho_f . U^2 (1-\epsilon)}{d_p . \epsilon^3} \quad ,$$

and later showed that this was a general equation and is valid over the whole range of Reynolds numbers.

In a fluidised bed at incipient fluidisation

$$\frac{\Delta P}{L} = (1 - \epsilon_{mf})(\rho_s - \rho_f) . g \quad ,$$

where ρ_s is the solid's density, ϵ_{mf} is the porosity at incipient fluidisation and g is the gravity constant. Since the bed at minimum fluidisation can be regarded loosely as a packed bed then the pressure drop can be approximated to the Ergun equation. Richardson has thus made use of these equations(67) (by substitution of $\Delta P/L$ in the last equation into the Ergun equation, and by multiplying both sides of the Ergun equation by $\rho_f . d_p^3 / U_{mf}^2 . (1-\epsilon_{mf})$) to obtain

$$\frac{\rho_f . (\rho_s - \rho_f) . g . d_p^3}{\mu^2} = \frac{150 . (1 - \epsilon_{mf}) . U_{mf} . d_p . \rho_f}{\epsilon_{mf}^3 . \mu} + \frac{1.75 . (U_{mf} . d_p . \rho_f)^2}{\epsilon_{mf}^3 \mu^2}$$

by substiting Re_{mf} for $U_{mf} . d_p . \rho_f / \mu$ and Ga for $\rho_f . (\rho_s - \rho_f) . g . d_p^3 / \mu^2$,

and ,by rearranging, one obtains

$$Re_{mf}^2 + 85.8(1 - \epsilon_{mf}) - \epsilon_{mf}^3 . Ga/1.75 = 0$$

where Ga is a dimensionless group called the Galileo number. This equation has been used to calculate the minimum flow velocity for Reynolds numbers upto 3000. Some measured values and those calculated from the above equation are given in figure 11 and show good agreement. The above equation applies to spherical particles; for non-spherical particles a shape factor must be used.(e.g. $K = \pi d_s^3/6.d_p^3$)

4.4 Flow Velocity and Bed Expansion.

Measurements of flow velocity and bed expansion by a number of workers(67) led Richardson to consider the following empirical relationship between bed voidage and flow velocity:

$$U_{mf}/U_i = \epsilon_{mf}^n$$

where U_i approximates to the terminal velocity of the particles. Using this relationship Richardson showed that U_i is slightly influenced by the ratio of diameters of the particle and the container, d_p/D_v, during fluidisation and that n is a function of d_p/D_v and Re_t (except for very high, $Re > 500$, and very low, $Re < 0.2$, values of Re_t) where Re_t is the Reynolds number under terminal free falling conditions. The following relationships were obtained for uniformly spherical particles by Richardson and Zaki(67), although they were slightly modified at a later date by Richardson(68)

$U_i = U_t$ in sedimentation

$\log U_i = \log U_t - d_p/D_v$ for fluidisation

for both the above situations then

$$n = 4.65 + 20.d_p/D_v \qquad (Re_t<0.2)$$

$$n = (4.4 + 18.d_p/D_v).Re_t^{-0.03} \qquad (0.2<Re_t<1)$$

$$n = (4.4 + 18.d_p/D_v).Re_t^{-0.01} \qquad (1<Re_t<200)$$

$$n = 4.4.Re_t^{-0.1} \qquad (200<Re_t\leqslant 500)$$

$$n = 2.4 \qquad (Re_t>500) .$$

When the particles are uniform but non-spherical n can be expressed in terms of the shape factor K. Values of n for $Re_t>500$ have also been given,

$$n = 2.7K^{-0.16}$$

Although Richardson's equation, $U_{mf}/U_i = \epsilon_{mf}^n$ has no theoretical basis, it is used extensively because it is simple and easily applied. Further, it more accurately represents the experimental results than any other equation which has been put forward to date.

4.5 The Particle Entrainment Velocity.

The encounter of fines in a fluidised bed is frequent and regardless, of the reason for particle breakdown, the fines will eventually require removal from the bed. One way of achieving this is by entrainment of the particles in the fluid. When wall effects and particle interaction are negligible the entrainment velocity is equal to the particle terminal velocity in a stagnant fluid.

The terminal velocity of a particle is attained when the gravitational forces and upward forces balance(59) and

it is also dependent upon the shape and density of the particles as well as upon the fluid properties. The terminal velocity occurs when

$$\frac{\pi}{6}.d_p^3.(\rho_s - \rho_f).g = 0.5C_D.\rho_f.\frac{d}{4}p^2.U_t^2$$

where C_D is the drag factor and;

$$C_D = 4.d_p.(\rho_s - \rho_f).g/3.U_t^2.\rho_f$$

C_D has been related to the Reynolds number by Leva(56) such that,

$C_D = 24/Re$ $\quad Re<2.0$

$C_D = 18.5Re^{-0.6}$ $\quad 2.0<Re\leq 500$

$C_D = 0.44$ $\quad Re>500$.

From the above equations and by using the relevant drag coefficient the following relationships for the entrainment velocity can be obtained:

$$U_t = \frac{1}{18}.(\rho_s - \rho_f).g.d_p^2 \qquad Re>2.0$$

$$U_t = \frac{0.152d_p^{1.14}.g^{0.714}.(\rho_s - \rho_f)^{0.714}}{\mu^{0.428}.\rho_f^{0.285}} \qquad 2.0<Re\leq 500$$

$$U_t = (38d_p.(\rho_s - \rho_f)/\rho_f)^{0.5} \qquad Re>500$$

In the above form, these equations are only useful for spherical particles. For non-spherical, but uniform, particles, e.g. cubes, cylinders or pyramids, the above equations should be multiplied by the shape factor K^*:

$K^* = 0.843\log \phi_s/0.065$, where ϕ_s is a sphericity factor (13).

5. MASS TRANSFER IN FLUIDISED BEDS.

5.1 Introduction.

The inert fluidised bed electrode and the conducting fluidised bed electrode are coming under increasing consideration in the electrochemical industry,as they allow good uniform deposition at high current densities on the one hand and good surface area to volume ratio, producing high currents , on the other.

In an inert fluidised bed ,the particles of the bed act as turbulent promoters around the electrode,thinning the diffusion boundary layer and mixing the electrolyte so that good uniform deposition can occur. Conducting fluidised beds, although they contain considerable turbulence within the bed, are considered more for the large surface area that they provide and upon which deposition can occur. In a conducting particle bed, the particles themselves are the electrode.

These two essentially different modes of operation make the fluidised bed useful in both electrowinning and metal finishing. In electrowinning,where metals in solution have to be concentrated, the conducting bed is able to provide an effective method of extracting metals from dilute solutions. It is able to do this because of its large surface area, which allows large currents to be obtained from the bed at low overall current densities. In electrofinishing, good quality deposition is required and the inert fluidised bed is capable of producing this type of finish easily and quickly at high current densities.

5.2 Mass Transfer between Particles and an Immersed Solid(Inert Bed).

5.2.1 Introduction.

Some early work by Jottrand and Grunchard(70),using an inert bed of silica particles, on the cathodic reduction of ferricyanide,showed that the presence of fluidised particles enhanced mass transfer rates to levels greater than those achieved by flowing electrolyte alone. Maximum currents were achieved at a bed voidage of 0.58; above this bed voidage increased flow rate resulted in a gradual decrease in the current density(fig 12). Coeuret et alia(71) have reported maximum currents in this type of system at bed voidages of 0.6 and Jagannadhareju et alia at voidages of 0.7. Carbin and Gabe have reported values between 0.51 - 0.57,depending upon the particle diameter of the bed(73). In all cases increasing the particle size of the bed gave an increase in the limiting current. The occurrence of a maximum limiting current in the voidage range of 0.5 - 0.7 has been established as being the optimum of two processes acting in opposition. First there is the increase in the kinetic motion of the particles that occurs when electrolyte flow is increased and resulting in more particle/electrode collisions and increased turbulence within the bed. Second, and as a direct result of the increased flow, there is an expansion of the bed height which increases the mean collision time between particles and the electrode. For bed porosities less than 0.5, the effect of the increased kinetic energy of the particles outweighs the longer collision times in the bed. Above porosities of 0.7,the reverse is the case. Somewhere within the porosity range 0.5 - 0.7 a balance point

is reached and optimum currents result.

The effect of particle size has been looked at by Brea(74) in heat transfer studies. Brea suggests that increasing the particle diameter increases the particle velocities within the bed and helps to reduce the diffusion boundary layer more efficiently than smaller particles and therefore gives higher mass transfer rates. Coeuret(75) has proposed that the increased mass transfer observed with large particles is due to an increase in the interstitial velocity,as previously proposed by Richardson(67). Carbin(76) has suggested that it is unlikely that the increased velocity of large particles are the sole cause of current increase and that the effect of particle agglomeration must also be considered. Coeuret(77) has shown that larger particles tend to agglomerate less than smaller particles and has suggested that there must therefore be more independent disruptive effects of the boundary layer, with larger particles resulting in greater mass transfer.

Apart from the effect of particle size it has also been observed(75 - 77) that higher mass transfer rates are achieved at the electrolyte entrance to the bed and are probably due to the disruptive effect of the distributor on the electrolyte. It is suggested that articles are not plated in this region because of the non-uniform effects encountered therein.

5.2.2 Inert Bed Technology.

A process for the electrodeposition of lead dioxide onto

graphite and titanium substrates in a silica sand bed has been reported by Le Goff(78) as giving an adherent uniform deposit which is pore-free. It was believed that this type of deposit was the effect of improved mass transfer and was particular to the fluidised bed. Thangappan(79) has studied the anodic polishing of copper in a bed fluidised by orthophosphoric acid. Higher limiting currents were obtained than in the presence of flowing electrolyte alone. The polishing was more effective when smaller particles were used although this also gave a reduction in the limiting current. Again anode dissolution was uniform. In comparison, the dissolution of an anode in flowing electrolyte alone was determined as being preferential at the electrode edges.

5.2.3 Mass Transfer Correlations.

The most frequently used method for correlating data for the fluidised bed has been with the aid of dimensionless groups (table 3), resulting in an equation of the form

$$St = k.Re^{a}.Sc^{b}.$$

However, uncertainty has often arisen in the selection of a characteristic length for the Reynolds number. Quantities that are available are:

(1) the cell diameter.

(2) the cell equivalent diameter.

(3) the particle diameter.

(4) the mean voidage diameter between the particles.

(5) the electrode length.

Original analysis was carried out by Leva(56) using the diameter of the particles as the characteristic length when he attempted a comparison between fixed and fluidised bed data. His choice of a Reynolds number was,

$$Re_{11} = U.d_p/\nu \ .$$

Later, Chu(80) surmised that the effect of voidage increase with increasing Reynolds number had to be significant and proposed a Reynolds number

$$Re_1 = U.d_p/\nu \ (1 - \epsilon) \ .$$

However although altering the Reynolds number he neglected to alter the Stanton number(K_m/U), which is also affected by this voidage term i.e. $St_1 = K_m.\epsilon/U$. Leva made a further data analysis using the results of McCune and Wilhelm(81) choosing a Reynolds number

$$Re_{111} = u.d_p/\nu.\epsilon$$ and a correctly modified Stanton number, St_1. Unfortunately he concluded that the modification of the Reynolds number to account for voidage gave no improvement in analysis.

Since then it has become widely accepted(82,83,84,85,86) that the most general method for plotting and interpreting mass transfer data is by using the Reynolds number as proposed by Chu , with a modified Stanton number, i.e.

$$Re_1 = U.d_p/\nu(1 - \epsilon) \quad , \quad St_1 = K_m.\epsilon/U \ .$$

Using this type of correlation Carbin and Gabe have obtained the analysis for the deposition of copper,

$$St = 1.22Sc^{-0.68}Re^{-0.52} \qquad (87)$$

with $$i_L = 1.22nF.C_b.(1-\epsilon)^{0.52}\epsilon^{-1.0}U^{0.48}d_p^{-0.52}\nu^{-0.166}D^{0.68}$$

Analysis of mass transfer data by other workers is given in table 4. Further data can be obtained in a definitive work by Upadhyay and Tripathi(87).

5.3 Mass Transfer Between the Fluid and the Particles(Conducting Bed).

5.3.1 Introduction.

In the application of electrochemical processes, one of the major problems is that of scale-up, because the system is always bounded by the available surface area of the electrodes. The use of a fluidised bed containing conducting particles is a possible way of overcoming this problem, in that it is a three dimensional electrode with a large surface area to volume ratio.

The concept of a conducting fluidised bed is not new(88), although little research was achieved with regard to its electrochemical applications before Backhurst(89) et alia(90) in 1966. Goodridge(91) has suggested that the fluidised bed has advantages,for instance, over the slurry electrode developed by Gerischer(92), in that costs are reduced by circulation of the electrolyte alone; a more uniform cell temperature is maintained; it is amenable to continuous operation and electrode replacement; and it offers a large surface area to volume ratio ,

typically 75cm^{-1} for 200μm particles. The fluidised bed is not without its disadvantages, such as non-uniformity of electrode potential throughout the bed possibly leading to unwanted side reactions; poor electronic conduction between the particles, particularly at high bed expansions; and the requirement of a porous diaphragm at all times(with inherent entry effect problems). Such disadvantages have been well documented by Smith(93) and Thangappan(94). (See also table 5)

Although the fluidised bed can operate in modes where the current flow is parallel or perpendicular to electrolyte flow, it has been suggested that the bed height is limited to 1 cm in the former mode(104) because of the lack of conduction which occurs between the bed top and the feeder electrode. Backhurst has shown that irrespective of the system size(90) the efficiency of this type of fluidised bed is minimal above 25% bed expansion.

5.3.2 Technological Aspects.

The application of the fluidised bed in the formation of compounds for electrosynthesis has been suggested(91). In particular its use has been related to where it will

(1) reduce the number of steps in the electrosynthesis production.

(2) produce a higher yield.

(3) reduce purification stages.

(4) allow continuous operation, thereby reducing labour costs.

(5) make use of lower cost materials.

Backhurst et alia(90) have investigated the cathodic reduction of m-nitrobenzene sulphonic acid to metanilic acid, and Hiddlestone and Douglas(95) have produced current potential curves for the ferrous/ferric redox reaction and also for the oxidation of methanol, using platinum coated carbon beads and palladium shot. In the former instance maximum currents were obtained when the bed was in the fluidised condition, whereas in the latter case maximum currents were obtained in a static bed and currents were nearly five times larger for equivalent conditions. The differences in the currents obtained may possibly be due to differences in bed conduction. Using platinum coated beads the resistance in the bed would be greater than using palladium shot if only because of the difficulties in getting the platinum to adhere to the carbon substrate. The bed might therefore be acting more in an inert bed type of fashion than like a truely conducting bed. Assuming reasonably good conduction between the palladium shot however, maximum currents might be expected when there was maximum electronic contact between the particles, which for a fluidised bed would be at the point of incipient fluidisation. Krishnamurthy(96) et alia have studied the reduction of sodium hydrosulphite to sodium bisulphite using nickel coated glass beads and found that fluidised bed electrodes gave better current efficiencies than planar ones.

The possible use of the fluidised bed in fuel cells has been studied by Berent et alia(97). One of the most important requirements of a fuel cell is a large surface area per unit volume of electrode. Berent looked at a number of systems such as methanol/potassium hydroxide and hydrazine hydrate/potassium hydroxide and determined that in such cells the use of a fluidised bed as a cathode warranted further investigation, but as anodes, they tended to deactivate with increasing fluidisation and were therefore of little use. Other preliminary reports have been produced by Backhurst et alia(98), on the zinc oxygen battery(where an advantage would be the prevention of dendrites of zinc from growing from the cathode to the anode and thereby shorting the cell), and by Hiddlestone and Douglas as outlined above.

5.3.3 Electrowinning and Metal Recovery.

The conducting fluidised bed should be particularly useful in electrowinning where metal concentrations are low. Under such conditions the fluidised bed makes makes efficient use of its large surface area to extract metal from dilute solution. Flett(99) has looked at the electrowinning of copper from acid plating solutions using plated ballotini and has found that good deposition occurs at concentrations down to 5 p.p.m. Further investigation led him to suggest that a cyclic anode, cathode operation(100) might be a feasible alternative to solvent extraction or ion exchange in metal ion concentration.

Wilkinson and Haines(101) have recovered copper from acid sulphate solution using particles upto 1200μm in diameter. Copper in solution was reduced from 3000 p.p.m. to 30 p.p.m. and power costs were estimated for various deposition currents. They found that current efficiency started to decrease for concentrations of less than 2500 p.p.m. and that the efficiency was dependent upon the current used. Extended experiments upto one hundred hours revealed a number of problems

(1) particles agglomerated if some of the bed became static.

(2) deposits grew on the membrane supporting the catholyte.

(3) dendritic growth from the feeder often occurred and incorporated particles.

These problems were overcome by using a more suitable cell design and by modifying the inlet system to give more uniform bed fluidisation.

In contrast to the above Surfleet and Crowle(1) found that copper removal from a fluidised bed became prohibitively low below 200 p.p.m.. Having compared the fluidised bed to other methods of metal recovery they consider that it would be most gainfully employed in removing copper down to 200 p.p.m. where ion exchange extraction could take over. From these varied results of Flett and Surfleet and Crowle it is obvious that the use of fluidised beds in extraction is still not clear. Barker and Plunkett(102) have more recently looked at the recovery of nickel using fluidised beds and have been able to reduce nickel concentrations to 30 p.p.m. Current efficiencies varied between 5% and 45% but were lower for the lower concentrations.

Low current efficiencies caused nickel hydroxide to precipitate and to prevent this boric acid was added. It was successful except where the nickel concentration dropped below 0.01% by weight. Additions of traces of chromium as an impurity had a marked inhibitive effect on nickel deposition suggesting that this system is very sensitive to chromium ion contamination.

Every fluidised bed investigator has indicated that problems will occur in bed scale-up resulting in increased operating difficulties. The tendency may therefore be to use a series of small cells rather than one large one. It has been reported(94) that at least one pilot plant size fluidised bed is operational, and is being used to investigate inorganic reduction reactions, organic syntheses, and the electrowinning and refining of metals. A recent large fluidised bed operation has been cited(108) and is giving good results. In this case instead of a single feeder electrode to supply the current there are a number of feeder electrodes situated within the cell.(fig.14)

5.3.4 The Fundamental Approach.

Fluidised bed investigations of a more theoretical nature have been carried out by a number of people. Goodridge(103) has proposed a mathematical model for the fluidised bed based upon charge transfer through discontinuous contact between the particles. Non-uniform behaviour at the distributor has been explained in terms of a variation in the charge transfer coefficient. Fleischmann and Oldfield(104) have used a simplified model previously used by Newman and Tobias(105) for the porous

electrode. (the essential difference being that in a porous electrode the matrix is fixed and continuous whereas in a fluidised bed it is not). Using this the fluidised bed was treated as a one dimensional model with variations in current and potential, being considered only as a function of the bed depth. Simplified equations were performed to describe the current and potential distributions in the bed, from which it was determined that a bed thickness of one centimetre is the maximum particle thickness for good bed conduction where both current flow and electrolyte flow are parallel. It was also found in this system that maximum current densities were obtained when the feeder electrode was placed at the furthest point from the counter electrode(fig. 14). Other simplified equations have been used by Fleischmann and Oldfield(106) to determine the effective resistivity of the metallic phase. These equations were based upon a number of assumptions and experimental attempts to verify the theory met with only limited success. Theoretically predicted values were compared with experimental values for the cathodic reduction of oxygen on silver but values only agreed when the feeder electrode was placed near the anode(107). Reasons for this lack of agreement were suggested either as being due to disturbance of the bed by the feeder, or because of non-uniform resistivity in the bed resulting from uneven porosity in the entrance region. This latter idea concurs with Goodridge's suggestion that a higher charge transfer coefficient occurs in this region(103).

Further work by Fleischmann and Oldfield has led to the suggestion that in all practical systems the electrolyte flow will have to be perpendicular to the current flow(110). This has since been shown to generally be empirically correct(95,100,109).

In conclusion it may be noted that the fluidised bed has numerous outlets in production, either for the uniform plating of components or for the electrowinning of metals from dilute solutions. In the latter case the conducting bed may be of particular service where a system is kinetically controlled by low reactant solubility or high reaction polarizability, and a lot of work is still necessary to determine the full scope of this electrode.

6. EXPERIMENTAL.

6.1 Ancillary Experiments.

6.1.1 Particle Size Determination.

As received copper powder was sieved in an automatic shaker for twenty four hours. The cut of powder between -212μm and +150μm(70 mesh to 100 mesh) was removed as this was the size range of powder which was to be used in the fluidised bed. A sample of powder from this cut was obtained by the method of 'Coning and Quartering' of these particles. Particles from this sample were sprinkled onto a slide smeared with oil and this was placed onto the stage of a 'Beck-Swift' optical microscope. The calibrated moving stage of the microscope allowed accurate diameter measurements to be made(±1μm). All particles under observation were within the range of values quoted by the mesh size. Although the majority of copper particles were spherical some of them consisted of two or three spheres joined together. In the determination of the diameter of such particles, the diameter of the two or three 'pseudo' spheres were measured. The surface areas of the spheres were then added and equated to a sphere of equivalent diameter.

6.1.2 Particle Density Measurement.

The density of the copper powder used was determined by the displacement of distilled water at 20°C, using a specific gravity bottle(Pycnometer). The usual precautions were taken to ensure the removal of any air trapped in the bottle. The copper powder was found to have a mean density of $8.96 \pm 0.2 g/cm^3$.

6.1.3 Electrolyte Density.

The densities of the electrolytes used were measured with a Hydrometer according to the method specified in B.S. 718/1960. One litre measuring flasks containing the various solutions were immersed in a tank containing forty litres of water at 20°C. Once the electrolyte temperature had reached equilibrium the Hydrometer was used to measure the specific gravity of the solution.

6.1.4 Viscosity Measurements.

A glass capillary (type B.S.U.-A) U tube viscometer was used to determine the kinetic viscosities of the electrolytes according to the method specified in B.S.- 188/1937. The viscometer was mounted vertically in a forty litre tank and equilibrated with water in the tank to 20°C. The fall time. for deionised water was used to calibrate the instrument. Absolute viscosities were determined using values from the 1953 ammendment of B.S.- 188/1937 Appendix C, and this allowed the kinematic viscosities of the electrolytes to then be determined.

6.1.5 Electrolytes:

All solutions were made up from 'Analar' grade hydrated copper sulphate $CuSO_4.5H_2O$, 'Analar' grade Sulphuric Acid, and deionised water. Initially concentrations of 7×10^{-2}M. and 1×10^{-2}M. copper sulphate were used in experiments to attempt comparability

with a previous study(73). However, because low ion concentrations are required for the establishment of limiting currents, 1×10^{-3}M. and 1×10^{-5}M. copper solutions were used as well. One strong solution of 0.7M copper sulphate was used primarily for surface morphology work, but was used in other experiments for the sake of experimental completeness.

6.1.6 Electrolyte Composition.

A 'Unicam' SP600 Spectrophotometer and a Hilger 'Spekker' H676 Spectrophotometer were calibrated against standard copper solutions. The copper ion concentration of the solution being used was checked daily and it was found that significant increases occurred with time for concentrations of 0.01 M. solution or less. Solutions were replaced when their optical density deviated by 5% or more from that determined in the standard solutions. This required replacement of 10^{-2}M. solutions weekly and 10^{-3}M. solutions daily. On runs using 10^{-5}M. solution, the solution was changed after each experiment. The standard copper solutions were made up from $CuSO_4.5H_2O$ dissolved in 0.5M. Sulphuric acid. The 'blank' solution was made from 0.5M Sulphuric acid alone.

The increase in the copper concentration found in the electrolyte was due to the superior current efficiency of the anode over the cathode in that the experiments were often taken into the range where hydrogen evolution occurred thus dropping the cathode efficiency. Chemical dissolution of the anode by the acid electrolyte may have had a minor effect.

Measurement of the hydrogen ion concentration using an

E.I.L. pH meter showed that the acid content of the electrolyte did not change significantly at any time. Because the solutions were changed frequently it was not thought necessary to check the pH after an initial check when the solution had first been prepared, but checks on the pH were still made when a lot of hydrogen was evolved during any one experiment.

The electrical conductivity of Sulphuric acid was determined over a range of concentrations from 0.1M. to 1.5M. using a Pye conductivity bridge. Although electrical conductivity plays an important part in fluidised bed behaviour 0.5M Sulphuric acid was used as the base electrolyte even though this did not give the most conducting solution. This particular acid concentration was chosen because, as found previously by Carbin and as was also found in this present work, the perspex cell used in the experiments tended to crack after a short period when stronger acid concentrations were used. Even in 0.5M Sulphuric acid some cracking was apparent after a number of months of service(plate 2)

6.1.7 Flow Measurement.

Flow rates were measured by leading the cell exit pipe directly into a measuring cylinder and measuring the flow for a given time interval, usually one minute. The flow for a given Rotameter reading was constant using this method. Bed expansion readings also gave consistent readings with the Rotameter readings. The Rotameters used were of the 100-type tapered glass tube.

They were fitted with ceramic floats (Korannite K-type) and had tantalum end springs to prevent corrosion by the electrolyte. The smaller Rotameter (7K) was used for flow rates upto 0.3 litres/minute, and the larger for flow rates upto 2.5 litres/minute. A three way Quick-Fit tap was fitted to switch flow from one Rotameter to the other.

6.1.8 Tubing.

A number of different types of tubing were used in conjunction with the pump. Initially Neoprene was used as recommended by the manufacturers, however the tube wore very rapidly and had to be replaced.'Silicone Rubber' tubing was considered, however it was not possible to obtain this rubber with wall thicknesses of greater than 2mm and rubber with this thickness caused uneven flow in the cell because of back pressure at the pump. Thick walled vacuum tubing was tried and gave excellent stable flow but had poor mechanical wear resistance, failing after only ten hours. Eventually clear flexible P.V.C. tubing was used which had excellent resistance to the solution lasting about 200 hours at pump speeds of 100 r.p.m..Its cost was also minimal.

6.2 Apparatus.

The fluidised bed used in this study is described schematically in figure 15. A photograph of the apparatus is given in platel.

6.2.1 The Cell.

The cell was constructed from perspex as shown in figure 16, and was essentially a long tube which had been split up into three lengths. The bottom two lengths both had two flanges, one at either end of the tube. The top tube had only one flange, at its base. Each flange was fitted with one or more 'O' ring seals to prevent seepage of electrolyte from the cell. Other features particular to each section of tubing were:-

1) The bottom section contained a base plate which had been drilled to admit an electrolyte entry pipe. It also had a grooved insert to take a porous plastic filter(Vyon). This was the filter upon which the fluidised bed rested. This section also had a small hole drilled in it to accept the reference electrode.

2) Two middle sections of the cell were constructed, differing in the diameter of the perspex tube from which they were made, Both sections were used in experiments at different times.

3) The top section of tubing had a hole drilled in its side to accept the electrolyte exit pipe. This hole was situated thirty millimetres below the uppermost point of the unflanged end of the tube. Directly opposite this hole and a further thirty millimetres below it, another hole of similar diameter was situated to accept the anode lead(6.25mm dia. hole).

The three cells were bolted together at the flanges by six equally spaced 2B.A. steel bolts (protected with an electroless nickel coating). Initially brass bolts were used but the heads wore very quickly,

especially as the cell had to be taken apart after each experiment. Uncoated steel bolts were corroded because of acid spillage and often seized up if the cell was not used for a few days. Table 6 gives the overall dimensions of the cell.

6.2.2 The Bed.

The bed consisted of small atomised particles of copper which were generally quite spherical. A particle range between 70 mesh and 100 mesh was used to construct the bed(see also section 6.1.1).Three bed weights were used,giving packed bed heights(i.e. the bed height with no electrolyte flow) of approximately one,two and three centimetres in the smaller cell. The bed weights were 16.67, 33.33, and 50g. In the larger cell a 50g. bed weight only was used with a packed height of approximately one centimetre(table6).

The bed rested on the porous filter in the lower section of the cell. The particular range of particle size was chosen firstly because it gave good bed fluidisation and secondly because it was more easily available than other particle size ranges. Other reasons for keeping to this size range were that particles less than 150μM tended to entrain in the electrolyte at low flow rates, and suffered from flotation problems if there was any air trapped in the system. Particles of greater than 212μM in diameter did not fluidise easily in this cell perhaps because of their mass. Larger particles were also less spherical. Very large particles could not be used because otherwise mass transfer effects between the wall and the particles would have become important.

6.2.3 The Electrode Arrangment.

The anode was made from a length of 'Analar' grade copper sheet 125mm×50mm×0.9mm which was coiled so that it could fit inside the cell. It was placed directly above the bed and about 150mm from it. The anode lead fitted into the cell through a rubber bung fitted into the anode entrance hole. The area around the bung was supported by perspex to give the bung extra support. Extra 'Perspex' was also placed around the electrolyte exit pipe to give the pipe more support. (see fig.16). At the very top of the cell a large rubber bung, drilled to take a stirrer gland, was placed. A glass tube fitted tightly down the centre of the stirrer gland and went from the stirrer gland down through the centre of the cell to a point 60mm above the height of the porous bed support. The cathode feeder to the bed went down the centre of this glass tube. This feeder electrode was 1.6mm in diameter , and was made from Shellac coated high purity copper wire. It was further insulated by a surround coating of P.T.F.E. tape. One end of the feeder electrode was connected to the Potentiostat and the other end rested on the porous support. A rubber bung, which made a water tight seal with the glass tube, surrounded the feeder electrode at the top of the cell. During experiments, that part of the feeder which was to be situated in the bed was stripped of all insulation to a height one millimetre less than the bed height. Electrical contact could then be made between the feeder and the copper particles in the bed (fig.15).

The reference electrode was placed just below the porous filter through a hole drilled there for that purpose. The reference

electrode was placed in this position both for convenience and because it ensured a consistency in the experimental procedure during potential sweep experiments. A saturated Calomel electrode (KCl) was used initially but this was replaced by a copper wire reference elctrode as this had proven to be both convenient and stable. The temperature of the cell was monitored by placing a thermometer in an inlet hole at the top of the cell.

6.2.4 The Circulating System.

The circulating system is shown schematically in figure 18 An eight litre electrolyte reservoir was placed in a fifty litre water bath fitted with a 'Cambridge-Tecam' temperature unit to maintain a constant temperature.The electrolyte was pumped via a variable speed peristaltic pump capable of flow rates upto thirty litres per minute. Two intermediate vessels were used to smooth out the pulsed flow from the pump. After passing through the cell the electrolyte returned to the reservoir via one of the Rotameters. From the Rotameter reading the flow in the cell could be determined. The temperature of the electrolyte was observed with the aid of a thermometer placed in the reservoir.

A framework of 'Climpex' tubing mounted on a wooden base supported the cell, the Rotameters and the smoothing vessels. The wooden base sat in a plastic tray and was mounted on foam rubber to reduce vibrations in the system caused by the pulsing action of the pump.

6.2.5 Flow Regulation.

The pump was capable of speeds upto 220 r.p.m. (equivalent to 100 cm/sec. for large bore tube) but it was found that for smooth running, speeds between 70 r.p.m. and 100 r.p.m. were necessary. Below 70 r.p.m. flow pulsations increased and the flow was not adequately smoothed by the time it reached the fluidised bed. Above 100 r.p.m. the tube life deteriorated quite rapidly and vibrations in the 'Climpex' support system were noticeable. In the range of 70 r.p.m. and 100 r.p.m. the flow , although smooth, was much higher than that required to fluidise the bed and would have entrained the copper particles in the cell. A by-pass valve was therefore installed to draw off some of the electrolyte before it reached the cell, thereby reducing the flow to the bed(fig.15). The pulsed flow from the peristaltic pump was smoothed using two vessels in series. The first of these was a two litre aspirator fitted with entrance and exit pipes. A small pressure release tap was fitted at the top of the aspirator. The second vessel was a 100 c.c. glass flask, again fitted with entrance and exit pipes and a pressure release vessel(fig15).

6.2.6 Temperature Control.

A single temperature of 23°C was used in the experiments, which was similar to room temperature. It was still necessary to install a temperature control regulator however to ensure that a constant temperature in the cell could be maintained. This was achieved by passing the electrolyte down a 'Leibig Condenser' in the flow circuit. Flowing water in the outer jacket of the condenser

raised or lowered the temperature as required.

6.2.7 The Electrical Supply.

Experiments were performed potentiostatically using a ten Amp./forty Volt 'Chemical Electronics' potentiostat and 'Linear Sweep Generator'. The potential across a standard one ohm resistor was fed into a Bryans 28000 chart recorder to give a direct potential-current conversion, and polarization currents could thus be monitored continuously during the potentiodynamic sweep of the electrode.

6.3 Procedure.

Initial experiments in the cell were carried out without a bed of particles being present in the cell. Instead cylindrical specimens similar to those used by Carbin and Gabe(73) were used and a number of polarization curves were obtained. These gave limiting currents for copper solutions under various conditions of flow and for different copper ion concentrations.

6.3.1 Cylindrical Specimens.

Cylindrical specimens were polished through various grades of silicon carbide paper to 800 paper and were degreased in acetone. Two methods of pretreatment of the samples were investigated, chemical polishing and electrochemical polishing. Both methods gave similar reproducible results for polarization curves above 100 mV. overvoltage, with limiting current densities varying by 2%. Below

100 mV. some differences existed in the polarization curves but this region was not of major importance to the study.(The discrepancies were probably an effect of crystallization overvoltage caused by the different methods of pretreatment). As such close agreement was achieved between the two methods of polishing, chemical polishing was used because it was a more convenient method. The chemical polish solution that was used contained 55% Orthophosphoric, 25% Acetic and 20% Nitric acids' by volume. The degreased specimens were immersed for one minute at room temperature(25°C), removed, washed with tap water, deionised water and finally in the electrolyte in which they were to be used.

After polishing the specimens were placed at various heights within the cell and in this instance, as no bed was present, the reference electrode was fitted two millimetres away from the cathode specimen.(fig.17). A flow rate of 1·4 cms/sec was used and polarization curves for the electrode were taken by potentiodynamically scanning the electrode upto 1200mV. overvoltage, or until the hydrogen evolution reaction was giving a current in excess of one Amp. A potential scan speed of 60 mV./min. was chosen for these experiments.

6.3.2 Electrode Geometry.

The cylindrical specimens used were cut from 6.32 mm.(1/4") diameter copper rod. Their end faces were squared on silicon carbide paper with the aid of a perfectly rectangular tool steel block drilled to take the specimens. Each specimen length was measured with

a microscope capable of reading to 0.1mm.. The ends of the specimens were laquered so that only the curved surfaces of the specimen took part in the experiments.

Various experiments were conducted to find out the hydrodynamic length of the cell and the effect of the porous membrane on this length.It has been suggested that filling the area below the membrane with glass ballotini helps reduce the hydrodynamic entry length(q_8), in the cell. This was tried out in this cell , but it did not have any noticeable effect on limiting current data. Limiting current data was obtained for copper ion concentrations of 0.07M. in 0.5M. Sulphuric acid, and the experiments were conducted at 23°C.

6.3.3 The Feeder Electrode.

Experiments on the feeder electrode were also carried out in the absence of a bed. In this case insulation was removed from the feeder to leave the required length of copper wire exposed. This was immersed in copper polish solution for ninety seconds or until there were no bubbles on the feeder surface. It was then washed in a similar manner to the cylindrical specimens. The feeder electrode was placed so that it was just touching the porous membrane and the reference electrode was placed below this filter(fig.15). Polarization curves were recorded by potential scanning of the feeder using similar conditions as for the cylindrical specimens. Care had to be taken that no copper from the feeder electrode became embedded in the filter as spurious polarization curves resulted. (This sometimes

occurred if burnt copper particles formed on the feeder electrode and then fell onto the filter). The cause of the spurious results was probably due to having a larger surface area cathode, caused by the copper particles embedded in the filter becoming part of the cathode.

Required feeder lengths were measured under the microscope and insulation was stripped from the feeder surface using a scalpel. Polarization curves were recorded at various flow rates in 0.07 and 0.01M. copper solutions for a number of feeder lengths. Great care was exercised when changing solutions to ensure that the system was entirely free of the old solution. This required draining the system, flushing with water, flushing with distilled water, and finally with three litres of new solution.

A small number of polarization curves were obtained using various feeder lengths in a fluidised bed. The length of the feeder electrode was varied; between being one third of the total height of the bed and the full height of the bed less one millimetre.

6.3.4 The Fluidised Bed.

In order to ensure that experimental values were comparable, reproducible conditions were necessary in the bed. Attempts were therefore made to polish the particles. Electropolishing was considered an unsatisfactory method of polishing because the behaviour of the fluidised bed had not been established, also it was apparent that as a continuously changing portion of the bed would be in contact with the anode, a range of results might be achieved caused by the variability in anode contact time with any given particle. The

results of the polishing might therefore have varied between light etching, through polishing to over etching and pitting. A second reason against the use of an electrochemical pretreatment was that due to the large surface area of the particles, the particles would be much more active than normal and it has been suggested(100) that under anodic fluidisation bed particles often become coated with a thin layer of oxide.

Chemical polishing of the particles did not prove successful as the large area to volume ratio of the particles catalysed the breakdown of the Nitric acid in the polishing solution resulting in the evolution of nitrogen dioxide. Diluting the solution with water also gave unsatisfactory results. Other milder forms of cleaning solution were tried using 15% Nitric acid(v/v) and 4% Nitric acid (v/v) in distilled water. These were not successful either as the solutions merely caused pitting of the particles thereby changing their surface area(plate 3). Consequently before being used in the experiments the particles were merely degreased. A thorough degreasing was obtained in the following manner. Initially the particles were cleaned in an ultrasonic bath containing soap and water. This was followed by a rinse in deionised water and then by immersion in boiling iso-propyl alcohol. Finally the particles were rinsed in the solution in which they were to be used. Scanning electron microscopy showed the particles to be oxide free. Once the particles had been degreased they were placed in the cell, the cathode feeder was then placed in the bed and the bed was fluidised to the required height. The reference electrode was placed just below the filter upon which the bed rested. Once a potentiodynamic sweep had been completed, the bed was removed and a new bed of particles was placed in the cell

before commencing the next sweep. Reusing a bed gave bad results.

When the smaller cell was in operation three bed weights were used (16.67,33.33,50.0g),In the larger cell one weight was used (50.0g). Each experiment was repeated twice or until experimental reproducibility was achieved. Polarization curves for various bed expansions upto double the original height of the bed were taken using the 7×10^{-1}M Cu^{++} solution in 0.5M Sulphuric acid. These curves were then repeated using other solutions containing 10^{-5}M., 10^{-3}M., 10^{-2}M., and 0.7M. Cu^{++} solution in 0.5M Sulphuric acid. Runs were also conducted using 0.5M. Sulphuric acid alone. The sweep rate used in these experiments was 15mV/min. and experiments were continued well into the hydrogen evolution range.

6.3.5 Particle Growth Experiments.

A number of experiments were carried out on the growth of particles under potentiostatic conditions. Using the smaller cell a bed weight of 16.67g was taken and fluidised to 1.3 cms in 0.7M. copper solution ($\epsilon = .46$) A potential difference of 60 mV was placed on the feeder electrode with respect to the reference electrode for times of 1, 5, 10, 25, 50, and 100 minutes. At the end of each of these times a sample was taken from the bed washed in water, dried in alcohol and stored in a dessicator. This procedure was repeated on samples for potential difference intervals of 60mV upto 420 mV. All the samples were examined under a Cambridge Mark V Stereoscan. (In the preparation of samples for the Stereoscan care had to be taken not to apply too much glue to the stub onto which the particles were to be sprinkled, otherwise the particles became completely immersed

in glue. The curvature of the copper particles did not cause any problems on this equipment because of the excellent depth of field this particular piece of equipment has.)

7. RESULTS.

7.1 Ancillary Results.

7.1.1 Electrolyte Viscosity and Density.

The kinematic viscosities of the electrolytes used in this study as well as data for distilled water are shown in table.7. This data is in good agreement with Selman et al.(112) which is also tabulated for ease of reference. The viscosities of the solutions containing only small quantities of copper are indistinguishable from each other.

The densities of the above electrolytes are tabulated in table 8 and again good agreement is obtained with the data of Selman in the appropriate ranges. For densities of less than 0.01M. values differed, however the empirical equation which Selman uses has not been validated for concentrations of 0.01M. or less.

7.1.2 Diffusion Coefficients.

The relationship proposed by Arvia(111) for obtaining diffusion coefficients for copper has been widely accepted(3,73) and was used here. Calculated values of D Cu^{2+} for the conditions investigated appear in table 9.

7.1.3 Spectrophotometer Calibration.

The two spectrophotometers which were used (section 6.1.6) were very useful in determining the quantity of copper in solution. The blue colour inherent in copper solutions meant that it was unnecessary to add any form of colour complexant to the solution and samples could be removed from the cell and analysed immediately.

Linear relationships existed between optical density and copper ion concentration over intervals within the ranges used, although no single linear function could be used to cover all the solution ranges. Figure 19 indicates a typical linear calibration line for copper ion density versus optical density for the Cu^{2+} concentration range 0.01M. to 0.1M..

7.1.4 Sulphuric Acid Conductivity.

The results for conductivity tests with Sulphuric acid are given in figure 20. An appreciable drop in conductivity occurs with decreasing acid concentration and in fact 0.5M. Sulphuric acid has only 41% of the conductivity of 1.5M. Sulphuric acid; however the life of the perspex cell is approximately ten times greater in the more dilute acid solution. The conductivity of the 0.5M solution is still good with a conductivity of $0.19\Omega^{-1}cm^{-1}$, and is sufficiently good to remove the copper ion contribution to the electrical conductivity i.e. $t \rightarrow 0$ for Cu^{2+}.

The overpotential at which hydrogen evolution starts on copper is about 16% greater in 0.5M Sulphuric acid than in 1.5M Sulphuric acid. Figure 21 indicates how the overpotential at which hydrogen starts to evolve drops, with increasing hydrogen ion concentration. It is noticeable that as the acid conductivity stabilises in the higher concentration regions, the overpotential at which hydrogen starts to evolve also stabilises.

7.1.5 Particle Size Determination.

A histogram and a graph of five hundred particles' size distribution are given in figures 22 and 23. The graph follows a normal distribution type function. The particles have a mean diameter of 184μM with a standard deviation of 17μM.

7.2 Apparatus.

7.2.1 Flow Measurement.

The calibration curves for the 7k and 14k Rotameters are shown in figures 24 and 25. Only very slight density and viscosity differences occur for solutions of 0.01M Cu^{2+} or less and calibration curves in these ranges are indistinguishable.

7.2.2 Effect of Potential Sweep Rates.

The 'Linear Sweep Unit' was calibrated against a standard 'Weston' cell to give a range of 3.0 volts on a ten turn potentiometer. One turn on the potentiometer was subdivided into one hundred divisions, each division resulting in a potential shift of 3mV. The accuracy of the calibration was checked against a standard 'Electrometer' and a straight line graph of overpotential versus potentiometer reading was obtained as shown in figure 26.

7.2.3 Polarization in Static and Flowing Electrolyte.

The effect of change of potential with time during a potentiodynamic sweep of a reaction is a major factor as to how a

reaction proceeds. If the sweep rate is too fast then the reaction does not have time to equilibrate at any one particular potential and current overshoot occurs i.e. the reaction proceeds faster than it normally would do at a given potential. If the sweep rate is very slow it allows the reaction to equilibrate at a particular potential very well, but it can allow large deposit growth to occur on the electrode causing an increase in electrode area. This latter effect is not normally noticeable at the sweep rates employed in many studies which have sweep rates down to 10mV/min.

The effect of sweep rate is clearly seen in figures 27 and 28. The first of these shows how current overshoot occurs at rates above 60mV/min. in acidified 0.07M. $CuSO_4$ during the plating of copper from stagnant solution. The second shows that the effect of agitation in the solution causes the deposition reaction to equilibrate more rapidly at a given potential,allowing sweep rates upto 300mV/min. to be used without overshoot occurring. The effect of sweep rate in a conducting fluidised bed is shown in figure 29.

7.2.4 Effect of Cell Design on Polarization Curves.

Initial experiments were carried out using the larger cell (31.68mm I.D.) in the presence of flowing electrolyte alone in order to determine the entrance effect of the cell. This effect had been found previously(70,71) using similar type cells. As this study was one of apparatus familiarisation samples similar to Carbin's were used. Cylindrical specimens of 6.35mm diameter×11mm in length were

placed at various heights above the porous filter and a family of polarization curves obtained for 0.07M $CuSO_4$ at a flow rate of 1·4 cm/sec (fig. 30). The above experiments were then repeated without the porous membrane in the cell in order to determine its effect on solution flow(fig. 31). The polarization curves for the specimens, both for the membrane present, and with it absent, exhibited well-defined limiting currents at all heights in the cell. Figures 32 and 33 indicate the effect of axial height on the measured values of i_L for both these cases.

7.2.5 Polarization Curves and Electrode length.

Polarization curves obtained using a variable size electrode(length variability) are shown in figure 34. The effect of electrode length on the average value of limiting currents is indicated in figure 35. Mass transport data reported by Bazan et al.(111) has indicated that electrode length affects mass transfer coefficients. These results tend to confirm this suggestion.

7.3 The Feeder Electrode.

7.3.1 Introduction.

The results of study on the fluidised bed electrode are shown in figures 46-74 .The connection to a conducting fluidised bed electrode is an electrode in its own right and is known as the feeder electrode. This electrode is often a wire, or wire mesh, and as such

must have some individual effects of its own. Typical results for the feeder electrode used in this study, without a fluidised bed present, are set out below.

7.3.2 The Effect of Flow on Polarization Curves.

The effect of flowing electrolyte on the feeder when no fluidised bed is present is shown for the polarization data for 0,01M and 0.07M Cu^{2+} solutions in figures 36 - 45. These experiments were carried out in the smaller cell(25.4mm I.D.) and in all cases limiting currents were clearly defined over a large range of overpotential values and limiting currents could be quite accurately measured to ±1%. (Although in this instance the limiting current was clearly defined , the limiting current of a polarization curve is often quite difficult to establish. In order to afford comparibility with other results the limiting current was stipulated as occurring, in this instance, at an overpotential of 400mV with respect to the rest potential.) The electrode was placed just above the porous membrane and was therefore always wholly or partly covered by the hydrodynamic entrance region; thus limiting currents much higher than those that would occur outside the hydrodynamic region were probably obtained.

7.3.3 The Hydrogen Evolution Reaction.

The effect of the feeder electrode length on the evolution of hydrogen during a potential sweep is adequately established in

figure 36 in the presence of flowing solution of 0.5M Sulphuric acid. Increasing the length of the feeder electrode causes a slight reduction in the overpotential necessary for a given current of hydrogen to be produced, This can be expected from the slight increase in area of the electrode. The effect of the agitation caused by circulating the electrolyte is to raise the potential at which hydrogen is given off.

7.4 Fluidised Bed Results.

7.4.1 Polarization Curves.

Figures 46 - 74 represent the polarization curves for the fluidised bed electrode and describe the effects of the variables investigated in this study. The main variables studied were the effect of: bed volume, bed porosity, electrolyte concentration, and cell size. These particlar variables were used in order to characterise conditions in a fluidised bed electrode and to determine the limitations of the system.

7.4.2 Bed Volume.

The effects of changing the volume of the bed by increasing the mass and number of particles in the bed are shown in figure 46. There is a large decrease in the 'apparent overpotential 'requirement necessary to produce a given current as the bed weight is increased. This might be predicted, as the bed's surface area obviously increases with increasing bed weight(for a constant particle diameter), and larger currents can thus be expected at smaller overpotentials.

From the overall shape of these polarization curves for different bed weights, one observes that after an initial overpotential region where the current is very small, a very rapid increase in current occurs with only small apparent increases in the overpotential. Increasing the weight of the bed increases the height of the bed which, in this case, is the same as scaling up the bed perpendicular to current flow. This type of scale-up is discussed more fully in section 8.2.2.

7.4.3 Bed Porosity.

The effect of fluidising the bed to different porosities causes a decrease in the current corresponding to a given 'apparent overpotential' as shown in figures 49 - 69. Initially it had been expected to find an optimum current(i.e. highest value current) occurring above the incipient fluidisation point where a balance occurred between particle-particle conductivity and electrode surface area; similar to the effect arising in inert particle fluidised beds for the effects of particle agitation and flow rate (fig. 12). This effect was not observed suggesting that mass transfer effects in the bed are not as important as bed conductivity.

At low bed expansions $\lesssim 20\%$ and at fairly high'apparent overpotentials' hydrogen evolved all over the top of the bed and a burnt copper deposit formed(This effect usually became noticeable for currents greater than ~ 2 Amps, and was preceded by parts of the top of the bed becoming burnt around the feeder electrode. These burnt areas would spread outwards,away from the feeder,and hydrogen

would evolve first from these sites.) The rate of hydrogen evolution was very large possibly because of the large number of nucleation sites available and a 'burst' effect was often observed just after the commencement of the reaction, with the speed of evolution being so fast that the solution above the bed turned opaque within a few seconds. This effect also made the electrolyte flow unstable.

At high bed expansions the hydrogen evolved from the feeder electrode only, implying that there was very little contact between the feeder and the bed particles. In this situation, at high over-potentials, the feeder electrode itself often had a burnt appearance although the total current delivered by the bed was generally quite small. The burnt effect increased as the bed height(porosity) increased. The current at a given overpotential decreased as the bed height increased.

7.4.4 Electrolyte Concentration.

A family of curves showing the effects of solution strength on bed porosity and bed volume are given in figures 49 - 69. It is noticeable that no limiting currents appear until very low copper ion concentrations are used i.e. 10^{-5}M.(fig. 64 - 66). As the solution strength is increased the overpotential at which hydrogen is evolved decreases. A third observation is that at very high currents 2 - 8 Amps. current increase no longer remains a linear function of overpotential increase(fig. 67 and 68). The reason for this latter observation is that at such high currents the top of the bed often solidifies causing instability in the bed

and making further use of the bed impracticable.

7.4.5 The Effect of Cell Size.

The effects of scale-up of the cell, parallel to the current flow of the system are shown in figures 67 - 69. The results are relatively similar to those achieved in a bed of one third the weight in the smaller tube(fig 49 - 51). The results perhaps emphasise the point made by Backhurst et alia(89) that scale-up of cells parallel to current flow may have severe limitations because the cells are governed by the position of the electrode and the potential distribution in the bed. The effects of scale-up perpendicular to the bed are given in section 7.4.2.

7.4.6 The effect of Variable Feeder Length in the bed.

Experiments were conducted to see the effects of the feeder electrode on the fluidised bed(fig. 47 and 48). Various lengths of feeder electrode were placed in the cell. When the feeder was greater than the bed height some spurious results were obtained which were probably due to uneven polarization of the electrode above the bed. To prevent this from happening that part of the feeder situated above the bed was covered in 'Lacomit' sealant and further covered with a layer of P.T.F.E. tape. The results show that as the length of the feeder is decreased in the bed the current decreases for a given overpotential. Because of these results, and after some initial experiments had been carried out, the feeder length was standardised at 1mm less than the porosity of the bed.

7.4.7 The Hydrogen Reaction.

The effect of the conducting fluidised bed on the hydrogen evolution reaction when no metal ions are present in the bed , and using a platinum anode,are given in figures 53,58 and 63. The over-potential at which hydrogen is generated is higher than that for when copper ions are present,(fig. 49 -52, 54 -57,59 -62), but is less than when no bed is present at all(fig. 36). A possible explan-ation for this is given in section 8.2.

7.4.8 The Effect of Reusing the Bed for more than One Experiment.

It was found that if a bed of particles was used more than once in a potentiodynamic sweep then some unusual polarization curves were obtained. For small bed expansions<20%,straight line relationships were obtained for overpotential versus current(fig. 70) and the same current/overpotential polarization curve was often maintained for different bed porosities. If a particular bed was used in more than two polarization runs, the bed generally became unstable and lumps of copper powder which had agglomerated together could be observed. A lot of fine copper powder of 10μM or less was also present in the bed. This generally became incorporated into the porous membrane and increased the surface area of the bed through contact with the feeder electrode which was touching the membrane.

7.5 The Structure of the Electrodeposits.

7.5.1 The change of Deposition Rate with Time.

Some experiments were conducted where the bed was left under a constant 'apparent potential' for various time periods in 0.7M $CuSO_4$ + 0.5M H_2SO_4. At various time periods for a given potential (i.e. 1,5,10,25,50, and 100 minutes) samples were taken from the bed to be looked at under the Scanning Electron Microscope (fig. 71 and plates 6-15). Although the current in the bed was expected to remain fairly constant for a given potential, in fact the current changed quite dramatically with time. Possible explanations for this behaviour are given in section 8.2.

8. DISCUSSION.

8.1 Cell Characteristics.

A preliminary investigation was carried out on the cell without the presence of the fluidised bed to determine the effect of some hydrodynamic parameters of the system. The results were compared to the results obtained by Carbin([76]) who used a similar type of fluidised bed cell. Similar cathode samples were also used.

8 1.1 The Effect of Axial Height.

The effect of limiting currents obtained during the variation of the cathode height in the cell were found to agree very closely with the results obtained by Carbin. A pronounced entry length was evident in the cell at heights of upto 40mm. above the porous membrane. This has been attributed to the distance required for a stabilised flow regime to become established. If the porous membrane(used to support the fluidised bed) is removed from the cell the flow characteristics of the cell change slightly and a further 20mm entry length is required before the flow regime estab-lishes itself to the same degree as when the membrane is present. (fig. 29 - 32).

8.1.2 The Effect of Electrode Length.

The effect of the electrode length is dependent upon the length from the leading edge of the sample. This is demonstrated in figures 34 and 35, the latter of which shows the limiting current per unit length of electrode decreases as the length of the cylinder increases. This effect may well be due to a flow regime which has

not fully developed by the time the cathode has been reached(fig. 12). Eddies may also form along the length of the sample because of its non-hydrodynamic shape and might thus be important. It would have been interesting to determine the effect of different shaped specimens on the limiting current data as this would have determined how much of the entry effect was due to the sample geometry and indicated the character of the entry length effect.

8.1.3 The Feeder Electrode.

Data on the feeder electrode for various conditions of flow rate and metal ion concentration and for different feeder lengths, is given in figures 36 - 45; characteristic limiting currents are observed for all conditions. Increasing the flow rate from 0cm/sec to 1.35cm/sec increased the limiting current by a factor of three to four times. The effect achieved by only a small amount of agitation, i.e. 0.25cm/sec, was sufficent to increase the limiting current values greater than that produced by a fivefold increase of the surface area of the electrode. This perhaps demonstrates the importance of the diffusion layer in reaction kinetics and also the type of beneficial effect agitation can have in reducing this diffusion layer. The effect of agitation on the potential sweep rate for the polarization curves is given in figures 27 and 28. In the absence of flow, sweep rates of 150mV/min. are required to prevent spurious results from being obtained. When a flow rate of 0.8cm/sec is used in the cell, then sweep rates of upto 300mV/min. produce good reproducible results.

8.1.4 The Hydrogen Reaction.

The evolution of hydrogen is always a problem in metal extraction and metal finishing because it causes a decrease in the current efficiency of the cell, it can cause embrittlement of the cathode deposit, and can prevent good deposits from forming. Polarization curves for the hydrogen reaction, under similar conditions of flow and for similar feeder lengths as those used when the fluidised bed is present in the cell, are given in figure 36. Although no limiting currents are observed, it can be noted how the hydrogen reaction moves to smaller overpotentials as the flow rate through the cell is increased. A similar effect has been observed by Carbin(76) using an inert fluidised bed. (In the presence of a fluidised bed in which metal ions are present the overpotential at which hydrogen is evolved increases with flow rate. See section 8.2.)

8.2 The Conducting Fluidised Bed.

In order to characterise the fluidised bed system a number of parameters have been considered. These are:-

1) The effects of flowing electrolyte.

2) The effect of bed volume- i.e. scale-up of the bed

(i) Perpendicular to current flow.

(ii) Parallel to current flow.

3) Electrolyte concentration.

4) Electrodeposit morphology.

The electrolyte chosen was acidified copper sulphate solution because during the deposition of copper from its ions there is no

chemical step involved(68), making the rate determining step either diffusion controlled or charge transfer controlled. This also meant that copper could be used as the cathode which was beneficial as copper is a very good electron conductor.

8.2.1 The Effect of Flowing Electrolytes.

The effect of agitation in an electrochemical cell has become of increasing importance to electrochemists in the last fifteen years ever since the kinetics of cell polarization have been realised. In the fluidised bed electrode the surface area of the electrode is large and the flow of electrolyte through the bed is turbulent. Increasing or decreasing the rate of electrolyte flow not only affects the degree of turbulence within the bed, but also the intrinsic nature of the electrode itself. An increase in the electrolyte flow through the bed causes an expansion of the bed which in turn causes an increase in porosity of the electrode. A number of polarization curves demonstrating the effect that this has on the efficiency of the bed are given in figures 49 - 69.
As the porosity of the bed increases with faster flowing electrolyte then, for a given overpotential, the current in the bed decreases. Maximum currents are obtained when the porosity of the bed is a minimum i.e. at the fluidisation point of the system. The deposition current also decreases quite rapidly above bed expansions of 20% ($\epsilon = .45$) and limiting currents are observed.

This behaviour of the fluidised bed with changing agitation may be explained in terms of resistance within the bed and the

corresponding changes in potential this causes. In a bed which has not been fluidised all the particles are in good electrical contact with each other. If a small potential is applied to one point within the bed through the feeder electrode all the particles in the bed will assume this potential and all the potential drop between the bed and the counter electrode occurs at the metal/solution interface. If a large potential is placed on the feeder with a corresponding high current flow, there is a very slight change in potential through the bed of particles because of this large current flow and the contact resistance between the particles becomes important.

When the bed is fluidised the potential distribution can change quite markedly. This has been demonstrated previously (95,100,104). The extent of change depends upon such factors as bed material and its conductivity, the particle size, the contact time between particles and the current flowing in the bed. The cell arrangement between the anode and cathode is also important as this determines the current paths between the electrodes and the efficiency of electrode design. An increase in the flow rate causes the bed to expand and the porosity of the bed to change. The mean contact time between particles also increases. Similarly the total number of particles in contact either directly or indirectly with the feeder(indirectly - i.e. by touching other particles which are in: contact with the feeder,) decreases. Parts of the bed which are no longer in contact with the feeder become deactivated and do not assume the bed potential. This type of behaviour has been observed by a number of authors(90,95). At very high flow.rates , and therefore very high porosities, there is very little contact between particles

and the feeder electrode ; the particles function more as an agitation medium than as a means of increasing the electrode surface area and the bed behaves more like an inert particle fluidised bed. The effect of increasing the flow through a fluidised bed when a potential is applied to the bed is to increase the inherent resistance of the electrode and make it function less efficiently.

The polarization curves of figures 49 - 69 describe the above effects in the following manner. At bed expansions upto 20% expansion there is a fall off of the current that is produced by the cell for a given feeder potential. This demonstrates the decreasing activity(and the increasing resistivity) of the bed with increased flow of electrolyte. Above 20% bed expansion 'quasi' limiting currents are observed(fig. 72-74). In so far as the currents are not perfectly limiting, it suggests that the particles are still having a slight effect on the cell current. Another possible reason why the currents are non-limiting is because of some hydrodynamic instability along the feeder electrode. (The feeder elctrode is in contact with the porous membrane in the cell and this is an area where hydrodynamic conditions are not stable. Non-uniform results may therefore be expected from this region which could effect the total current of the cell.)

The highest currents were obtained at the fluidisation point of the system probably because this is where the electrode has the best conduction and works most efficiently. At the fluid-

isation point however the electrode tended to suffer from the effects of slowly moving particles which, because of the long particle-particle contact time, often allowed particles within the bed to agglomerate, upsetting the stability of electrolyte flow through the bed and causing the electrode to break down. This effect was more prominent whilst using the more concentrated electrolytes and at high bed overpotentials(fig.67). In the use of this type of fluidised bed a balance may have to be obtained between operation current and bed height to prevent this type of agglomeration from occurring.

8.2.2 The Effect of Bed Volume.

The designs of fluidised cells are based on two main types of cell configuration.

1) Where current flow and electrolyte flow are parallel.

2) Where current flow and electrolyte flow are perpendicular.

Both of these designs have been discussed in section 2.4.3. Problems in scale-up of processes are very common in most industries, and one of the factors in determining the success or failure of the fluidised bed electrode will be its ability to cope with any scale-up problems. In this area Backhurst's findings are quite significant(90). He believes that increasing the dimensions of the cell perpendicular to current flow will allow linear scale-up of the cell whereas scale-up of the bed parallel to current flow is not advisable above one centimetre because of deactivation of parts of the bed.He points out however that because the current carrying capacity of the bed is large(Backhurst suggests 300A/^{2} related to a cell χ section of $1ft^2 \times 1''$ deep. (500μm particles)

then this is a small limitation and that a number of small cells may even work more efficiently than one big one.

In this study little benefit was obtained in improved current capacity of the cell by scale-up of the bed parallel to the current flow. This is demonstrated by the polarization curves in figures 49 - 51; 67 - 69. The results suggest that the feeder electrode is bounded by a zone of conducting particles $\simeq$ 1cm outside of which good electrical contact is lost between the particles and the feeder. Problems other than conduction became apparent during scale-up of the bed parallel to current flow. The stability of the bed deteriorated. This deterioration became more noticeable as the bed was expanded to higher porosities. Stressing of the membrane upon which the bed rests although not a problem in this study , might become one in a larger cell. This would require replacement of the porous membrane with one of increased rigidity but probably with less permeability.

A theoretical and experimental study by Fleischmann and co-workers led them to a similar conclusion on the maximum useful size of a fluidised bed where current flow and electrolyte flow are parallel, via the concepts of a bed effective resistivity ρ_m of the discontinuous metal phase and an effective solution resistivity. Assuming that charge is shared between particles, following elastic collisions in the bed, they gave an estimation of the current capacity of a given bed as,

$$\rho_m = \frac{0.28\epsilon^{0.33}(\epsilon^{0.33} - 1.0)\gamma_s^{0.33}.\rho_s}{\rho^{0.33}.\nu_p^{0.66}}$$

where ρ is the particle density, ρ_m and ρ_s are the metal and solution

effective specific resistivities, ν_p is the free particle velocity, γ_s is Young's modulus and ϵ is the electrode length normalised with respect to the bed height. The difficulties in relating this theoretical equation to experimental data are large in so far as a free particle velocity determination of particles in the bed is not easy.

Experimentally measured values of I m by Fleischmann were less than 1/7th of that predicted by the equation(110). The discrepancy was ascribed to non-uniform fluidisation(see section 4.3.2) of the bed and possible stagnation of the bed around the feeder electrode. It also demonstrates that a substantial amount of work is still required on the fluidised bed and fluidised bed parameters before the electrode will be completely characterised.

The limitations imposed by the cell during scale-up of the cell parallel to current flow led to the consideration of cell scale-up perpendicular to current flow. In this type of scale-up the 'zone' type conduction problems of above were no longer apparent and larger currents were obtained as the surface area of the electrode was increased. Polarization curves for this mode of operation are given in figures 49 - 66. The relationship between current and electrode surface area is not a linear one for this cell, but this is not unexpected. Some authors have observed(95,103,110) in fluidised beds of both a conducting and non-conducting nature that there is a region of hydrodynamic instability just above the membrane on which the bed rests and as demonstrated in this thesis(section 8.1.1). In this region flow is more turbulent, contact between particles is therefore more frequent and the diffusion layer around the particles is probably thinner. Goodridge has suggested that higher currents

are produced in this region because of a higher transfer coefficient K_m between particles, where

$$I_m = -K_m.A.d\phi_m/dx$$

and I_m is the transfer current. Upon scale-up of the bed the percentage volume of this region decreases and its effect on the total current is therefore diminished. Current achieved when the bed is scaled-up may therefore be slightly less than that expected with a linear current/area ratio.

Other factors which may contribute to this non-linearity in current/electrode area ratio are:-

1) The effects of the potential gradient of the bed which will vary as the bed volume is increased both because of the extra bed resistance between the top and the bottom of the bed and because of a larger concentration gradient between the top and the bottom of the bed(see section 8.2.3 following)

2)The electrode arrangement of the cell which makes the throwing power of the system more important. Where the anode is placed above the cathode the effects of increasing the bed volume in the direction of the anode is to increase the number of available current paths to the cathode. Most of these paths will have an associated increased resistance , and will carry a smaller quantity of current than other current paths. The benefits of an increased bed volume(i.e. scale-up of the bed perpendicular to current flow) will therefore be a diminishing one and smaller increases in current may be expected as the cell is scaled-up.

8.2.3 Concentration Effects.

In this study electrolyte concentrations were varied between 0.7M and 1×10^{-5}M and the results obtained are perhaps the most interesting but also the most difficult to explain. From observation of the results the following comments can be made:-

1) As the electrolyte concentration is increased the apparent overpotential at which hydrogen evolves decreases.
2) The overpotential required to produce a given deposition current decreases with increasing electrolyte concentration.
3) Apart for the 1×10^{-5}M solution no other solution exhibited a limiting current in the active bed range. (25% bed expansion)
4) Scale-up of the bed perpendicular to current flow emphasised the above observations.

These observations are shown graphically in figures 49 - 69.

The results obtained in the fluidised bed by changing the bulk concentration of the electrolyte demonstrates the nature and the limitations of the electrode. The large current obtainable from a fluidised bed of conducting particles may be attributed to the two effects of 1)A large surface area of electrode, 2)A decrease in the diffusion layer thickness around the particles. In an inert particle fluidised bed the increase in current is due solely to the improvement in diffusion conditions. For example, Kreysa et alia(109) have shown that increases of current of

5 or 6 maybe expected in copper solutions using an inert particle bed rather than a non-agitated planar electrode. In this study of the conducting bed even higher ratios were achieved but a comparison between the electrodes is not easy as they operate with different electrode areas.

In conventional planar cells such as the parallel plate cell(section 2.2) concentration changes in the electrolyte tend to affect only the limiting current of the system and the relationship between current and overpotential is similar,upto the limiting current, for different electrolyte concentrations. The results obtained for,the fluidised bed used in this study differ from those obtained for a planar electrode in that when no limiting current is apparent different electrolyte concentrations give different deposition currents, at low overpotentials, when all other experimental parameters appear constant.

The reaction in the fluidised bed does not appear to be kinetically limited by diffusion because the limiting currents which characterise diffusion control are absent. In that different currents are obtained from different strength electrolytes under a constant set of conditions, it would suggest that there is little activation limitation either. Obviously there is a certain parameter which is applied for plane electrodes that cannot be applied in this work.In plane electrodes the potential over the whole of the electrode surface under consideration is taken as a constant value whereas for this fluidised bed electrode this assumption is probably not valid.

In section 8.1.1 it was suggested that changes in bed porosity caused changes in the metal potential of the electrode, by altering the 'contact resistance' between particles in the bed, and that this could eventually lead to deactivation of parts of the bed. It is also possible that changes in electrolyte concentration within the bed affect the metal/solution potential of the system. Consider the following example:-

Let a fluidised bed , through which acidified copper sulphate is flowing, have a porosity ϵ to ensure the bed is active. If a small cathodic current is applied to the bed copper will deposit on the electrode. The deposition current will flow through the paths of least resistance within the bed and because the metal particles have a small contact resistance, more deposition is likely to occur on those particles whose potential is close to that of the feeder, rather than on those whose potential is reduced by this resistance. It is likely therefore that deposition will be greater in the close proximity of the feeder than at points further away.

If more deposition occurs near the feeder electrode , this region will become more depleted in copper ions than an equivalent volume further away. A concentration gradient will tend to set up across the bed. Counteracting this concentration gradient will be the electrolyte's turbulence within the bed which will quickly equalize any concentration differences. When small overpotentials are applied to the feeder concentration gradients will probably have a negligible effect, because of the small amount of current that is being drawn, but this may not be the case when the current is increased.

The effects of concentration changes across the bed will probably be a lot more minor than concentration changes parallel to electrolyte flow. As the electrolyte percolates up through the bed, the effect of an applied potential to the feeder will cause copper to deposit continually from the electrolyte. Electrolyte of decreased concentration will flow out of the top of the bed. The longer the contact time within the bed for the electrolyte, the more copper that will have deposited, and the greater change in values there will be in the inlet and outlet values of the copper ion concentration of the bed.

During a potentiodynamic sweep of the electrode the copper deposition reaction is pushed further and further away from its equilibrium value and greater deposition currents result. Eventually some of the solution may become so depleted in copper, because of the rate of deposition of copper as the electrolyte moves up through the bed, that the deposition current will limit. The part of the bed that will limit first will be in that area where particle contact resistance is least, and where the solution contact time is a maximum i.e. at the top of the bed next to the feeder electrode. This effect was observed(see section 7.4.3).

Taking the above ideas in slightly more fundamental terms, the electrode potential of a system may usually be calculated from the equation

$$E = E' - E_o^*$$

where E is the overpotential, E' is the metal solution potential and E_0^* is the equilibrium potential for the reaction. In a fluidised bed it is not quite so easy to define an overpotential E because of the concentration gradient up the electrode which will affect

the metal/solution potential E'. For a fluidised bed the above equation must be rewritten as

$$E = E'_{(x)} - E^{*}_{o}$$

where $E'_{(x)}$ is the local potential of the system at a given point in the bed. When no potential is applied to the bed the overpotential is zero and $E'_{(x)} = E^{*}_{o}$. Upon applying a cathodic potential to the feeder electrode current will flow, as the reaction moves away from equilibrium, and metal will deposit in the bed. The feeder electrode was made of copper, a good conductor, so the potential along the feeder will be uniform and equal to the potential applied. The potential at the metal/solution interface will vary however because of the difference in ion concentration at the feeder electrode.

At the entrance of the bed, before any concentration changes occur, the bed may be likened to a planar electrode (i.e $E'_{(x)} = E'$) and for example for a 1.0M Copper ion solution ($E^{*}_{0} = E^{o} = +0.34V_{s.h.e.}$) where a potential of -20mV. has been applied to the feeder then,

$$E'_{(x)} = E^{*}_{o} + E = +340 + (-20) = 320mV_{s.h.e.}$$

At the top of the bed solution depleted in copper will be present and therefore the potential at the solution/metal interface will vary with respect to that at the entrance of the bed, i.e. $E'_{(x)}$ will have varied. Taking the Nernst equation

$$E^{*}_{o} = E^{o} - \frac{RT}{nF} \ln \frac{a_{Cu}}{a_{Cu^{2+}}}$$ where a is activity

which for convenience is usually taken to be

$$E^{*}_{o} = E^{o} + \frac{RT}{nf} \ln . C_{Cu^{2+}}$$ where C is concentration

One may easily obtain E^{*}_{o} values for different copper ion concentrations.

For a given solution concentration,

$$E'_{(x)} = E^{*}_{o} + \frac{RT}{nF} \ln . C_{Cu^{2+}}$$

and a decrease in the copper ion concentration will cause a decrease in $E'_{(x)}$. Thus in the fluidised bed the decrease in copper ions up through the bed will cause a decrease in the potential through the bed $E'_{(x)}$; $E'_{(x)}$ at the top of the bed will be more negative than $E'_{(x)}$ at the bottom of the bed under an applied potential as,

$$E = E'_{(x)} - E^{*}_{o}$$

and at the bottom of the bed

$$E = E'_{(B)} - E^{*}_{o}$$

whereas at the top of the bed

$$E = E'_{(T)} - E^{*}_{o}$$

and because the activity of copper ions will be less at the top of the bed than at the bottom because of the deposition reaction in the bed, $a^{T}_{Cu^{2+}} < a^{B}_{Cu^{2+}}$, then

$$E'_{(T)} < E'_{(B)}$$

This means that the polarization at the top of the bed will be greater than at the bottom. Further, as the potential on the feeder is increased during a potentiodynamic sweep, the deposition current will increase. Electrolyte entering the bed will remain of constant concentration equal to the bulk concentration of solution; however the higher deposition current imposed by the higher potential at the feeder will cause a steeper concentration gradient in the bed and therefore a steeper potential gradient up through the bed. The relative potentials between the top and the bottom of the bed will diverge and the local potential at the top of the bed will become

more negative.

The maximum potential difference through the bed should occur at the top of the bed once the top of the bed has reached its limiting current potential. It might be considered that electro-potential changes at the top of the bed should now only be governed by changes in potential of the feeder and that the gradient in the bed will decrease as the potential on the feeder increases until all of the bed reaches the potential established at the top and that a limiting current will now be observed. However, if the top of the bed limits this implies that the potential gradient through the rest of the bed will become steeper in that the gradient will be acting through a smaller bed height(equal to the total bed height minus that volume which has limited). Because of the effects of a progressively increasing potential gradient in the bed due to the increasing potential on the feeder electrode and a steeper potential gradient over an increasingly small volume of the bed once the top of the bed limits, it is unlikely that limiting current data will ever be available from this type of fluidised bed.An additional factor which will make the observation of limiting currents even less likely is that at the top of the bed,where the current has limited, the potential on the feeder electrode will still be increasing continually as the electrode is being potentiodynamically swept and this extra potential can push the local potential at the top of the bed into the hydrogen evolution domain. Once this has happened no limiting currents will be observed because they will be masked by the hydrogen reaction.(In fact although the top of the bed may

be of a sufficiently negative potential for the hydrogen reaction to occur, the rest of the bed may not even have limited).

It has already been suggested that there is a potential gradient through the bed. If this is the case then hydrogen should evolve first from the top of the bed, In all experiments using the fluidised bed burnt deposits characteristic of limiting currents were always first noted at the top of the bed, by the feeder electrode, and hydrogen evolution always first became apparent at the top of the bed next to the feeder.

From the foregoing discussion it is apparent that concentration and concentration gradients within the bed play a major role in the electrochemical behaviour of the bed. The ideas put forward may be substantiated by looking at the effect of changes made in the bulk electrolyte. It has been suggested that concentration gradients up through the bed cause differences in the electrode potential of the bed. The equilibrium potential of copper E_o^* is determined by the initial quantity of copper ions in the electrolyte. The major effect of changing the electrolyte concentration will be to change the value of E_o^*. This value will become more positive as the electrolyte concentration is increased, and more negative as it is decreased. Returning to the polarization equation

$$E = E'_{(x)} - E_o^*$$

if E_o^* becomes more positive (by using a more concentrated electrolyte) then the variation between E_o^* and $E'_{(x)}$ can become greater before the limiting current is reached. This means that the overpotential E at the top of the bed will be greater and thus the potential

gradient in the bed will be steeper during a potentiodynamic sweep. In the reverse case where the value of E_o^* is less(using a dilute solution the variation between E_o^* and $E'_{(x)}$ will be less and thus the potential gradients in the bed will be smaller. In the ultimate case when the solution is made dilute enough that it limits before concentration gradients become established, or have any real effect anyway, then all the bed will polarize at approximately the same potential and some limiting currents may be observed.(The potential at the top of the bed will be very slightly more negative than at the bottom but because all, or nearly all,the bed will have limited at a potential too positive for the hydrogen reaction to be observed limiting currents will show up).

The ideas just discussed will show up in polarization curves in the following manner:-

1) At a given overpotential as shown by the potentiostat, currents will increase as the bulk electrolyte concentration increases.
2) The increased polarization at the top of the bed in a more concentrated electrolyte means that hydrogen will evolve at a smaller apparent overpotential in more concentrated electrolytes than in dilute ones.
3) The increased polarization at the top of the bed over the bottom in a given electrolyte means that hydrogen will evolve from the top of the bed first.
4) The increased current deposition obtained,at a given apparent overpotential,from more concentrated solutions means that potential gradients are steeper in more

concentrated solutions than dilute ones.

8.2.4 Other Effects.

(1) Bed Height: The potential gradient set up in a bed during a potentiodynamic sweep forms over the whole length of the bed provided that none of the bed has limited. The current which is drawn at any point in the bed will determine the quantity of copper available for deposition further up the bed. For larger beds more deposition will occur as electrolyte flows up through it simply because of the size of the bed. Electrolyte flowing out of the top of a tall bed will be less concentrated, under similar flow conditions, than electrolyte flowing out of a small bed. Necessarily therefore the potential between the top and the bottom of a tall bed will be also greater.The bed will be more polarized and hydrogen will be observed at smaller apparent overpotentials in larger beds.
(2) Concentration. For more concentrated electrolyte solutions, at a given apparent overpotential, the currents drawn at a given point in the bed will be higher than for dilute solutions because at any given local potential concentration polarization will be less pronounced in the bed(given that concentration polarization starts having a small effect any time after 1/10th of the limiting current for that concentration has been reached). The higher currents will enhance polarization in the bed with hydrogen coming off at lower overpotentials.
(3) Bed Porosity. The porosity of the bed is determined by the rate of electrolyte flow through the bed. For a given porosity steeper potential gradients occur in more concentrated electrolytes and

therefore currents are higher at a given overpotential. As copper deposits throughout the bed the surface roughness ,and therefore probably the electrolyte's turbulence as well , will increase. The number of contact sites between particles will change. It has already been shown that the contact contribution between particles is more important than the degree of electrolyte's turbulence(section 8.2.1). It also seems more likely that the resistance changes in the bed caused by the deposition of metal will also be more important than the way the deposition affects the electrolyte's turbulence within the bed. The extra contact sites caused by deposition(plates 6-16) will probably lower the resistance in the bed(which is equivalent to having a bed of lower porosity), and this will increase the effective electrode area of the bed and thus the current in the bed, The larger currents will then increase the potential gradient in the bed; the bed will become more polarized. Currents produced by the more concentrated electrolytes are larger than those produced by the dilute ones therefore more contact sites will be produced when the more concentrated electrolytes are used. Thus more concentrated electrolytes will enhance any decrease in the bed resistivity and by the higher currents produced will increase the polarization in the bed. Hydrogen evolution will therefore be observed at smaller apparent overpotentials in more concentrated solutions.

4) The Hydrogen Reaction. The evolution of hydrogen on a bed of copper particles using 0.5M H_2SO_4 electrolyte in which no copper ions are present is shown in figures 61 - 63. Hydrogen evolves at lower potentials than it does on a planar electrode(fig. 36), but at higher potentials than when copper ions are present in the solution(e.g. fig.52 -54). The reason for this behaviour is thought

to be twofold:(i) The evolution of hydrogen from the bed will cause a small polarization up the bed which will slightly reduce the potential at which hydrogen is observed from the top of the bed (compared to that at a planar electrode),also the amount of hydrogen coming from the bed because of the bed's surface area will mean that hydrogen will be observed slightly earlier than on a planar electrode. (ii)The evolution of hydrogen will occur at higher potentials than when copper ions are present in the solution because there will be no copper ions to preferentially polarize the bed, or to increase the surface roughness of the particles in the bed and thereby also further polarize the bed.

5) Sweep Rate. In point three of this section(bed porosity) it was suggested that the longer that copper was depositing in a fluidised bed, the more the bed would preferentially polarize, because the resistance of the bed would be continually changing thus affecting the potential gradients in the bed.If this is the case the rate of change in potential on the feeder electrode during a potentiodynamic sweep will be important because if the sweep rate is very fast then the reaction will not reach equilibrium at any given potential, but if it is slow the copper depositing from the bed will affect the resistance of the bed and preferentially polarize the bed. Polarization curves will therefore not only be a function of copper ion concentration but also of sweep rate.The effect of sweep rate in a fluidised bed is demonstrated in figure 29.

6) Reuse of the bed. Figure 70 shows the effect of reusing the bed for more than one potentiodynamic sweep(see section 7.4.8).The

results are unusual and probably reflect the effects caused by surface roughness produced in the bed in the previous experiment and also the unstable flow of the electrolyte because of the roughness and/or agglomeration of particles in the bed.

7) Low Copper Concentration in the Bed. When a very low copper ion concentration was used in the electrolyte i.e. 10^{-5}M then some limiting currents were observed in the fluidised bed(fig. 64 - 66). The fact that these limiting currents were observed suggests that the copper ion concentration was so low that the bed limited before concentration gradients in the bed could have much effect on preferentially polarizing it.(see section 8.2.3)

8) Corrosion Effects. A number of authors have found that in a fluidised bed, particularly at low overpotentials, some of the bed is not protected and parts of the bed corrode(100,113,114).In the bed used in this study it is believed that these effects could occur at porosities where the bed is still active but when not all the bed is active. In this instance a number of particles will be touching each other for a short period of time whilst not in contact with the feeder. For a group of particles in this situation particles at one end of the group could well be in contact with solution of a different concentration to particles at the other end of the group. A concentration cell will be established for a short period of time. Particles in the more dilute solution will then be anodic, and thus corrode, whilst particles in the more concentrated solution will be more cathodic and copper will deposit. The anodic part of the cell will be higher in the bed because solution of a lower concentration will be found there.

9)Apparent Overpotential. The potential of the working electrode is maintained with respect to a non-polarizable electrode(e.g. saturated Calomel electrode) with the aid of a potentiostat. An overpotential on the working electrode is maintained,or applied, by allowing current flow through the potentiostat to the secondary electrode,until the required potential is achieved at the working electrode. For the fluidised bed electrode,because of the concentration gradients set up, a whole range of potentials are acquired,although the feeder will be measuring only a small potential change with respect to the original potential set up on the feeder before current was passed. The overpotential on the feeder will therefore be indicative of the potential in the bed with respect to the original solution/metal potential whereas the potential at the top of the bed will be much more negative with respect to this. The overpotentials measured for polarization curves are therefore really only 'apparent overpotentials' reflecting the overpotential of just a small volume of the bed and with respect to this overpotential hydrogen will appear to be given off at extremely low overpotentials.

8.3 Apparent Potential/time Polarization.

The experiments carried out for various time periods under a constant 'apparent overpotential' gave results where the current varied with time. This would be unusual for a planar electrode but considering the effects of concentration and time on the potential gradients in a fluidised bed as discussed previously it is perhaps not unusual for this electrode. Figure 71 shows the 'constant potential' time polarization curve for 0.7M Cu^{2+} electrolyte. Samples were

removed from the bed during these runs to determine how particles were growing in the bed.To do this the electrolyte flow in the bed had to be halted once the potential on the bed had been removed. It is noticeable from the figure that on restarting the flow again in the bed after the sample had been removed and after the potential had been reapplied to the bed, that the current is always less than the value it had been before the sample was removed. There was of course a slightly smaller amount of copper particles in the bed, but the amount of copper particles removed would not be sufficient to cause the current decrease.(0.1% of the bed was removed). Although the reason for this current decrease is not known, some factors which might have been important are (i)The particles- In the fluidised state the particles which have become slightly roughened due to deposition will perhaps interlock together and decrease the resistance of the bed.When electrolyte is no longer flowing through the bed the particles will settle on the porous membrane and many of the optimum interlocking points will be disrupted, Upon refluidisation of the bed, the bed will now have a greater resistance than it had before the electrolyte flow was stopped and lower currents will ensue.(ii) Concentration effects- Before a sample was removed from the bed there would be a concentration gradient in the bed polarizing the bed. Once the potential was removed from the bed and the electrolyte flow had been stopped, any concentration gradient would have time to equalise out. On restarting the experiment a finite time would be needed for the concentration gradient to become reestablished and until this had happened the current in the bed would be less than that before the sample was removed from the bed.

8.4 Other Considerations.

Cell design in highly industrialised countries is usually a compromise between capital costs and power consumption costs. In view of this a lot of development time has been spent on upgrading electrochemical systems which have already proved themselves, as, for instance, in the electrolysis of brine to chlorine, by decreasing the power losses and increasing the cell capacity. As the kinetic limitations of cells have been realised a number of mass transport correlations have evolved incorporating many cell geometries(110). In particular the effect of cell agitation has been considered in relation to cell design. It has been recognised that in order to obtain good electrodeposits one can only operate within a certain percentage of the limiting current(e.g 0.4 in the case of the rotating cylinder(3)). If the limiting current can be increased however, then so can the operating current. This current increase may be achieved by (i) raising the electrolyte concentration, (ii) increasing the temperature of operation, (iii) reducing the diffusion limitations of the system. If only because of solubility considerations and temperature considerations (i.e. the solubility limit, and the boiling point of the electrolyte) the first two of these methods are very limited.

Reduction of the diffusion layer has been widely studied using methods of forced agitation(115 - 119), although some systems such as in copper refining have achieved a modicum of stirring by promoting the natural convection in the system caused by electrolyte density differences in the electrode vicinity. Ibl has stated that

a typical metallurgical bath containing 0.6M copper sulphate in 1.5M Sulphuric acid gives limiting currents under natural convection in the range 0.5 - 2kA/m^2 whereas if forced convection is also used currents upto 100kA/m^2 can be achieved(120). This shows that although natural convection may improve cell performance, to achieve high currents forced convection is required. Artificial stirring, however brings its own problems; it raises the permissible operating current but also raises the power losses in the cell P.L. = I^2R) Apart from this the cost of stirring itself is important. It is always necessary to balance any saving in labour cost achieved by higher cell performance with the increased cost of power and wear to the system when artificial stirring is used.

The use of artificial agitation is always dependent upon the economics of the situation and any method that is used will nearly always be the one which will provide the cheapest form of stirring. The use of gas bubbling or sparging as a form of stirring is important because although it doesnot decrease the diffusion thickness very much(δ = 0.1 - 0.2mm for copper(120)) costs are also low. Gas bubbling from the electrode also decreases the diffusion layer and can produce values for of 0.02 - 0.03mm (= 20kA/m^2) which are probably about as small as can be achieved by most methods of mechanical stirring. However this type of gas evolution decreases the efficiency of the reaction, increases power wastage and causes a deterioration of the product. In cases where gas is evolved from the anode, such as in electrowinning, the gas creates its own turbulence and no extra agitation is required.

Other systems in which artificial stirring is employed are generally ones which mechanically move the electrode with respect to the solution or vica versa. In an attempt to compare power costs for these type of systems Ibl(120) has compared power costs at similar limiting currents for the rotating disc, the rotating cylinder and a pumped flow cell(fig.75). In all cases as the limiting current required is increased so also do the power costs increase and thus the range for increasing currents is small because of the extra power and capital costs required to achieve them.

8.4.1 Scaling-Up.

In the application of electrochemical processes one of the main difficulties is scaling-up of the process. The surfaces at which electrochemical reactions occur are the electrodes and it is these that determine the capacity of the cell. Because of the dependence of cell capacity upon electrode area not very much scale-up advantage can be achieved by conventional planar electrodes. Problems in scale-up of planar electrodes are mainly concerned with:-

(1) The voltage drop across the cell

(2) The cell resistance

(3) The current density

The voltage drop across the cell consists mainly of the electrolyte resistance and the resistances due to the polarization of the anode and the cathode. Assuming that the activation potential of the reaction is minimal then the scaling-up procedure can be considered

under the headings of

(1) Ohmic resistance in the cell

(2) Convection control

The first of these will follow Ohm's law and assuming operation at constant current and voltage ,the resistance should be similar. The result of scale-up on the convective control of the system will be to change parameters affecting the concentration overpotential of the system. It is not easy to determine the effects prior to scale-up and consequently an empirical approach,using dimensionless analysis to determine what factors most affect the mass transfer of the system, is often carried out on a small scale. Values of current can then be determined using correlations such as

$$i = k.(Gr.Sc)^{a}(d/r)^{b}$$

where k is a constant, d is the electrode length, r is the electrode separation and Gr and Sc are the dimensionless groups(see table4). A typical correlation of this sort for the flow of electrolyte up an empty tube is given in section 9.2.

Because not much advantage is achieved in the scale-up of the above cells in terms of space, more modern cells have been produced which act in a three dimensional mode ,are therefore very compact and save a lot of cell space compared to the above cells. The particular advantage of such cells is the high current/ low cell volume principle on which they operate. Such cells are the porous bed, the restrained bed and the fluidised bed.

The determination of the problems associated with these three dimensional type cells such as the fluidised bed cell is not easy, because as well as having the problems that planar cells

encounter during scale-up they also have extra problems associated with the extra dimension of the cell. The fluidised bed suffers particularly in that it is not a continuous electrode. The ohmic resistance of the cell requires an extra term ρ_m which will be equal to the resistance of the bed. It has already been shown in section 8.2 that this resistance cannot be easily disregarded, and cannot be easily accounted for in bed scale-up(e.g it has a maximum effectiveness over only 10mm in one direction in the bed). In fact the results of the fluidised bed suggest that scale-up of the bed will only be effective when current flow and electrolyte flow are perpendicular. Against this scale-up perpendicular to the bed causes potential distribution problems in the bed. It might be preferable therefore to have a number of small fluidised beds rather than one large one; a proposal originally supported by Backhurst(90). In this way potential gradients in the bed could be reduced, or at least minimized.

It is not only the fluidised bed which has scale-up problems. For instance there is the porous bed. This does not have the same resistance problems as the fluidised bed because the electrode is a continuous metal matrix, but it suffers problems such as localised pH changes in the electrode pores and fast methods of removing reaction products from the electrodes. Potential gradients in the bed are still a problem, perhaps even a greater one than for the fluidised bed and the size of the electrode may often be limited by the potential gradient that will form between one end of the cell and the other. Bennion and Newman have discussed the removal of copper

using a porous bed(121) and have shown hydrogen evolution in the bed, caused by the potential gradient in the bed,to be a limiting factor.

For all the inherent limitations of the modern electrodes which have to be overcome they do usually have good performance compared to planar cells and are generally superior in comparison. Kuhn and Houghton have compared the restrained bed cell with four other non-three dimensional cells, the inert fluidised bed, a parallel plate cell, an expanded mesh cell, a parallel plate cell packed with Netlon. In terms of removal of antimony the restrained bed was almost an order of magnitude better than the other cells, reducing the level to 5 p.p.m.. This demonstrates the effective removal of ions that modern cells can achieve by virtue of their large electrode surface area and the low current densities required by these cells to operate at reasonable current levels.(125)

Future Application of Modern Cells.

Modern cells , which one can classify into two types, are generally used in and/or create turbulent flow conditions in the cell.The main difference between the two types is in the principle on which they operate. One type (I) operates in a purely agitational mode and decreases the diffusion boundary layer by causing electrolyte turbulence around the electrode. The other type (II) also decreases the diffusion layer around the electrode, but it also works on a small volume/high surface area principle by being a very large surface area electrode. The inert fluidised bed is a type I electrode and the conducting fluidised bed is a type II electrode. Both electrodes

have possible industrial outlets although many of the areas where each type will be used will not necessarily be similar.

In electrorefining an impure anode is corroded whilst purified metal is deposited on the cathode. Under normal operating conditions the cell voltage and therefore power consumption is lower than in all other forms of electrolysis; this industry is therefore more able than most to tolerate higher operating currents without power losses making the process unviable. The increased currents obtainable from modern electrodes may thus be used to advantage. One problem is that a good surface finished product is often required and many of the modern cells are not designed to give this. One that is however is the inert fluidised bed. The use of inert material in this cell results in uniform and intense agitation at the electrode/electrolyte boundary and creates enhanced mass transfer rates in this region. The fundamental effects of the continual bombardment of particles at the cathode surface is as yet unknown but the macroscopic effects have been observed. Vergnes(122) et alia have demonstrated that the deposit of nickel from a fluidised bed gives a surface finish comparable to that of conventional cells when only 20 - 50% of the brightening agent is used(butyene-1-4-diol) and when the limiting current is five times higher than that normally found. Other workers have also found that the fluidised bed tends to give better quality deposits(78,123, 124) and suggest that this relates to better current distribution over the electrode with the rapid removal of hydrogen bubbles from the electrode surface. In particular Le Goff has studied the formation of lead dioxide on graphite anodes. Using a fluidised bed the copper cathode remained clean and black dense and highly adherent deposits of lead dioxide

formed on the graphite. In the absence of such a bed lead was found to deposit on the cathode, and a non-uniform pitted deposit formed on the graphite. These results are interesting and perhaps could be followed on in areas where hydrogen evolution is a problem and plating itself is difficult e.g. in the plating of chromium or the platinum metals.

In electrowinning electrodes of type II will probably be more successful than the others because with their high surface area of electrode they will be able to deal with a high throughput of dilute solution . Perhaps the main advantage will go to cells like the conducting fluidised bed which can operate on a continuous basis rather than those which operate on a batch process. In particular the treatment of leach liquors from in situ leaching sites might become viable. At the moment these sites are treated by methods such as cementation ,ion exchange and solvent extraction methods.

Fuel cells are becoming more important today as methods of storing and controlling stored energy are being explored. An important requirement of fuel cells and batteries is a large area per unit volume so type II electrodes would appear to be ideal in this situation. A number of authors have investigated this field(97, 98) and it has become apparent , in the case of the fluidised bed, that it is more effective as a cathode than as anode. A major reason is that the bed particles oxidise very easily when they are used as an anode. This rapidly increases the resistance in the bed and power costs become very high.

Goodridge has pointed out that there are a number of opportunities for the conducting fluidised bed in electrosynthesis(91) although this must extend to all type II electrodes. Many organic compounds have been produced in the laboratory on a small scale by electrolysis , but the method usually cannot be produced on a large scale because of the high activation potential requirements of the reaction. Because of the high potentials required for the reaction and the high currents required to make a process feasible industrial cells have to dissipate heat away very quickly as organic reactions tend to be very temperature sensitive. Electrodes such as the fluidised bed overcome the problems of most other cells in this field because only a low overpotential is required at the electrode to produce high currents (albeit at a very low current density) and heat transfer away from the electrode is excellent. It is important to note , as Goodridge points out, that the replacement of a chemical step by an electrochemical one is unlikely to be of any real advantage unless it is accompanied by the reduction or elimination of the use of an expensive catalyst.

In recovery and effluent control it is difficult to decide whether the high agitation or the high surface area electrodes will find more use. Industrial effluents containing metal finishing wastes are toxic, corrosive and harmful. Due to the renewed interest in pollution control these wastes must now be pretreated before dumping into sewers. Many methods of removal of metals from waste waters are in operation. Ion exchange methods are quite widely used as a means of concentrating metal ions so that they can be reclaimed by other methods and alkali oxidation with hypochlorite is used widely in the destruction of cyanide wastes.

Using modern cells concentration of effluent metals can be achieved by the mesh electrode, the swiss roll electrode and the porous bed electrode in a batch process and for instance by the fluidised bed electrode, both conducting or inert, or the Eco-cell in a continuous process. The amount of copper recovery in Great Britain would not make development of any of these cells economic (< 10 tonnes/year) in a commercial sense, but as stricter methods of control are levied against industry some of them are bound to be considered. For this reason it will probably be the cells which can reduce metal concentrations to a very low level that will become important, providing of course that they can deal with a high throughput of waste solution. An extra advantage will be if they can separate metals during treatment. Of the cells available the ones that seem to be the most efficient at metal recovery from solutions containing 5 p.p.m. or less are the extended mesh electrode and the swiss roll electrode. In U.S.A. the quantity of metal effluent discharged is higher than in Britain e.g. in New York 250 Kg Cu, 160 Kg Cr(6^+), 500 Kg Ni, and 320 Kg Zn are discharged every day of which 85% is treated. The possibility of using the above electrodes in this situation would be even more favourable than in Britain and even without legislature being implemented necessitating trying them out an economic method of waste treatment may be possible.

The future role of modern electrodes is likely to be diverse: each have their own advantages and disadvantages. In particular the swiss roll electrode is good at treating very low concentration

solutions and may be the successor to ion exchange methods in the treatment of effluents. The porous electrode has already been used in fuel cells and is likely to become more firmly established. The inert fluidised bed must surely have some outlets in electrorefining as must the conducting fluidised bed in electrowinning and organic synthesis, provided that potential distribution problems in the bed can be overcome in the latter case. Perhaps it is finally worth noting some observations about electrolysis in general which apply equally to old and new cells alike.(120)

1) An important factor in any electrolysis is optimisation of the current density.

2) Increases in current density imply increases in power costs but a corresponding decrease in required capital investment.

3) An optimum current will therefore be achieved which will be a minimum for the total of the investment costs and the power costs.

4) Assuming a linear relationship between current, voltage and investment cost and electrode area for a given product,one can use an equation for obtaining the optimum current density,

$$i_{opt} = a/bR$$

where R is the cell resistance $/m^2$, b is the investment price £/KWh and a is the specific investment cost $£m^2/h$.

5) typical values for a and R in copper refining are $£0.0025/m^2h$ and $6\ 10^{-4}\ m^2$, giving an optimum current density of $906A/m^2$.(1975)

6) In normal practise one operates at $200A/m^2$ ($i_L = 675A/m^2$ but one only obtains bad deposits) in natural convection. In forced convection keeping the same i/i_L ratio then the current can be increased

by a factor of 906/200 in a pumped flow plate cell under optimum conditions. The extra power required is about $5W/m^2$ or about £0.05/ton which is only about ten per cent of that consumed by electrolysis ($50W/m^2$). The saving achieved by the increased i_{opt} justifies the cost saving about £7/ton of Cu produced and demonstrates the effectiveness of forced convection.

9. MASS TRANSFER CORRELATIONS IN INERT FLUIDISED BEDS.

9.1 Inert Fluidised Bed Characteristics.

In a previous work, Carbin and Gabe(73) have discussed the effects of particle motion on the mass transfer rates of copper ions in a fluidised bed of silica spheres and have compared it with mass transfer rates in concentric annuli alone. Their results were correlated into a dimensionless equation of the form,

$$St = k\,Re^{a}.St^{b}$$

As shown in section 5.2.3 there has been some uncertainty in the past over the appropriate form of the Reynolds number containing the characteristic length of the system. Carbin and Gabe used the accepted relationship of a modified Stanton and Reynolds number with a porosity term included, i.e.

$$St = k.Re^{a}.Sc^{b} \qquad \text{where } Re' = \frac{U.dp'}{\nu(1-\epsilon)},\ St = \frac{K_m.\epsilon}{U}$$

and obtained the equation,

$$St_I = 1.22\,Re_I^{-0.524}.Sc^{-0.68}$$

which in terms of a limiting current gave,

$$i_L = 1.22\,n.F.C_b.(1-\epsilon)^{-0.52}.\epsilon^{-1.0}.U^{0.48}.\nu^{-0.16}.D^{0.68}$$

The data was processed using a Hewlett Packard desk top calculator model 1900 B, and the equation was solved by least squares regression analysis. There are three major problems inherent in using this method.

(1) There is no easy method of checking whether or not a mistake has been made whilst entering the data into the calculator i.e. there is no data print out and internal programme control.

(11) Cnce a wrong figure has been entered into the computer, it cannot easily be removed and replaced, and all the data has to be reprocessed.

(111) In the method of least squares analysis logs of the data had to be taken(Appendix I) and because in the case of the Schmidt number

the number of different data results were small, the Schmidt numbers for these numbers ,when logged, were very similar. This similarity would allow errors to creep into the least squares analysis of the data.

Due to the above limitations of the desk top calculator the scope for error during data processing was large, the data has therefore been reprocessed on a larger I.C.L. computer. Even in this situation, because of the small variations in Log Sc, round up errors from the computer may have affected the correlation. An assessment of the correlation however does show that it is more accurate mathematically than the Carbin correlation. The results of this assessment are given below and a computer programme for the correlation is given in Appendix I . Although the general equation

$$St_I = k.Re_I^a.Sc^b$$

is the most widely accepted, for the sake of completeness correlations using other modified Reynolds and Stanton numbers are also given.

Thus:-

$$St_I = 0.384\ Re_I^{-0.538}Sc^{-0.772}$$

is the new correlation (as compared to $St_I = 1.22.Re_I^{-0.524}Sc^{-0.68}$). The differences in the correlations is quite large and a computer check was therefore made on both correlations to determine their accuracy.

The ideal line for a two dimensional regression analysis plot is one on which all the points fit. In this case the square of the difference, in distance, between any point and the line of best fit is zero. In most analysis the line of best fit does not pass through all points and the line of best fit is the one where the

square of the distance between the points and the line are kept to a minimum. In the above situation,although it is a three dimensional analysis,a similar situation applies but in this case the square of distances between points and a plane are taken as the minimum value required. Taking the two correlations the square of the differences between the line of best fit and the experimental data is,

1) 0.802332×10^{3} Carbin analysis.

2) 0.975609×10^{1} New analysis.

showing that this later correlation is a much more accurate representation of the data. The new correlation is therefore,

$$St_I = 0.384\ Re^{-0.54}.Sc^{-0.77}$$

and $$i_L = 0.38\ n.F.C_b.(1 - \epsilon)^{-0.54}\epsilon^{-1.0}U^{0.46}d_p^{-0.54}\nu^{-0.16}D^{-0.77}$$

Correlations assuming other Reynolds numbers and Stanton numbers which have been modified (see section 5.2.3) give,

$St = 0.87\ Re_I^{-0.63}.Sc^{-0.84}$ Chu correlation
(Analysis error = 0,41 10^2)

$St_I = 0.64\ Re_{III}^{-0.67}.Sc^{-0.87}$ Leva- 2nd correlation
(Analysis error = 0.247 10^2)

$St = 0.822\ Re_{II}^{-0.71}.Sc^{-0.91}$ Leva- 1st correlation
(Analysis error = 0 395 10^2)

9.2 Flow with no bed.

Results published by Carbin and Gabe were subject to some scrutiny by Wragg(69). The results reported electrolytic mass transfer measurements between flowing electrolyte and a cylindrical electrode positioned with its axis in the flow direction.(See also sections 6.3.1 and 6.3.2). The results were correlated by

$$Sh = 3.93\ Re^{0.32}.Sc^{0.33}(d_e/l)^{0.35}$$

where the characteristic length was taken as the equivalent diameter of the annulus. This equation was derived from another equation given by Carbin and Gabe as

$$Sh = 3.93\ Sc^{0.33}Re^{0.32}$$

Wragg expressed doubts about the validity of the first of these two equations in that by introducing the length to diameter term the constant in the equation must surely change from that as expressed in the second equation. In fact the above equation had a printing error and the equation originally derived is

$$Sh = 2.93\ Re^{0.32}.Sc^{0.33}(d_e/l)^{0.35}$$

Carbin and Gabe compared this correlation with that of other authors(23,33,71) which Wragg suggests is not meaningful in that the flow conditions are not similar, Although the comparison was given the dissimilarity in flow conditions had been noted previously (76).

Wragg suggests that because hydrodynamic flow had not fully developed in the above experiments a more meaningful analysis might be obtained by treating the data in a similar fashion to that of a plate in developing heat transfer flow. This leads to a solution where the characteristic length for the Reynolds and Sherwood number is taken as the length of the leading edge of the sample. Using this as the characteristic length the following correlation is obtained, (fig. 76).

$$Sh = 2.253\ Re^{0.316}Sc^{0.33}$$

CONCLUSIONS

1. The particle-particle contact resistance in a fluidised bed is of prime importance in the cell's efficiency of operation. Bed expansions of $< 25\%(\epsilon < 0.5)$ are required if the cell is to act efficiently and, the current capacity of the cell increases as the porosity of the bed decreases.

2. Above 25% bed expansion the fluidised bed acts more as an agitation promoter for the feeder electrode than as a fluidised bed cell. This behaviour becomes more pronounced as the bed porosity is increased.

3. Scale-up of the bed parallel to current flow is limited by the distance of particles from the feeder electrode. To prevent some parts of the bed from becoming inactive particles must be kept within a zone of one cm. radius from the feeder electrode.

4. Scale-up of the bed perpendicular to current flow is limited by potential gradients within the bed. A maximum is reached when a secondary reaction starts occurring, at the same time as the primary reaction, even when the overpotential on the electrode is low.

5. The potential distribution in the bed generally prevents limiting currents from being observed.

6. Concentration gradients in the bed cause potential distribution problems and allow corrosion to occur at inactive sites in the bed.

7. There are possible future applications for the fluidised bed in the electrowinning industry. There are still many problems to be overcome however before this cell will be useful as its operation at the present time is too complex.

8. A reassessment of some mass transfer data obtained by Carbin and Gabe(73,76) in an inert fluidised bed gave the following correlation:

$$St_I = 0.38.Re^{-0.54}.Sc^{-0.77}$$

9. A reassessment of mass transfer data for electrolyte flow through an annulus(73,76) using a Reynolds number and a Stanton number based on the leading edge of the sample rather than on the annulus equivalent diameter gave:

$$Sh = 2.25.Re^{0.316}.Sc^{0.33}$$

LIST OF SYMBOLS

a	Specific investment cost £ m^2/h.
A	Area
α	Activity of element.
b	Investment price £/KWh.
C	Concentration.
C_b	Bulk concentration.
C_D	Drag factor.
C_s	Concentration at the surface of an electrode.
D	Diffusion coefficient.
dc/dt	Change in concentration with time.
dc/dx	Concentration gradient.
d_e	Annulus equivalent diameter.
d_m	Stable bubble diameter.
d_p	Particle diameter.
d_s	Solid's diameter.
D_v	Container diameter
E	Overpotential
E'	Metal/solution potential.
E'(B)	Local potential at the entrance to a fluidised bed.
E'(T)	Local potential at the top of a fluidised bed.
E'(x)	Local potential at a particular point in a fluidised bed.
E^o	Standard electrode potential.
E_o^*	Equilibrium potential.
F	The Faraday constant(96,540 coulombs).
Fr	The Froude number.
g	The acceleration due to gravity $9.8ms^{-2}$.
Ga	The Galileo number.

h	Electrolyte thickness.
I	Current.
I_m	Current capacity.
i	Current density
i_L	Limiting current density.
i_{opt}	Optimum current density.
J	The diffusion flux.
k	A constant.
K'	A shape factor.
K^*	A shape factor.
K_m	Mass transfer coefficent.
L	Length.
l	Characteristic length.
L_{ent}	Entry length.
L_h	Bed height.
m	A number.
n	A number.
P	Pumping energy.
ΔP	Pressure drop.
R	Cell resistance.
Re	Reynolds number $U.l/\nu$
Re_I	Modified Reynolds number $U.d_p/\nu(1-\epsilon)$
Re_{II}	Modified Reynolds number $U.d_p/\nu$
Re_{III}	Modified Reynolds number $U.d_p/\nu.\epsilon$
Re_t	Terminal particle Reynolds number $U_t.d_p/\nu$
N_{Re}	Reynolds number based on channel width.

S	Surface renewal factor.
Sc	Schmidt number /D.
Sh	Sherwood number $K_m.l/D$.
St	Stanton number K_m/U
St_I	Modified Stanton number K_m. /U.
t	Transport number.
T	Temperature
U	Free flow velocity.
U_i	Sedimentation velocity.
U_{mf}	Minimum fluidisation velocity.
U_s	Slugging velocity.
U_t	Terminal particle velocity.
x	A direction(e.g. the diffusion direction).
γ_s	Young's modulus.
δ	Diffusion layer thickness.
δ_c	Diffusion layer thickness.
δ_u	Prandtl boundary layer thickness.
ϵ	Bed porosity.
ϵ_{mf}	Porosity at bed fluidisation.
η, η_p	Overpotential.
θ	Solution packet residence time.
μ	Fluid dynamic viscosity.
ν	Fluid kinematic viscosity.
ν_p	Free particle velocity.
ρ_f	Fluid density.
ρ_s	Solids density.
ϕ_M	Metal potential.
ϕ_s	Sphericity factor.
ω	Angular momentum .

1. Surfleet B. and Crowle V.A., Trans. Inst. Met. Fin. 1972 50 227-232

2. Robinson D. and Gabe D. R., Trans. Inst. Met. Fin. 1970 48 35-42

3. Robinson Ph.D. thesis University of Sheffield 1970

4. Rudge A.J., Chapt.1 'Industrial Electrochemical Processes' Ed. Kuhn A.T. 1-65 Elsevier, Amsterdam 1971

5. Rudge A.J., Chapt. 2 ibid. 70-88

6. Cooke B.A., Ness M.N. and Pallvel A.L.L., ibid. 417-465

7. Levich V.G., 'Physico-chemical Hydrodynamics' Prentice-Hall 1962

8. Kuhn A.T., J. Appl. Electrochem. 1974 4 173-190

9. Schreiber M.L., J. Soc. Motion Picture Engrs. 1965 74 505

10. Garbutt F.E., U.S. Patent 1,866,701 1931

11. Ibl N., Chem. Ing. Tech. 1963 35 353-361

12. King J.S., J. Electrochem. Soc. 1955 102 193

13. Beck F. Electrochim. Acta 1973 18 355

14. Tobias C.W., J. Electrochem. Soc. 1959 106 833

15. Fainstein L.B., MAMAKOV A.A., ELEKTRON OBRAB MATER 1970 50

16. see ref. 8

17. Kuhn A.T., Chem. and Ind. May 1st 1971

18. Beck F. and Guthke H., Chem. Ing. Techn. 1969 41 943-950

19. Eisenberg M 'Advances in Electrochem.and Electrochem. Engng.' Vol. 2 Ed. Delahay P. Interscience New York 1962

20. Goldstein S., 'Modern Developments in Fluid Dynamics' Vol 1 319 Oxford University Press 1952

21. Schlichting H., 'Boundary Layer Theory' (translated by Kestin J.) 2nd edition McGraw and Hill 1960

22. Leveque M., Ann. Mines 1928 13 (12) 381

23. Ross T.K. and Wragg A.A., Electrochim Acta 1965 10 1093

24. Le Goff P. Vergnes F. Coeuret F. et al., J. Electrochem. Soc. 1973 120 140C abstract 246

25. Surfleet B.R. 'Symposium on Electrochemical Treatment of Effluent' 1973 April University of Salford.

26. D. O. S. 1,917,43 (Application 11/11/1968) German Patent.

27. Adams R.N., 'Electrochemistry at Solid Electrodes' Marcel Dekker New York 1969

28 Taylor G.I. Phil. Trans. Roy. Soc. London 1923 A223 289

29. Flower J.R. Macleod N. Shahbenarian A.P., Chem. Eng. Sci. 1969 24 673

30. Gabe D.R. and Robinson D., Electrochim. Acta 1972 17 1121

31. Kappesser R., Cornet I. and Grief R., J. Electrochem. Soc. 1971 118 1957-1959

32. Gabe D.R. J. Applied Electrochem. Soc. 1974 4 91

33. Arvia A.R. Carozza J.S.W., Electrochim Acta 1962 7 65

34. Colquhoun-Lee I. Stepanek J.P., Chem. Eng. London 1974 282 108

35. Houghton R.W. and Kuhn A.T, J. Appl. Electrochem. 1974 4 69-73

36. Armstrong R.D. Brown C.R. Giles R.D. and Harrison J.A., Nature 1968 219 94

37. U.S. Patent 3,180, 810 1965

38. German Patent 954,056 1956

39. Chu A.K.P. and Hills G.J., J. Appl. Electrochem. 1974 4 324-336

40. Bennion D. and Newman J., ibid 1972 2 113-122

41. Nanis L. Mclarnon F., J. electrochem. Soc. 1970 117 157-159

42. Backhurst J.R. Fleischmann M. and Goodridge F., Brit. Patent application 23,070 1966

43. Flett D.S. Chem. and Ind. December 16th 1972 983-988

44. Shchukarev Z. Phys. Chem. 1891 8 76

45. Nernst W. ibid 1904 47 58

46. Brunner J.A.V. 1904 47 56

47. Fage and Townsend Proc. Roy. Soc. London A135 1932 656

48. see ref. 7

49. Vielstich W., Z. Elektrochem. 1953 57 646

50. Prandtl L. and Taylor Phys. Zeit. 1910 11 1072
Prandtl L. ibid 1928 29 487

51. Von Karman J. Aero. Sci. 1934 1

52. Adams R.N. 'electrochemistry at Solid Electrodes ' Marcel Dekker New York 1969.

53. Higbie R., Trans. A.I.Che. J. 1935 31 365

54. Danckwerts P.V., ibid 1933 29 174

55. Toor and Marchello, ibid 1958 54 97

56. Leva 'Fluidisation' Mcgraw and Hill New York 1959

57. Kwauk and Wilhelm, Chem. Eng. Prog. 1948 44 201

58. Harrison D. and Davidson J.F., Trans. Inst. Chem. Eng. 1961 39 202

59. Richardson J.F. and Zaki W.N., ibid 1954 32 35

60. Storrow et alia, Chem. Eng. Sci. 1957 6 204

61. Ergun S., Anal. Chem. 1952 24 338

62. Herman de Groot 'Proc. symp. Fluidisation' Ed Drinkenberg A. 1967

63. Williams J. and Keating K. Dupont Innovation 1975 6(3) 6-10

64. D.O.S. 1,917,438 Application 11/11/68

65. Robertson P. Scholder B. Theis G. and Ibl N., Chem and Ind 1978 July 1st 459-465

66. Holland F.S., Chem and Ind. 1978 July 1st 453-458

67. Richardson J. and Zaki W., Trans. Inst. Chem. Engrs. 1954 32 35

68. C.R.C. 'Handbook of Chemistry and Physics' 56 Ed.

69. Wragg A.A., Electrochim Acta 1975 20 917

70. Jottrand R. and Grunchard., J. Appl. Chem. London 1952 2 Supplimentary issue 1 S17-S26

71. Coeuret F. Le Goff P. Vergnes F., Proc. Int. Symp. Fluidisation Eindhoven 1967

72. Jagannadharaju G.V. and Rao V.C. Indian J. Technol. 1965 3 201

73. Carbin D.and Gabe D.R., Electrochim Acta 1974 19 653

74. Brea F.M. and Hamilton W. Trans. Inst. Chem. Eng. 1971 49 196

75. see ref. 71

76. Carbin Ph.D. thesis University of Sheffield 1973

77. Coueret M.F. and Vergnes F., Chim. et Industrie, Genie Chemique 1972 15 1000

78. Le Goff P. Vergnes F. Coueret F and Bordet J., Ind. and Eng. Chem. 1969 61 10 8-17

79. Thangappan R. Nachiappan S. and Sampath S., see ref. 62 609

80. Chu J.C. Kalil J. and Wetteroth W., Chem Eng. Prog. 1953 49 141-9

81. McCune and Wilhelm, Ind. Eng. Chem. 1949 41 1124

82. Theones D and Kramers H Chem. Eng. Sci. 1958 8 251

83. Beek W.J., see ref. 62 507

84. idem 'Fluidisation' Eds. Davidson J.F. and Harrison D., Academic press Inc.(London) 1971 431

85. Parkash S. Lele P.S. and Das B.N., Indian Chem. Engr. 1968 January 3-8

86. Richardson J.F. and Szekely J., Trans. Inst. Chem. Engrs. 1961 39 212

87. Upadhyay S.N. and Tripathi G., J. Scient. Ind. Res. 1975 34 10-35

88. Tomasi W. and Houwalt A. Przemysl Chem. 1963 42 285-289

89. Backhurst Ph.D. thesis 1967 University of Newcastle

90. Backhurst J. R. Coulson J.M. Goodridge F. and Plimley R.E., J. Electrochem. Soc. 1969 1600-1607

91. Goodridge F., Chem. Proc. Eng. 1968 February 93-95, and 100

92. Gerischer Brit. Patent 1,098,837 (Shell)

93. Smith D.H. Chem. Processing 1969 15 4

94. Thangappan R. Uduppa H.U.K., Trans. of S.A.E.S.T. 1974 April-June Vol. 9

95. Hiddleston J.N. and Douglas A.F. Electrochim Acta 1970 15 431-443

96. Krishnamurthy R. Laslo J. Thangappan R. and Udupa H.U.K., 12th Seminar on Electrochemistry Karaikudi India May 1972

97. Berent T. Fells I. and Mason R., Nature 1969 223 1054-1055

98. Backhurst J.R. Goodridge F. Plimley R.E. and Fleischmann M., Nature 1969 223 55

99. Flett S., Chem and Ind. 1971 300-302

100. Flett S., ibid 1972 983-988

101. Wilkinson and Haines A.I.M.M.E. 1972 September C157-C162

102. Barker B.D. and Plunkett B.A., Trans. Inst. Met. Fin. 1976 54 104-112

103. Goodridge F. Holden D. Plimley R.F. and Murray H.D., Trans. Inst. Chem. Eng. 1971 49 137

104. Fleischmann M. and Oldfield J.W., J. Electroanal. Chem. 1971 29 211-230

105. Newman J. and Tobias C.W., J. Electrochem. Soc. 1962 109 1183

106. Fleischmann M. and Oldfield J.W., J. Electroanal. Chem. 1971 29 231-240

107. idem ibid 1971 29 241-253

108. Heiden van der G. Raats C.M. Boon H.F., Chem. and Ind. 1978 465

109. Kreysa G. Piontech S. and Heitz E., J. Appl. Electrochem. 1975 5 305-312.

110. Fleischmann M and Oldfield J.W. J. Appl. Electrochem. 1971 1 103-112

111. Arvia A.J. Bazan J.C. Carrozza J.S.W. Electrochim. Acta 1966 11 881-889

see also Milora C.J. et al. J. Electrochem. Soc. 1973 120 488-492

112. Selman J.R. Hsueh L. and Newman J., 'physical Properties of $CuSO_4$ - H_2SO_4 Solutions' Inorg. Mater. Research Div. Annual report 1966. U.C.R.L. 17330

113. Hutin D. and Coeuret F., J. Appl. Electrochem. 1977 462-471

114. Germain S. and Goodridge F., Electrochim Acta 1976 21 545- 550

115. Newman J., 'Electrochemical Systems' Englewood Cliffs: Prentice Hall.

116. Wragg A., Chem. and Ind. 1975 April 19th 330-332

117 Lopez-Cacicedo C.L., Trans Inst. Met. Fin. 1975 53 74-77

118. Eisner S, Trans. Inst. Met. Fin. 1973 51 13-16

119. Ibl N., Chem. Ing. Technik. 1971 43 202

120 idem Chem. and Ind. 1975 April 19th 326-328

121. Bennion D. and Newman J., J. Appl. Electrochem. 1972 2 113-122

122. Vergnes F. et al. , Corrosion (Rueil-Malmaison) 1969 17 131-136

123. Thangappan. R. et al. Metal. Fin. 1971 69 43-45

124. Krishnamurthy B. Thangappan R. and Sampath S., Metal Fin. 1971 69 43-49

125. Kuhn A.T. and Marquis B. J. of Appl. Electrochem. 1972 2 275-281

Additional references.

a) 'Canning Handbook' on Electroplating.

b) Electrodeposition and Corrosion Processes, J. M. West Van Nostand 1965

c) 'Modern Electroplating' Ed. Lowenheim F.A. Wiley-Interscience New York 1974

d) Canadian J. of Chem. Engrg. 1973 51 521-534

e) Raub E. and Muller K. 'Fundamentals of Metal Deposition' North Holland Publishing Co. New York 1970

f) Bockris J.O.M. and Reddy T 'Modern Aspects of Electrochemistry' vols 1 and 2

g) Monhemius A.J., Hydrometallurgy 1 1975 183-203

h) Paulin M. Hutin D. and Coueret F., J. Electrochem. Soc. 1977 180-188

i) Alkire R. and Plichta R., ibid 1973 1060-1066

j) Ibl N., Proceedings of "Surface 66" 48-61

k) Rao A.S. J. Appl. Electrochem. 1974 4 87-89

l) Proc. 27th Meeting C.I.T.C.E., 1976 No16-23

m) Podkolinski A.K., Trans Inst. Metal Fin. 1976 54 133-137

n) Clarke M ibid 155-158

o) Wragg A.A., Electrochim. Acta. 1968 13 2159

p) Wagner C., J. Electrochem. Soc. 1949 96 161

q) Eisenberg M. et. alia J. Electrochem. Soc. 1953 100 513

r) Ibl N., Helv. Chim. Acta 1954 37 1149

s) Ross T.K. and Wragg A.A., Electrochim. Acta 1965 10 1093

t) Wranglen G. et alia ibid. 1962 7 121

u) Diessler R.G. N.A.C.A. report 1955 1210

v) Everett M The Chem. Engr. 1969 231 159

w) Fouad M.G. and Zatout A.A., Electrochim. Acta 1969 14 909

APPENDIX 1

Computer Analysis of Data

A large number of variables can be reduced to a few dimensionless groups to make the plotting of data more convenient. Where the number of dimensionless groups required is greater than two, or where the amount of data is large, it is often more convenient to plot the data using the aid of a computer as this normally eliminates most of the tedium and the errors that are often made whilst transforming data to a handcalculator.

In mass transfer studies the form of the equation most often used for plotting data is given dimensionlessly by

$$Sh = k.Re^{a}.Sc^{b}$$

or

$$St = k.Re^{a}.Sc^{b}$$

where the values of k, a, and b must be determined. Linear equations are generally much more eay to solve than power function equations so the above equation is normally changed to its Log format i.e.

$$LogSt = aLogRe + bLogSc + k$$

which is the linear equation of a plane ($y = mx + nz + k$).

Once in this form the data can be analysed by using a method of numerical analysis called 'the least squares regression analysis'. The least squares criterion requires that

$$S = \sum(Y_i - y_i)^2$$

is a minimum where $(Y_i - y_i)$ is the distance of a data point from the plane. For S to be a minimum the partial derivatives ds/da, ds/db, ds/dc must equal zero and three simultaneous equations are therefore obtained.

$$\frac{ds}{da} = \sum_{i=1}^{n} \frac{d}{da}(ax_i + bz_i + c - y_i)^2 = \sum 2x_i(ax_i + bz_i + c - y_i) = 0$$

$$\frac{ds}{db} = \sum_{i=1}^{n} \frac{d}{db}(ax_i + bz_i + c - y_i)^2 = \sum 2z_i(ax_i + bz_i + c - y_i) = 0$$

$$\frac{ds}{dc} = \sum_{i=1}^{n} \frac{d}{dc}(ax_i + bz_i + c - y_i)^2 = \sum 2(ax_i + bz_i + c - y_i) = 0$$

and one has,

$$\sum y_i = a\sum x_i + b\sum z_i + c$$

$$\sum x_i y_i = a\sum x_i^2 + b\sum x_i z_i + c\sum x_i$$

$$\sum z_i y_i = a\sum x_i z_i + b\sum z_i^2 + c\sum z_i$$

Applying the least squares method to the mass transfer data the following equations are obtained which must be solved.

$$St = a\sum Re + b\sum Sc + c$$

$$Re.St = a\sum Re^2 + b\sum Re.Sc + c\sum Re$$

$$St.Sc = a\sum Re.Sc + b\sum Sc^2 + c\sum Sc$$

where Re, St, Sc are in log format

Solutions of these equations are performed readily using the computer programme set out overleaf.

Errors.

Although the programme will solve the above equations, because values of Re, Sc, and St are in log format round-up errors can occur during the analysis if there are only a few values of any one of the variables. In mass transfer data there are generally only a few values of the Schmidt number and so round-up errors are possible.

A COMPUTER PROGRAMME FOR A THREE DIMENSIONAL 'LEAST SQUARES ANALYSIS' OF DATA.

```
   MASTER TIME
   DIMENSION E(3), F(3), G(3,3), E1(3), P(360), Q(360), R(360)
60 FORMAT(3F0.0)
61 FORMAT(3F0.0)
70 FORMAT(1H ,11HREYNOLD NO.,5X,11HSTANTON NO.,5X,11HSCHMIDT NO.,
  15X,6HLOG RE,5X,6HLOG ST,5X,6HLOG SC,5X,2HA ,10X,2HB ,10X,2HC )
71 FORMAT(1H ,3(F10.5,5X),3(F7.4,5X),3(F7.5,5X))
   WRITE(2,70)
   DO 22 I = 2,360
   READ(1,60)AK,EF,V
   IF(AK.EQ.999) GOTO 41
   READ(1,61)CF,FF,D

   C- THE VARIABLES TO BE USED IN THE REYNOLDS,SCHMIDT AND STANTON
      NUMBERS HAVE JUST BEEN READ IN FROM THE RELEVANT DATA CARDS
      THREE VARIABLES ON EACH DATA CARD.

   ST=(AK*EF)/V
   RE=(V*CF)/(FF*(1.0-EF))*0.0001
   SC=FF/D

   C- THE EQUATIONS FOR THE REYNOLDS STANTON AND SCHMIDT NUMBERS
      HAVE JUST BEEN ENTERED AND WILL NOW BE PUT INTO LOG FORM

   P(I)=ALOG10(RE)
   Q(I)=ALOG10(ST)
   R(I)=ALOG10(SC)

   C- IN ORDER TO DO A THREE DIMENSIONAL ANALYSIS A THREE DIMENS-
      IONAL MATRIX IS REQUIRED IN THE FORM OF THE EQUATION
      COEFFICIENTS.

   G(1,1)=G(1,1)+P(I)
   G(3,2)=G(1,1)
   G(2,1)=G(2,1)+R(I)
   G(3,3)=G(2,1)
   G(1,2)=G(1,2)+P(I)*P(I)
   G(2,3)=G(2,3)+R(I)*R(I)
   G(2,2)=G(2,2)+P(I)*R(I)
   G(1,3)=G(2,2)
   G(3,1)=I-1.0
   F(1)=F(1)+P(I)*Q(I)
   F(2)=F(2)+Q(I)*R(I)
   F(3)=F(3)+Q(I)
   IF(I-4)22,101,101
101 CONTINUE
   CALL GAUSS (E,F,G)

   C- GAUSS IS A SUBROUTINE WHICH ANALYSES THE DATA ENTERED. AT
      LEAST FOUR SETS OF DATA POINTS ARE REQUIRED FOR THE PROGRAMME
      TO WORK. (N.B. THIS MEANS THAT DIFFERENT RE, ST AND SC VALUES
      ARE REQUIRED FOR EACH POINT)
```

```
      WRITE(2,71)RE,ST,SC,P(I),Q(I),R(I),E(1),E(2),E(3)
   22 CONTINUE
   41 CONTINUE
      DO 14 J=1,2
      READ(1,11)E1(1),E1(2),E1(3)
   11 FORMAT(3F0.0)
      DO 16 L=2,360

      C- THE ERROR IN THE ANALYSIS WILL NOW BE CALCULATED

      ERROR1=ERROR1+(Q(L)-E(1)-E(2)*P(L)-E(3)*R(L))*(Q(L)-E(1)-E(2)*P(L)
     1-E(3)*R(L))

      C- THE ERROR OF ANY OTHER ANALYSIS CAN NOW BE CALCULATED

      ERROR2=ERROR2+(Q(L)-E1(1)-E1(2)*P(L)-E1(3)*R(L))*(Q(L)-E1(1)-E1(2)
     1*P(L)-E1(3)*R(L))
   16 CONTINUE
      WRITE(2,12)ERROR1,ERROR2
   12 FORMAT(1H ,28HTHE SUMS OF SQUARES I GET = ,E17 10,5X,30HTHE SUMS O
     1F SQUARES HE GETS = ,E17.10)
   14 CONTINUE
      STOP
      END


      SUBROUTINE GAUSS (X,W,PW)
      DIMENSION X(3),Y(3),B(3,3),PW(3,3),W(3)
      DO 60 I=1,3
      DO 60 J=1,3
      Y(I)=W(I)
      B(I,J)=PW(I,J)
   60 CONTINUE
      IF(ABS(B(1,1)).GE.ABS(B(2,1)).AND.ABS(B(1,1)).GE.ABS(B(3,1)))
     1GOTO 4
      IF(ABS(B(2,1)).GE.ABS(B(3,1))) GOTO 2
      NPIV=3
      GOTO 3
    2 NPIV=2
    3 CONTINUE
      DO 13 J=1,3
      HOLD=B(NPIV,J)
      B(NPIV,J)=B(1,J)
      B(1,J)=HOLD
   13 CONTINUE
      HOLD=Y(NPIV)
      Y(NPIV)=Y(1)
      Y(1)=HOLD
    4 RMULT=B(2,1)/B(1,1)
      DO 5 I=2,3
    5 B(2,I)=B(2,I)-B(1,I)*RMULT
      Y(2)=Y(2)-Y(1)*RMULT
      RMULT=B(3,1)/B(1,1)
      DO 6 I=2,3
```

```
    6 B(3,I)=B(3,I)-B(1,I)*RMULT
      Y(3)=Y(3)-Y(1)*RMULT
      IF(ABS(B(2,2)).GE.ABS(B(3,2))) GOTO 8
      DO 7 I=2,3
      HOLD=B(2,I)
      B(2,I)=B(3,I)
    7 B(3,I)=HOLD
      HOLD=Y(2)
      Y(2)=Y(3)
      Y(3)=HOLD
    8 RMULT=B(3,2)/B(2,2)
      DO 9 I=2,3
    9 B(3,I)=B(3,I)-B(2,I)*RMULT
      Y(3)=Y(3)-Y(2)*RMULT
      X(3)=Y(3)/B(3,3)
      X(2)=(Y(2)-B(2,3)*X(3))/B(2,2)
      X81)=(Y(1)-B(1,2)*X(2)-B(1,3)*X(3))/B(1,1)
      RETURN
      END
```

TABLE 1 (see ref. 5 page 212)

Metal	Quantity produced by electrowinning.(tons)	% of total production	Comments
Al	8,400,000	100	
Zn	2,400,000	53	
Cu	540,000	10	
Na	163,000(U.S.A.)	100	
Mg	206,000	80	
Ni	48,000	11	
Mn	37,500	?	Free world
Co	10,000	50	
Cd	6,500(U.S.A.)	50	
Cr	3,000(approx.)	75(U.S.A.)	
Li	250	100	
B	100	-	U.S. Atomic Energy cojectural.
Ta	-	-	At present only H.C.Starck produces by electrolysis. Total U.S capacity 300 tonnes both Nb/Ta only Misch metal in tonnage amounts
Nb	pilot scale	-	
rare earths	a few tonnes	-	
Ga	0.5(U.S.A)	-	mostly by electrolysis
Tl	-	-	
Ti	pilot scale	-	Total U.S. product approx 20,000 ton
In	-	-	Total production 100 tonnes.

TABLE 2 (see ref. 5 page 73)

Typical products obtained by electrochemical fluorination		
Starting material	Principle products	Remarks
$CH_3(CH_2)_nCH_3$	$CF_3(CF_2)_nCF_3$	Poor yields
$CF_3(CH_2)_nCH_3$ or $CH_3(CF_2)(CH_2)_{n-1}CH_3$	$CF_3(CF_2)_nCF_3$	Moderate to good yields.
Cyclohexane, benzene napthalene	-	no fluorination
$CCl_2:CCl_2$	$CFCl_2:CFCl_2$	High yield
$CH_3(CH_2)_nOH$	perfluoro/carbons, ethers,acidfluorides	Poor yields
n and cycloethers, polyethers	perfluoro analogues	Moderate to poor yields
n-carboxylic acids, acid anhydrides	perfluoro/carbons, ethers,acid fluorides	Poor yields*
n-acid chlorides and fluorides	''	Moderate to* very good
n-diacid fluorides	perfluorodiacid fluorides, perfluoroacid fluorides, perfluorocarbons	Poor yields
aldehydes,ketones	perfluoro/acids,carbons	No perfluoro aldehydes,ketones
esters	perfluoroacid fluorides	No perfluoro esters
primary/secondary/ tertiary amines	n-fluorinated perfluoro amines,NF_3, perfluoro tertiary amines	Moderate yields
n-alkyl sulphides	$(RF_2)SF_4$, $RFSF_5$	moderate yields
$CH_3(CH_2)_nSO_3OH$	perfluorocarbons$(CF_3)_2(CF_2)_{n-1}$	Poor yields
NH_3**, H_2O, CS_2.	NF_3, F_2O, $CF_3:SF_5$, SF_6, CF_4	
K_2SO_4	SO_2F_2, SOF_2, F_2O	

* n-carboxylic acids containing six or more carbon atoms give perfluorcyclic ethers, frequently as major products

** Caution NF_2H and NFH_2 maybe among the products, these are unstable and NF_2H may detonate spontaneously when in the liquid state.

TABLE 3 (see ref. 3)

Dimensionless Groups

Problems involving fluid flow and mass transfer are complicated by the number of relevant variables. In general the variables include: fluid density (ρ_f), viscosity (μ or ν), velocity(U), diffusion coefficent(D), characteristic length(d), characteristic length of mass transfer surface(x), the gravitational acceleration (g), and the diffusion flux(J). The large number of experiments required to test all the variables is greatly reduced by combining the parameters into dimensionless groups which, when adequately tested will show the role of each particular term. The most common such groups used in electrochemistry are:

Reynolds number	$Re = \frac{U.d}{\nu}$	- flow of fluids
Taylor number	$Ta = Re \sqrt{\frac{R_2 - R_1}{R_2 + R_1}}$	- flow of fluid between concentric rotating cylinders
Schmidt number	$Sc = \frac{\nu}{D}$	- dynamic similarity
Stanton number	$St = \frac{k_m}{U}$	- forced convection mass transfer
Sherwood number, Nusselt number	$Sh = \frac{k_m . x}{D}$	- forced convection mass transfer
Grashoff number	$Gr = \frac{g . x^3}{\eta^2 . \rho}$	- natural convection mass transfer.
Froude number	$Fr = U^2/d\rho . g$	

It has been common to the Sherwood number in laminar mass transfer studies, and to the Stanton number when turbulence is involved, but either can be used since $St = Sh/Re.Sc$

TABLE 4

Mass Transfer Correlations For Various Flow Systems

SYSTEM	CORRELATION	REF. (3)
Natural Convection a) Horizontal Plate - Laminar Flow	$Sh = 0,64\ (Sc \ldots)^{1/4}$ $i_L = 0.64\ zF\ C_b\ D^{3/4}\ x^{-1/4}(g\Delta\rho/\rho\nu)^{1/4}$	E(O)*
b) Horizontal Plate - Turbulent Flow**	$Sh = 0.16\ (Sc \cdot Gr)^{0.33}$ $i_L = 0.16\ zF\ C_b\ D^{2/3}\nu^{-1/3}(g\Delta\rho/\rho)^{1/3}$	E(O)*
c) Vertical Plate -Laminar Flow	$Sh = 0.51\ (Sc \cdot Gr)^{1/4}$	T(7)
d) Vertical Plate - Laminar Flow	$Sh = 0.805\ (Sc \cdot Gr)^{1/4}$	T(P)
e) Vertical Plate - Laminar Flow	$Sh = 673\ (Sc \cdot Gr)^{1/4}$	E(Q)
f) Vertical Plate - Laminar Flow	$Sh = 0.66\ (Sc \cdot Gr)^{1/4}$	E(R)
g) Vertical Plate -Turbulent Flow (Artificially Roughened- factor increases with roughness)	$Sh = 0.052\ 0.087\ (Sc \cdot Gr)^{0.32}$	E(W)
Forced Convection a) Concentric Annuli	$Sh = 1.76\ (Re \cdot Sc \cdot d_e/x)^{1/3}$ $i_L = 1.76\ zF\ C_b\ D^{2/3}U_e^{1/3}x^{-1/3}d_e^{-1/3}$	T,E(S)

---

* T,E refer to theoretical and empirical studies respectively.

** The most important parameter in Gr is x^3; when Sc . Gr is large enough, which usually implies that x is large, the flow becomes turbulent and i_L loses its dependence on x.

(Continued).

SYSTEM	CORRELATION	REF.
b) Concentric Annuli - Turbulent Flow	$St = 0.276\ Re^{-0.42} Sc^{-2/3}\ (d_e/x)^{1/3}$	T,E (S)
	$i_L = 0.276\ zF\ C_b\ D^{2/3} \nu^{0.24} U^{0.58} x^{-1/3} d_e^{-0.09}$	
c) Square Pipe - Laminar Flow	$Sh = 0.331\ Re^{1/2}\ Sc^{1/3}$	T(b)
	$i_L = 0.331\ zF\ C_b\ D^{2/3} \nu^{-1/6} d^{-1/2} U^{1/2}$	
d) Square Pipe -Turbulent Flow	$St = 0.143\ Re^{-2/5} Sc^{-2/3}$	T(b)
	$i_L = 0.143\ zF\ C_b\ D^{2/3} U^{3/5} d^{-2/5} \nu^{-4/15}$	
e) Circular Pipe - Turbulent Flow	$St = 0.079\ C_f^{1/2}\ Sc^{-3/4}$	T(u)
f) Circular Pipe -Turbulent Flow (Heat Transfer)	$St = 0.0204\ Re^{-0.195}\ Sc^{-0.585}$	E(y)
	$i_L = 0.02\ zF\ C_b\ D^{0.585} \nu^{-0.390} d^{-0.195} U^{0.805}$	
g) Circular Pipe - Laminar Flow	$Sh = 1.614\ (Re \cdot Sc \cdot d/L)^{1/3}$ (see a)	E,T(S)
h) Circular Pipe -Turbulent Flow	$St = 0.276\ Re^{-0.42} Sc^{-2/3}\ (d_e/L)^{1/3}$ (see b)*	E,T(S)
i) Rotating Disc	$Sh = 0.62\ Re^{1/2} Sc^{1/3}$	(7)
	$i_L = 0.62\ zF\ C_b D^{2/3} \nu^{-1/6} w^{1/2}$	
j) Rotating Disc - Turbulent Flow	$St = \underline{0.01}\ Re^{-0.1} Sc^{-3/4}$	(7)
	$i_L = \underline{0.01}\ zF\ C_b\ D^{3/4} \nu^{-0.65} \omega^{0.9} R^{0.8}$	

---

* These correlations indicate rather poor overall agreement for a pipe which is probably the most important flow geometry.

TABLE 5 (see ref.[129])

Advantages and disadvantages of fluidised beds			
Active material bed (e.g. Metal beads, Metal coated glass beads or plastic beads etc.)		Inert material bed (e.g. Glass beads, Silca sand, Quartz particles or granules)	
Advantages	Disadvantages	Advantages	Disadvantages
1. Provides high surface area.	In a highly expanded bed electronic contact is poor.	Provides uniform and intense agitation at the electrode.	Increases cell voltage because particles are non-conducting.
2. Enhances mass transfer and heat transfer rates .	Non-uniform electrode potential may give undesirable products.	Enhances mass transfer and heat transfer rates.	Attrition of particles can lead to fines in the bed.
3. Allows continuous reactor operation	Evolution of gas during reactions may affect the bed performance.	Maintains a uniform temperature throughout the cell.	Erosion of cell and electrode by abrasion may be large.
4. Maintains a uniform temperature under all conditions	Requires a diaphragm for all reactions.	Acts as a degasifier in the bulk of the electrolyte.	Requires additional equipment e.g. a pump.
5. Replacement of the electrode is easy	Attrition of particles and formation of fines causes loss of electrode.	Gives uniform bright smooth deposit.	–
6. Over-all cell voltages are low.	Erosion of cell and diaphragm may be high.	Reduces the requirement of addition agents.	–
7. Could easily be adapted for high pressure operation.	Requires extra equipment such as pump, particle separator, filter etc..	Allows use of high current densities.	–
8. Amenable to automatic control of process	–	–	–
9. Gives better current efficiency with some reactions in a low ion solution			

TABLE 6

CELL DIMENSIONS

Overall height			710mm.
length of upper section			320mm.
length of middle section			320mm.
length of lower section			70mm.
Tube dimensions			
larger tube	O.D.		38mm.
	I.D.		31.68mm.
smaller tube	O.D.		32mm.
	I.D.		25.40mm.
Flange dimensions			
overall diameter			100mm.
core diameter			32 @ 38mm.
thickness			6mm.
Counter electrode			
overall length			220mm.
overall width			40mm.
Working electrode			
copper powder	-70 mesh to +100 mesh		
bed weights	1cm bed		16.66g.
	2cm bed		33.33g
	3cm bed		50g.
larger tube	1cm bed		50g.

TABLE 7

Viscosity data for solutions of $CuSO_4$ + 0.5M H_2SO_4					
Cu^{2+} concentration:	0.7M	0.07M	0.01M	0.001M	10^{-5}M
Viscosity(cp) :	1.29	0.995	0.966	0.962	0.962

TABLE 8

Density data for solutions of $CuSO_4$ + 0.5M H_2SO_4					
Cu^{2+} concentration:	0.7M	0.07M	0.01M	0.001M	10^{-5}M
Density(g/cm^3) :	1.13	1.04	1.033	1.031	1.029

TABLE 9

Diffusion data for solutions of $CuSO_4$ + 0.5M H_2SO_4					
Cu^{2+} concentration :	0.7M	0.07M	0.01M	0.001M	10^{-5}M
Diffusivity(cm^2/sec x10^6) :	7.88	5.876	5.674	5.645	5.642

See reference 112

figure 1

A fluidised bed cell arrangement with electrolyte flow parallel to current flow.

figure 2

A fluidised bed arrangement with electrolyte flow perpendicular to current flow.

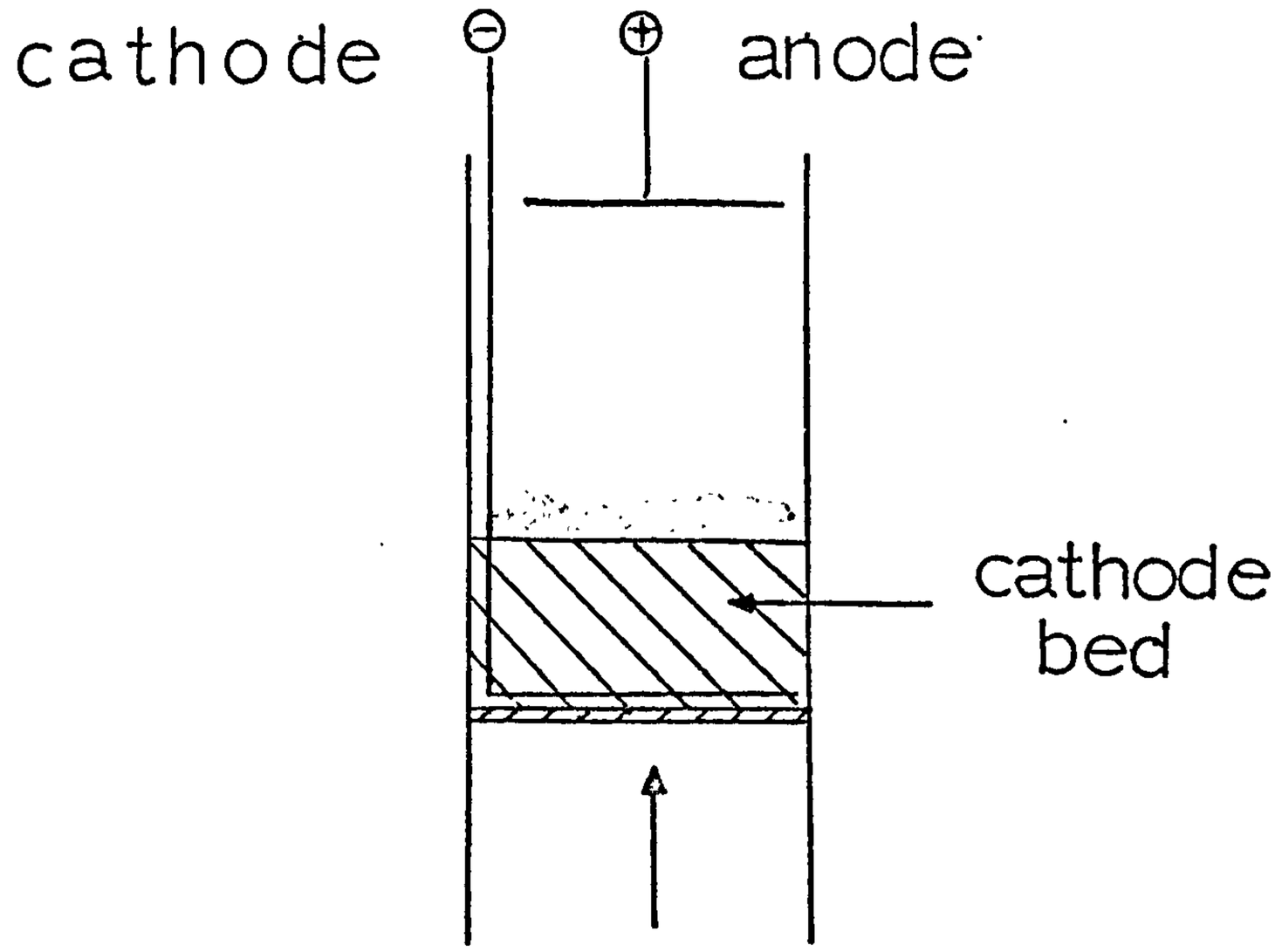
cathode
anode
cathode
bed

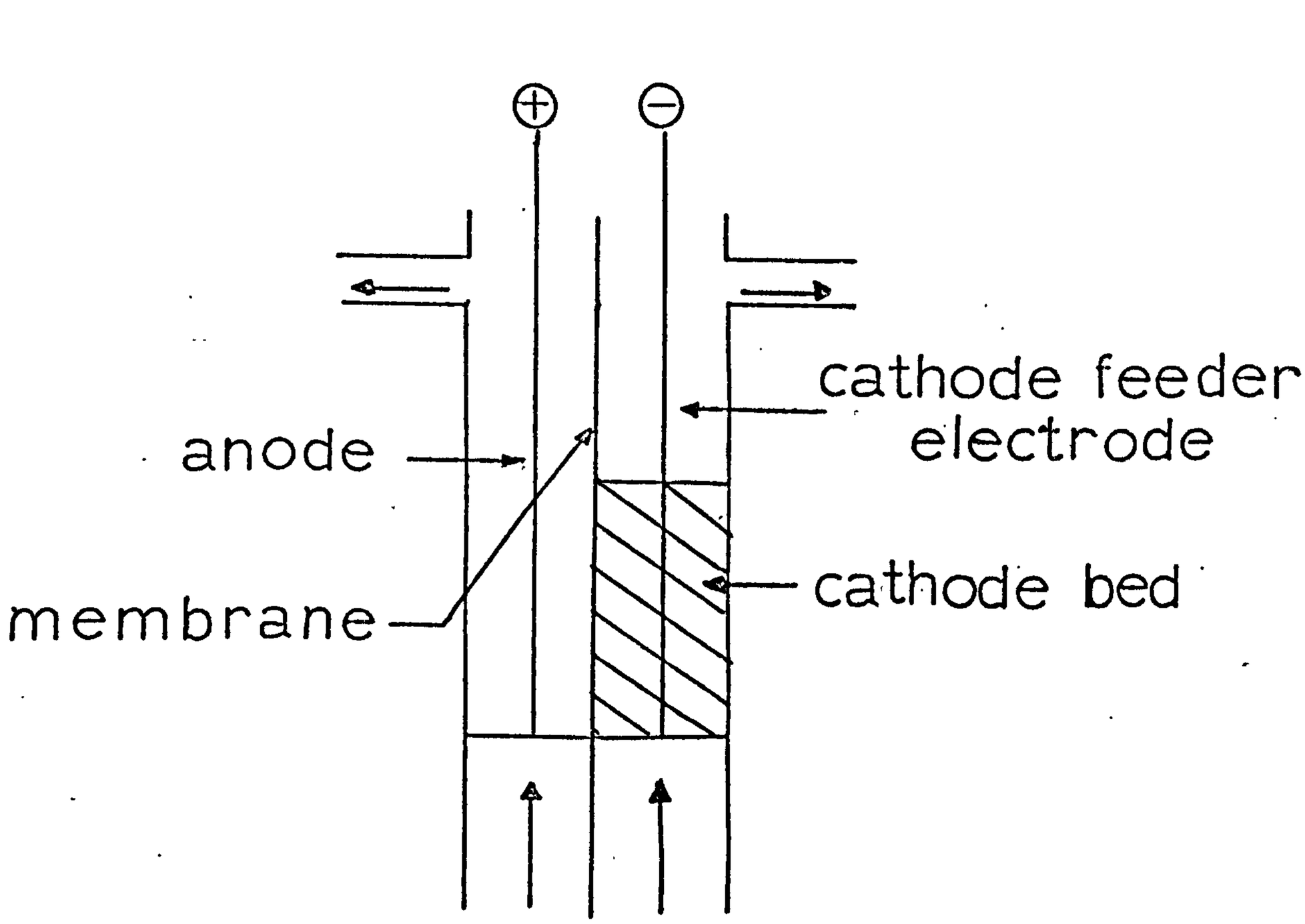
cathode feeder
electrode
anode
membrane
cathode bed
anolyte
catholyte

figure 3

Schematic figure of the Nernst diffusion layer. The metal ion concentration is a function of distance from the electrode.

figure 4

Variation of the velocity in the boundary layer according to the Nernst theory.

figure 5

Variation of the velocity in the boundary layer according to the Levich theory.(7)

figure 6

Variation in the thickness of the Prandtl layer(d_u) and the diffusion layer (δ) with distance (x) from the point where flow of liquid reaches the electrode.(7)

figure 7

The four layer theory as proposed by Levich and Landau. (7).

figure 8

Variation of concentration and flow velocity with distance (x) from the electrode surface.

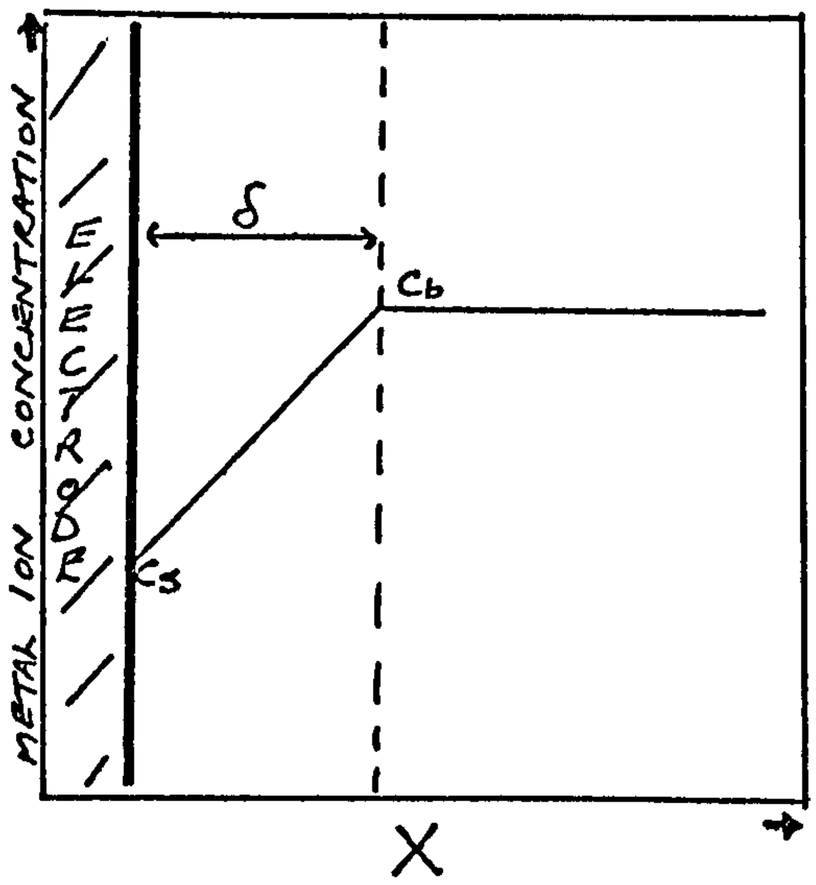
METAL ION CONCENTRATION
BOUNDARY LAYER
δ
C_b
C_s
X

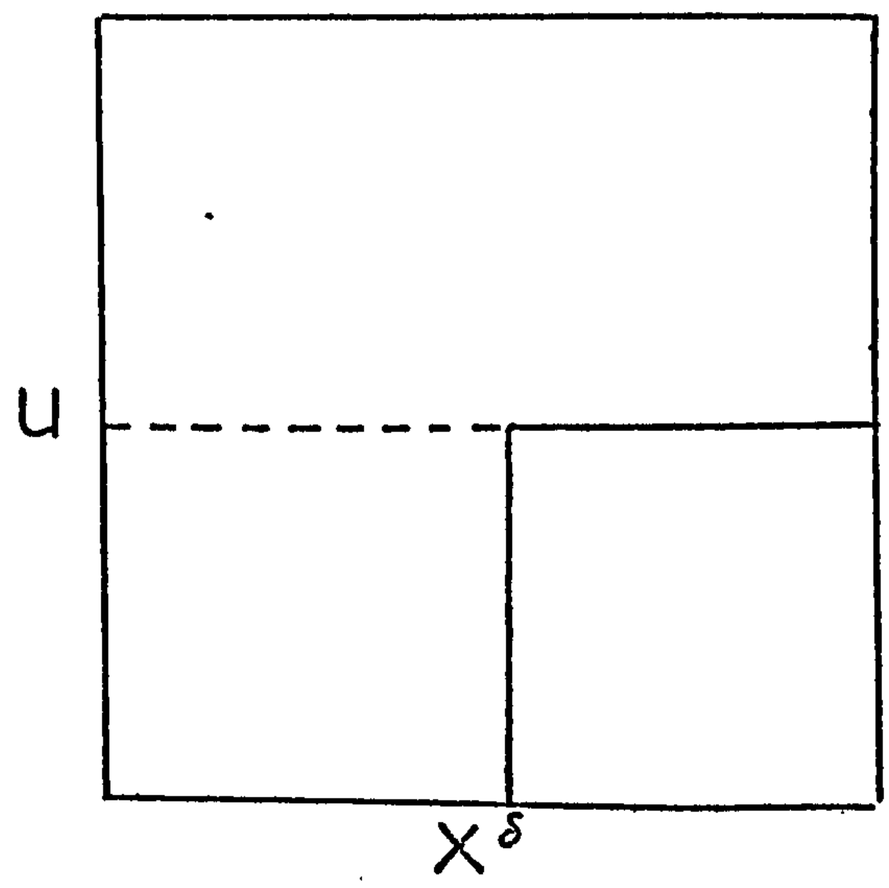
U
X
δ

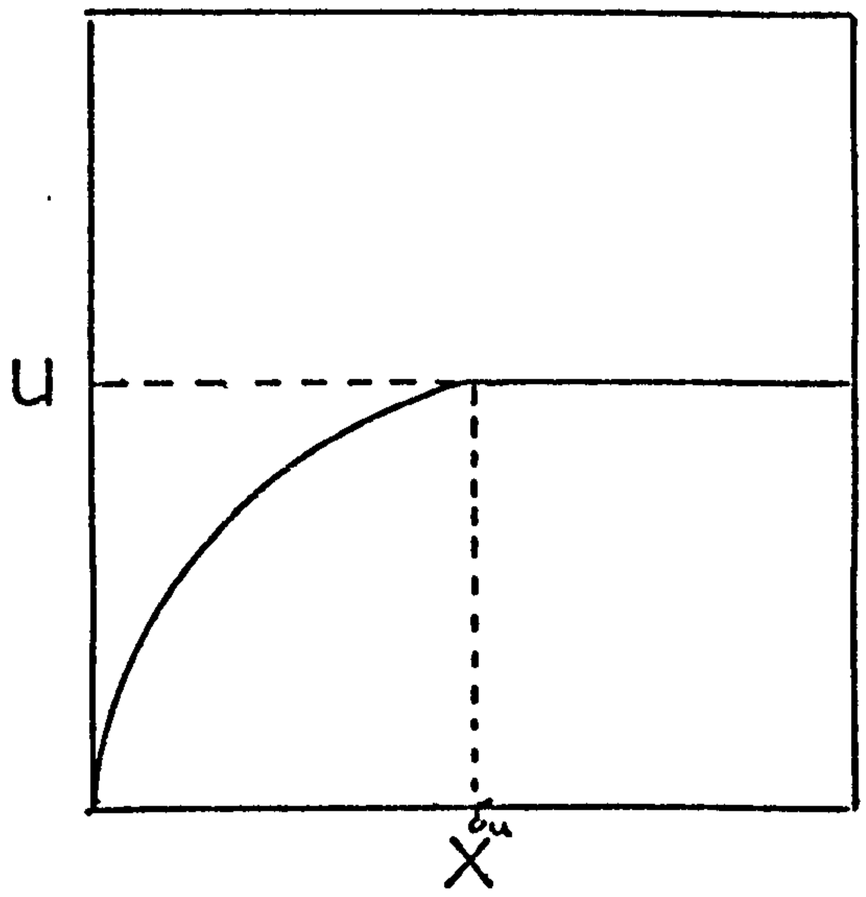
U
X
δ_u

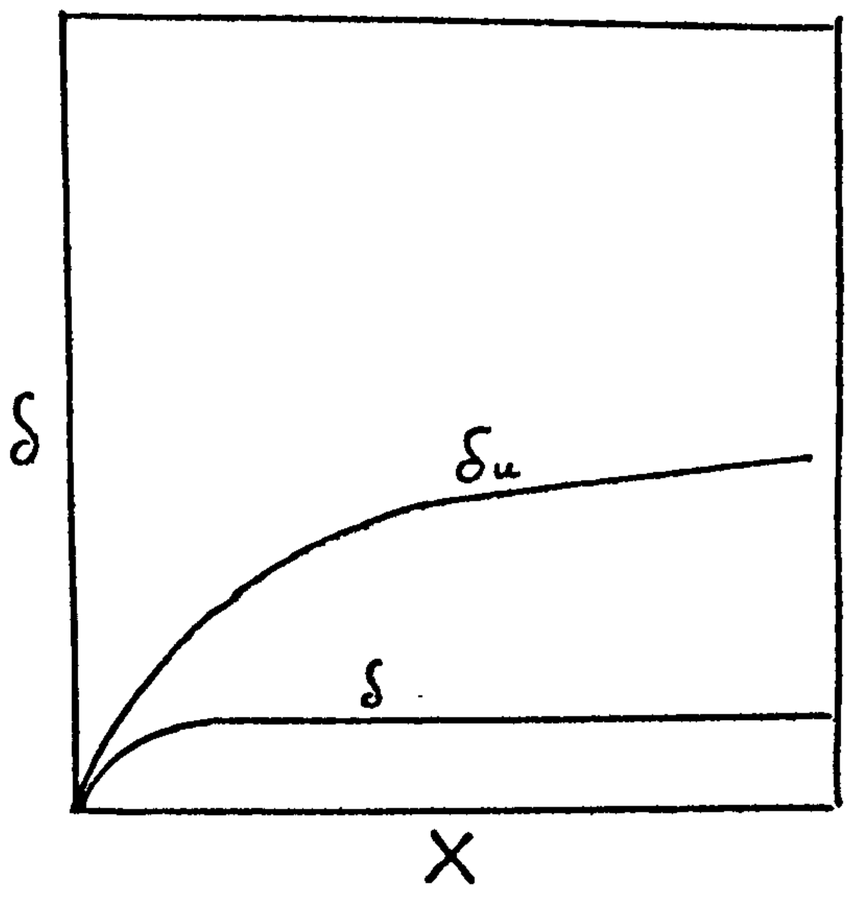
δ
δ_u
δ
X

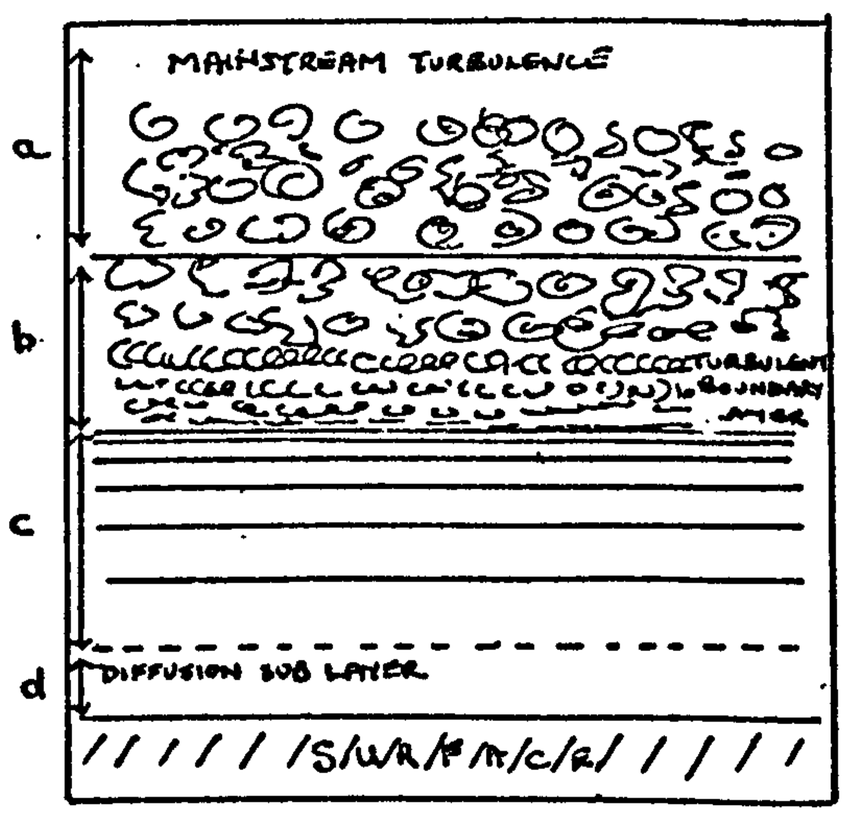
MAINSTREAM TURBULENCE
a
b
TURBULENT
BOUNDARY
LAYER
c
d
DIFFUSION SUB LAYER
SURFACE

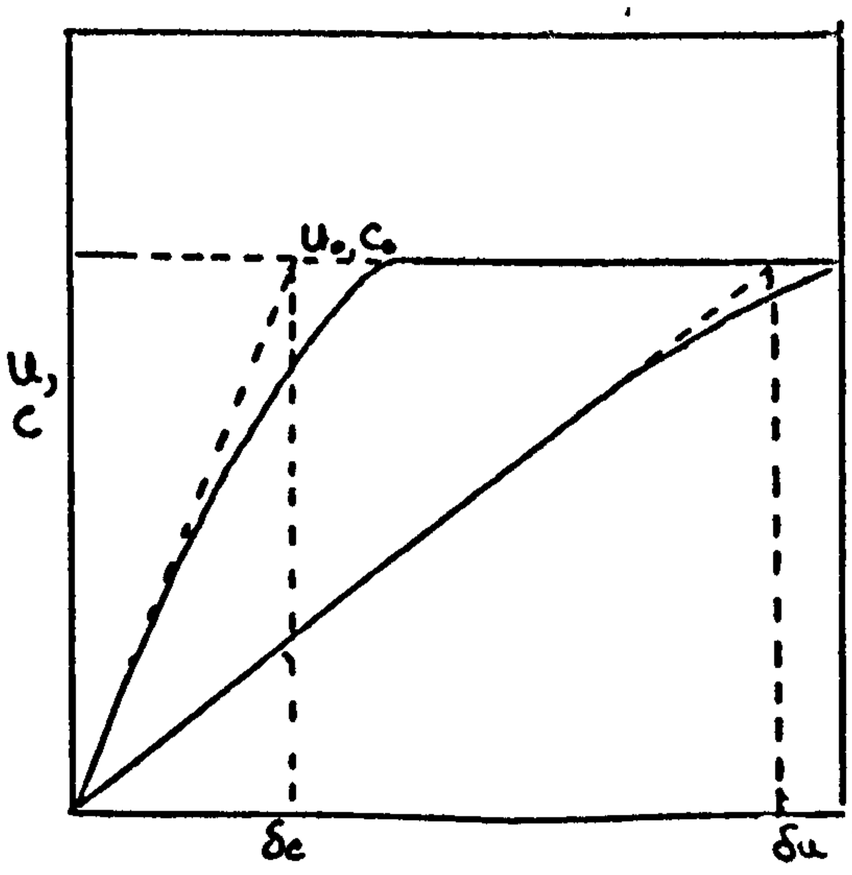
U_o, C_o
U, C
δ_c
δ_u

figure 9

Bed voidage at incipient fluidisation.(84)

figure 10

Channelling.(56)

figure 11

Experimentally measured mass transfer values.

figure 12

Optimum porosity for inert beds.(76)

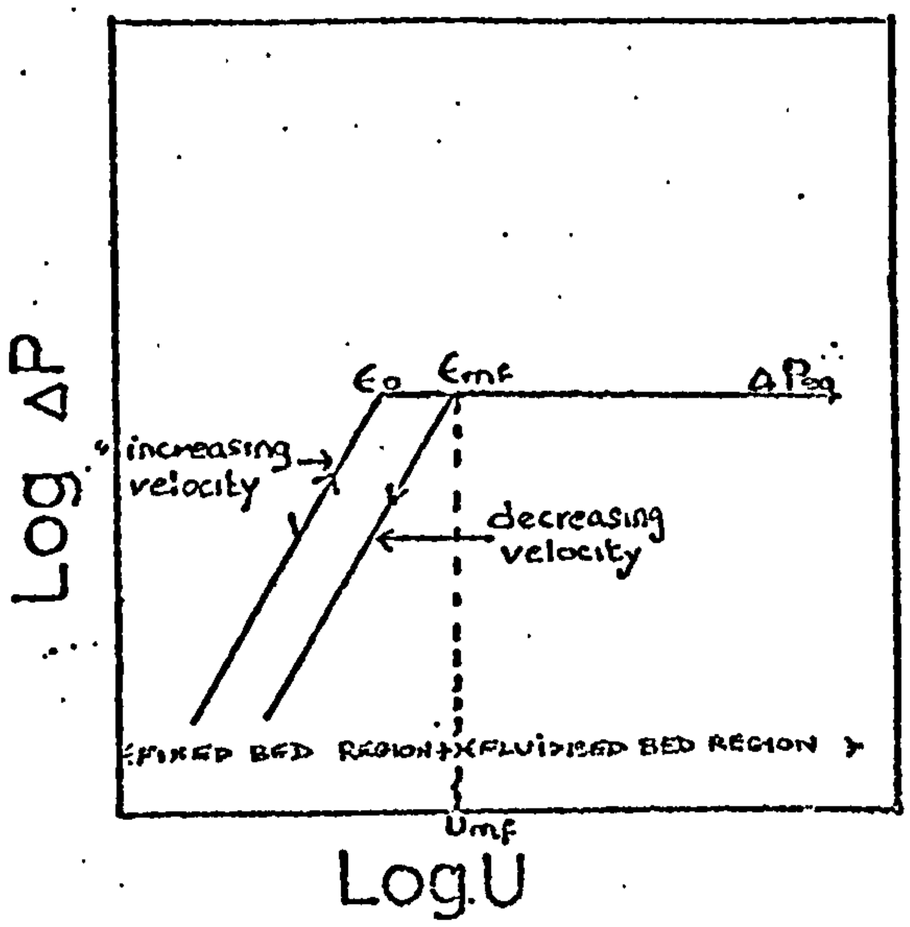
Log ΔP
ϵ_0 ϵ_{mf}
ΔP_{eq}
increasing velocity
decreasing velocity
FIXED BED REGION
FLUIDISED BED REGION
U_{mf}
Log U

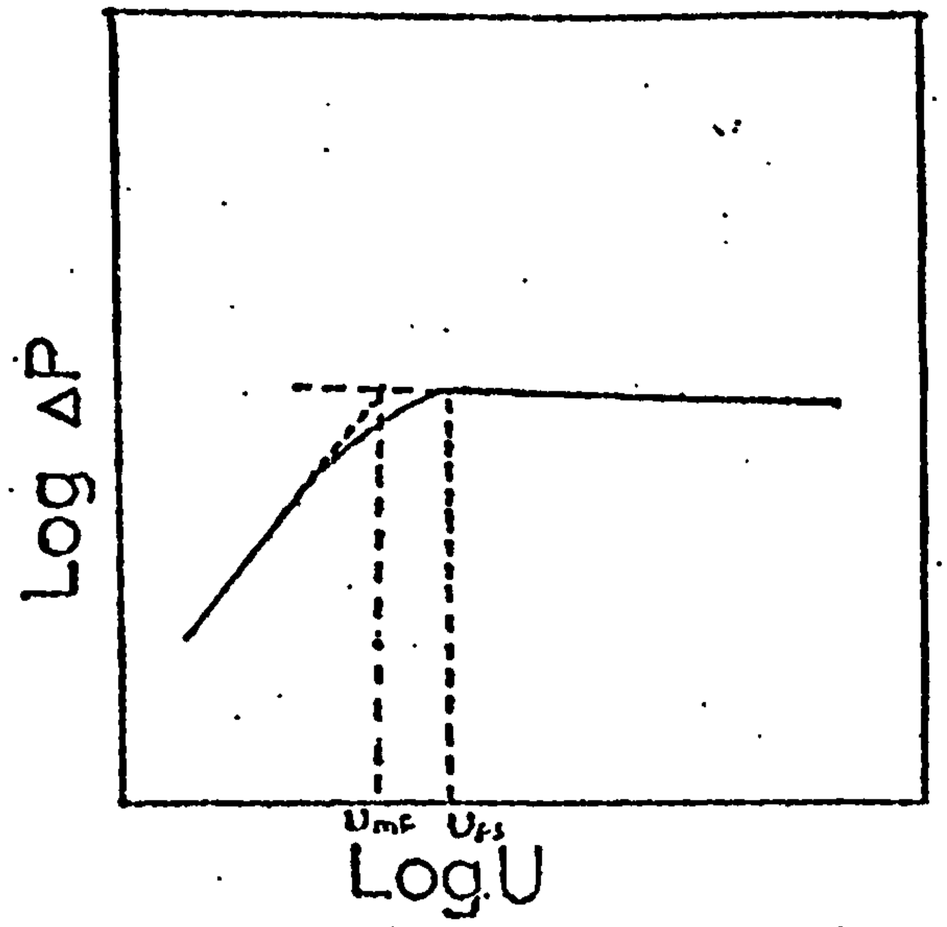
Log ΔP
U_{mf} U_{fs}
Log U

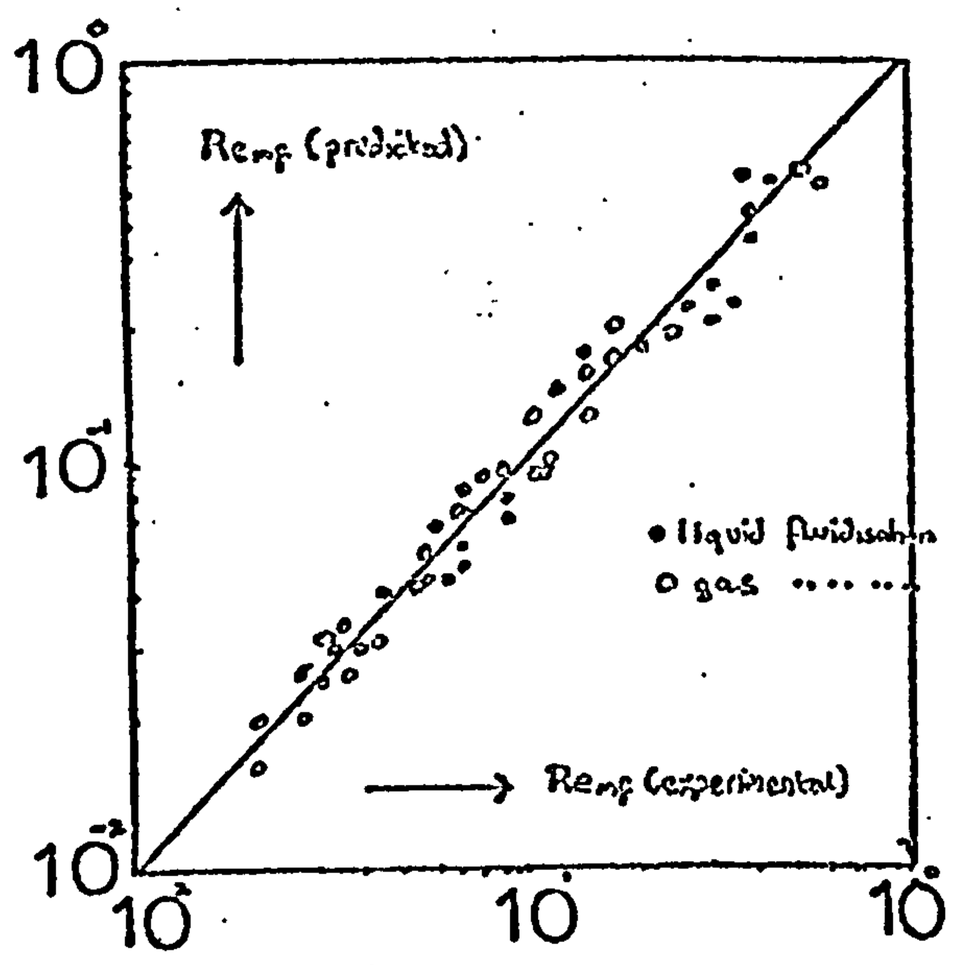
10^0
10^{-1}
10^{-2}
10^{-2}
10^{-1}
10^0
Re_{mf} (predicted)
Re_{mf} (experimental)
• liquid fluidisation
o gas

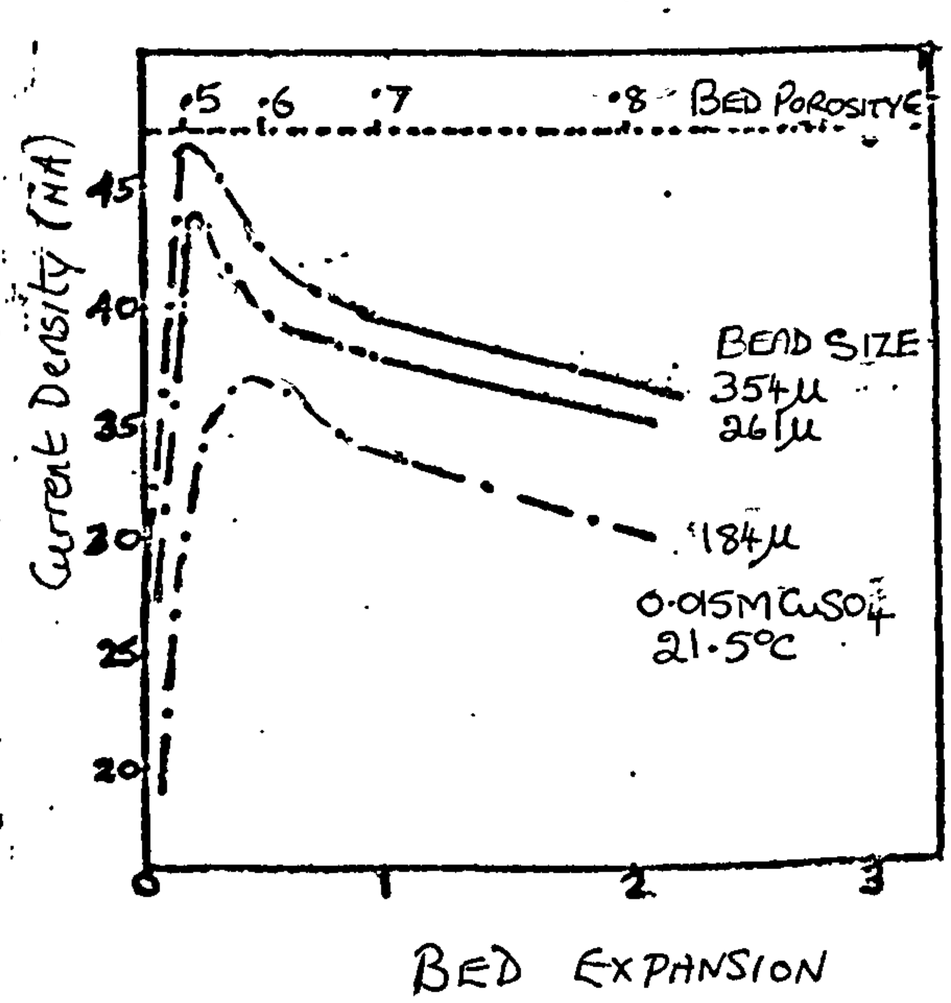
·5 ·6 ·7 ·8 BED POROSITY
Current Density (mA)
45
40
35
30
25
20
0
1
2
3
BED SIZE
354μ
261μ
184μ
0·015M CuSO4
21·5°C
BED EXPANSION

figure 13

Position of the feeder electrodes
in the Fleischmann model.
a) where the fluidised bed is between
the feeder and the counter electrode.
b) where the feeder is closest to the
counter electrode.

figure 14

A new type of fluidised bed with a
number of feeder electrodes situated
in the bed.(108)

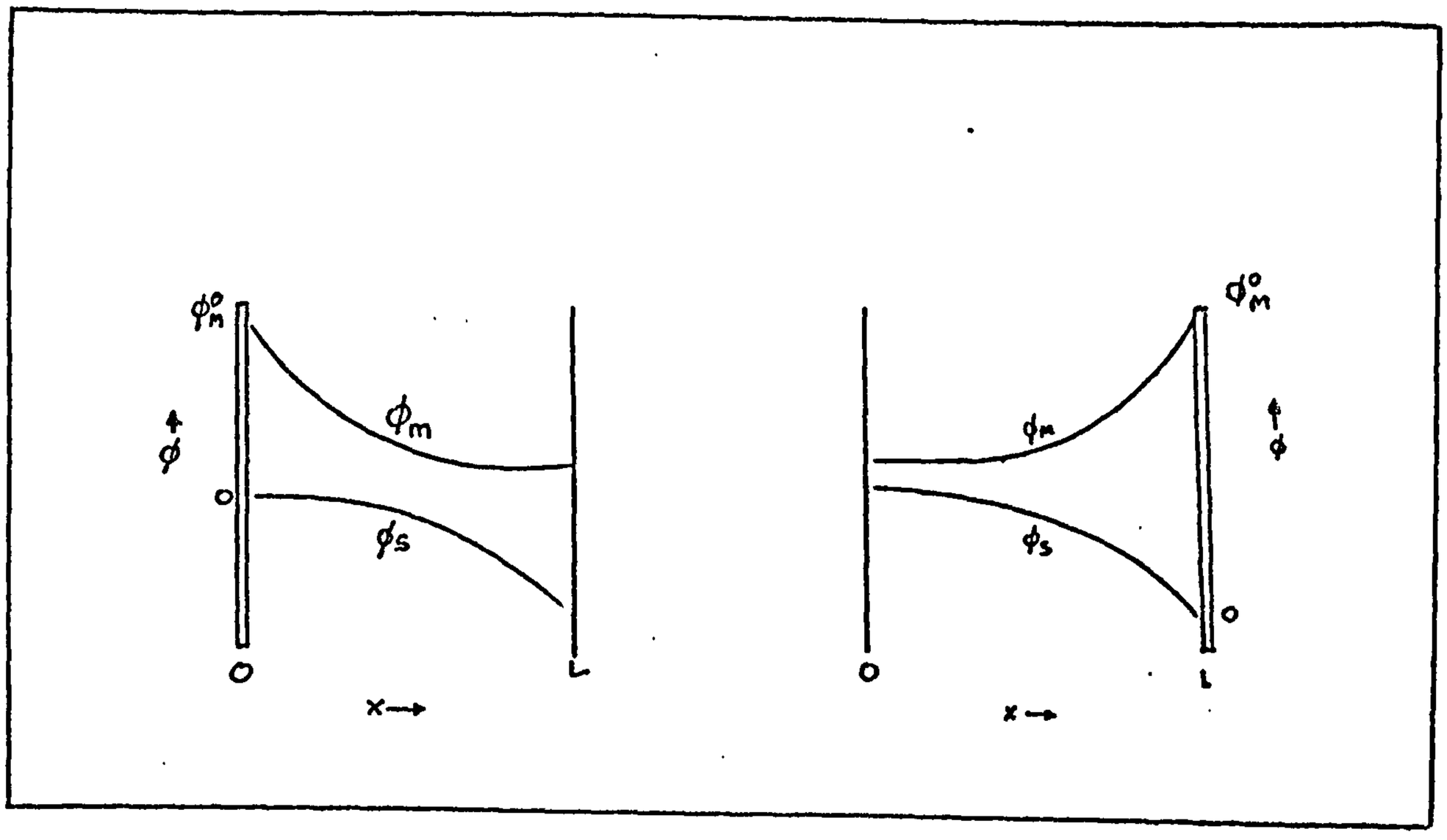
ϕ_m^o
ϕ
ϕ_m
0
ϕ_s
0
L
x→
ϕ_m^o
ϕ_m
ϕ
ϕ_s
0
0
L
x→

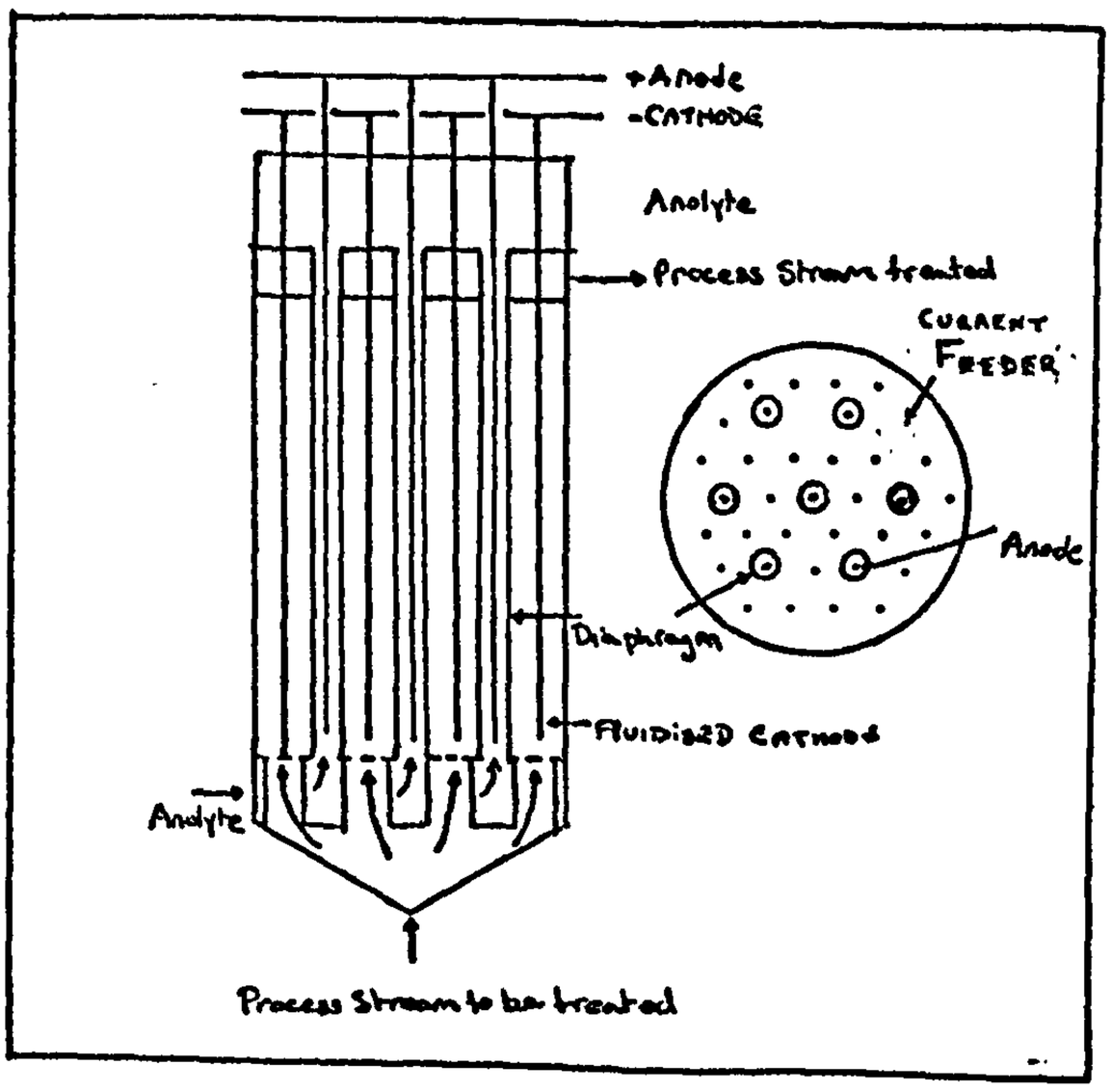
+Anode
-CATHODE
Anolyte
Process Stream treated
CURRENT FEEDER
Anode
Diaphragm
FLUIDISED CATHODE
Anolyte
Process Stream to be treated

figure 15

Schematic diagram of apparatus

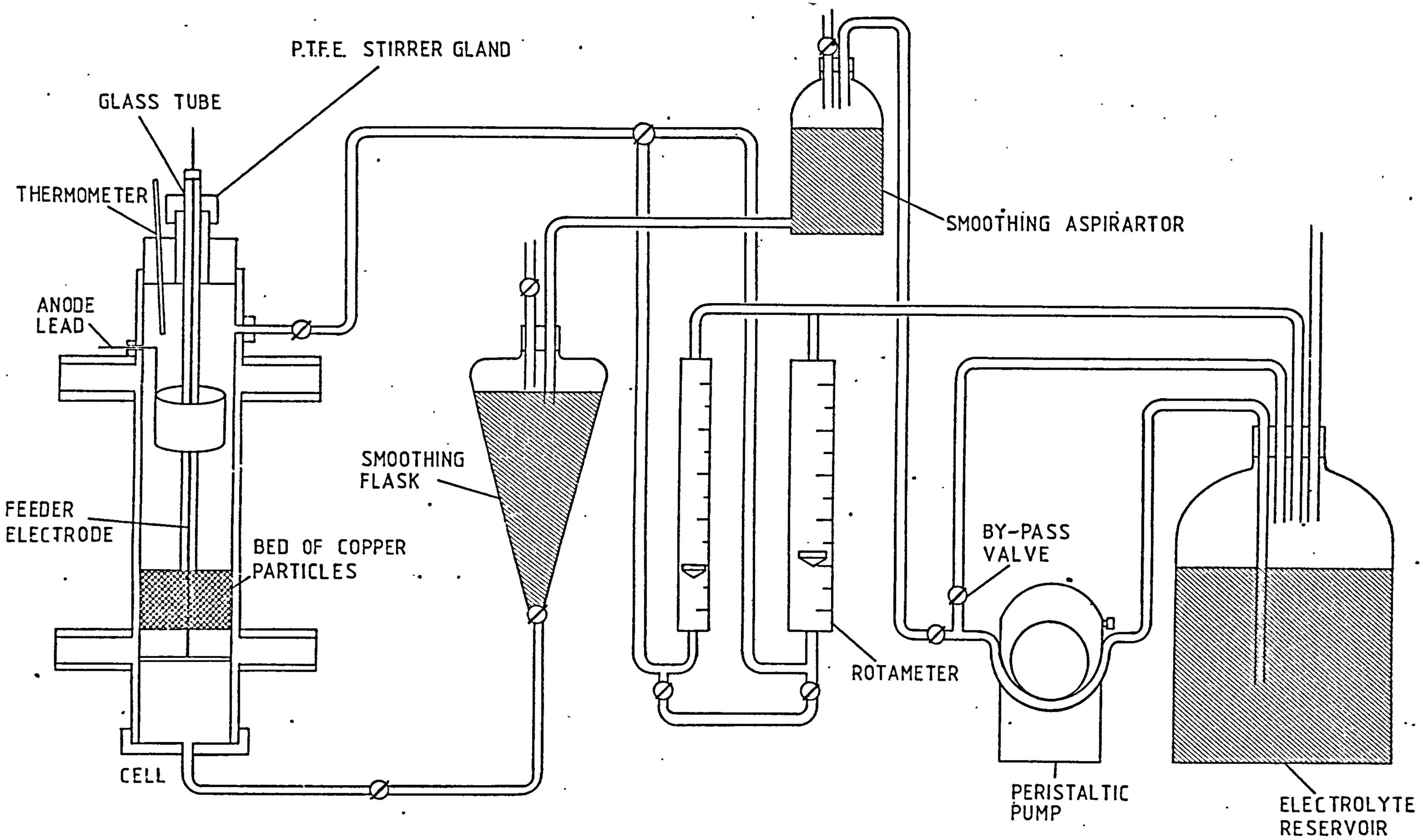
P.T.F.E. STIRRER GLAND
GLASS TUBE
THERMOMETER
ANODE LEAD
FEEDER ELECTRODE
BED OF COPPER PARTICLES
CELL
SMOOTHING FLASK
SMOOTHING ASPIRATOR
ROTAMETER
BY-PASS VALVE
PERISTALTIC PUMP
ELECTROLYTE RESERVOIR

figure 16

Schematic diagram of apparatus

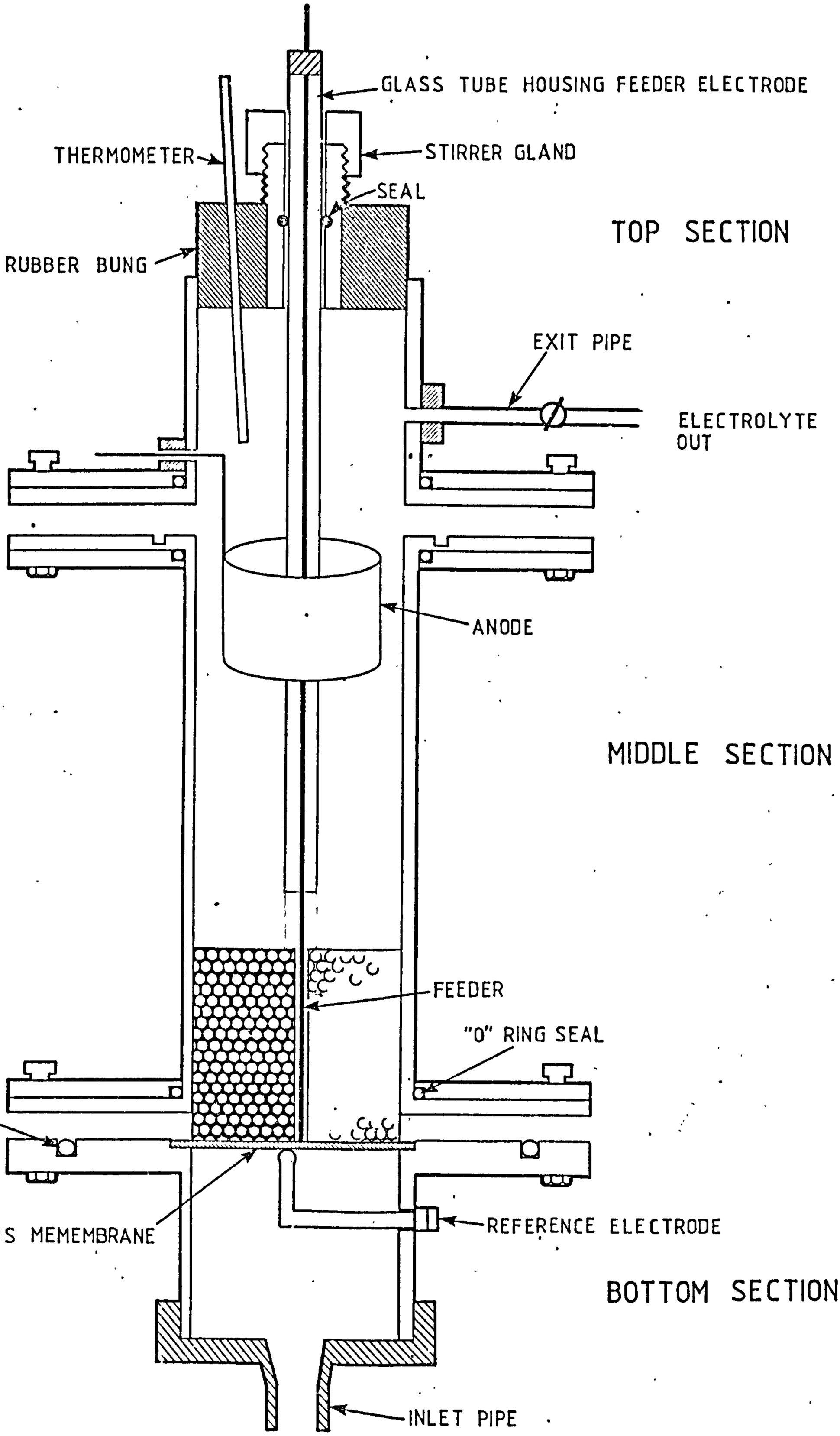
GLASS TUBE HOUSING FEEDER ELECTRODE
THERMOMETER
STIRRER GLAND
SEAL
RUBBER BUNG
TOP SECTION
EXIT PIPE
ELECTROLYTE OUT
ANODE
MIDDLE SECTION
FEEDER
"O" RING SEAL
"O" RING-SEAL
VYAN POROUS MEMEMBRANE
REFERENCE ELECTRODE
BOTTOM SECTION
INLET PIPE
ELECTROLYTE IN

figure 17

Schematic diagram of the apparatus
used with cylinder cathodes

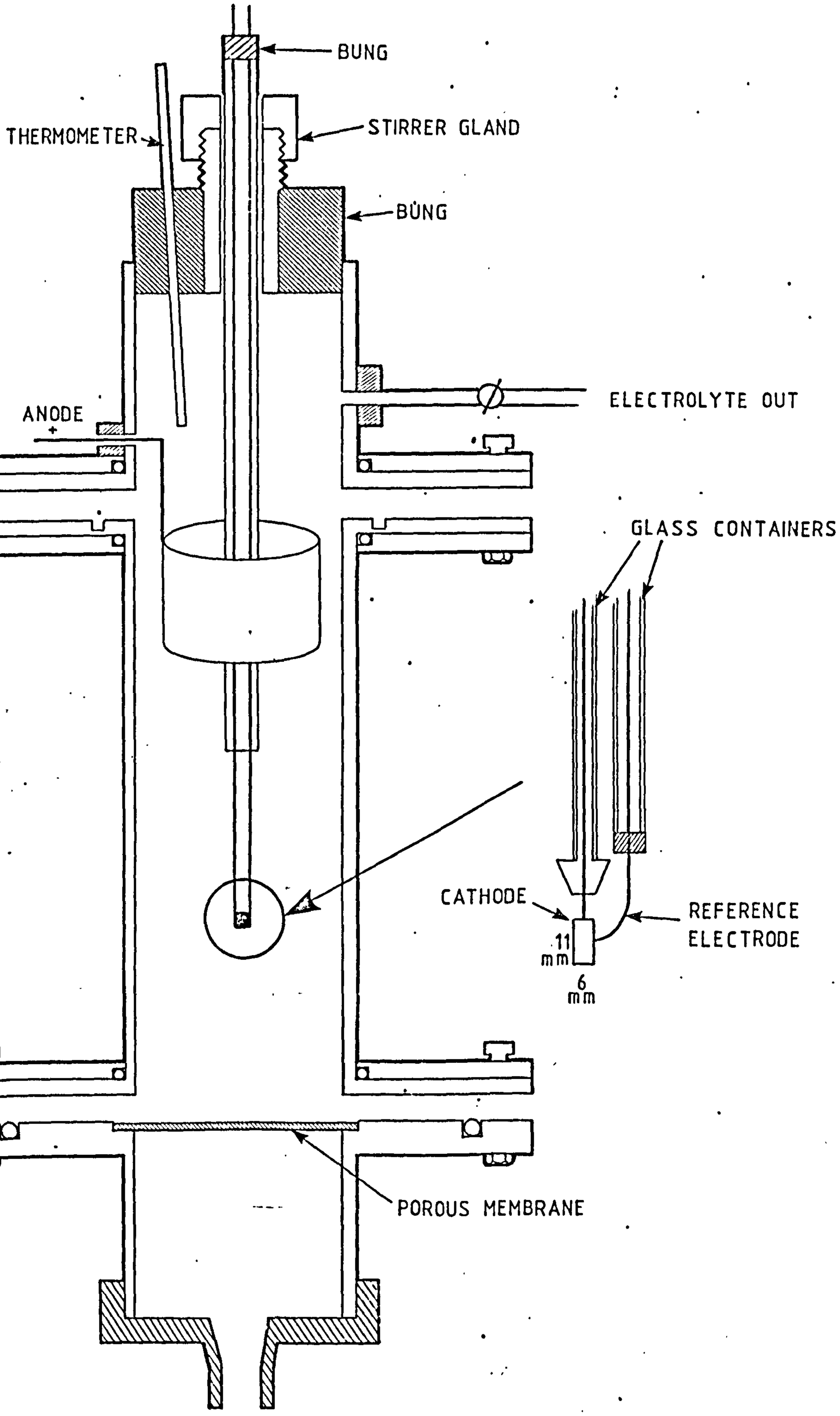
BUNG
THERMOMETER
STIRRER GLAND
BÜNG
ANODE
+
ELECTROLYTE OUT
GLASS CONTAINERS
CATHODE
REFERENCE ELECTRODE
11 mm
6 mm
POROUS MEMBRANE
ELECTROLYTE IN

figure 18

Diagrams to indicate the different conditions that can exist at an electrode.

a) Fully developed hydrodynamic conditions.

b) Non-fully developed hydrodynamic conditions.

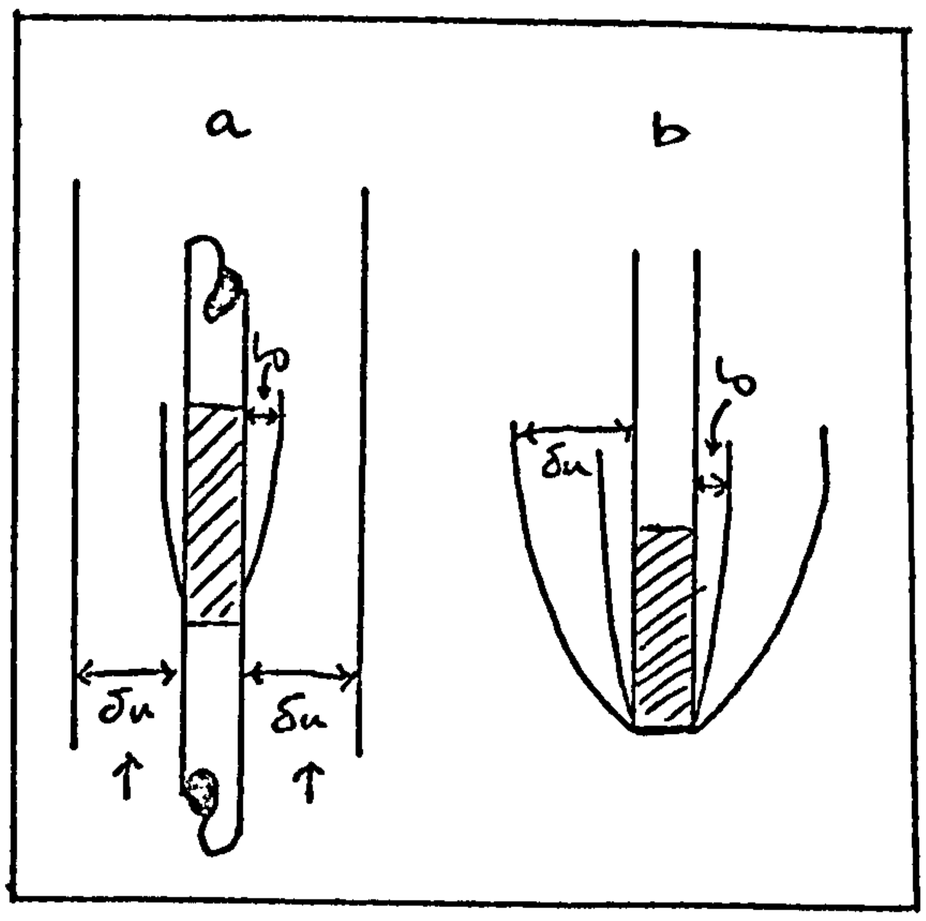
a
b
δ_0
δu
δu
δu
δ_0

figure 19

Change in the optical density of of a $CuSO_4$ solution with changing Cu^{2+}.

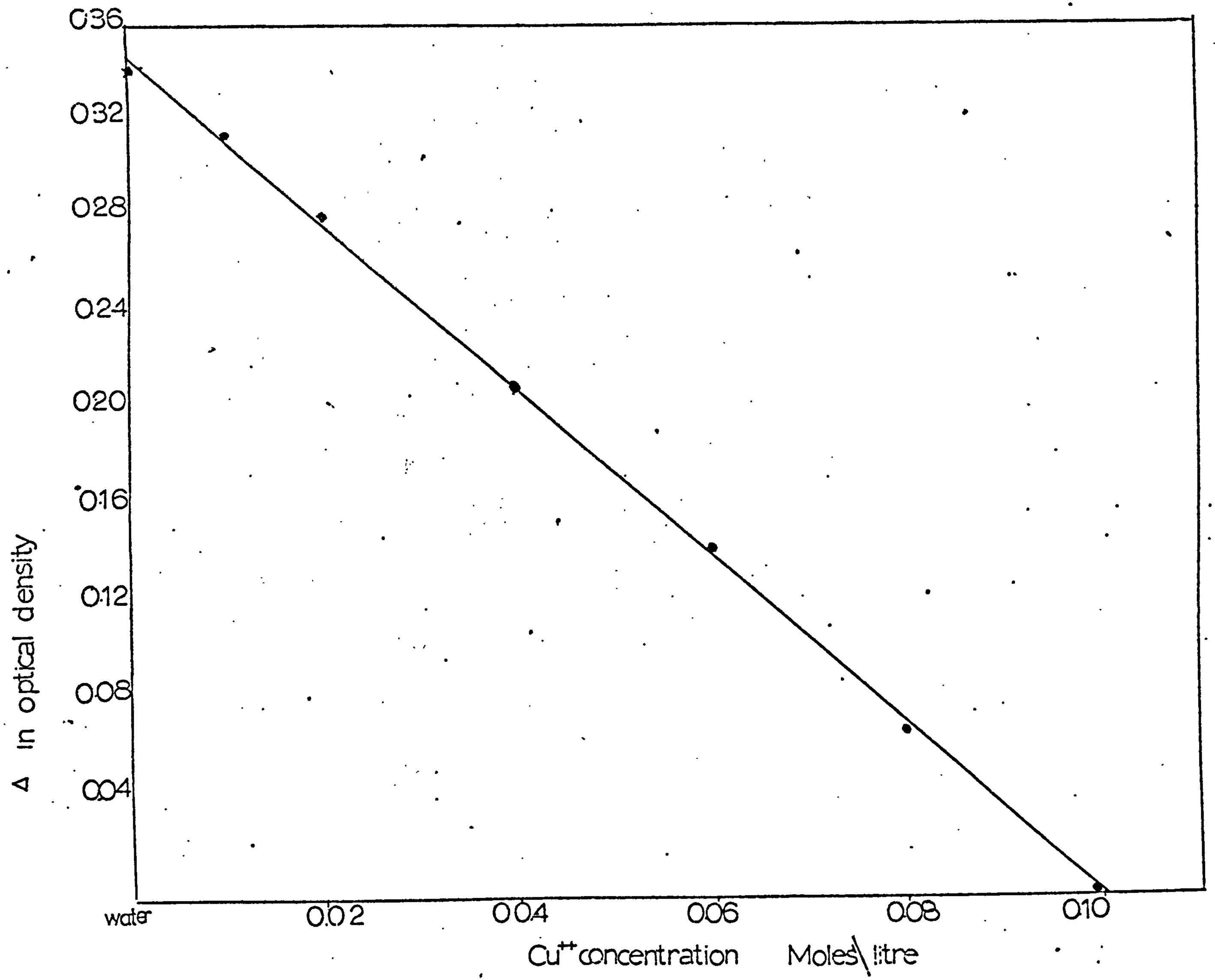
036
032
028
024
020
016
012
008
004
Δ In optical density
water
0.02
0.04
0.06
0.08
0.10
Cu++ concentration Moles\litre

figure 20

The conductivity of H_2SO_4 in water.

figure 21

Variation in the overpotential of hydrogen evolution on copper with sulphuric acid concentration.

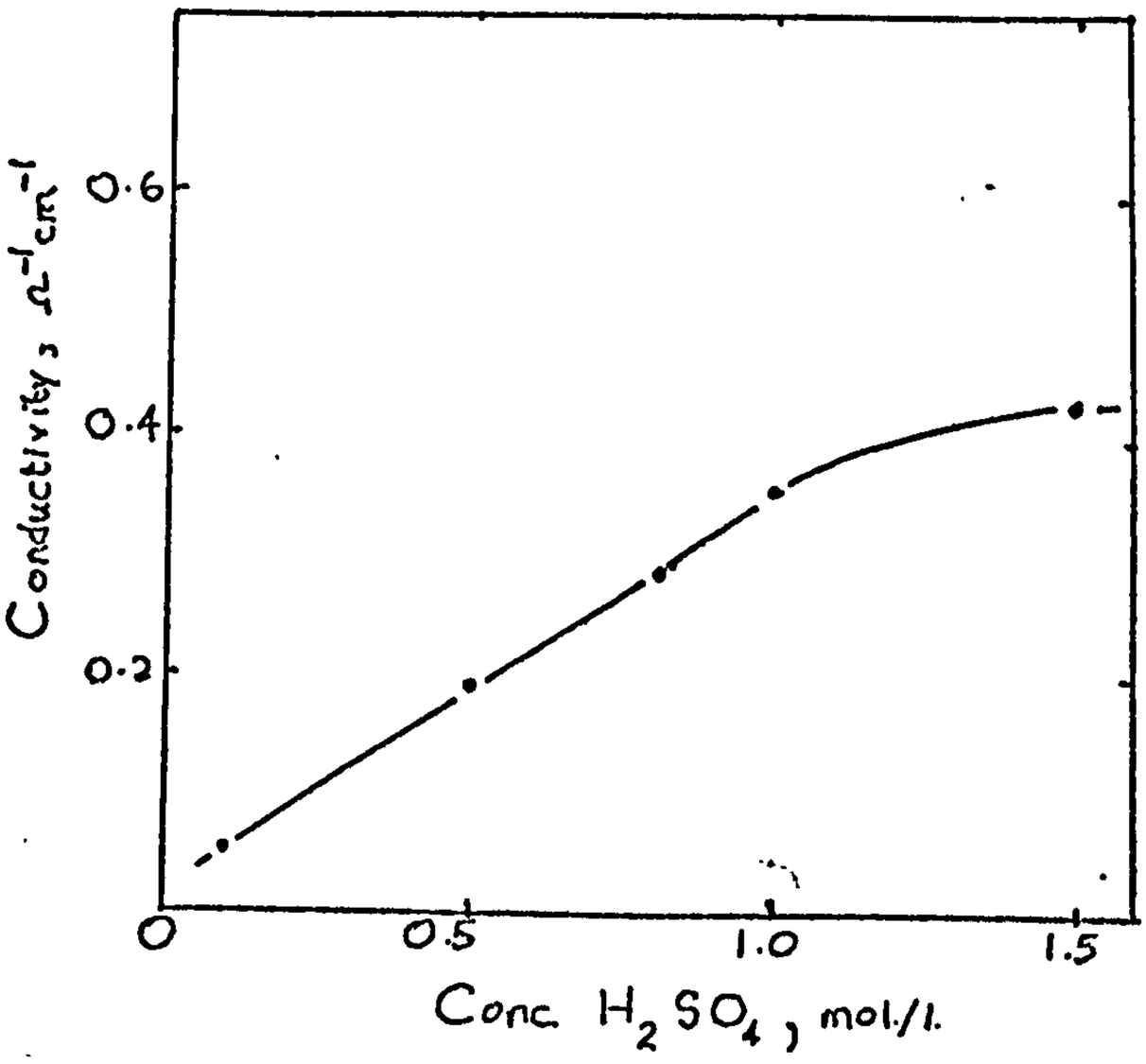
Conductivity, $\Omega^{-1}cm^{-1}$
0·6
0·4
0·2
0
0.5
1.0
1.5
Conc. H_2SO_4, mol./l.

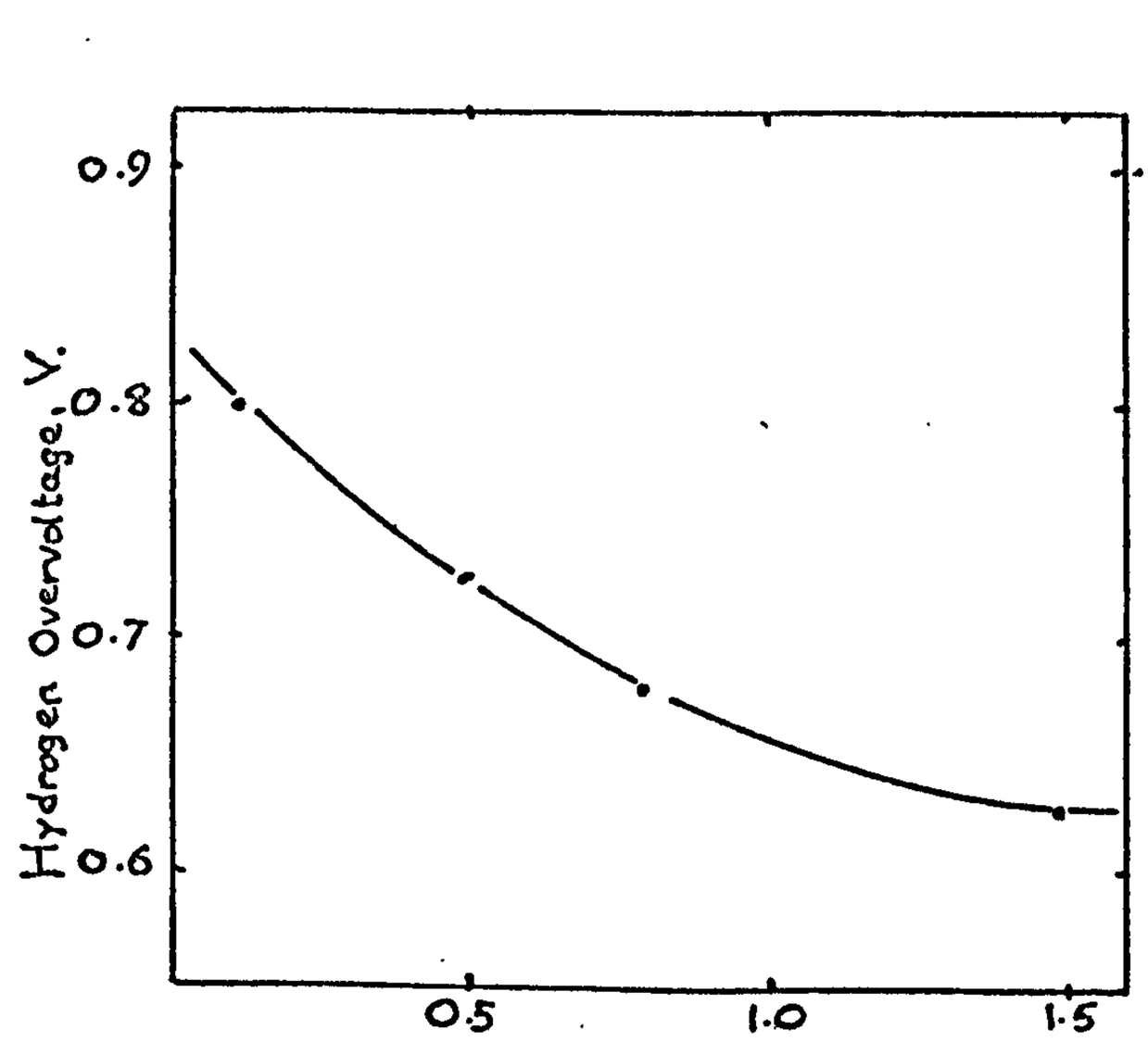
Hydrogen Overvoltage, V.
0.9
0.8
0.7
0.6
0.5
1.0
1.5
Conc. H_2SO_4, mol./l.

figure 22

Histogram of particle size distribution for 500 copper particles in the cut -70 - +100 mesh.

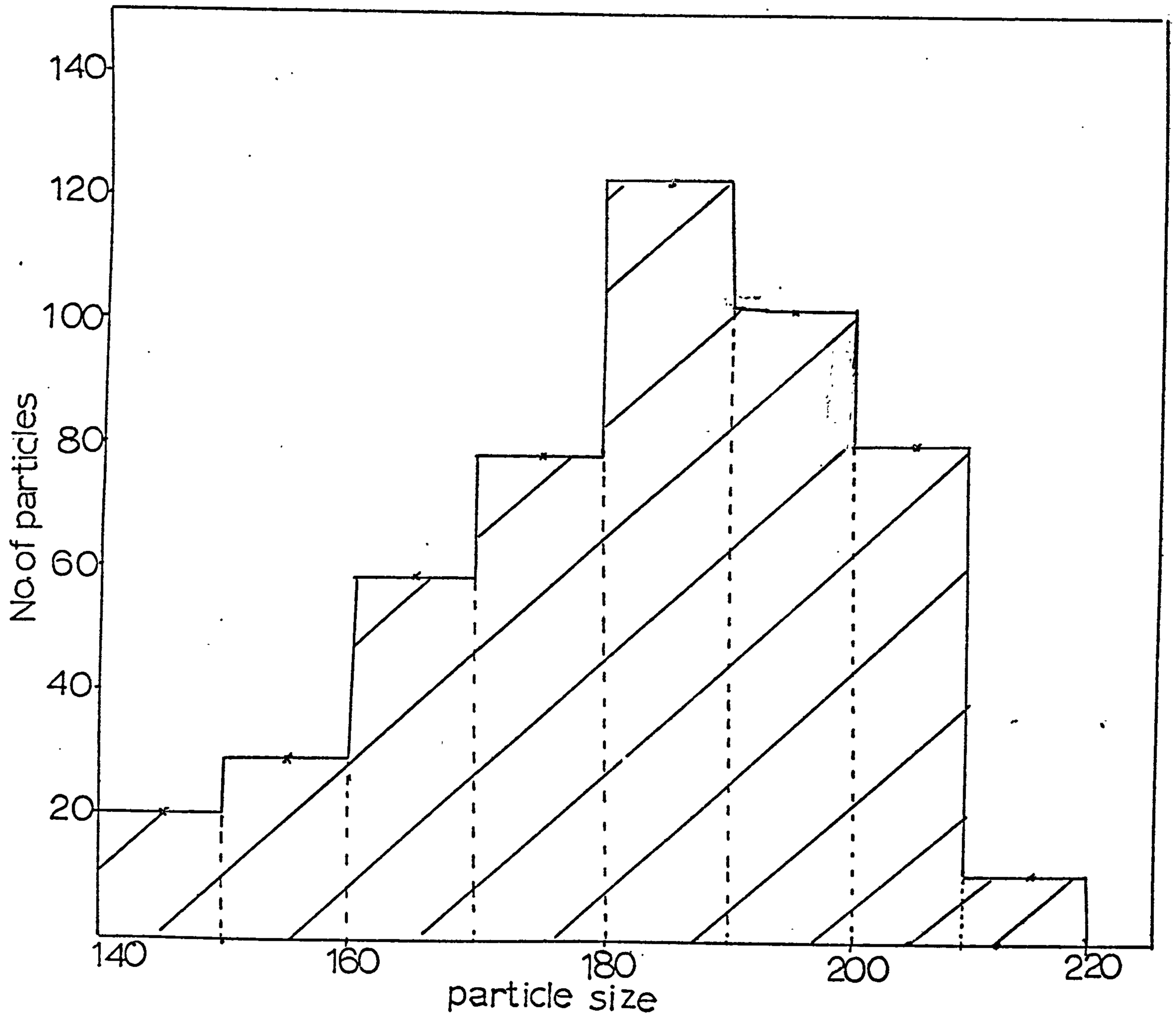
140
120
100
80
60
40
20
No of particles
140
160
180
200
220
particle size

figure 23

S curve distribution for 500 copper particles in the cut -70 to +100 mesh.

mean particle size = 184 μm

standard deviation = 17 μm

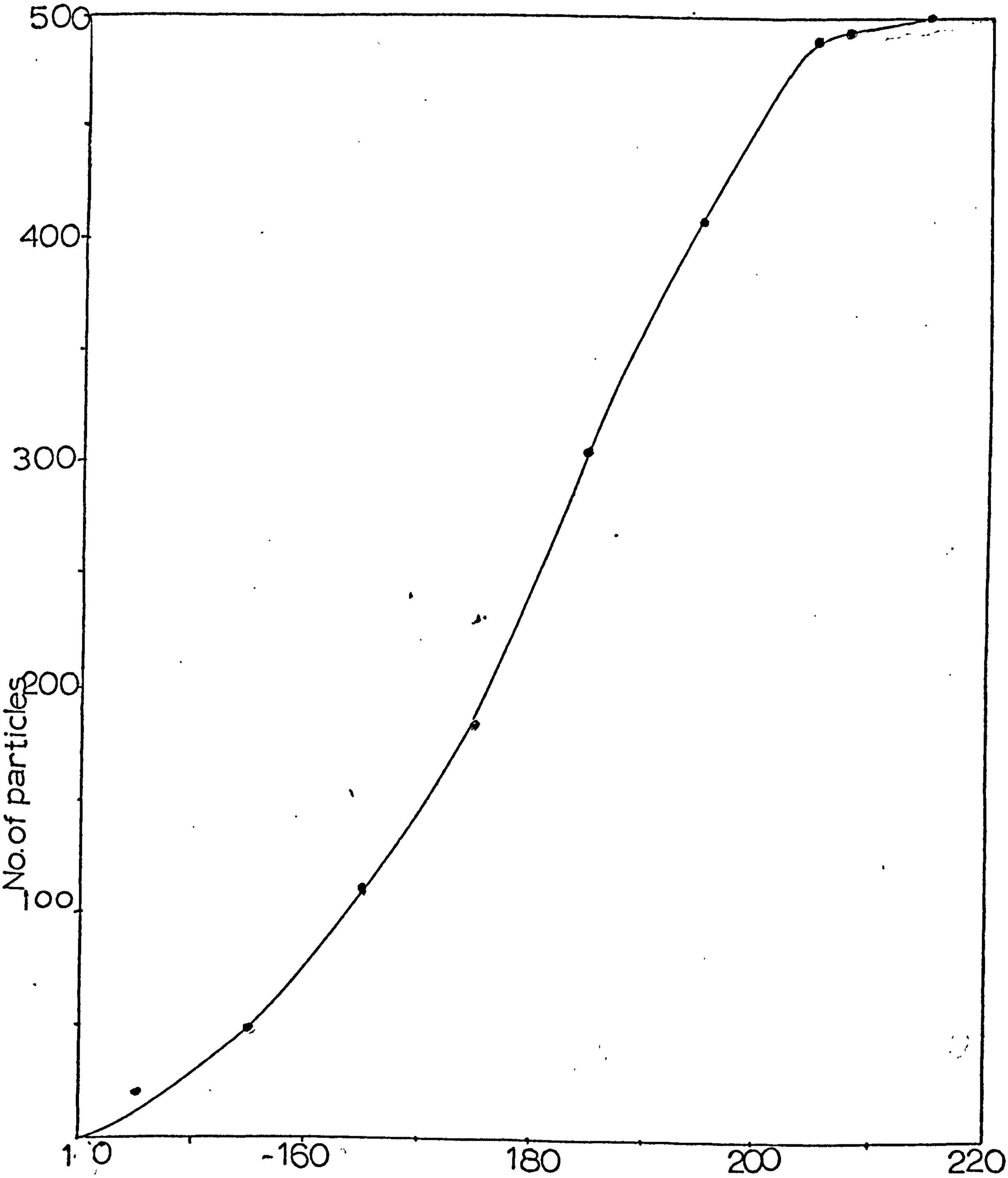
500
400
300
200
100
No. of particles
1·0
-160
180
200
220
particle size

figure 24

Rotameter calibration curves using the '7K' Rotameter.

a) 0.07M $CuSO_4$ + 0.5M H_2SO_4

b) H_2O

figure 25

Rotameter calibration curves using the '14K' Rotameter.

a) 0.07M $CuSO_4$ + 0.5M H_2SO_4

b) H_2O

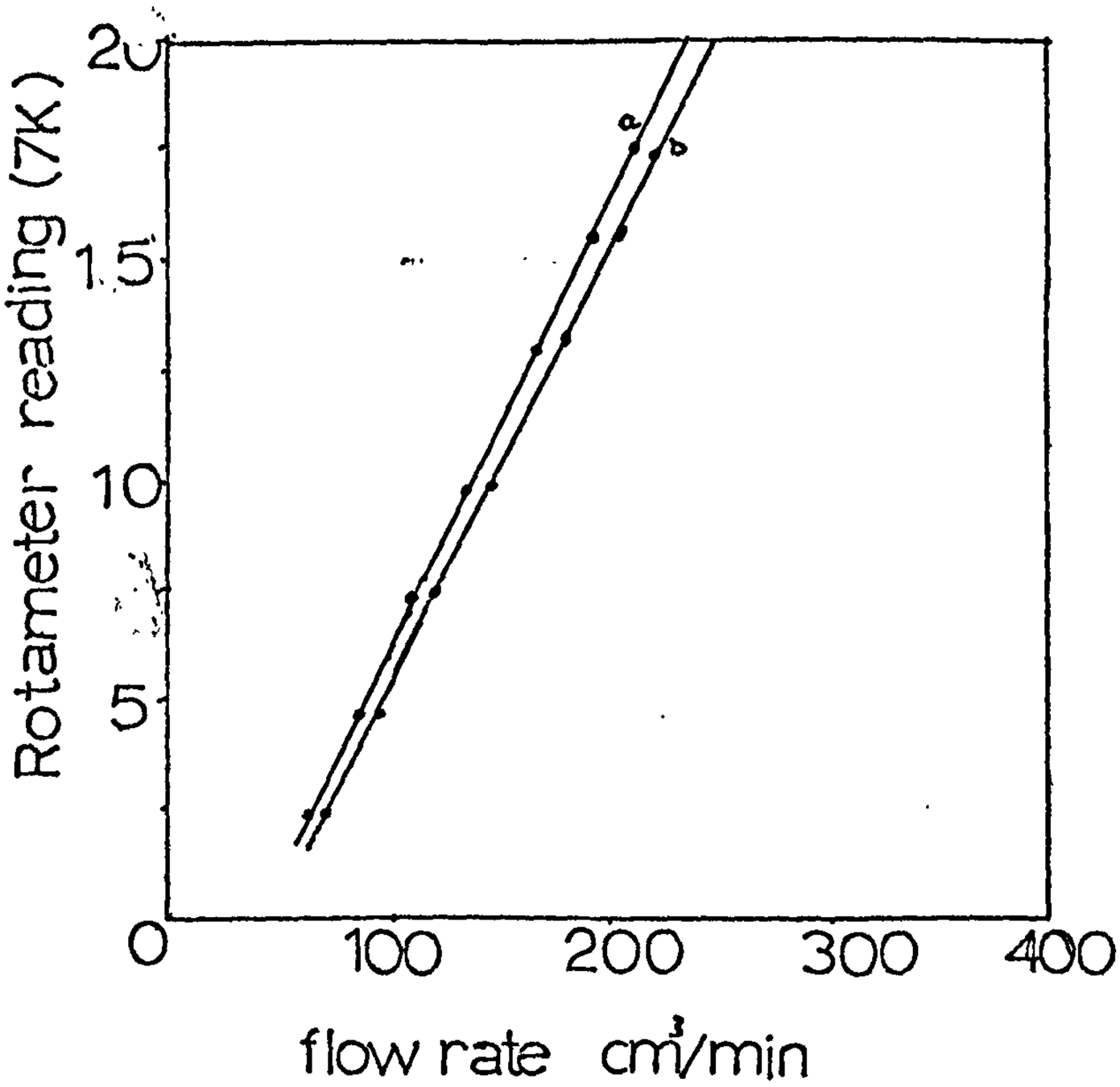
Rotameter reading (7K)
2
1.5
1
0.5
0
a
b
0
100
200
300
400
flow rate cm³/min

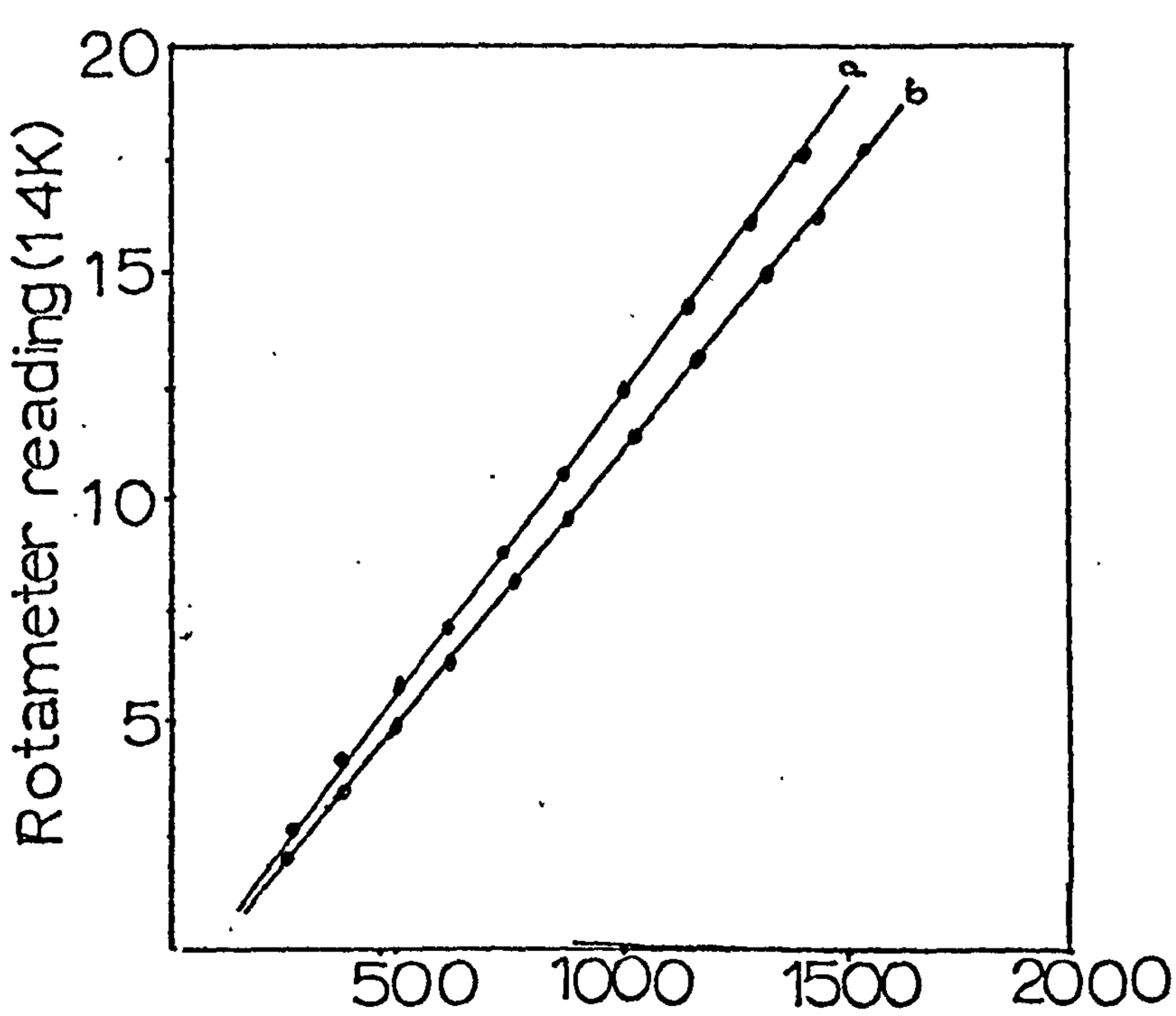
Rotameter reading(14K)
20
15
10
5
a
b
500
1000
1500
2000
flow rate cm³/min

figure 26

Calibration of the 'Linear Sweep Generator' against a Vibron Electrometer.

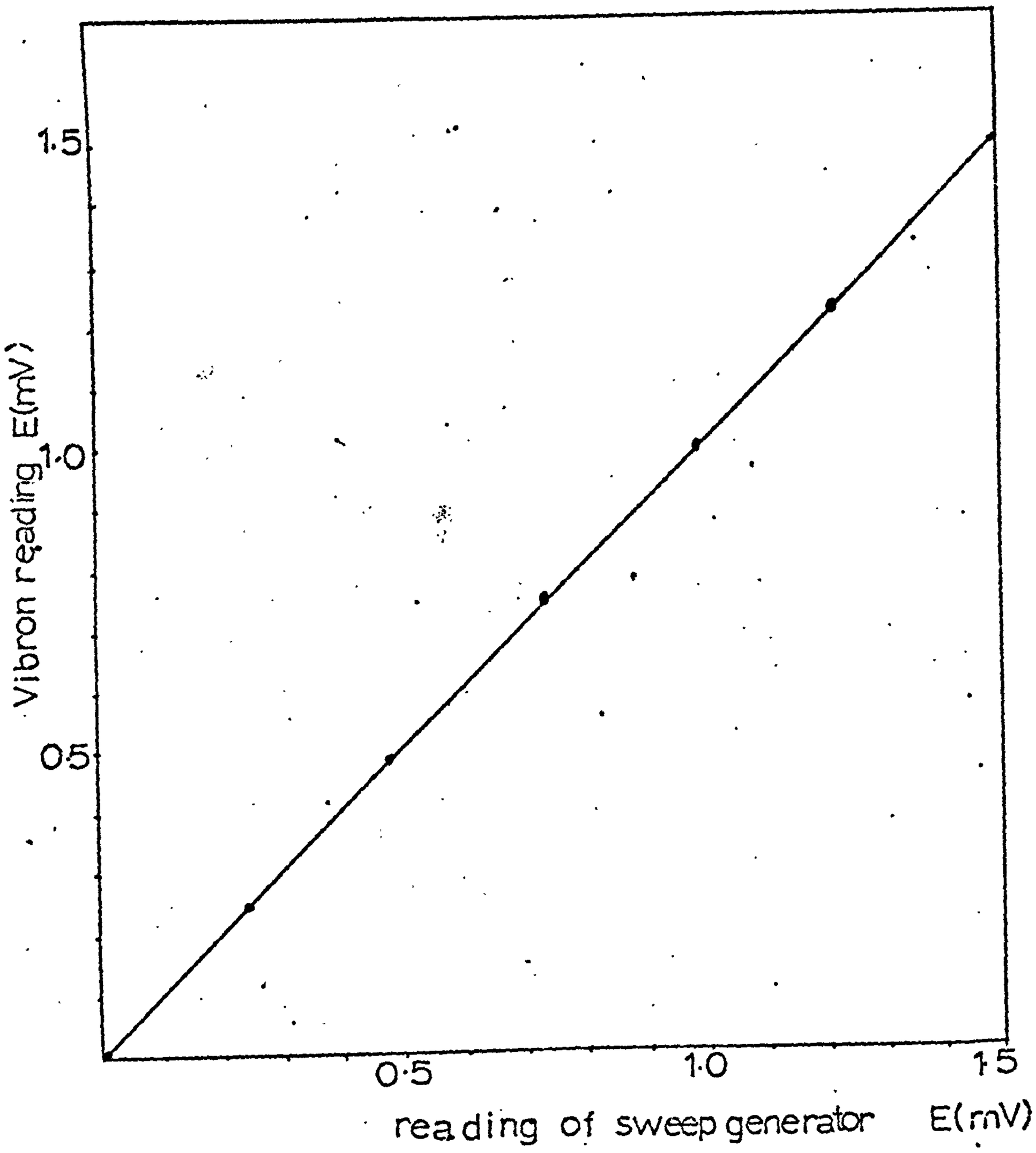
1·5
1·0
0·5
Vibron reading E(mV)
0·5
1·0
1·5
reading of sweep generator E(mV)

figure 27

Effect of sweep rate on polarization curves in stagnant solution. 0.07M Cu^{++}. feeder electrode length: 3.2cms

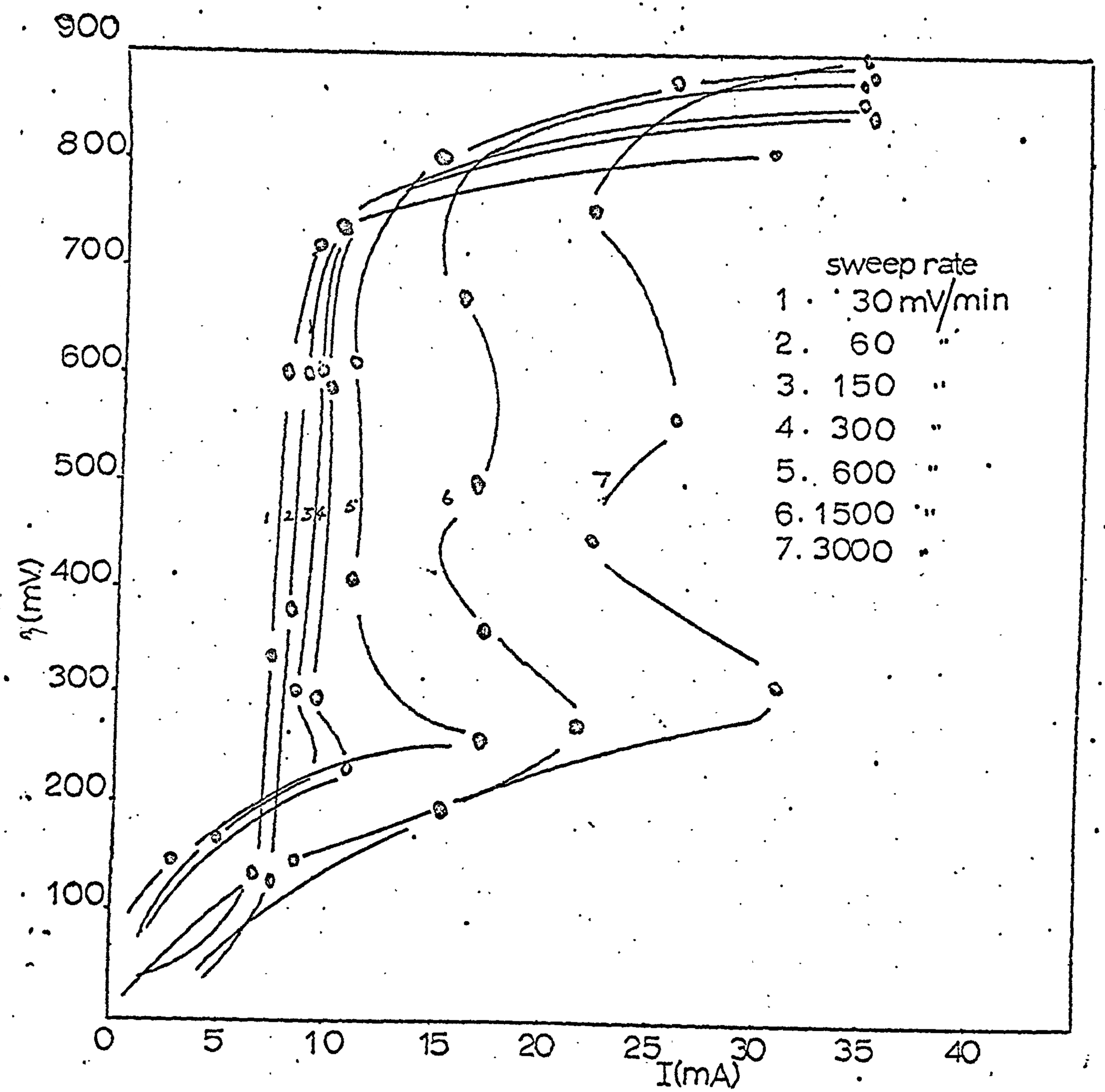
900
800
700
600
500
400
300
200
100
η(mV)
0
5
10
15
20
25
30
35
40
I(mA)
sweep rate
1. 30 mV/min
2. 60 "
3. 150 "
4. 300 "
5. 600 "
6. 1500 "
7. 3000 "

figure 28

Effect of sweep rate on polarization curves in flowing solution. 0.07M Cu^{++}., feeder electrode length 3.2 cms, flow rate 0.5 cm/sec.

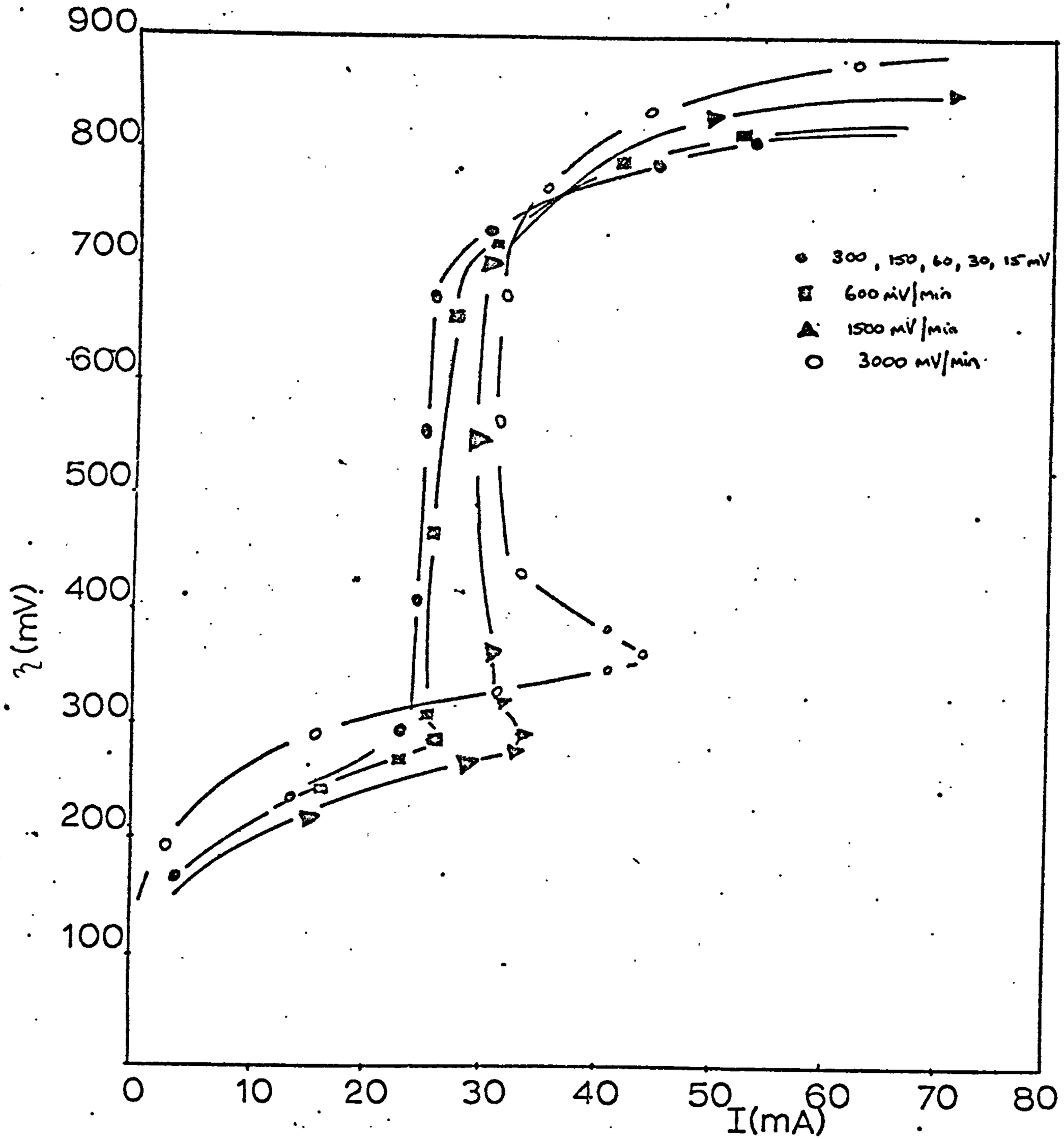
900
800
700
600
500
400
300
200
100
η (mV)
0
10
20
30
40
50
60
70
80
I(mA)
300, 150, 60, 30, 15 mV
600 mV/min
1500 mV/min
3000 mV/min

figure 29

Effect of sweep rate on polarization curves in a fluidised bed of copper particles. Static bed height 3.0cms.

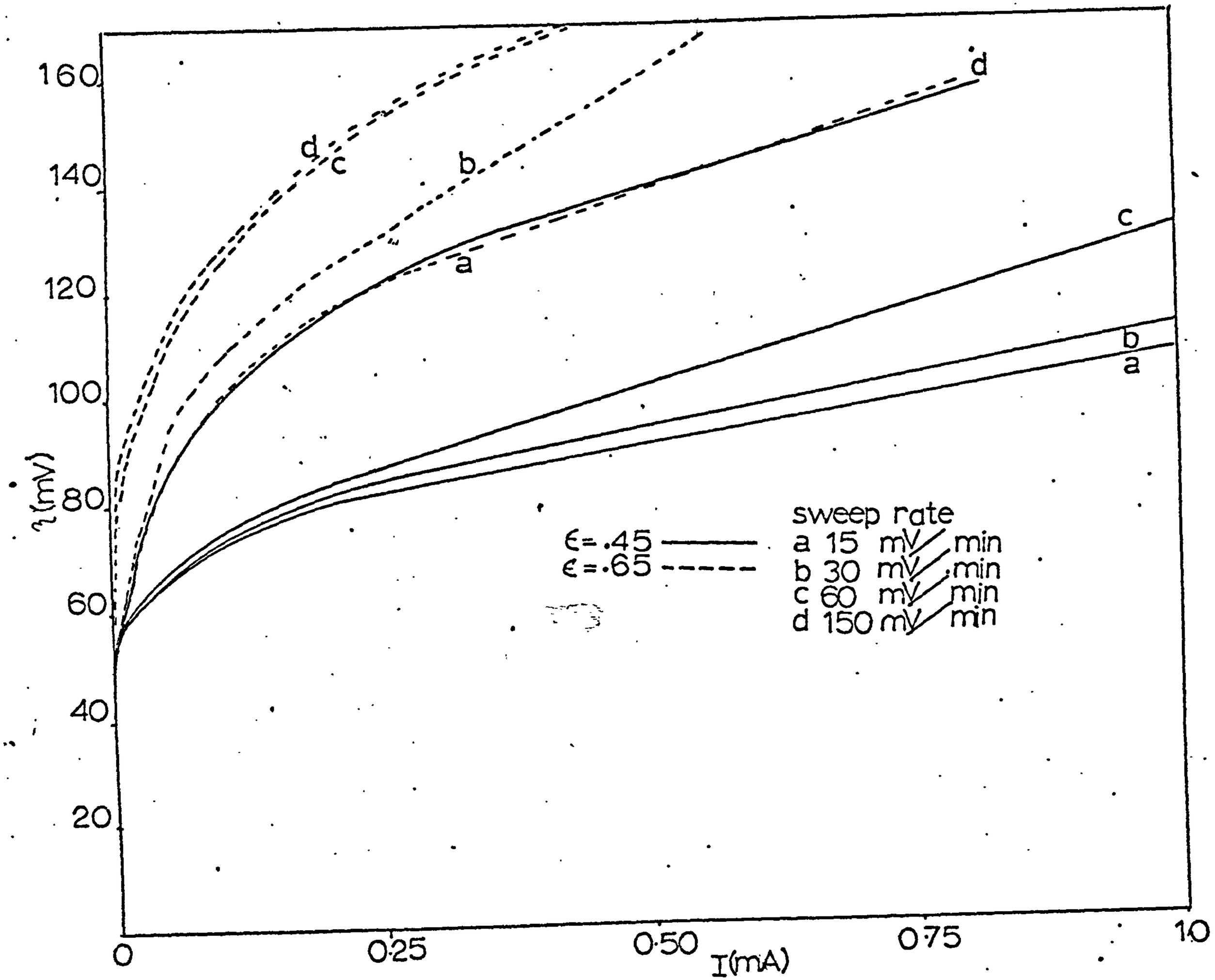
160
140
120
100
80
60
40
20
η(mV)
0
0·25
0·50
0·75
1·0
I(mA)
d
c
b
a
d
c
b
a
ϵ=.45
ϵ=.65
sweep rate
a 15 mV/min
b 30 mV/min
c 60 mV/min
d 150 mV/min

figure 30

The effect of axial height on the cathodic polarization curves for flow past cylindrical specimens in a tube. Specimen length 1.1cm dia. 0.625 cm .(0.07M $CuSO_4$ + 0.5M H_2SO_4)

Height above membrane:	10.1	8.0	6.0	5.8	4.9	4.1	2.9	1.8	1.0cms
Specimen No.	9	8	7	6	5	4	3	2	1

membrane present.

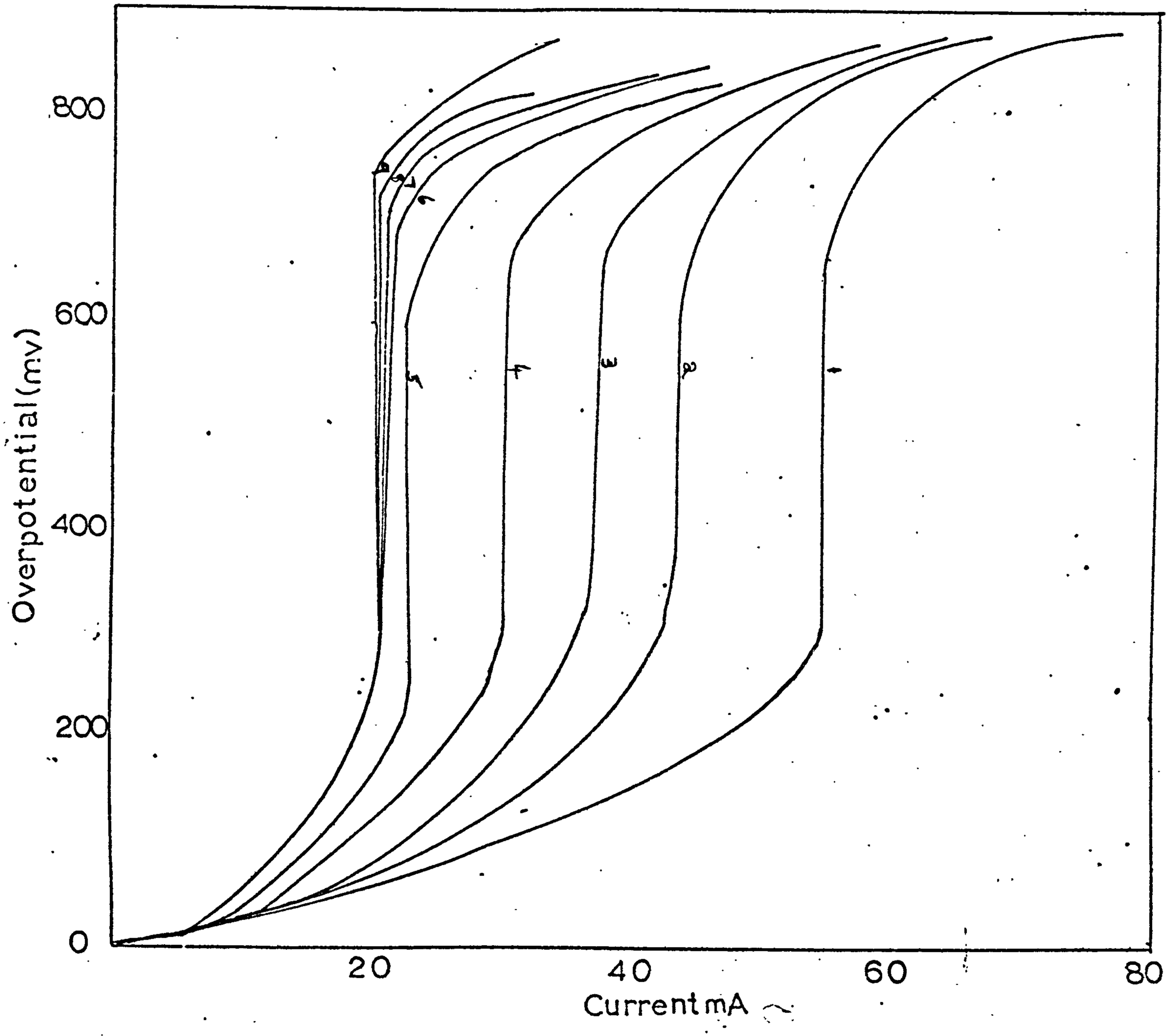
800
600
400
200
0
Overpotential(mv)
20
40
60
80
Current mA
1
2
3
4
5
6
7

figure 31

Effect of axial height on the cathodic polarization curves for flow past cylindrical specimens in a tube with no membrane present. Specimen length 1.1 cm dia. 0.625 cm. Solution 0.07M$CuSO_4$ + 0.5MH_2SO_4.

Height above membrane's normal position in the tube:	2.0	4.0	6.0	8.0	10.0	10.4	cms.
Specimen No. :	1	2	3	4	5	6	

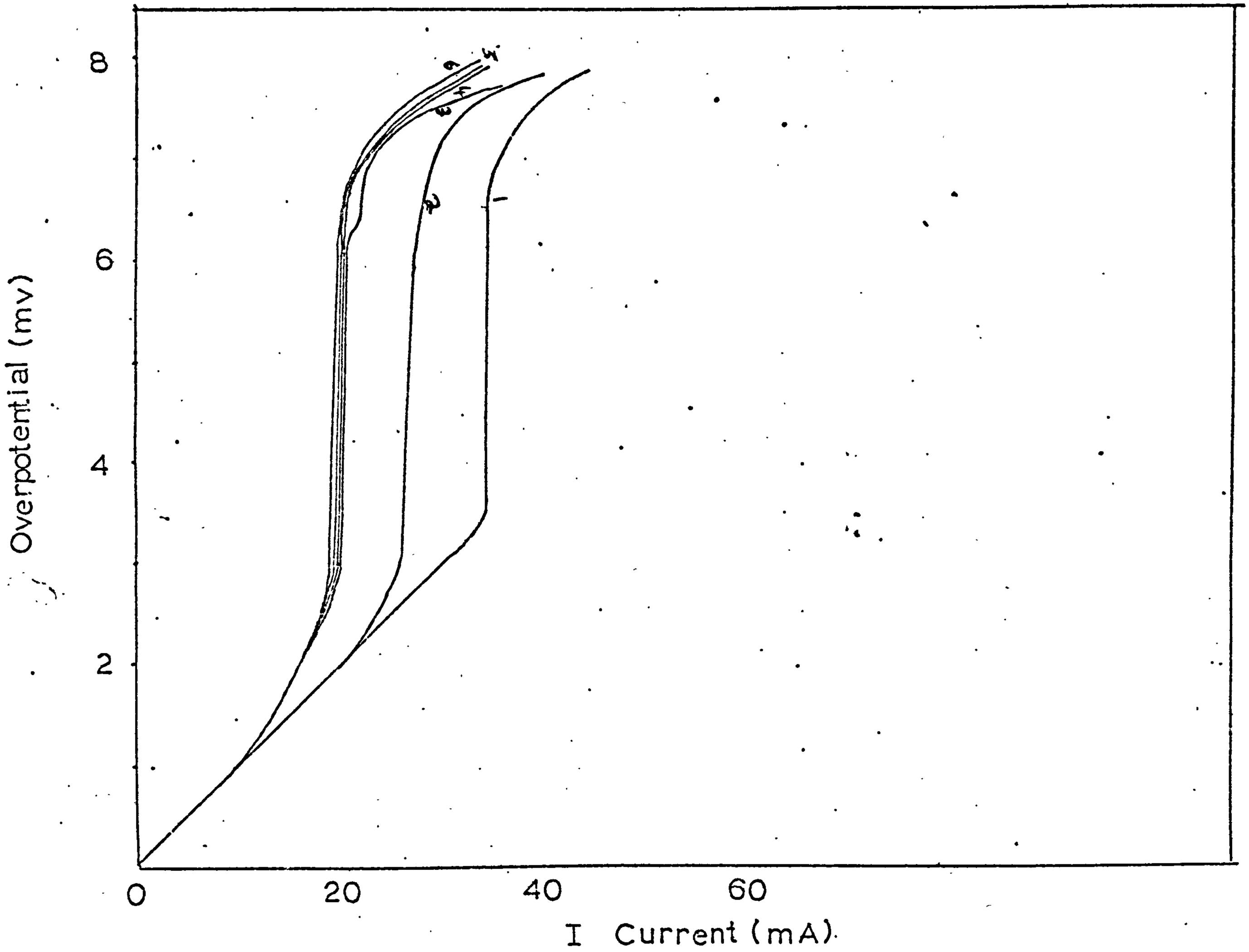
Overpotential (mv)
8
6
4
2
0
20
40
60
I Current (mA)
1
2
3
4
5

figure 32

Effect of axial height on limiting current values for flow past cylindrical specimens in a tube

□ = current values

× = current density values

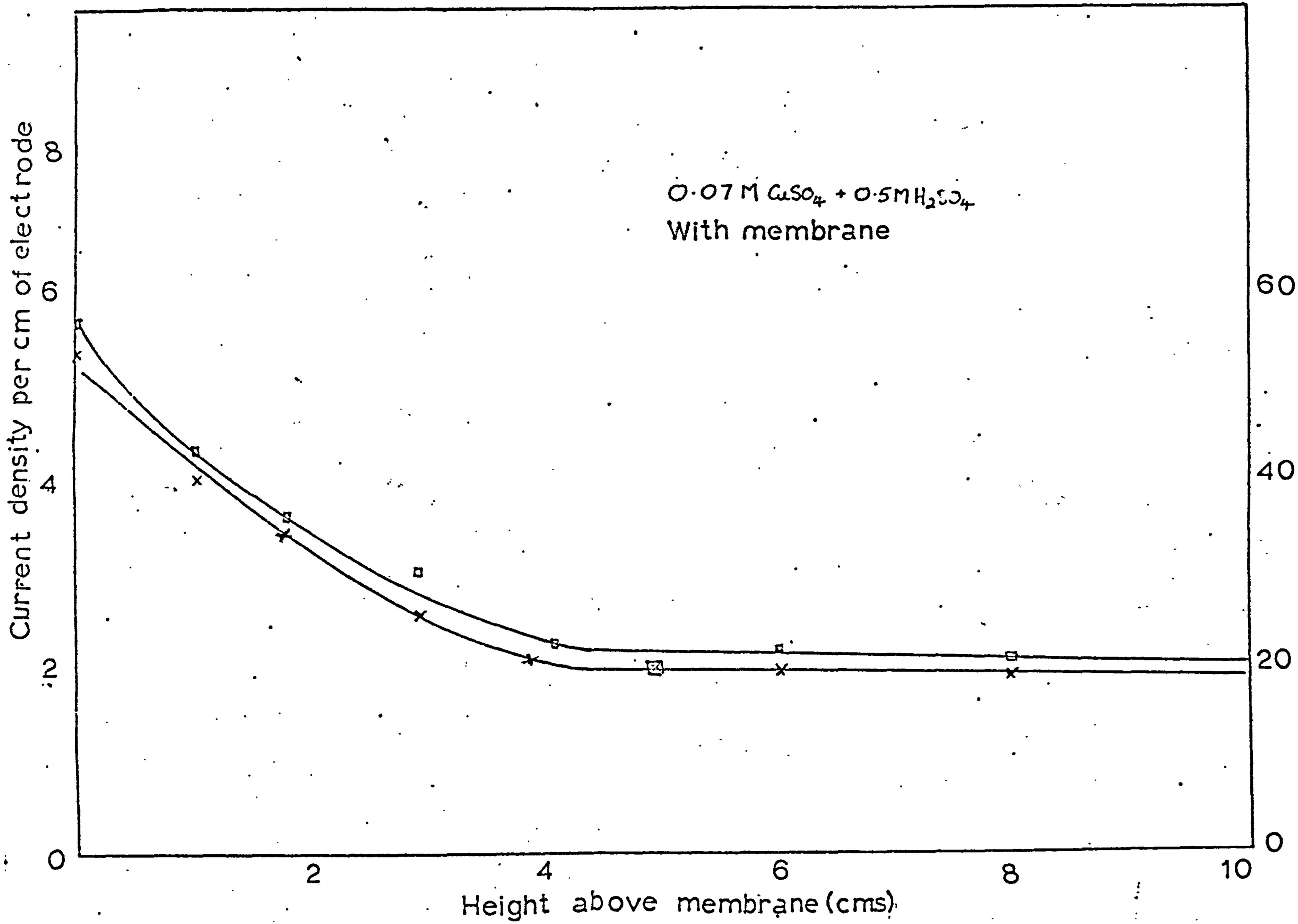
0·07 M CuSO4 + 0·5 M H2SO4
With membrane
Current density per cm of electrode
I
Height above membrane (cms)
0
2
4
6
8
10
20
40
60

figure 33

Effect of axial height on limiting current values for flow past cylindrical specimens in a tube.

0 07M $CuSO_4$ + 0.5M H_2SO_4.

specimen size 1.1 cm long 0.625 cm dia.

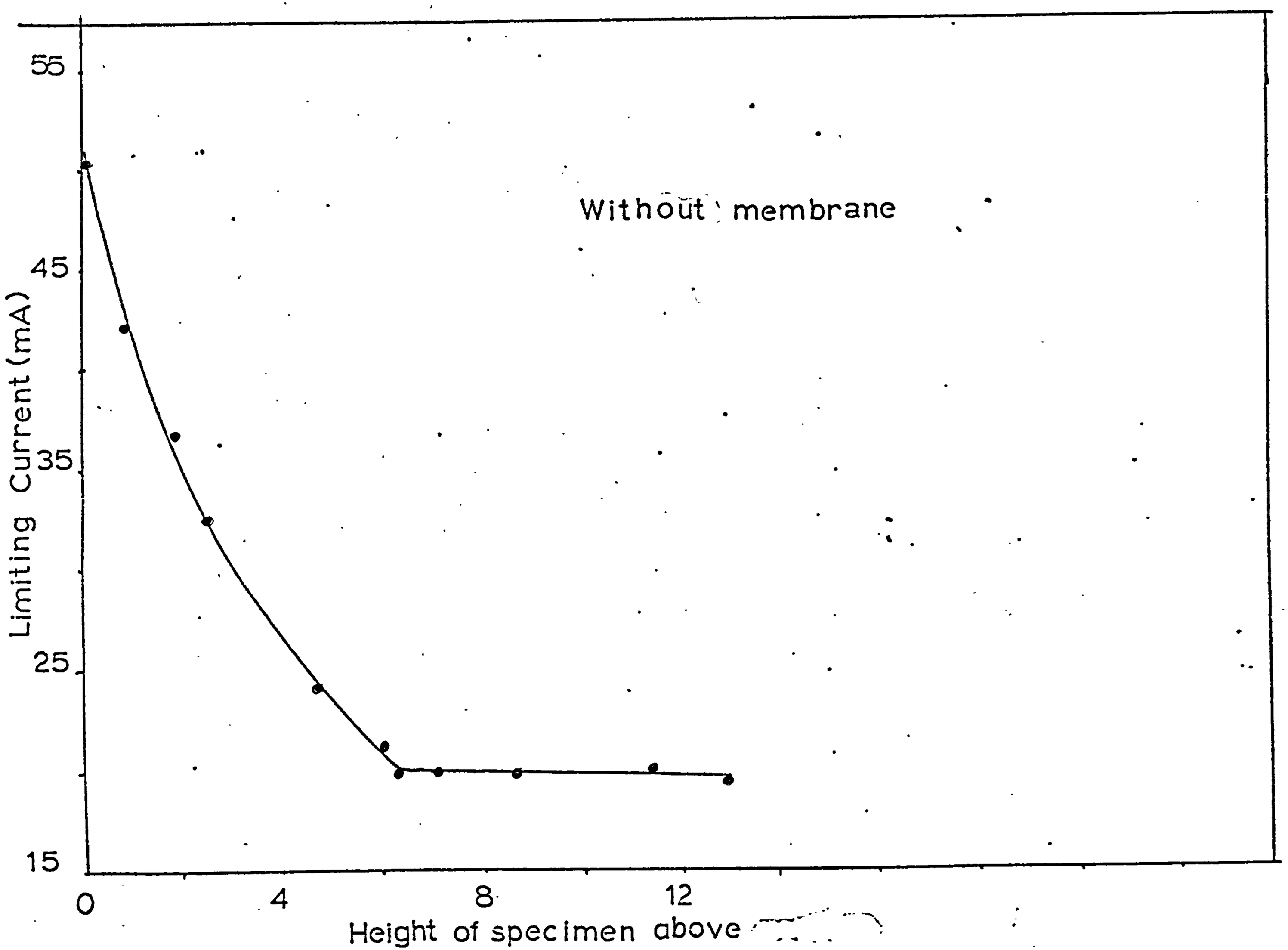
Without membrane
55
45
35
25
15
Limiting Current (mA)
0
4
8
12
Height of specimen above

figure 3¼

Polarization curves for different specimen lengths in flowing electrolyte in an annulus.

Solution: 0.07M $CuSO_4$ + 0.5M H_2SO_4

flow rate: 1.4cm/sec

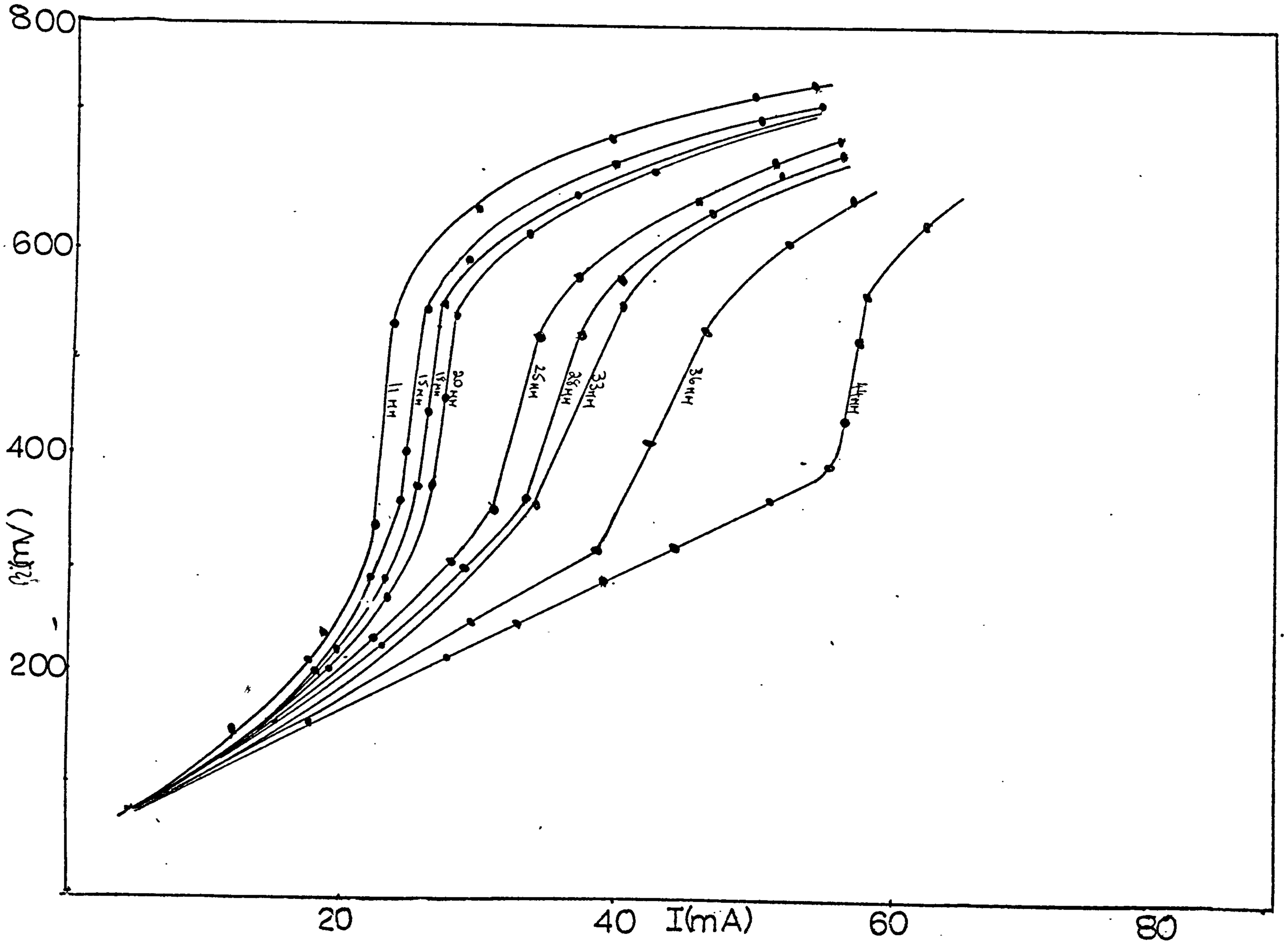
800
600
400
200
(mV)
20
40
I(mA)
60
80
11 MM
15MM
18MM
20 MM
25MM
29MM
33MM
36MM
44MM

figure 35

Effect of varying the specimen length on limiting currents for cylindrical specimens dia. 0.625 cm. Specimens placed 5cm above membrane. 0.07M $CuSO_4$ + 0.5M H_2SO_4 solution.

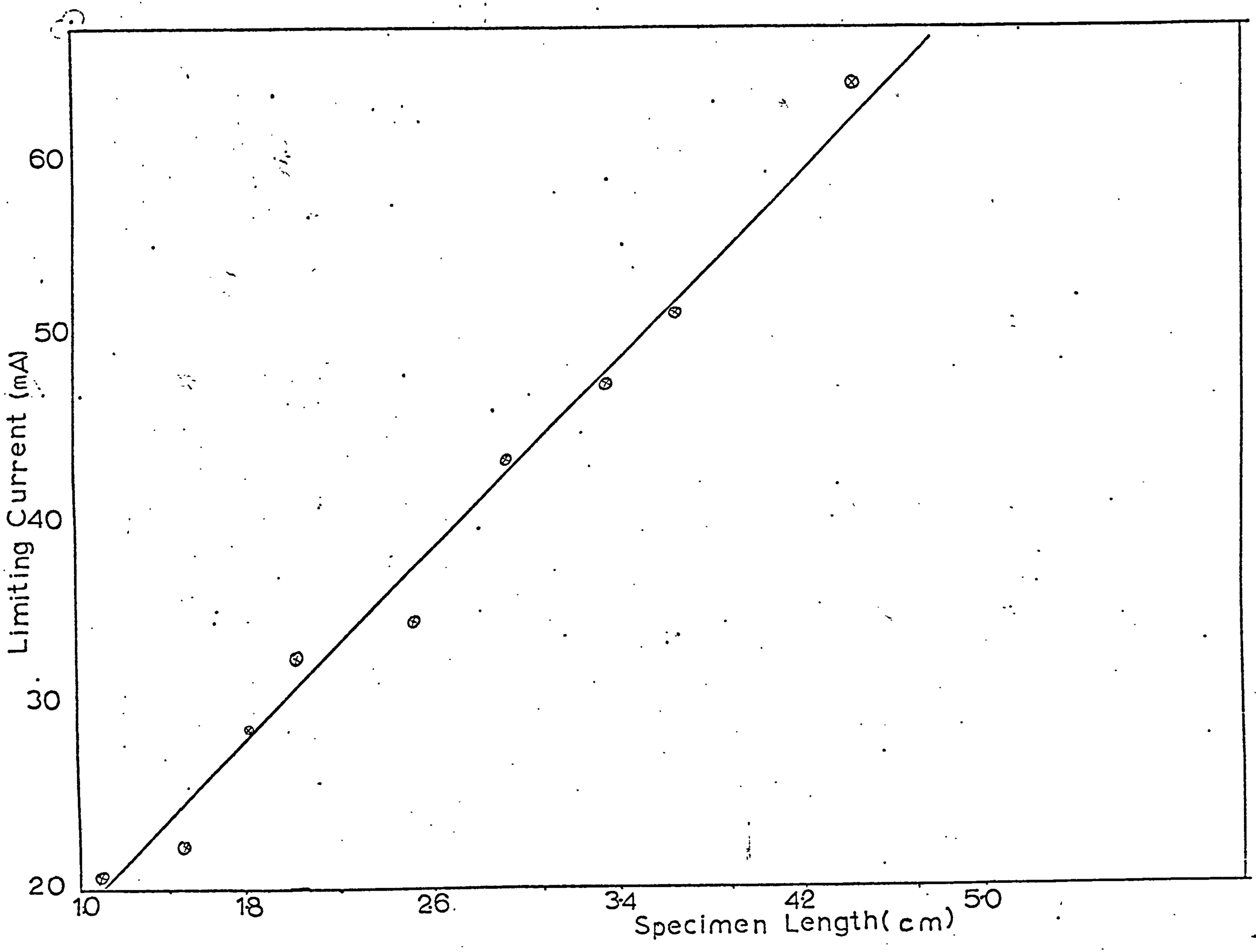
60
50
40
30
20
Limiting Current (mA)
10
18
26
34
42
50
Specimen Length(cm)

figure 36

Effect of flow rate on the hydrogen reaction at a copper feeder electrode in a tube, for various feeder lengths.

Equiv.ϵ is the equivalent porosity a fluidised bed would have if it were present.

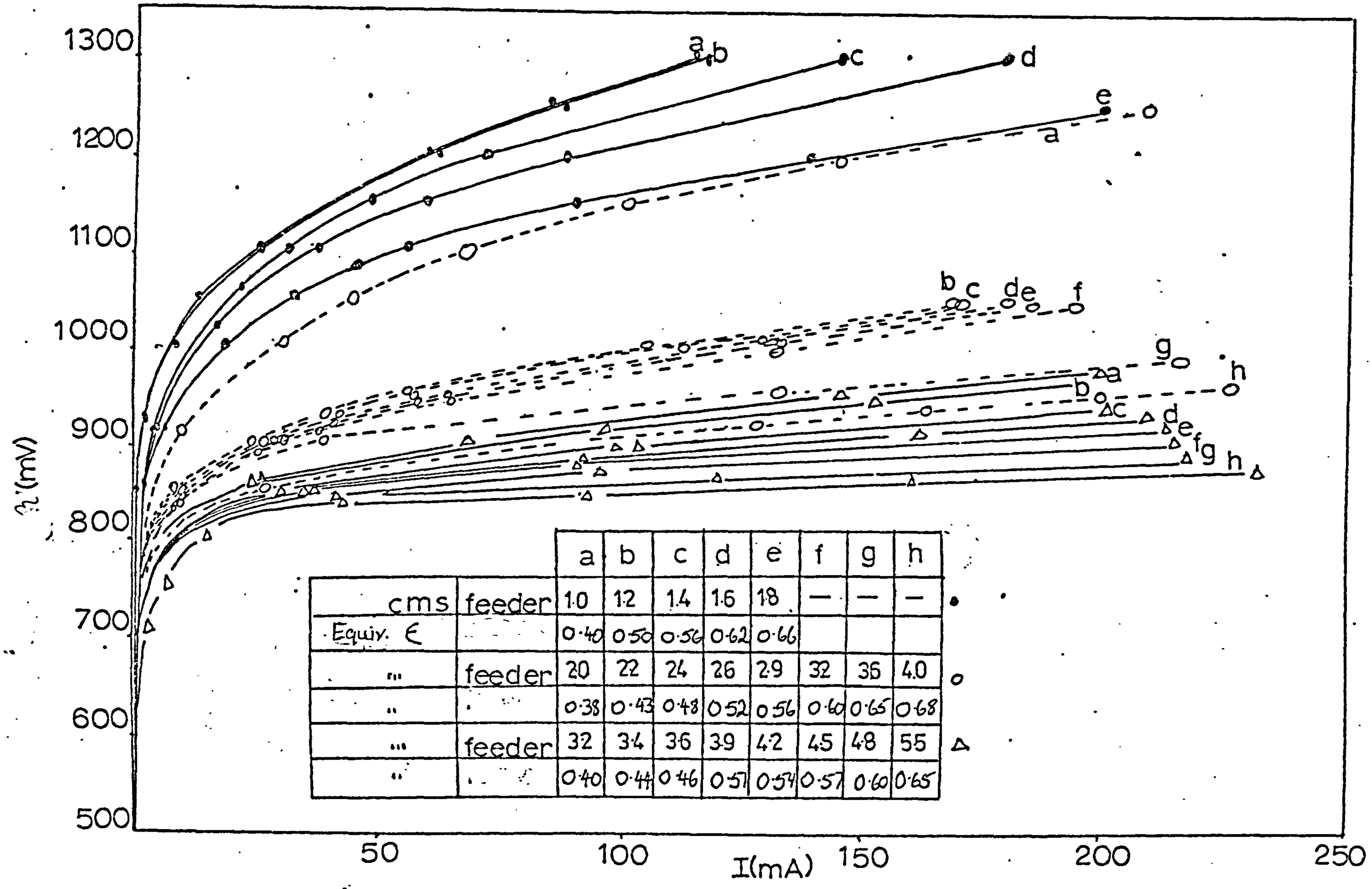

		a	b	c	d	e	f	g	h
cms	feeder	1·0	1·2	1·4	1·6	1·8	—	—	—
Equiv. ∈		0·40	0·50	0·56	0·62	0·66			
,,	feeder	2·0	2·2	2·4	2·6	2·9	3·2	3·6	4·0
,,		0·38	0·43	0·48	0·52	0·56	0·60	0·65	0·68
,,	feeder	3·2	3·4	3·6	3·9	4·2	4·5	4·8	5·5
,,		0·40	0·44	0·46	0·51	0·54	0·57	0·60	0·65

figure 37

Effect of feeder length on cathodic polarization curves in a tube. No electrolyte flow. 0.07M $CuSO_4$ + 0.5 H_2SO_4 solution.

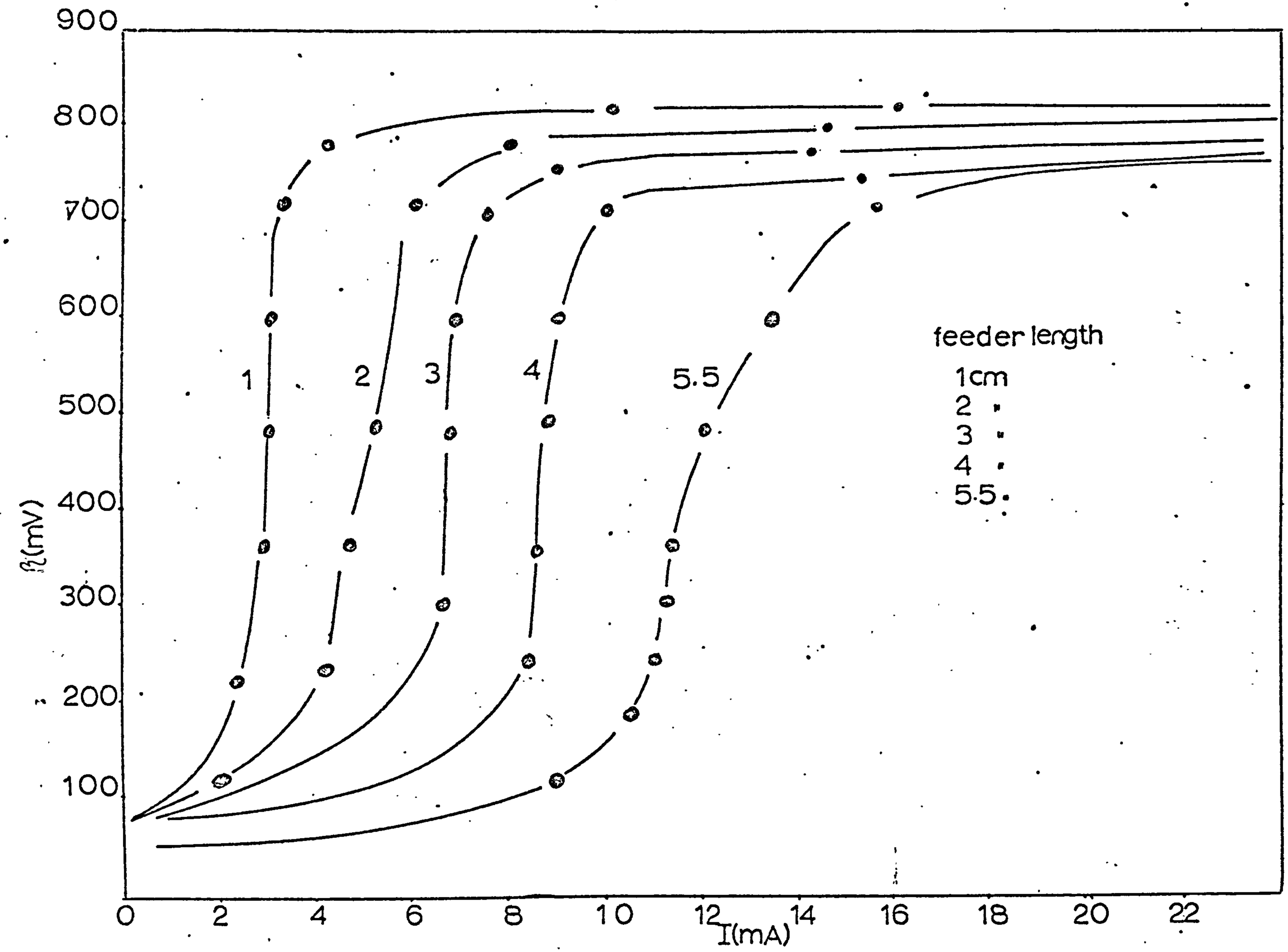
900
800
700
600
500
400
300
200
100
R(mV)
0
2
4
6
8
10
12
14
16
18
20
22
I(mA)
1
2
3
4
5.5
feeder length
1cm
2 "
3 "
4 "
5.5"

figure 38

Effect of flow rate on cathodic polarization curves in a tube.
Feeder length 1.0 cm.
0.07M $CuSO_4$ + H_2SO_4 solution.

Flow rate: :	0.19	0.38	0.58	0.77	0.96	1.16	cms/sec
Specimen No:	1	2	3	4	5	6	

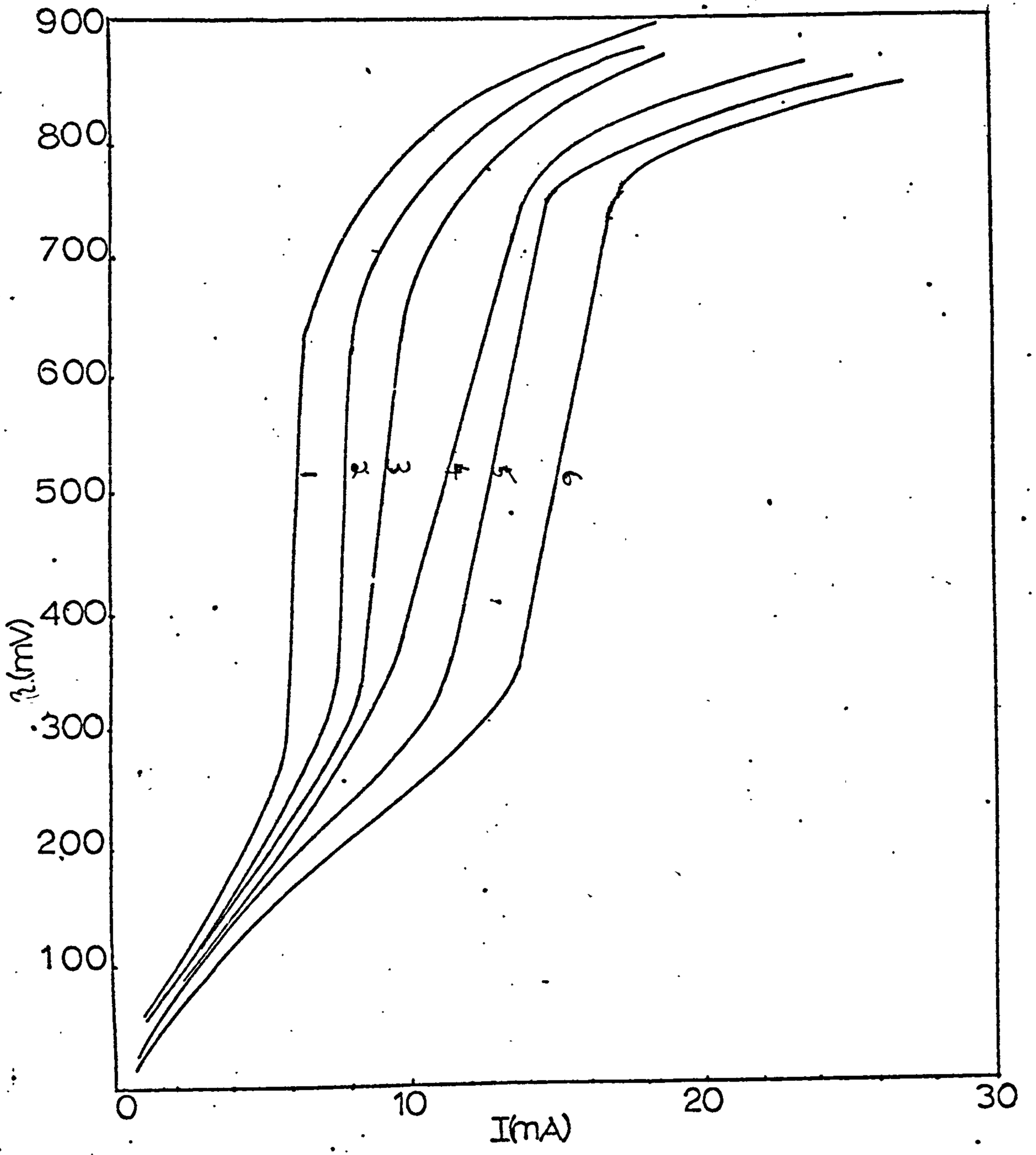
900
800
700
600
500
400
300
200
100
V(mV)
1
2
3
4
5
6
0
10
20
30
I(mA)

figure 39

Effect of flow on cathodic polarization curves, in a tube.
Feeder length = 3.2 cm.
0.07M $CuSO_4$ + 0.5 H_2SO_4

Flow rate :	0.19	0.38	0.58	0.77	0.96	1.16	cms/sec
Specimen No:	1	2	3	4	5	6	

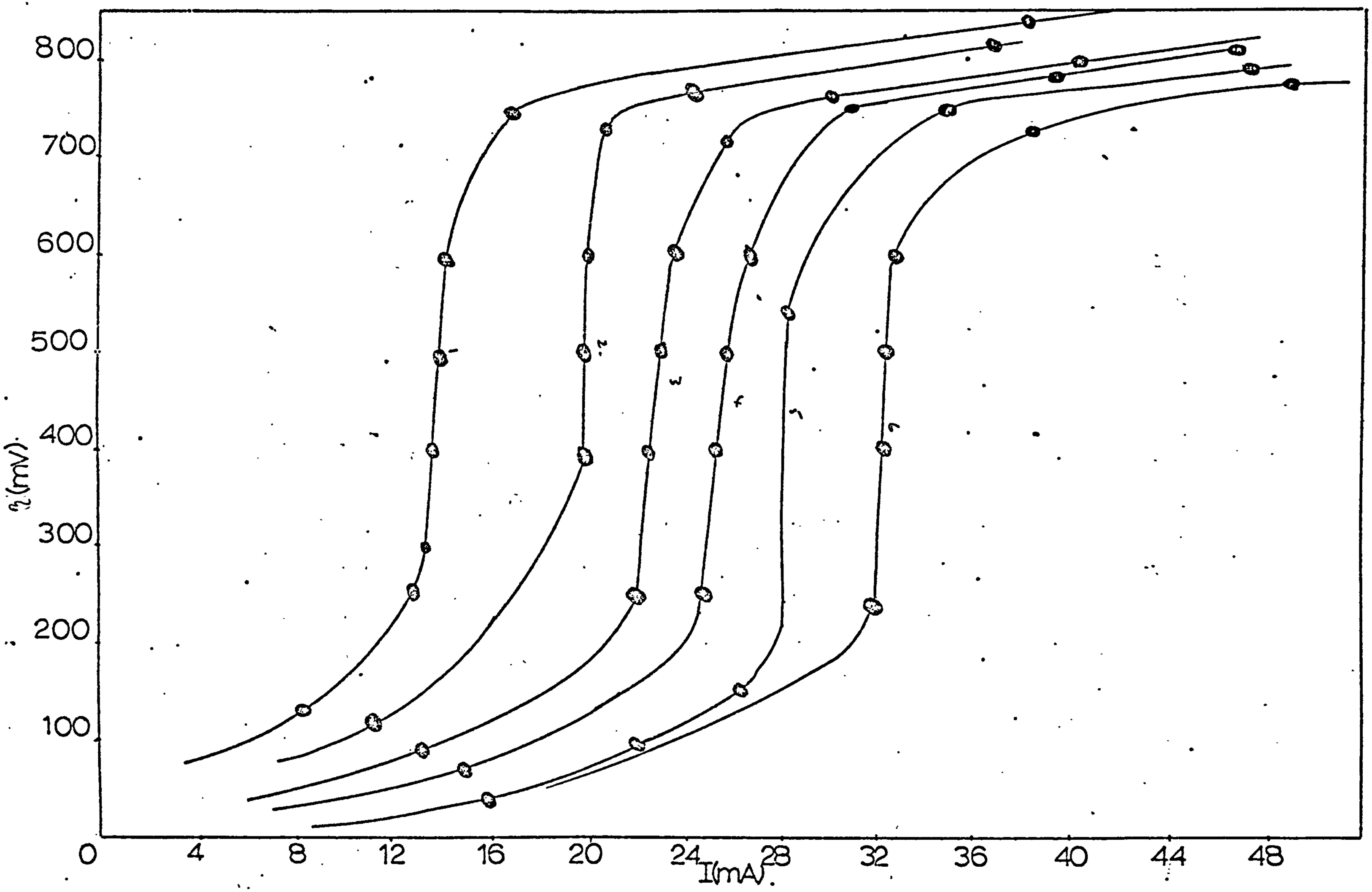
800
700
600
500
400
300
200
100
0
4
8
12
16
20
24
28
32
36
40
44
48
V(mV)
I(mA)
1
2
3
4
5
6
7

figure 40

Effect of flow on cathodic polarization curves, in a tube.
Feeder length = 5.0 cm
0.07M $CuSO_4$ + 0.5M H_2SO_4

Flow rate :	0.19	0.38	0.58	0.77	0.96	1.16	cms/sec
Specimen No:	1	2	3	4	5	6	

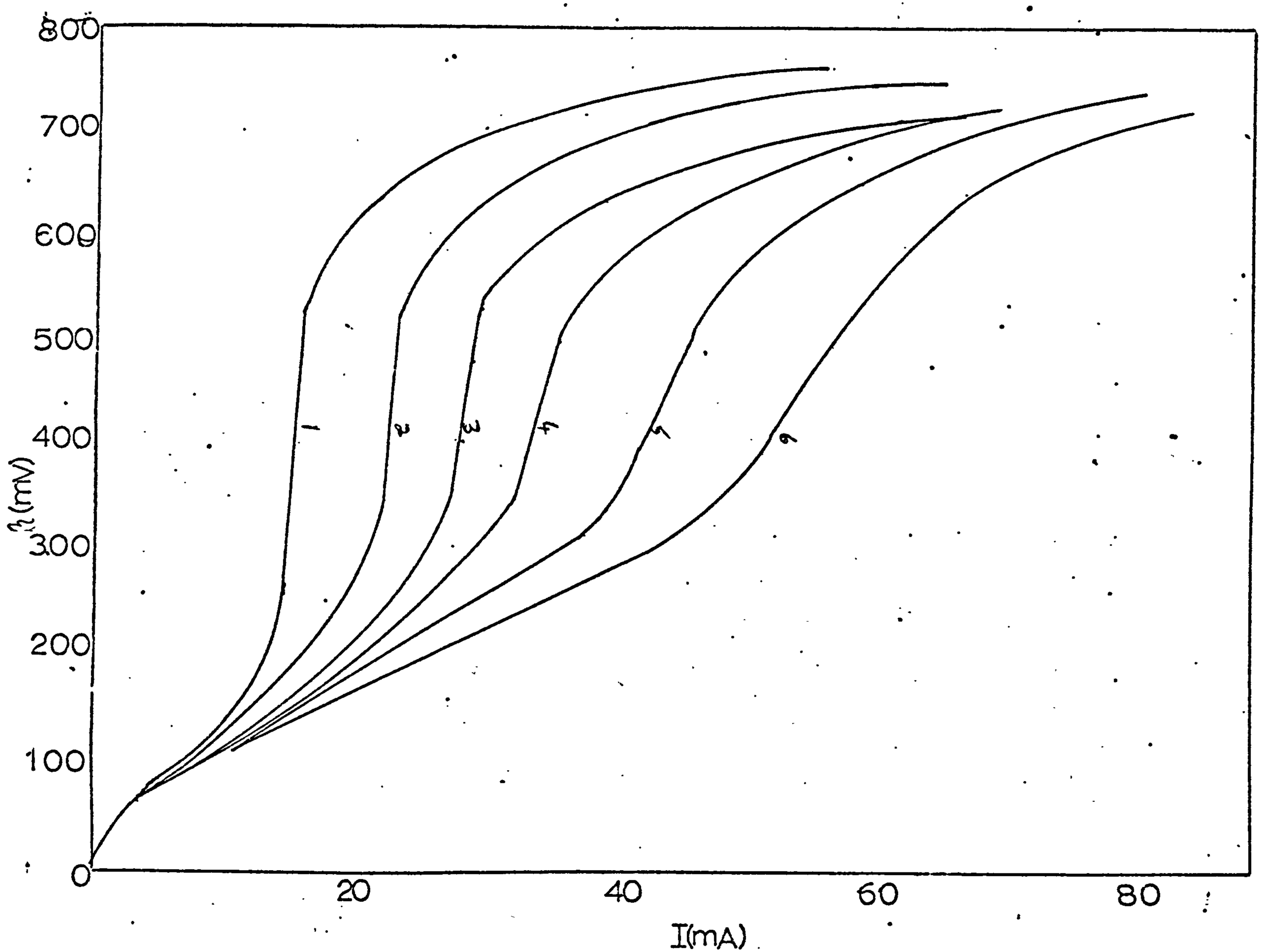
800
700
600
500
400
300
200
100
0
η(mV)
20
40
60
80
I(mA)
1
2
3
4
5
6

figure 41

Effect of flow rate on limiting currents for different size feeder electrodes. Limiting current taken at 400mV. overpotential.
0.07M $CuSO_4$ + 0.5M H_2SO_4

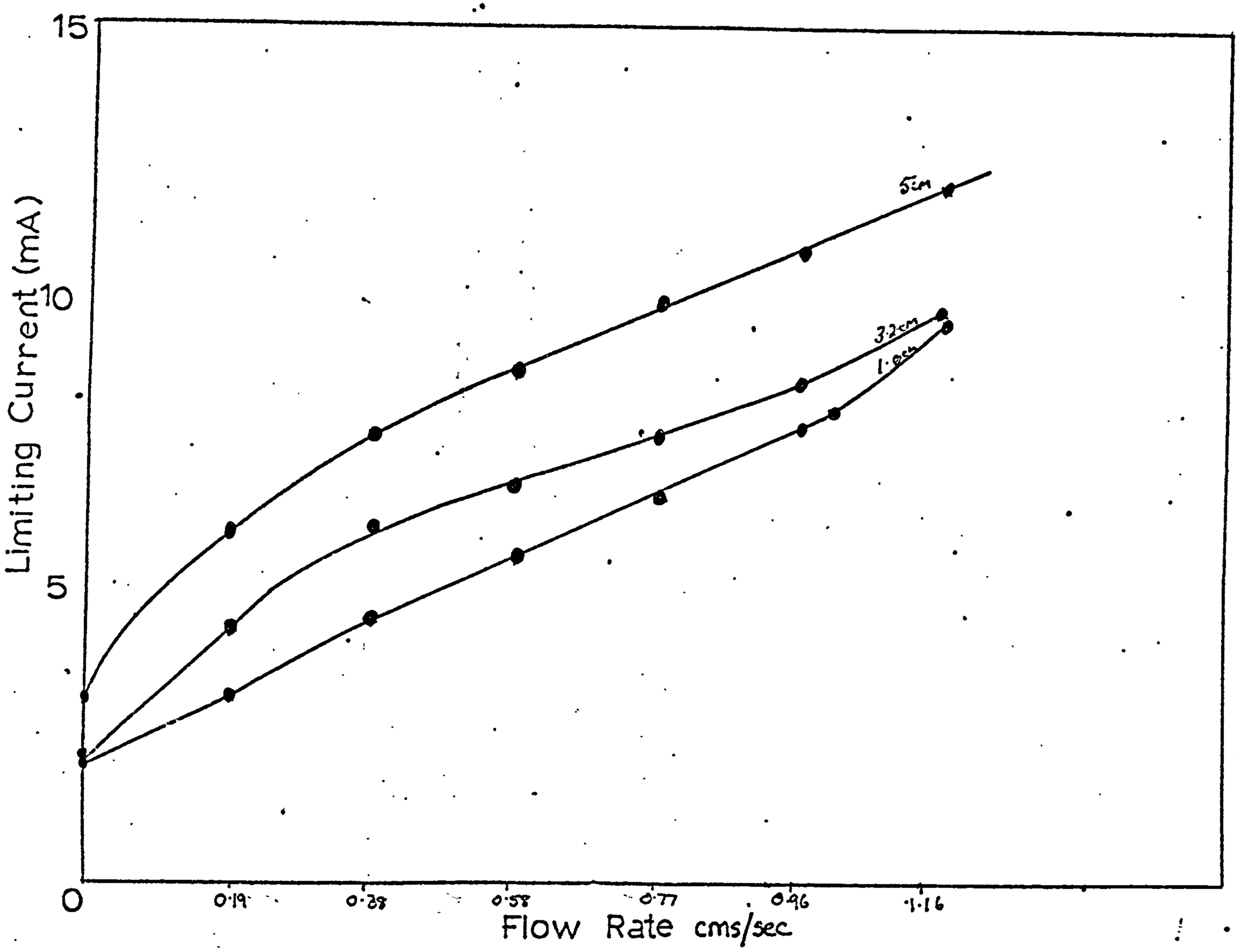
15
10
5
0
Limiting Current (mA)
5cm
3·2cm
1·0cm
0·19
0·28
0·58
0·77
0·96
1·16
Flow Rate cms/sec

figure 42

Effect of different feeder electrode sizes and different flow rates, on a given electrode, on polarization curves for the deposition of copper(in a tube)

0.01M $CuSO_4$ + 0.5M H_2SO_4

Specimen No. :	1	2	3	4	5	6	
flow rate :	.19	.38	.58	.77	.96	1.16	cms/sec
Feeder length:	1.0	2.0	3.0	4.0	5.0		cms.

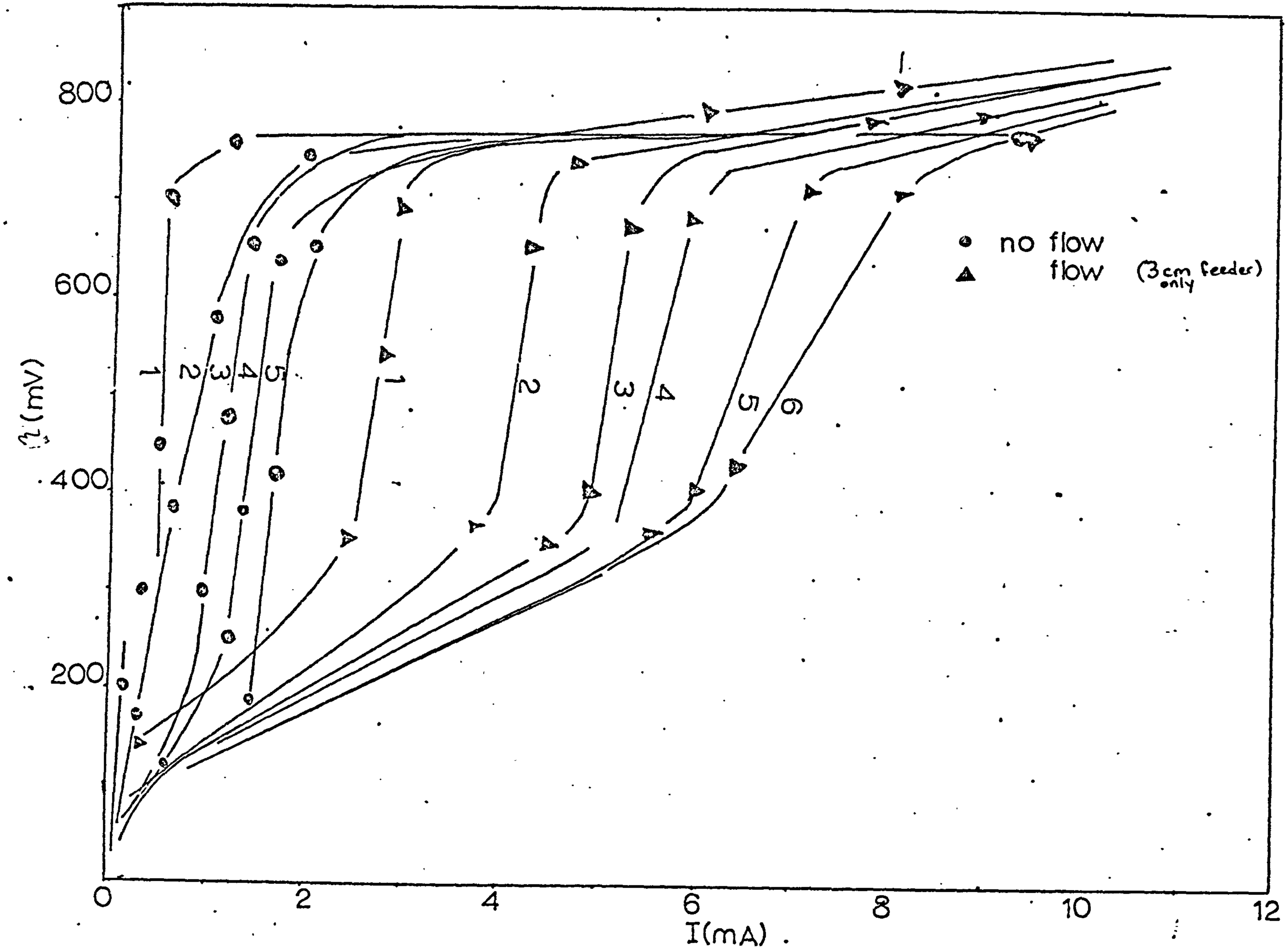
800
600
400
200
0
2
4
6
8
10
12
I(mA)
V(mV)
no flow
flow (3 cm only feeder)
1
2
3
4
5
6

figure 43

Effect of flow on cathodic polarization curves for the deposition of copper onto a feeder electrode in a tube.
Feeder length = 5.0 cm.
0.01M $CuSO_4$ + 0.5M H_2SO_4

Flow rate :	0.19	0.38	0.58	0.77	0.96	1.16 cms/sec
Specimen No:	1	2	3	4	5	6

figure 44

As for figure 44 except that the feeder electrode length is 1.0 cm.

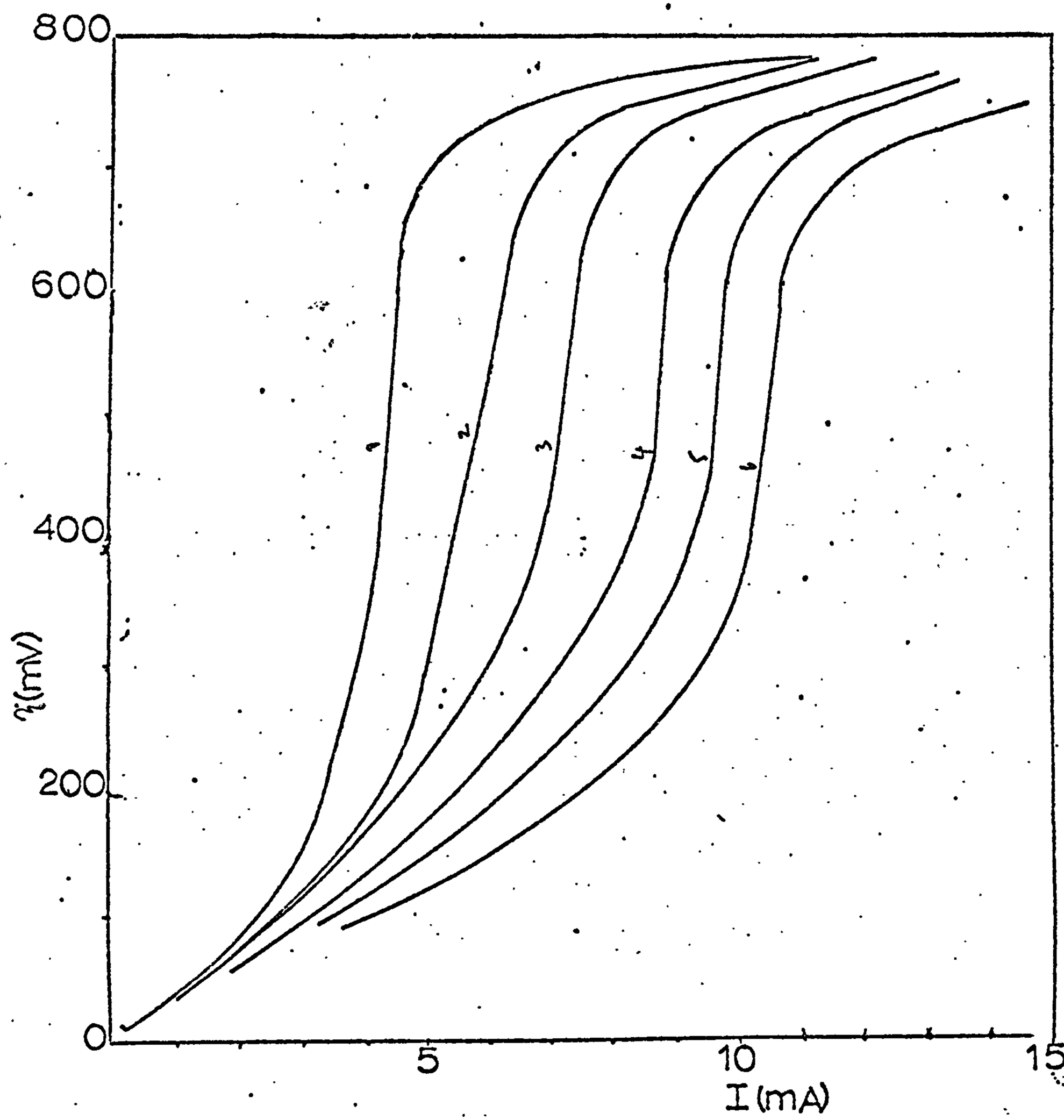
800
600
400
200
0
V(mV)
5
10
15
I(mA)
1
2
3
4
5
6

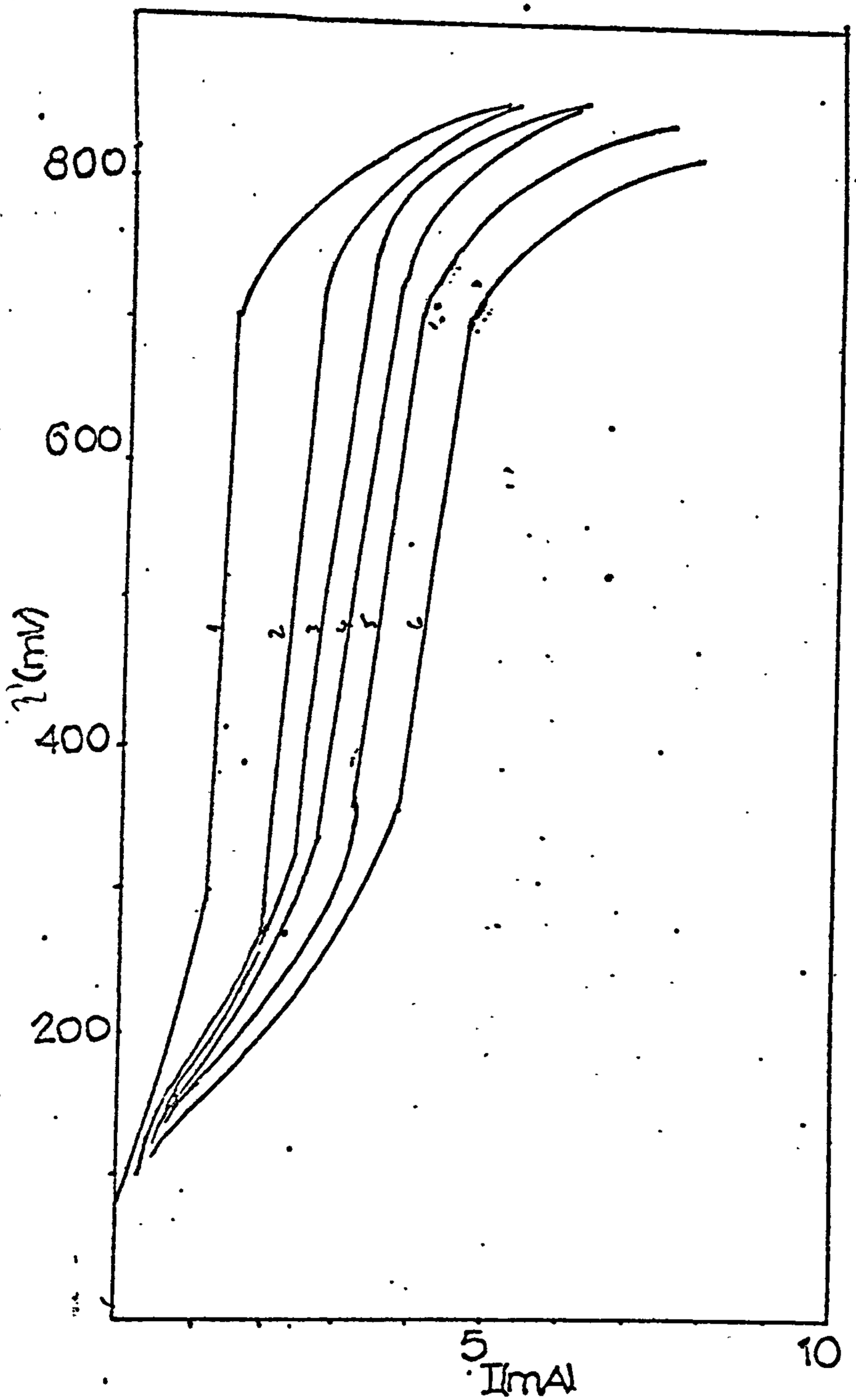
800
600
400
200
V(mV)
5
10
I(mA)
1
2
3
4
5
6

figure 45

Effect of flow rate on limiting currents for different size feeder electrodes. Limiting currents taken at 400mV overpotential.

Solution: 0.01M $CuSO_4$ + 0.5M H_2SO_4

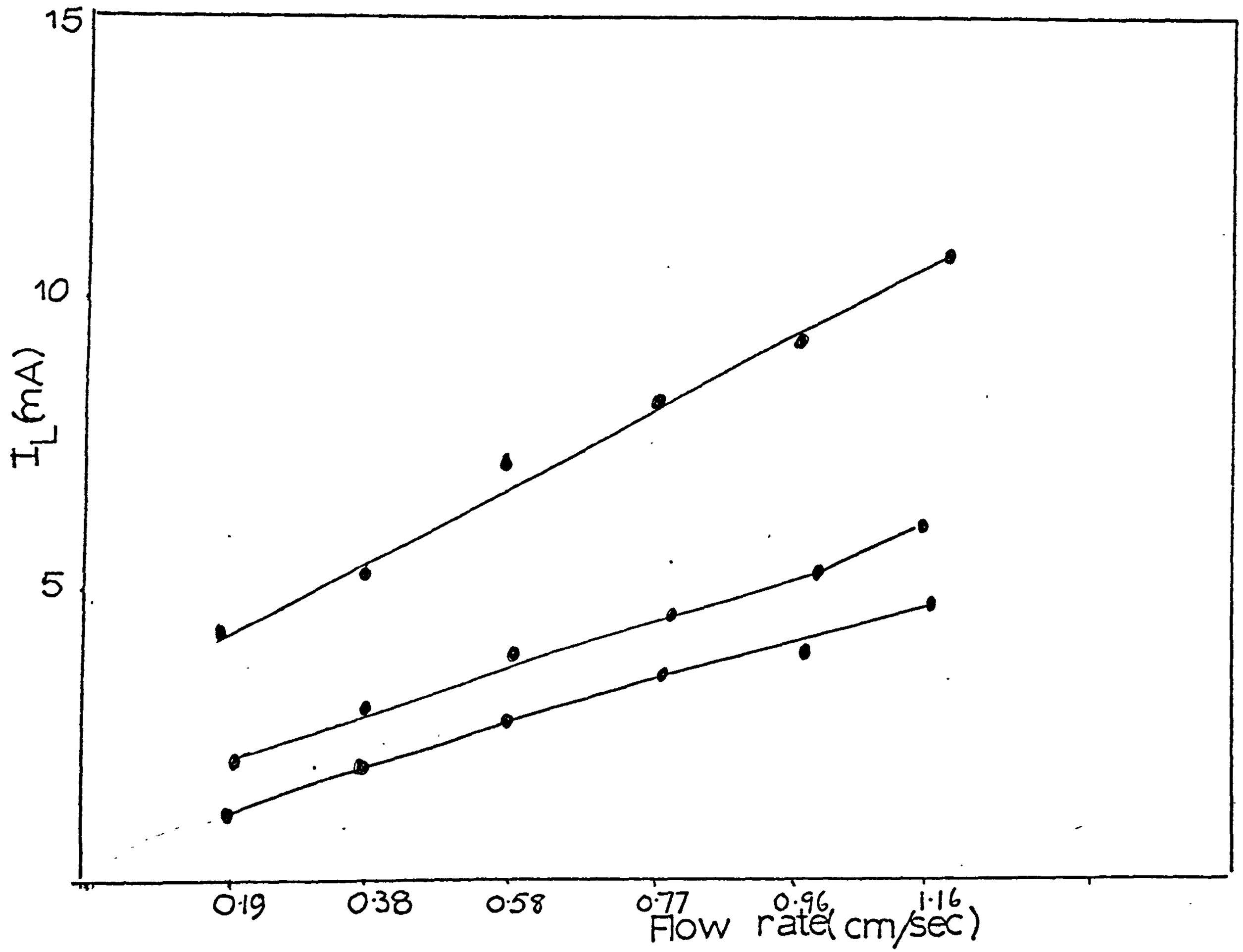
15
10
5
I_L (mA)
0·19
0·38
0·58
0·77
0·96
1·16
Flow rate (cm/sec)

figure 46

Comparison of polarization curves in different size fluidised beds.

Static bed sizes: 3cm, 2cm, 1cm.
porosities : 0.4and0.65
Solutions: 0.7M $CuSO_4$, 0.001M $CuSO_4$ both in 0.5M H_2SO_4

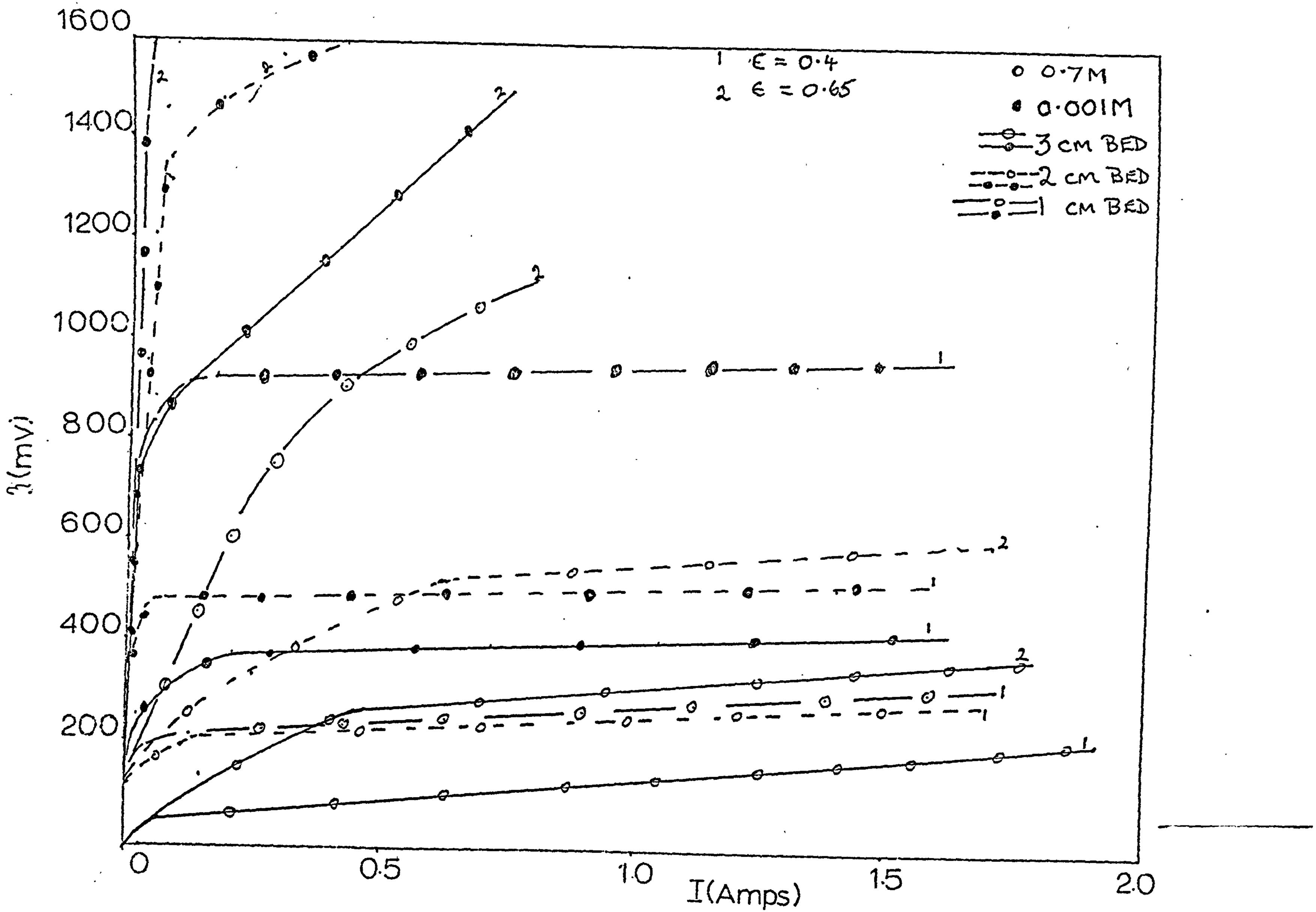
1600
1400
1200
1000
800
600
400
200
V(mV)
0
0.5
1.0
1.5
2.0
I(Amps)
1 ∈ = 0·4
2 ∈ = 0·65
o 0·7M
• 0·001M
3 CM BED
2 CM BED
1 CM BED

Figure 47

Effect of a variable size feeder electrode in a fluidised bed. The feeder electrode was placed one mm. below the top of the bed.

Solution: 0.07M $CuSO_4$ + 0.5M H_2SO_4

Feeder length
1 cm △
2 cm ○
3 cm ▼

Porosity

1	0.4
2	0.44
3	0.51
4	0.55
5	0.61

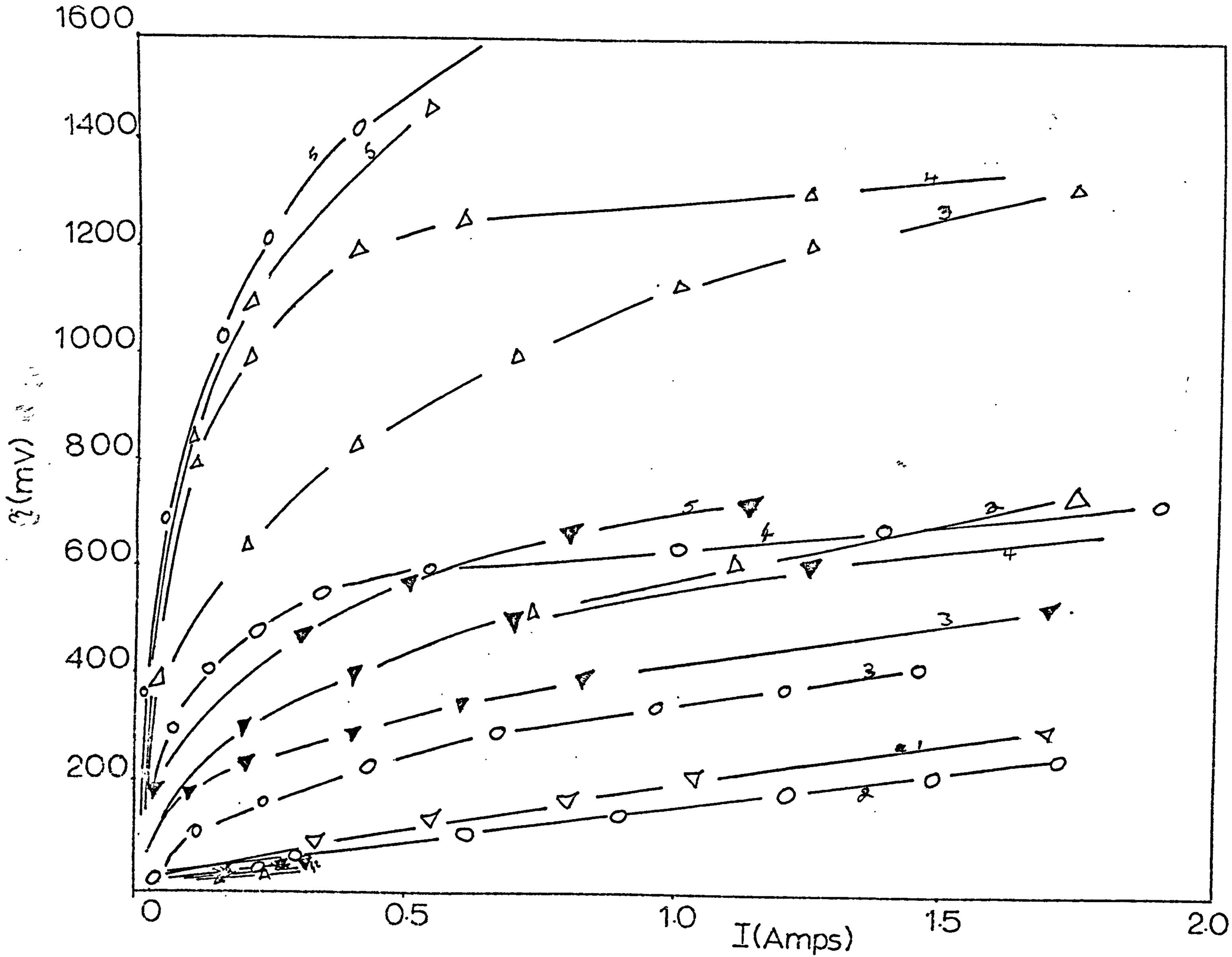
1600
1400
1200
1000
800
600
400
200
0
0.5
1.0
1.5
2.0
I(Amps)
5
4
3
2
1

figure 48

Effect of a variable size feeder electrode in a fluidised bed. The feeder electrode was placed 1 mm. above the bottom of the bed.

Solution: 0.07M $CuSO_4$ + 0.5M H_2SO_4

Feeder length	1 cm	△	Porosity	1	
	2 cm	o		2	0.44
	3 cm	▽		3	0.51
				4	0.55
				5	0.61

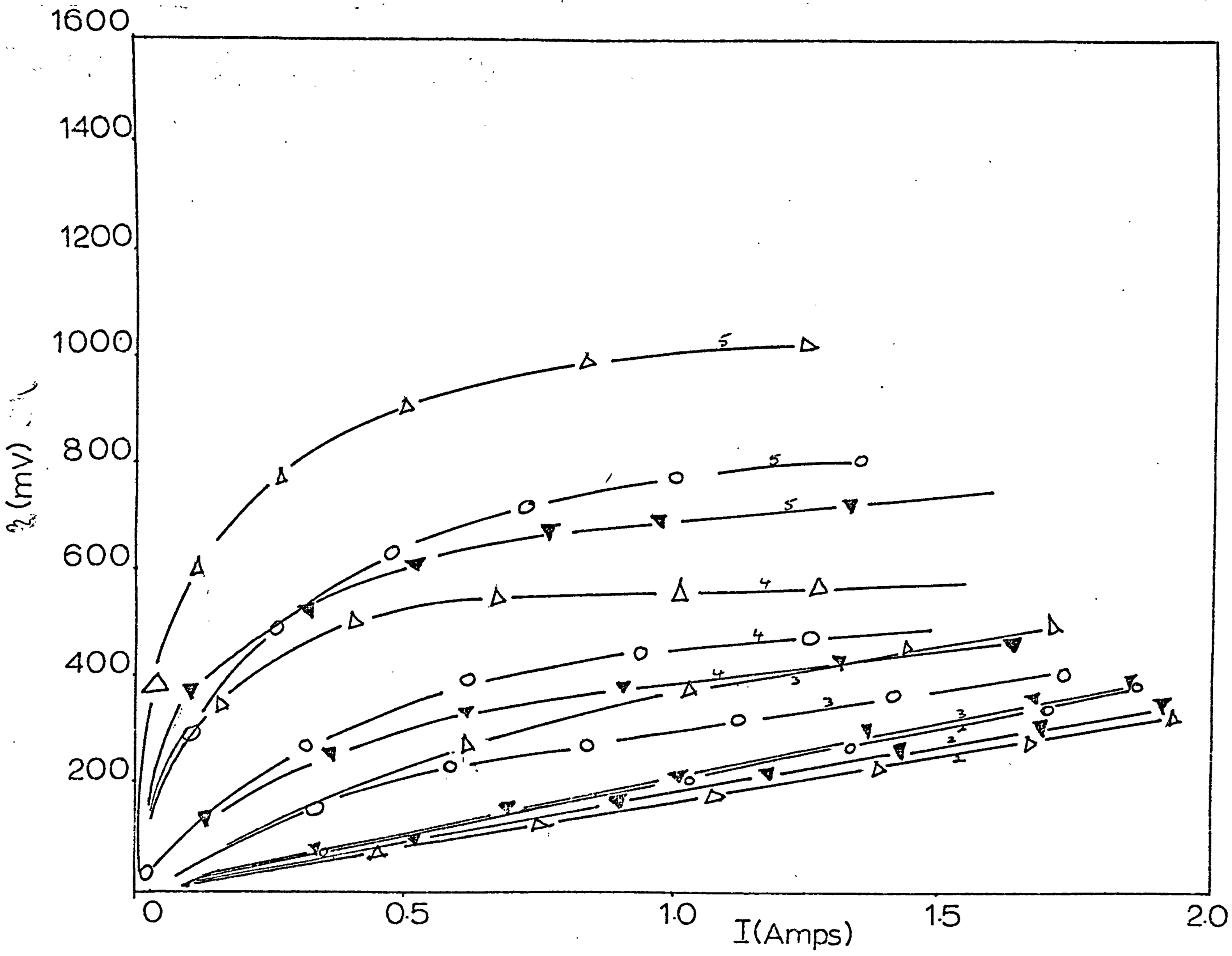
1600
1400
1200
1000
800
600
400
200
0
0.5
1.0
1.5
2.0
I(Amps)
5
5
5
4
4
4
3
3
3
2
2
1

figure 49.

Polarization curves for the deposition of copper in a fluidised bed.

Packed bed height 1 cm.

Solution: 0.7M $CuSO_4$ + 0.5M H_2SO_4.

Sample No.	1	2	3	4	5	6
Porosity	0.40	0.45	0.53	0.59	0.63	0.67

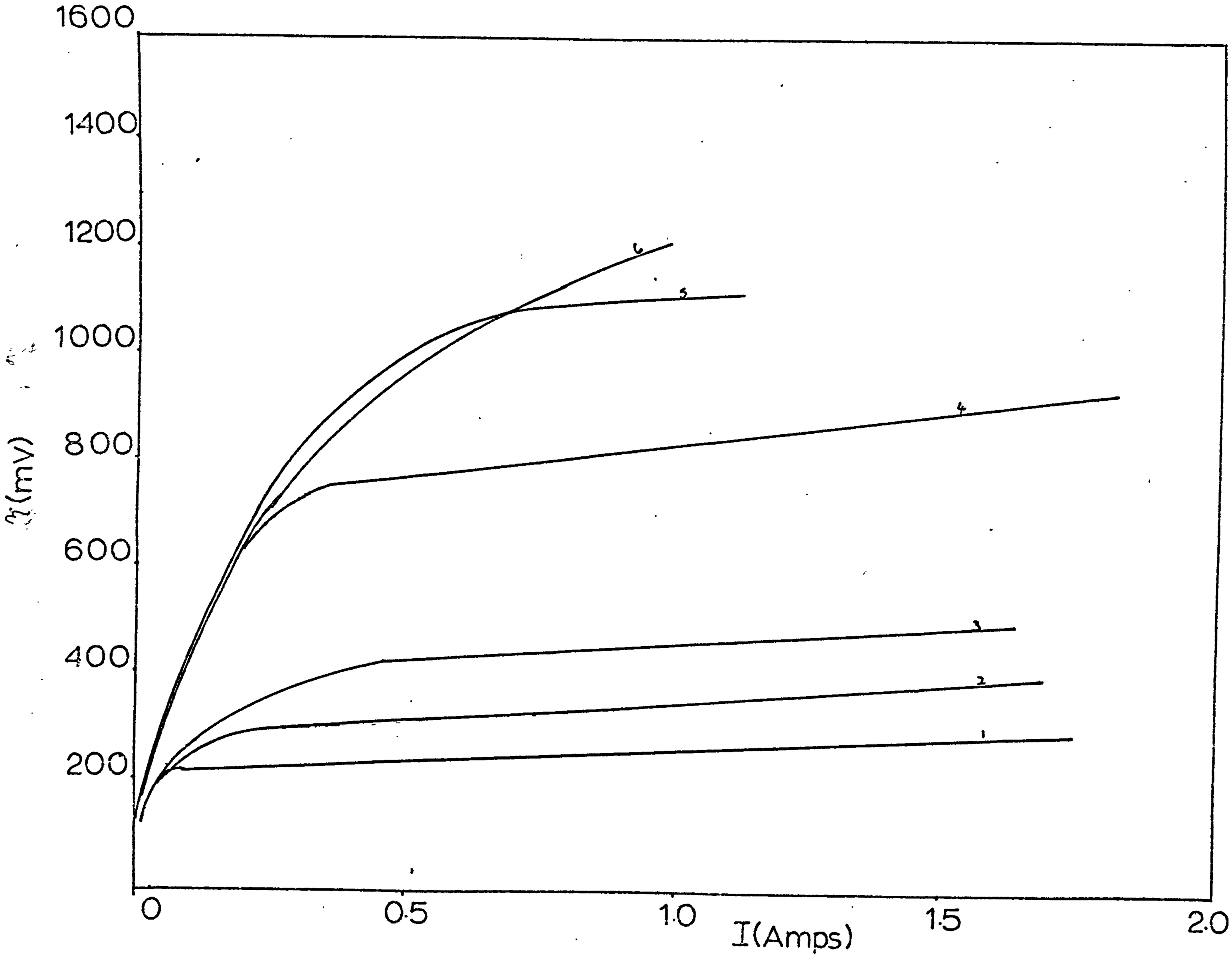
1600
1400
1200
1000
800
600
400
200
V(mV)
0
0.5
1.0
1.5
2.0
I(Amps)
6
5
4
3
2
1

figure 50

Polarization curves for the deposition of copper in a fluidised bed

Packed bed height 1 cm.
Solution: 0.07M $CuSO_4$ + H_2SO_4

Sample No.	1	2	3	4	5	6
Porosity	0.40	0.45	0.53	0.59	0.63	0.67

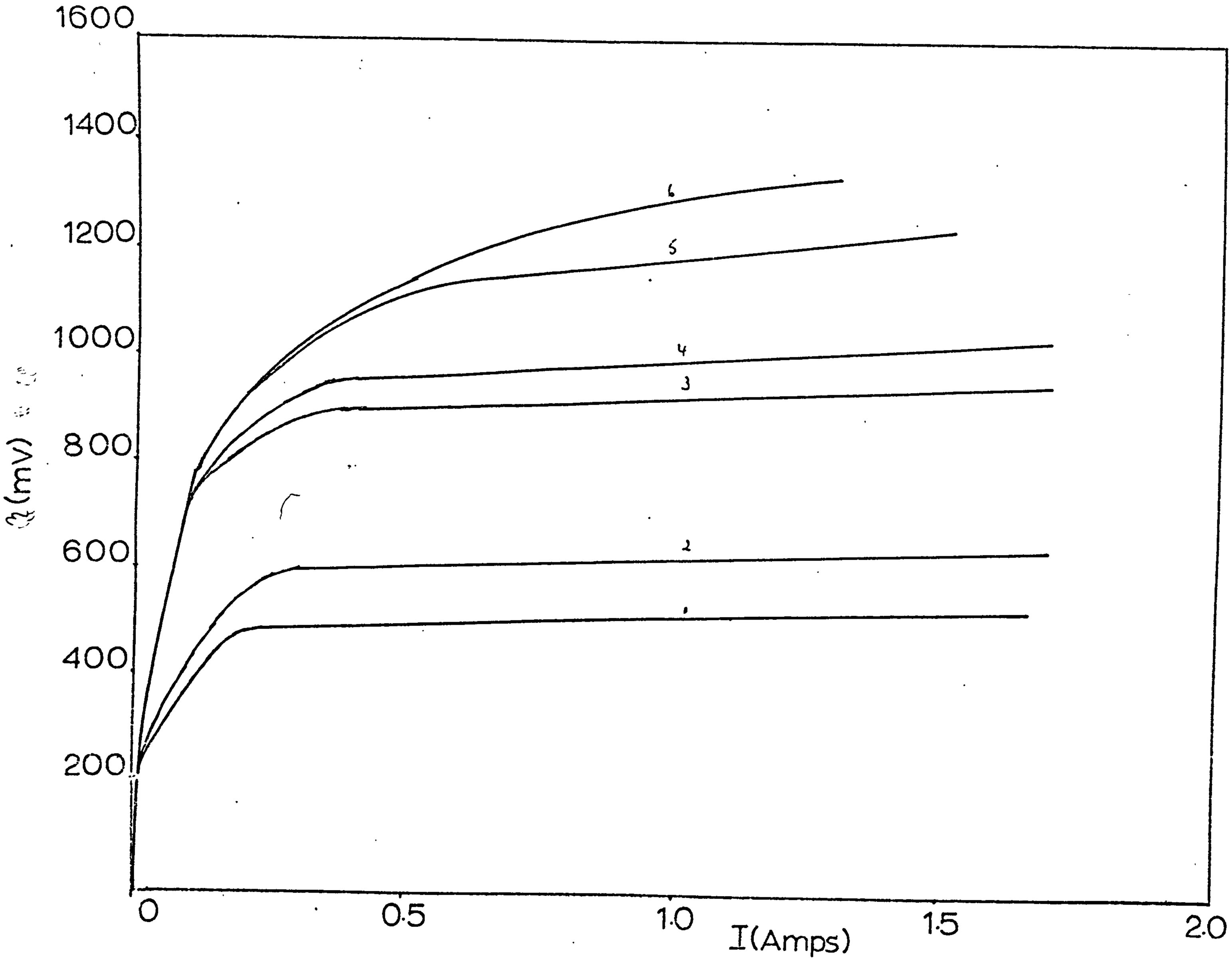
1600
1400
1200
1000
800
600
400
200
V(mV)
6
5
4
3
2
1
0
0.5
1.0
1.5
2.0
I(Amps)

figure 51

Polarization curves for the deposition of copper in a fluidised bed.

Packed bed height: 1 cm
Solution: 0.01M $CuSO_4$ + 0.5M H_2SO_4

Sample No.	1	2	3	4	5	6
Porosity	0.40	0.45	0.53	0.59	0.63	0.67

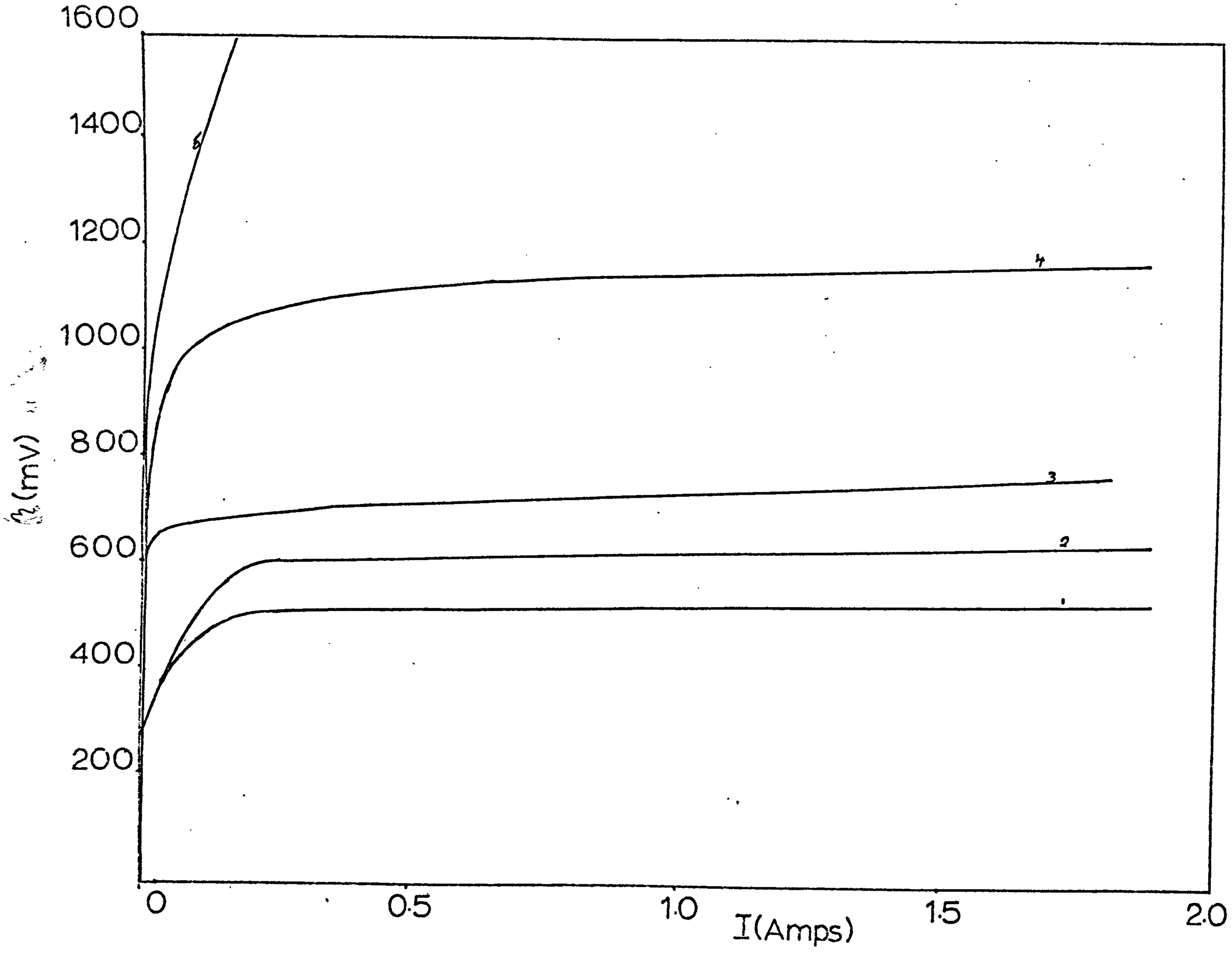
1600
1400
1200
1000
800
600
400
200
V (mV)
0
0.5
1.0
1.5
2.0
I(Amps)
5
4
3
2
1

figure 52

Polarization curves for the deposition of copper in a fluidised bed.

Packed bed height: 1 cm

Solution: 0.001M $CuSO_4$ + 0.5M H_2SO_4

Sample No.	1	2	3	4	5	6
Porosity	0.40	0,45	0.53	0.59	0.63	0.67

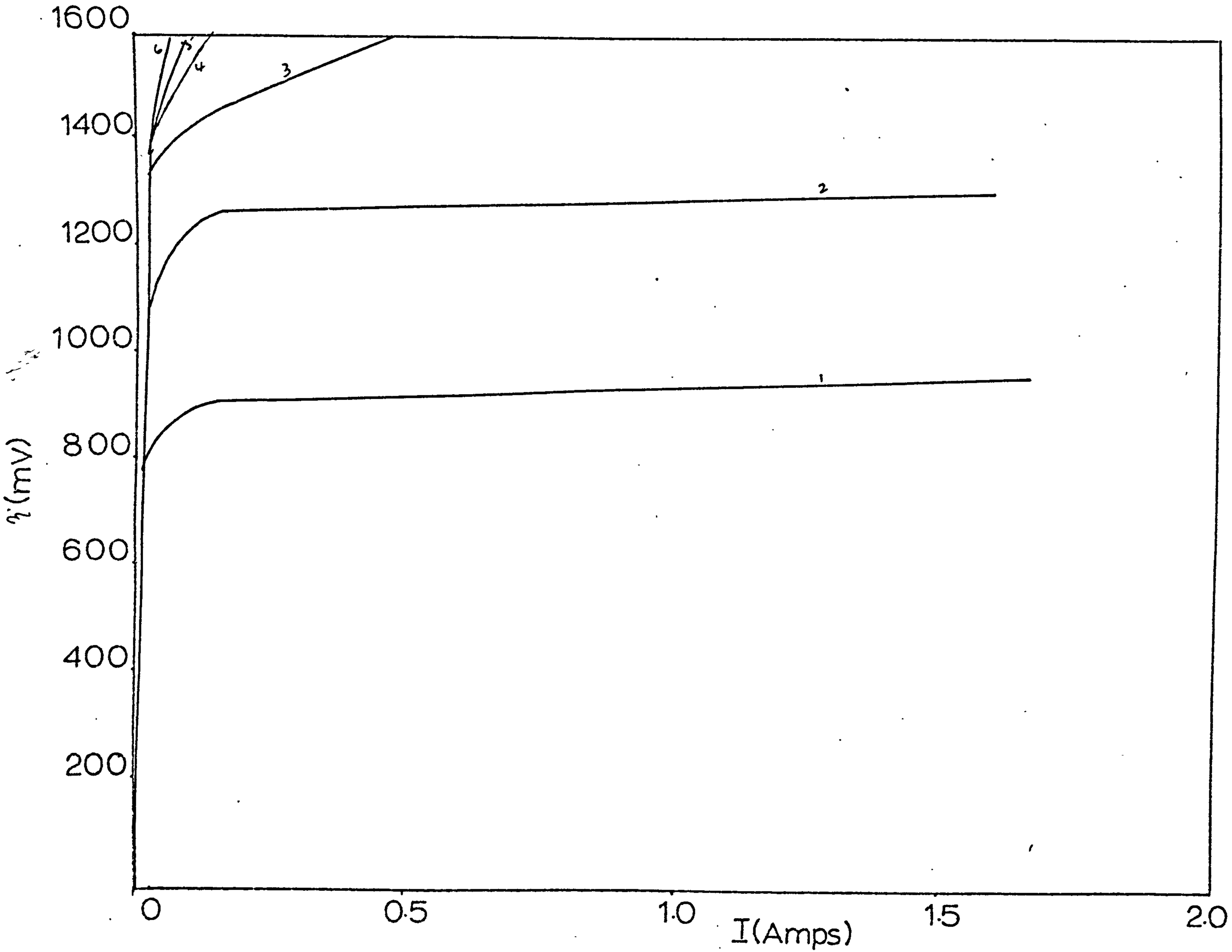
1600
1400
1200
1000
800
600
400
200
η(mV)
0
0.5
1.0
1.5
2.0
I(Amps)
1
2
3
4
5
6

figure 53

Polarization curves for the hydrogen reaction in a fluidised bed.

Packed bed height: 1 cm
Solution: 0.5M H_2SO_4 only

Sample No.	1	2	3	4	5	6
Porosity	0.40	0.45	0.53	0.59	0.63	0.67

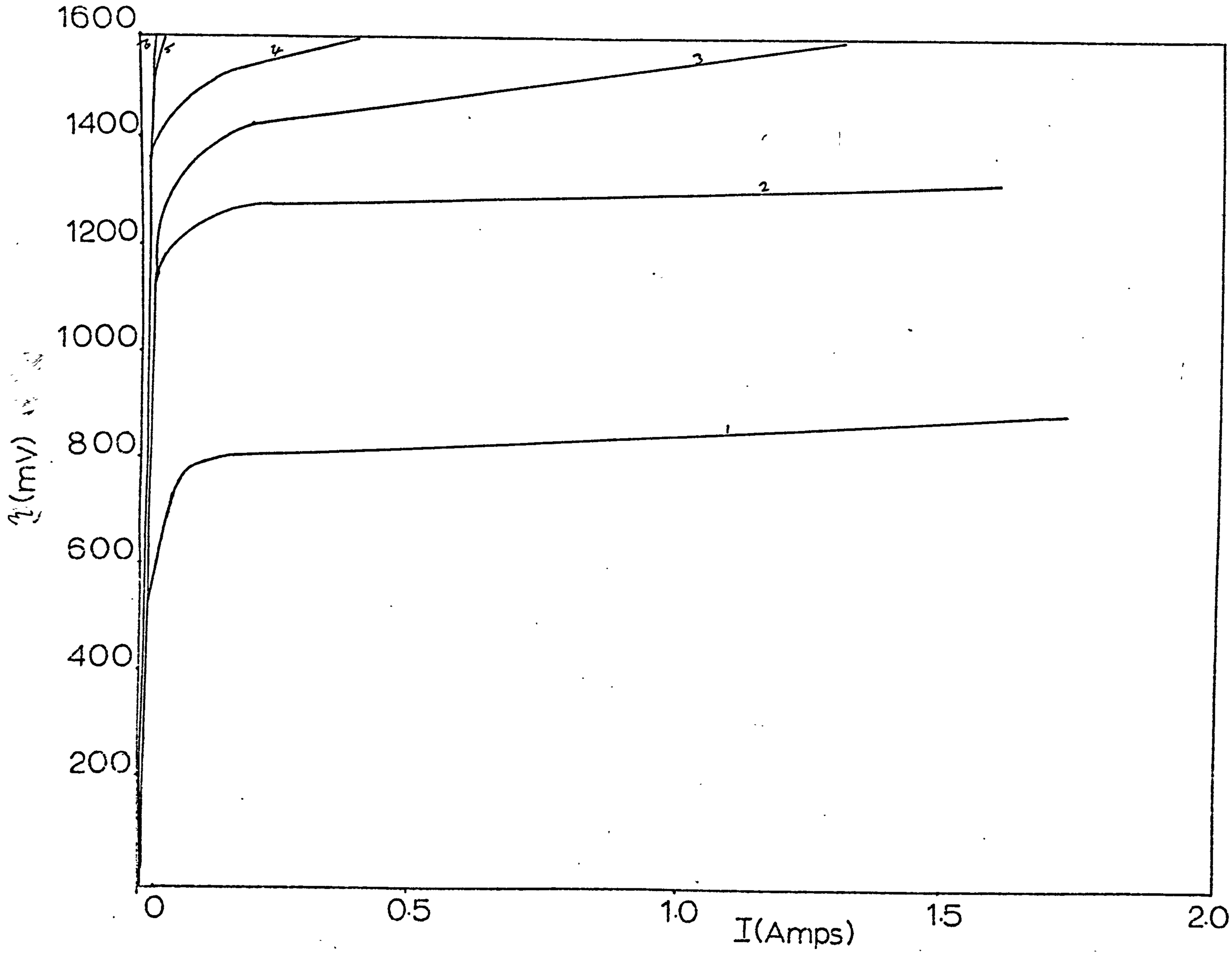
1600
1400
1200
1000
800
600
400
200
η(mV)
0
0.5
1.0
1.5
2.0
I(Amps)
1
2
3
4
5
6

figure 54

Polarization curves for the deposition of copper in a fluidised bed.

Packed bed height: 2 cm
Solution: 0.7M $CuSO_4$ + 0.5M H_2SO_4

Sample No.	1	2	3	4	5	6	7	8	9
Porosity	0.40	0.43	0.45	0.47	0.51	0.56	0.60	0.65	0.68

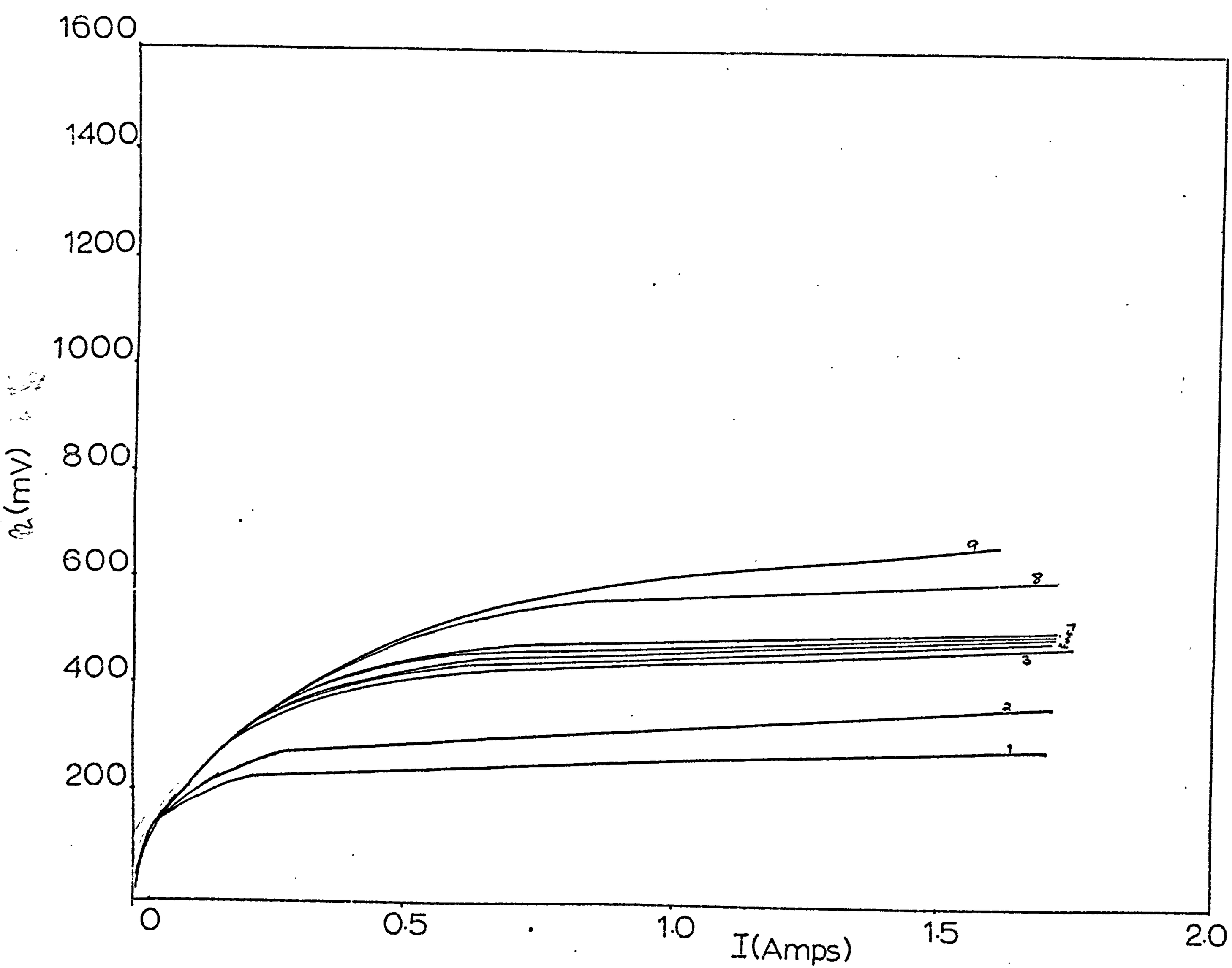
1600
1400
1200
1000
800
600
400
200
0
0.5
1.0
1.5
2.0
I(Amps)
9
8
3
2
1

figure 55

Polarization curves for the deposition of copper in a fluidised bed.

Packed bed height:2 cm.
Solution:0.07M $CuSO_4$ + 0.5M H_2SO_4

Sample No.	1	2	3	4	5	6	7	8	9
Porosity	0.40	0.43	0.45	0.57	0.51	0.56	0.60	0.65	0.68

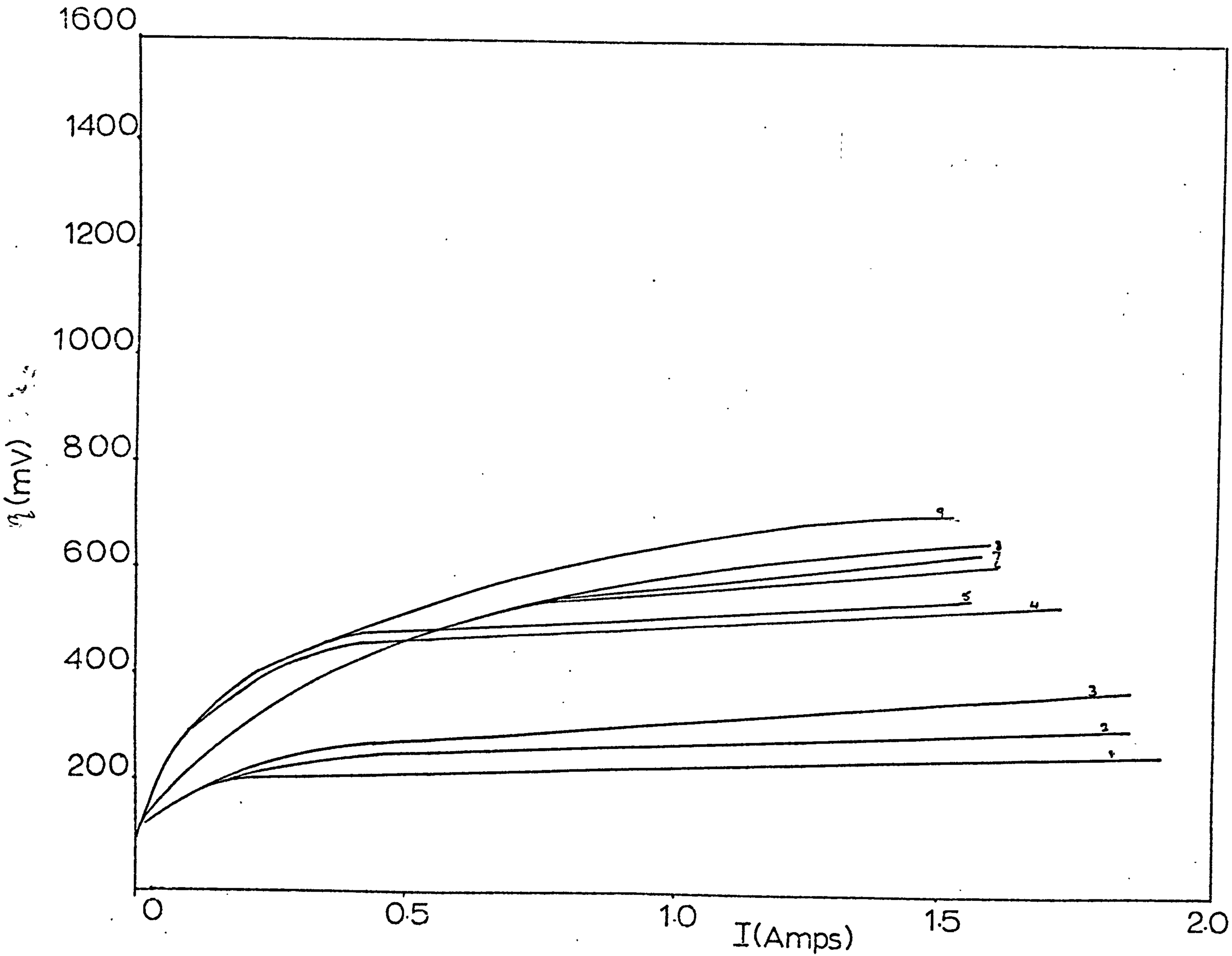
1600
1400
1200
1000
800
600
400
200
η (mV)
0
0.5
1.0
1.5
2.0
I(Amps)
9
8
7
6
5
4
3
2
1

figure 56

Polarization curves for the deposition of copper from a fluidised bed.

Packed bed height: 2 cm

Solution: 0.01M $CuSO_4$ +0.5M H_2SO_4

Sample No.	1	2	3	4	5	6	7	8	9
Porosity	0.40	0.43	0.45	0.47	0.51	0.56	0.60	0.65	0.68

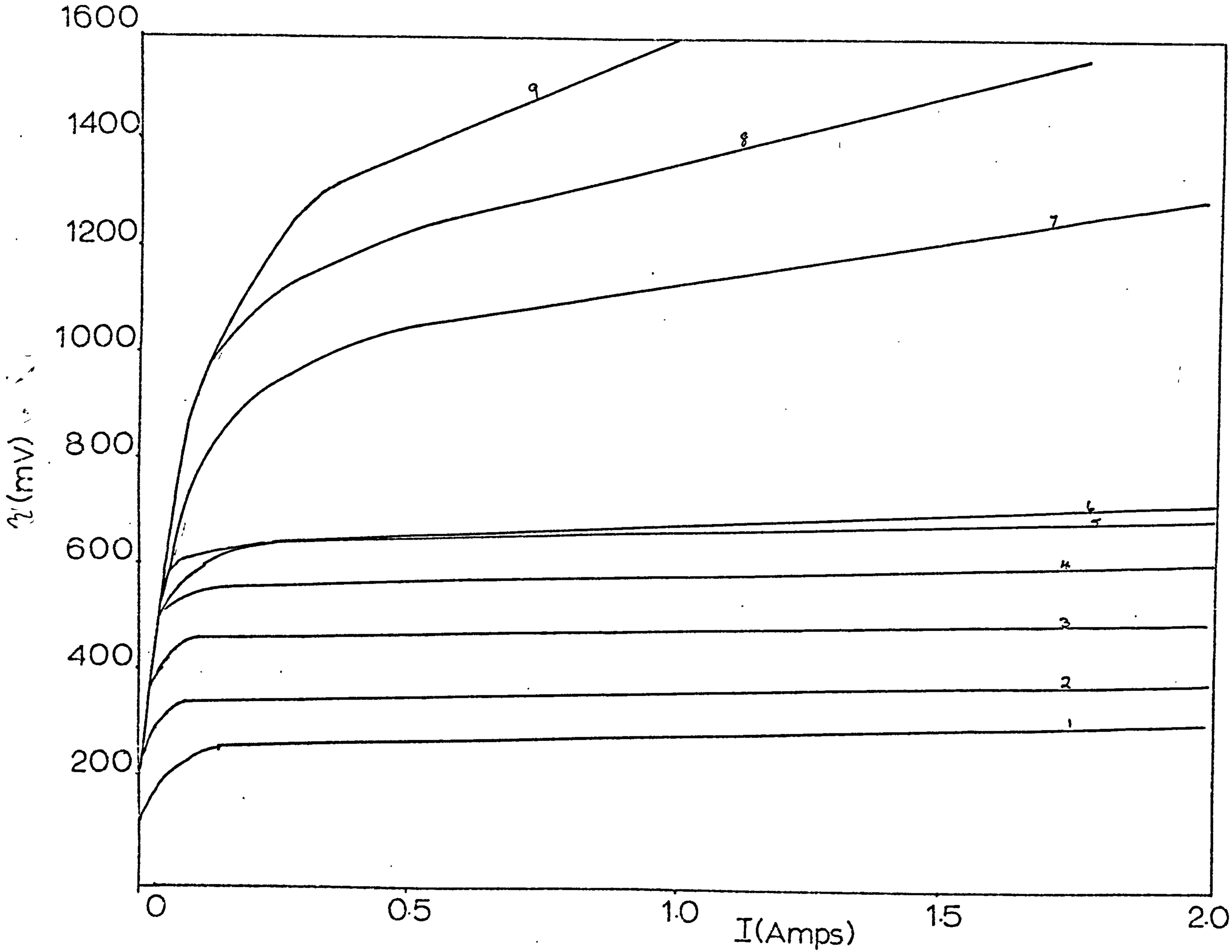
1600
1400
1200
1000
800
600
400
200
η (mV)
0
0·5
1·0
1·5
2·0
I(Amps)
9
8
7
6
5
4
3
2
1

figure 57

Polarization curves for the deposition of copper in a fluidised bed.

Packed bed height: 2 cm

Solution: 0.001M $CuSO_4$ + 0.5M H_2SO_4

Sample No.	1	2	3	4	5	6	7	8
Porosity	0.40	0.43	0.45	0.47	0.51	0.56	0.60	0.65

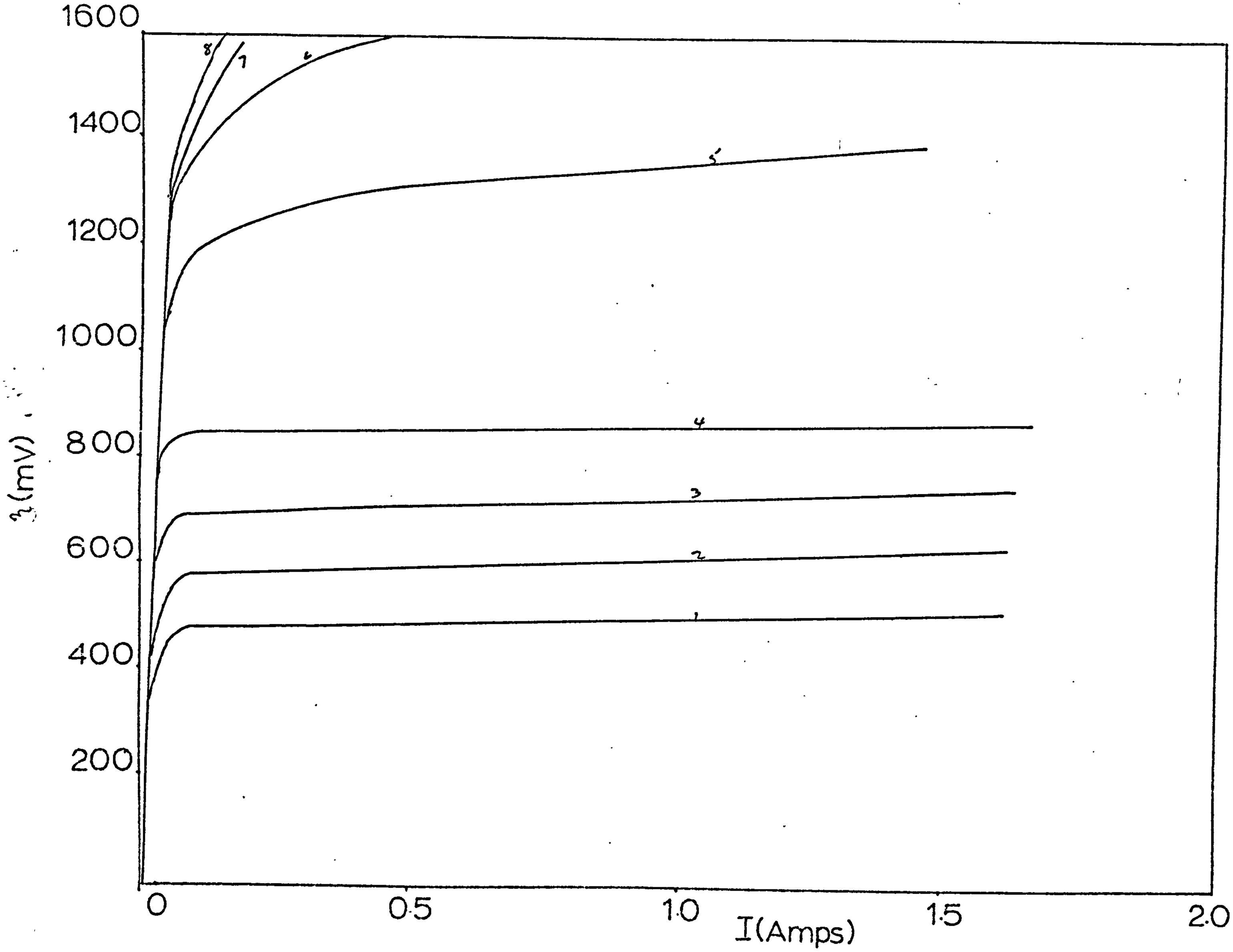
1600
1400
1200
1000
800
600
400
200
V (mV)
0
0.5
1.0
1.5
2.0
I(Amps)
1
2
3
4
5
6
7
8

figure 58

Polarization curves for the hydrogen reaction in a fluidised bed.

Packed bed height: 2 cm
Solution: 0.5M H_2SO_4

Sample No.	1	2	3	4	5	6	7
Porosity	0.40	0.43	0.45	0.47	0.51	0.56	0.60

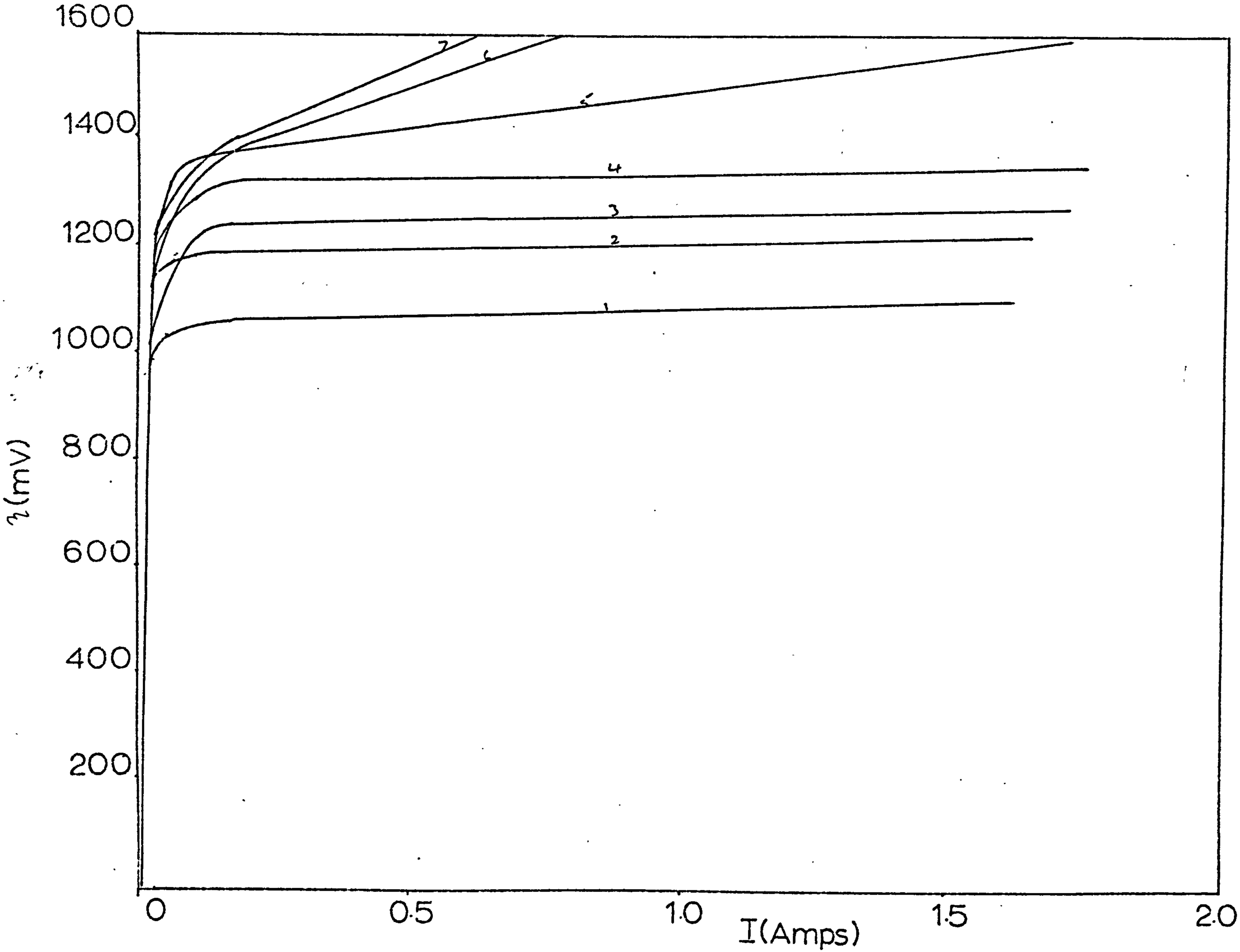
1600
1400
1200
1000
800
600
400
200
η(mV)
0
0.5
1.0
1.5
2.0
I(Amps)
1
2
3
4
5
6
7

figure 59

Polarization curves for the deposition of copper in a fluidised bed.

Packed bed height:3 cm.
Solution:0.7M $CuSO_4$ + 0.5M H_2SO_4

Sample No.	1	2	3	4	5	6	7
Porosity	0.40	0.44	0.47	0.51	0.54	0.57	0.60

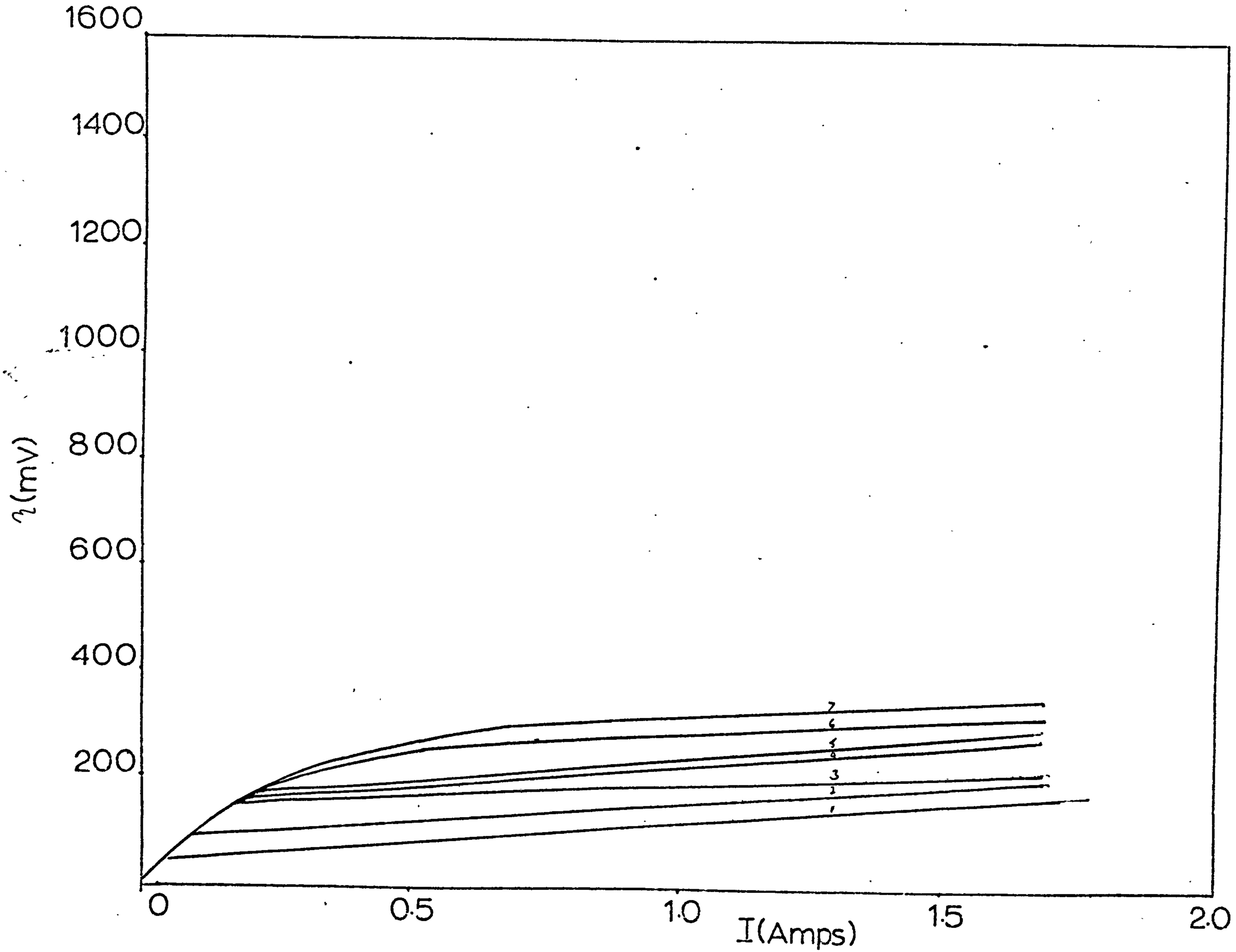
1600
1400
1200
1000
800
600
400
200
η(mV)
0
0.5
1.0
1.5
2.0
I(Amps)
7
6
5
4
3
2
1

figure 60

Polarization curves for the deposition of copper in a fluidised bed.

Packed bed height:3 cm.
Solution:0.07M $CuSO_4$ + 0.5M H_2SO_4

Sample No.	1	2	3	4	5	6	7	8
Porosity	0.40	0.44	0.47	0.51	0.54	0.57	0.60	0.65

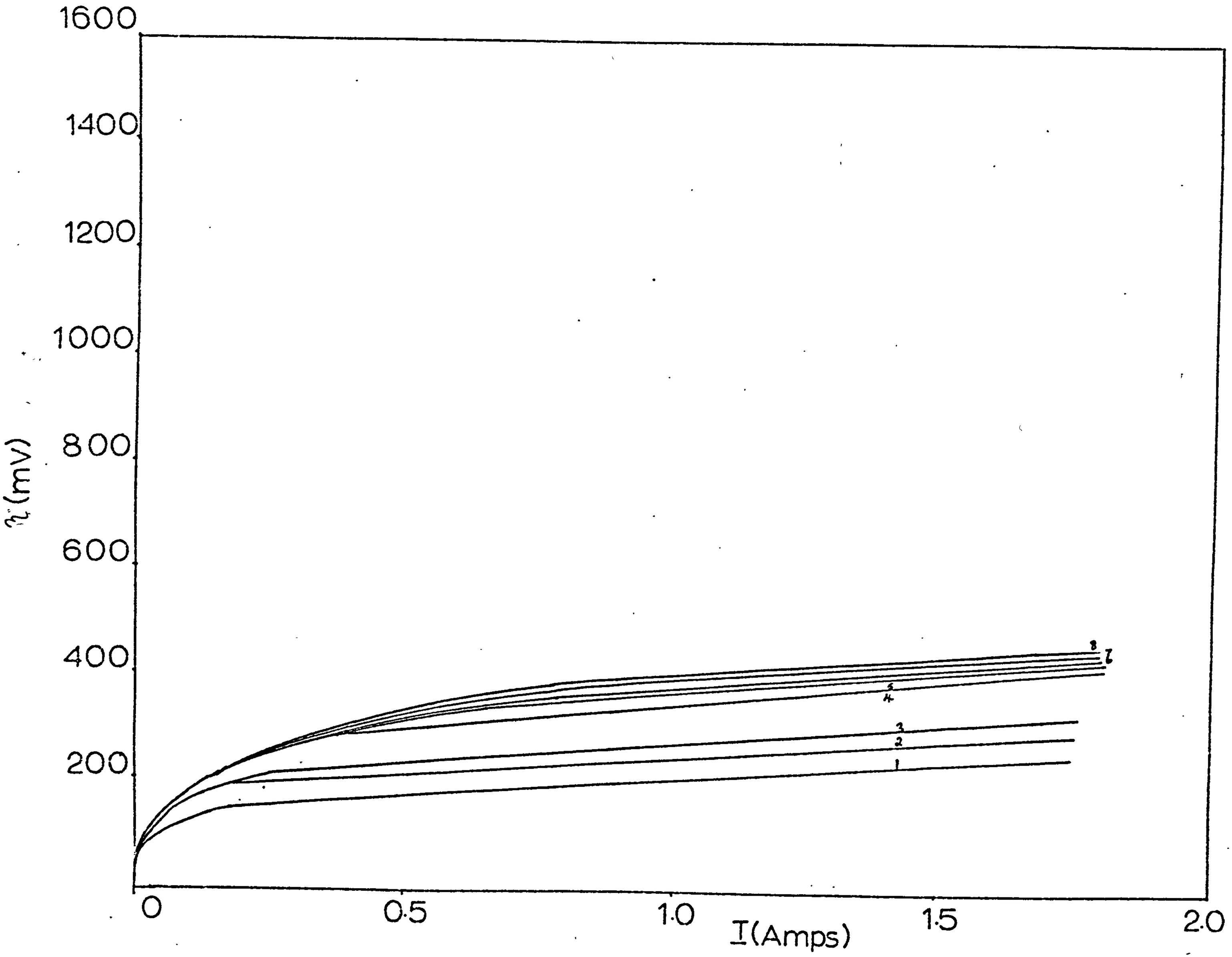
1600
1400
1200
1000
800
600
400
200
η (mV)
0
0.5
1.0
1.5
2.0
I(Amps)
1
2
3
4
5

figure 61

Polarization curves for the deposition of copper in a fluidised bed.

Packed bed height:3 cm
Solution:0.01M $CuSO_4$ + 0.5M H_2SO_4

Sample No.	1	2	3	4	5	6	7
Porosity	0.40	0.44	0.47	0.51	0.54	0.57	0.60

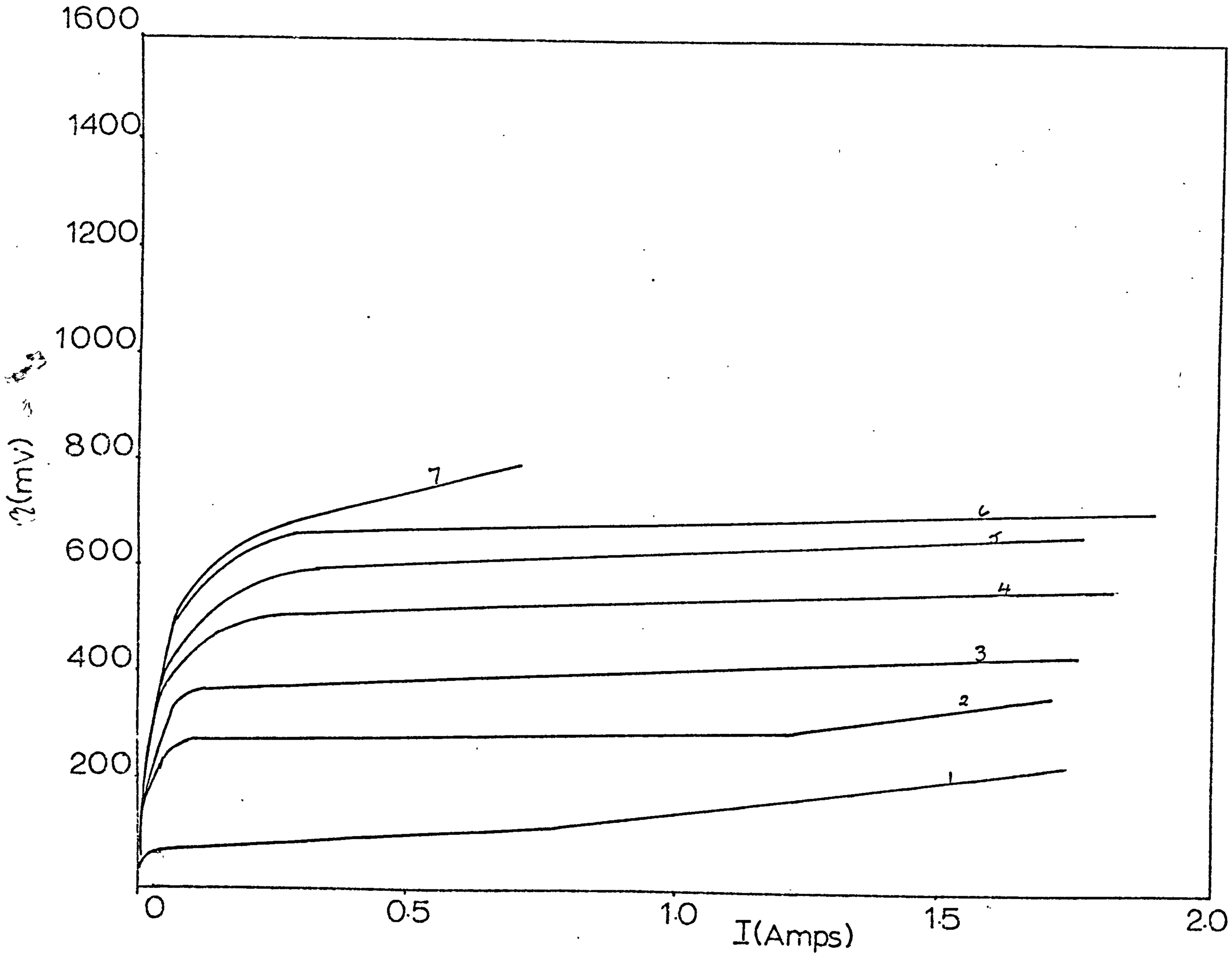
1600
1400
1200
1000
800
600
400
200
0
0.5
1.0
1.5
2.0
I(Amps)
7
6
5
4
3
2
1

figure 62

Polarization curves for the deposition of copper in a fluidised bed.

Packed bed height:3 cm.
Solution:0.001M $CuSO_4$ + 0.5M H_2SO_4

Sample No.	1	2	3	4	5	6	7
Porosity	0.40	0.44	0.47	0.51	0.54	0.57	0.60

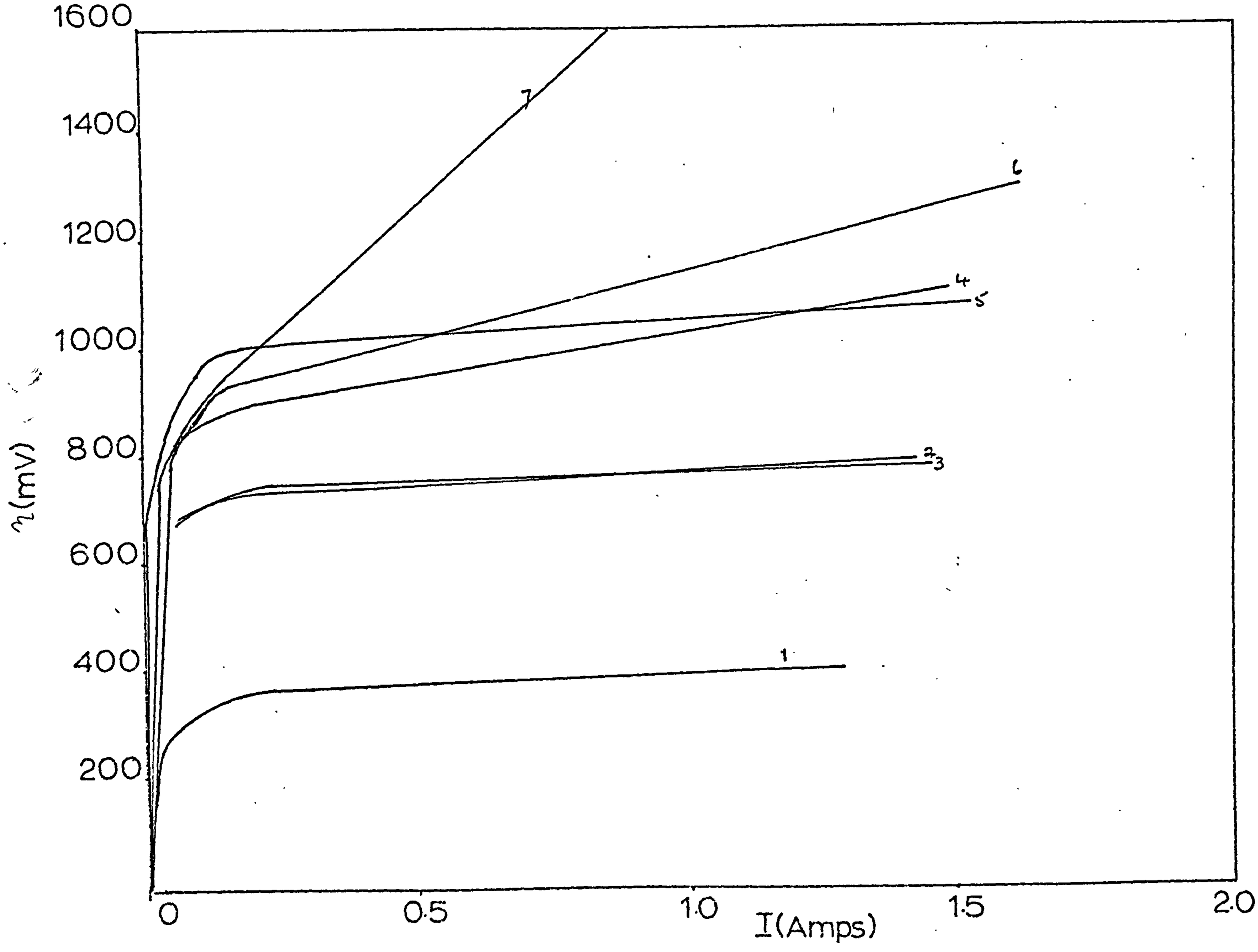
1600
1400
1200
1000
800
600
400
200
η(mV)
0
0.5
1.0
1.5
2.0
I(Amps)
7
6
4
5
2
3
1

figure 63

Polarization curves for the hydrogen reaction in a fluidised bed.

Packed bed height: 3 cm.
Solution: 0.5M H_2SO_4

Sample No.	1	2	3	4	5	6	7
Porosity	0.40	0.44	0.47	0.51	0.54	0.57	0.60

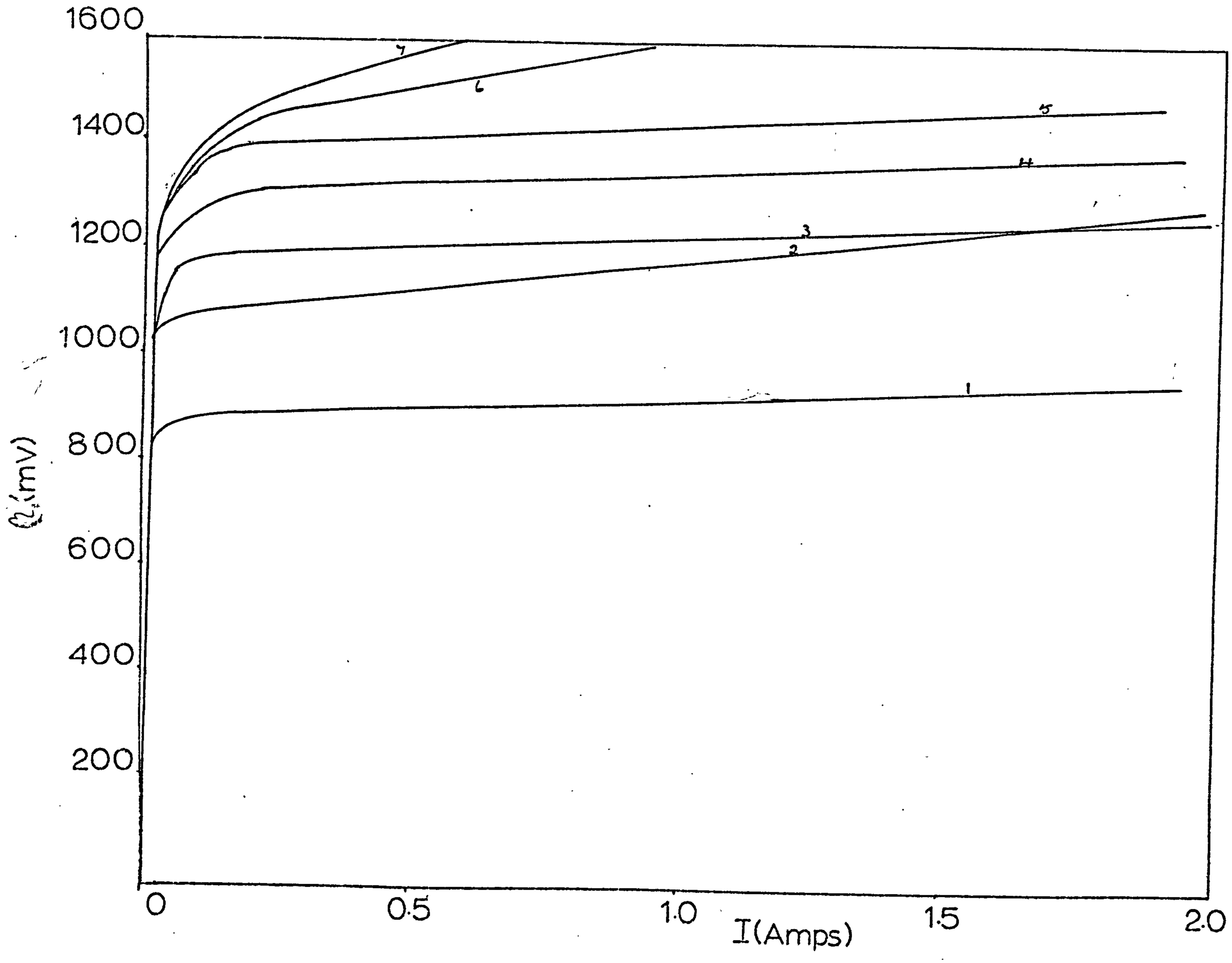
1600
1400
1200
1000
800
600
400
200
V(mV)
0
0.5
1.0
1.5
2.0
I(Amps)
7
6
5
4
3
2
1

figure 64

Deposition of copper from very dilute solution using a fluidised bed.

Packed bed height: 1 cm

Solution: 10^{-5}M $CuSO_4$ + 0.5M H_2SO_4

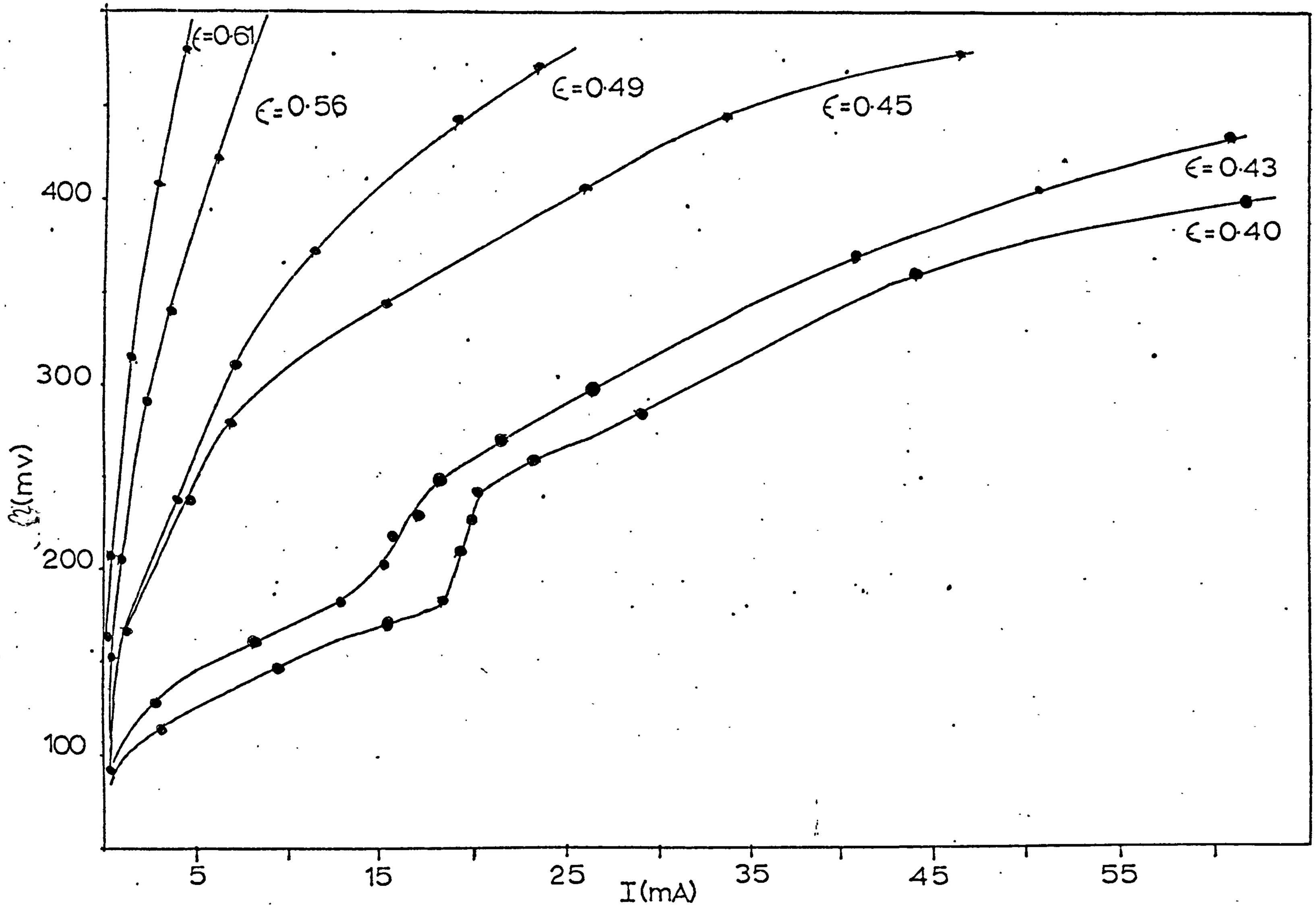
ϵ=0·61
ϵ=0·56
ϵ=0·49
ϵ=0·45
ϵ=0·43
ϵ=0·40
400
300
200
100
V(mV)
5
15
25
35
45
55
I(mA)

figure 65

Deposition of copper from very dilute solution using a fluidised bed.

Packed bed height: 2 cm

Solution: 10^{-5}M $CuSO_4$ + 0.5M H_2SO_4

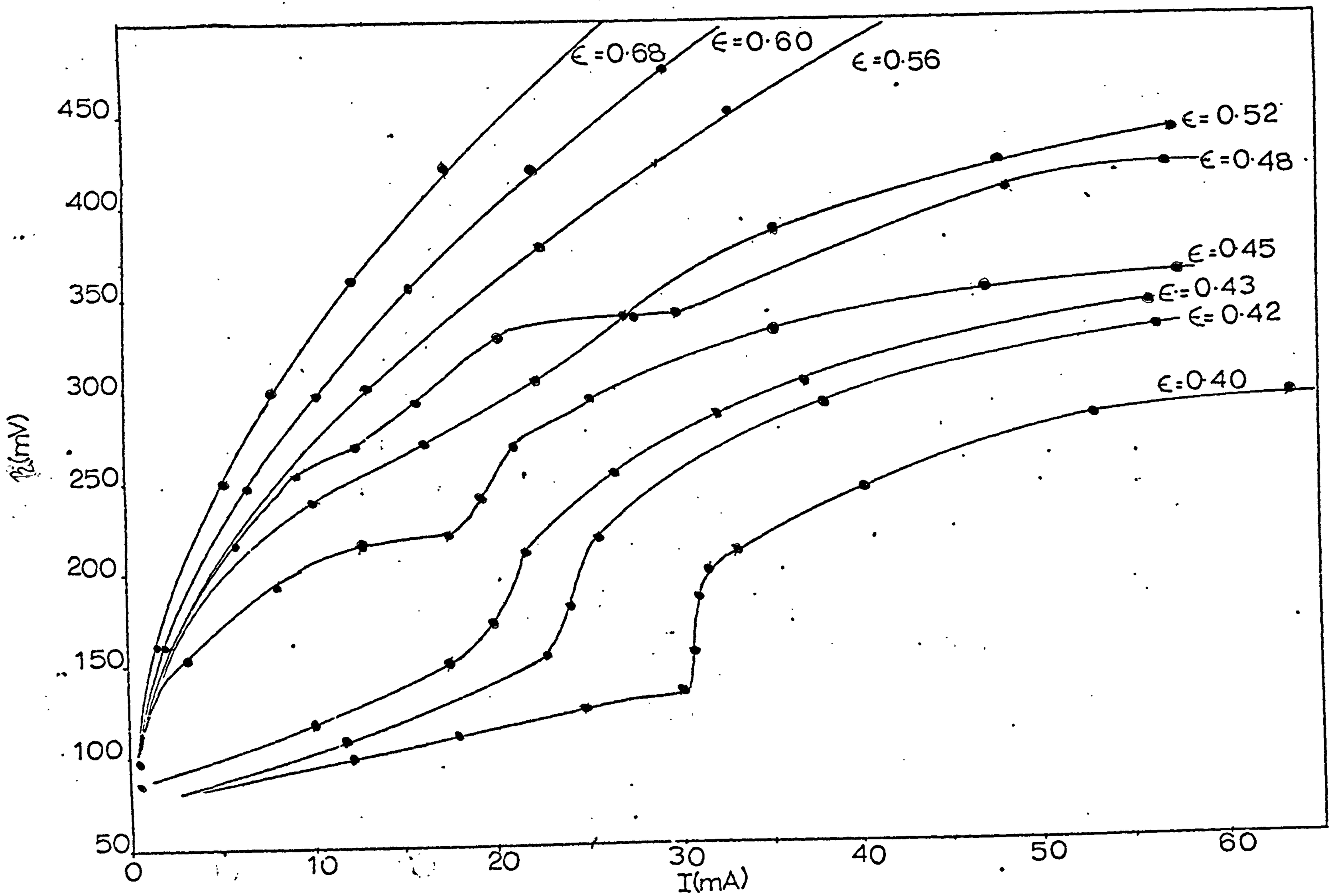
ϵ=0·68
ϵ=0·60
ϵ=0·56
ϵ=0·52
ϵ=0·48
ϵ=0·45
ϵ=0·43
ϵ=0·42
ϵ=0·40
450
400
350
300
250
200
150
100
50
0
10
20
30
40
50
60
I(mA)

figure 66

Deposition of copper from very dilute solution using a fluidised bed.

Packed bed height: 3 cm.

Solution: 10^{-5}M $CuSO_4$ + 0.5M H_2SO_4

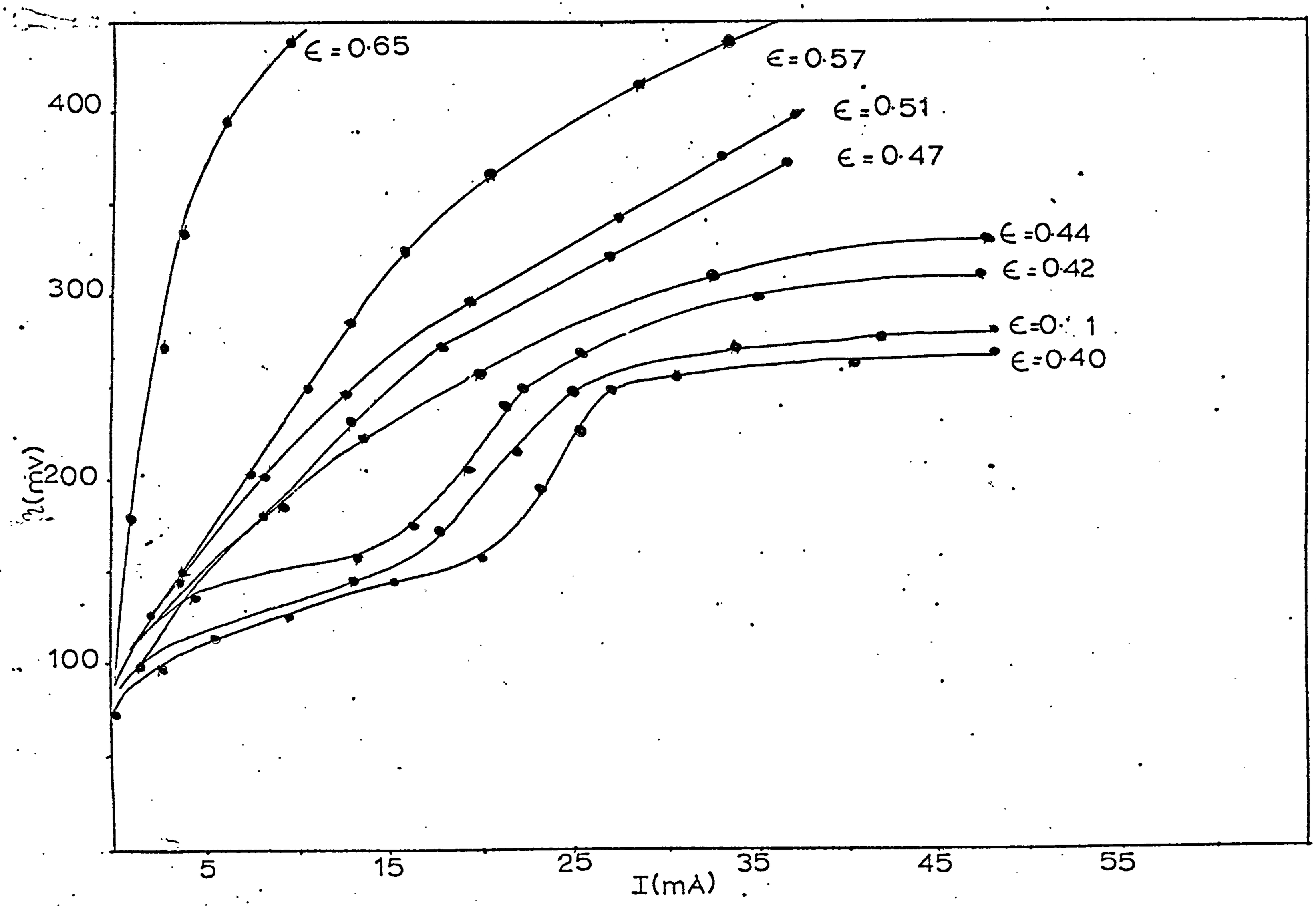
ϵ = 0·65
ϵ = 0·57
ϵ = 0·51
ϵ = 0·47
ϵ = 0·44
ϵ = 0·42
ϵ = 0·41
ϵ = 0·40
400
300
200
100
5
15
25
35
45
55
I(mA)

figure 67

Polarization curves for the deposition of copper from a fluidised bed. The larger cell was used (I.D. 31.68mm) to contain the bed.

Packed bed height: 1 cm
Solution: 0.7M $CuSO_4$ + 0.5M H_2SO_4

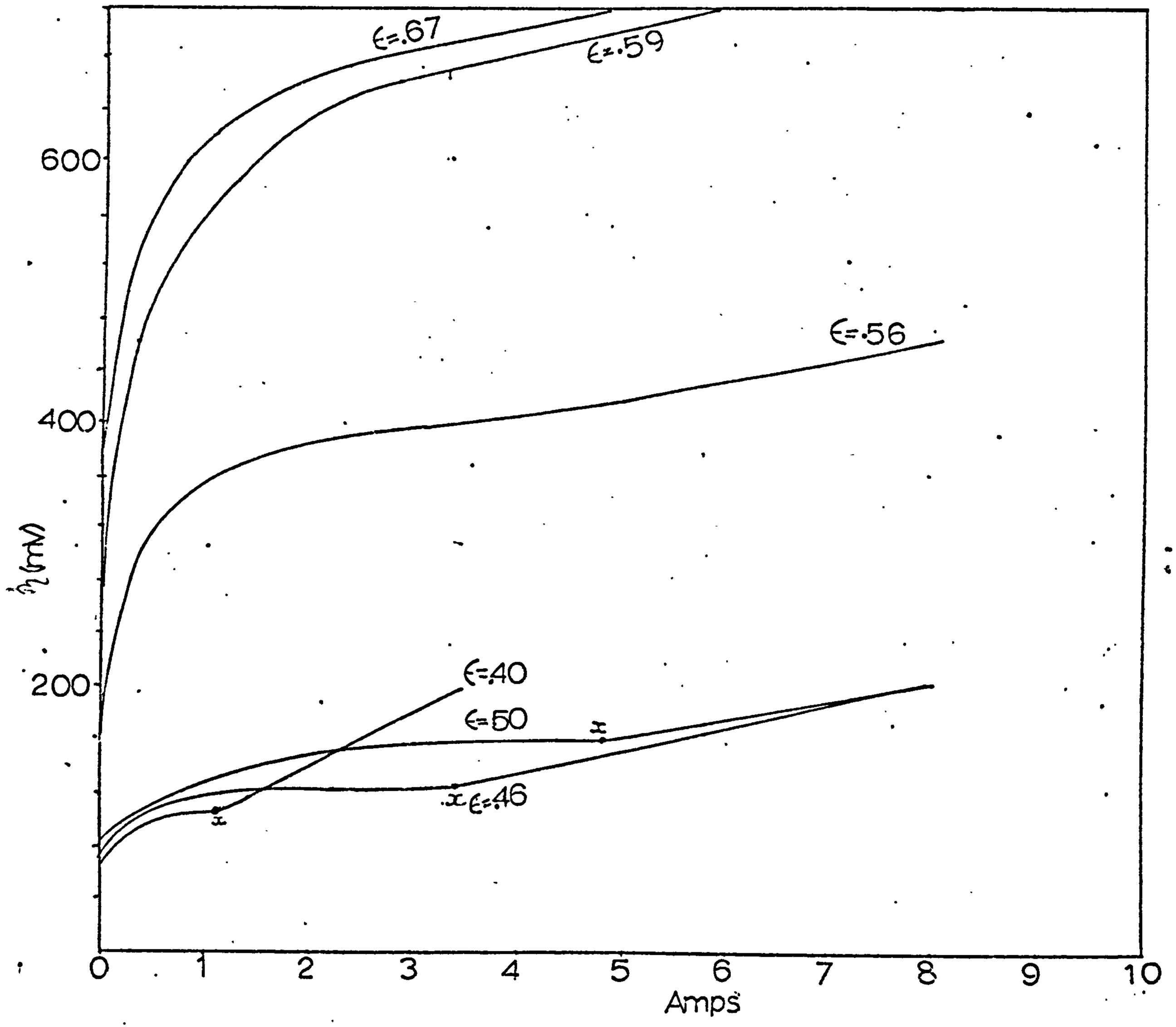
ϵ=.67
ϵ=.59
ϵ=.56
ϵ=.40
ϵ=.50
ϵ=.46
600
400
200
η (mV)
0
1
2
3
4
5
6
7
8
9
10
Amps

figure 68

Polarization curves for the deposition of copper from a fluidised bed. The larger cell was used(I.D. 31.68 mm) to contain the bed.

Packed bed height: 1 cm.
Solution: 0.07M $CuSO_4$ + 0.5M H_2SO_4

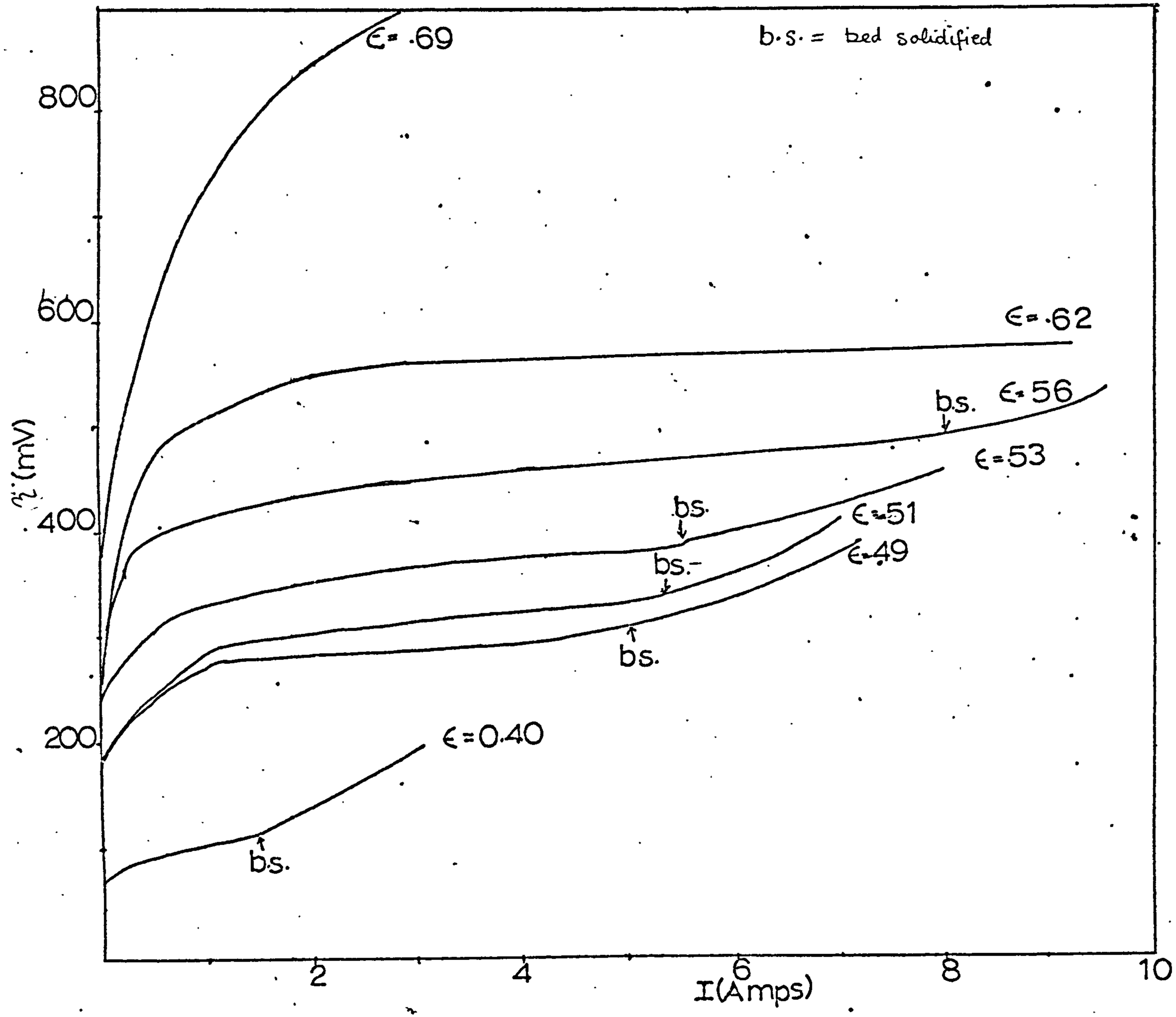
b.s. = bed solidified
ϵ= .69
ϵ=.62
b.s.
ϵ=.56
ϵ=53
bs.
ϵ=51
bs.
ϵ=49
bs.
ϵ=0.40
bs.
800
600
400
200
2
4
6
8
10
I(Amps)
(mV)

figure 69

Polarization curves for the deposition of copper from a fluidised bed. The larger cell was used(I.D. 31.68 mm) to contain the bed.

Packed bed height:1 cm.
Solution:0.01M $CuSO_4$ + 0.5H_2SO_4

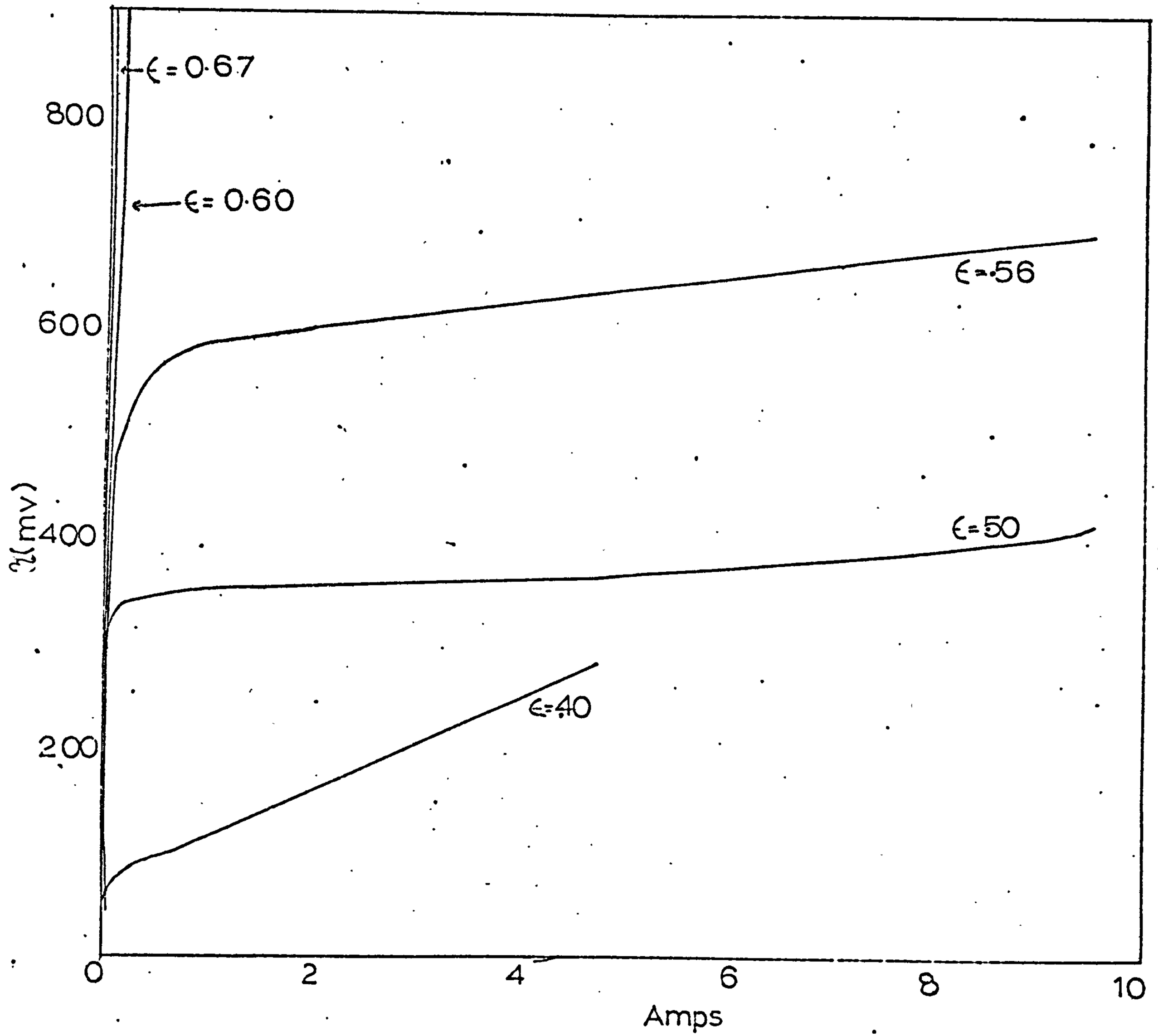
ϵ = 0·67
ϵ = 0·60
ϵ=·56
ϵ=50
ϵ=40
800
600
400
200
0
2
4
6
8
10
Amps

figure 70

The effect of reusing the same bed of copper powder on two consecutive potentiodynamic sweeps.
First sweep: see fig.60
Second sweep: this figure.

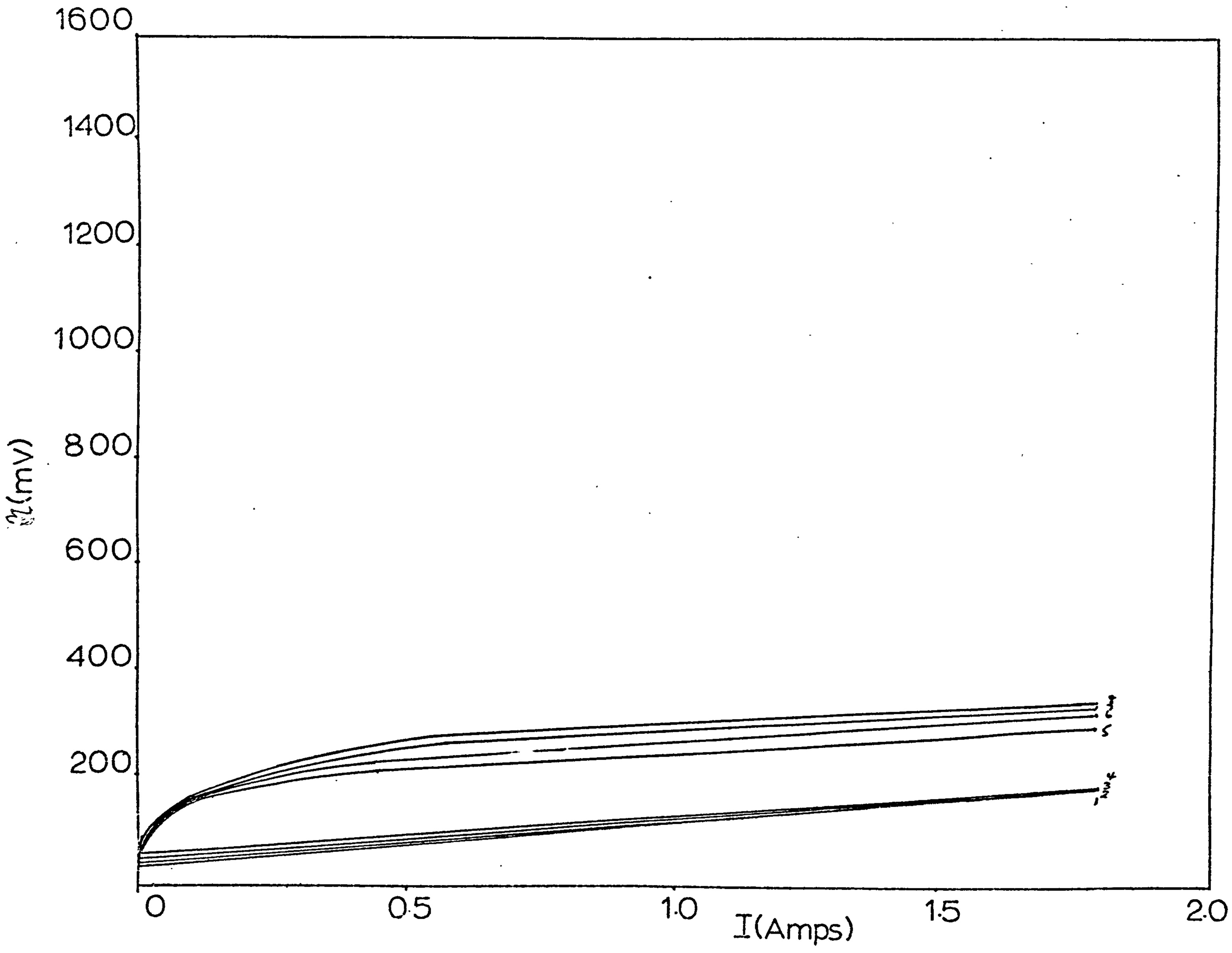
1600
1400
1200
1000
800
600
400
200
V(mV)
0
0.5
1.0
1.5
2.0
I(Amps)
1
2
3
4
5

figure 71

Effect of 'constant' potential/time curves on the current obtained from a fluidised bed.

Solution: 0.7M $CuSO_4$ + 0.5M H_2SO_4

Packed bed height: 1 cm

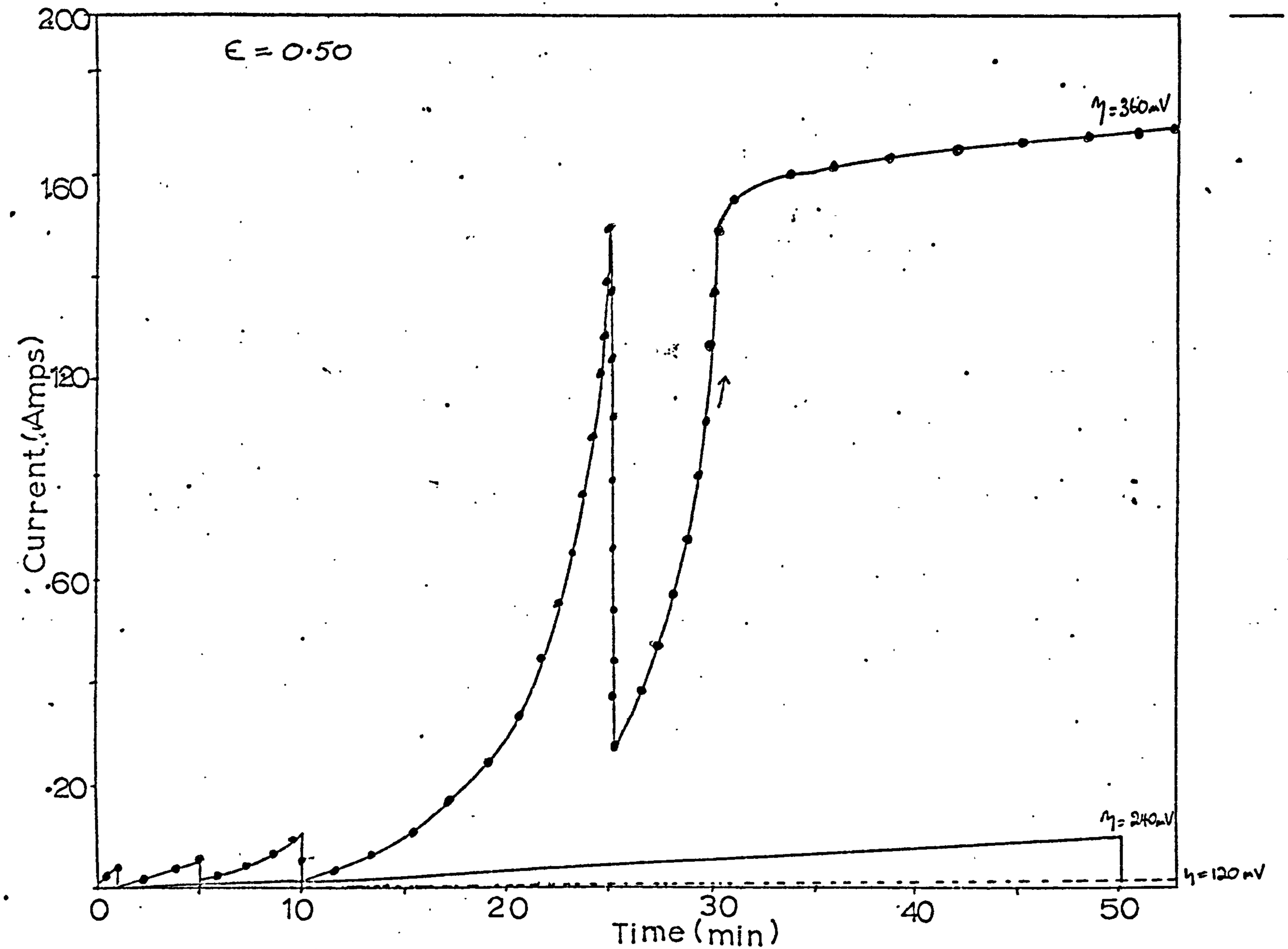
ϵ = 0·50
η=360mV
η= 240mV
η= 120 mV
Current (μAmps)
200
160
120
60
20
0
10
20
30
40
50
Time (min)

figure 72

Diagram showing 'quasi limiting currents' in a fluidised bed at high bed expansions. ($\epsilon > 0.5$)

Packed bed height: 1 cm

Solution: 0.001M $CuSO_4$ + 0.5M H_2SO_4

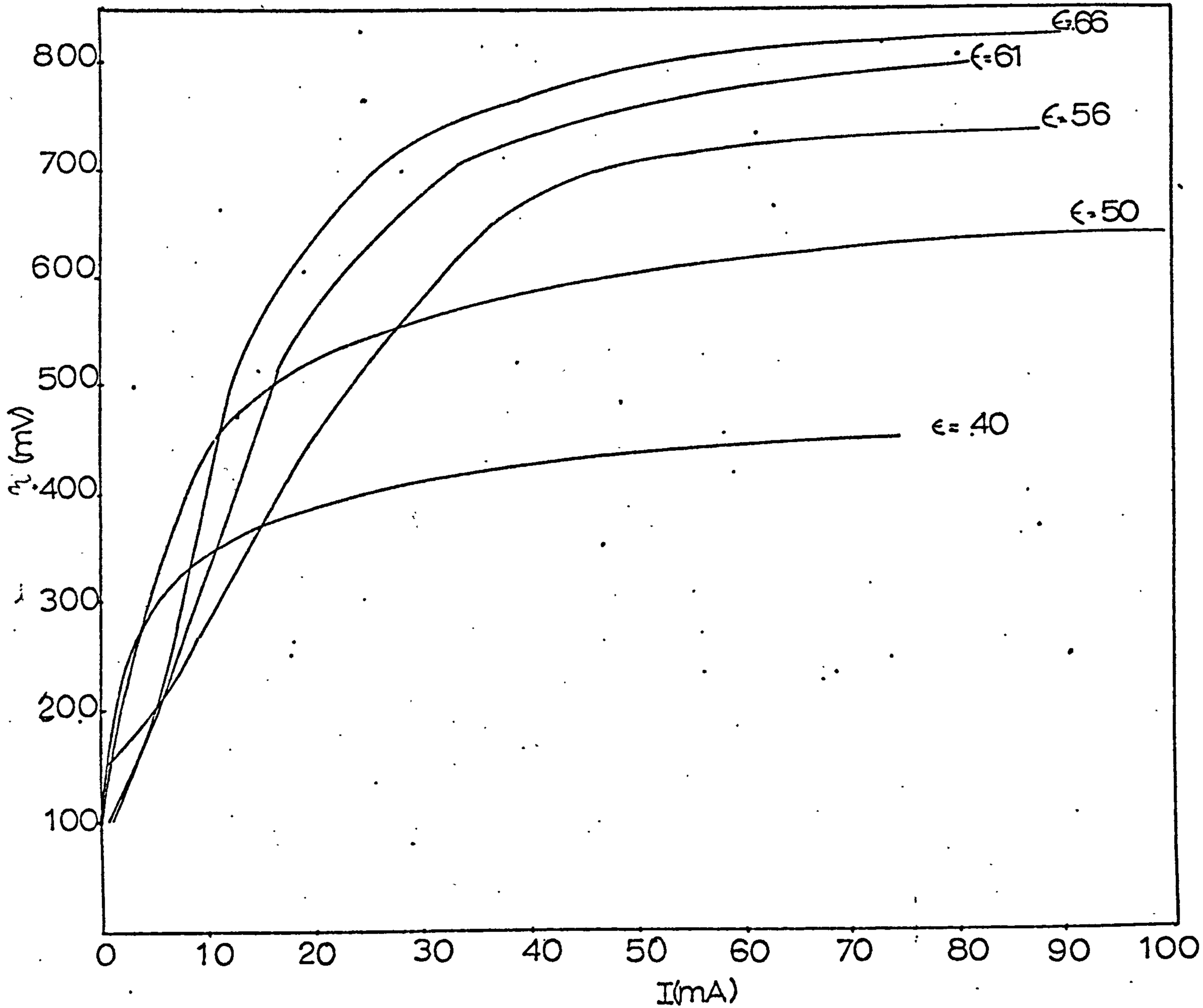
800
700
600
500
400
300
200
100
V (mV)
0
10
20
30
40
50
60
70
80
90
100
I(mA)
ϵ=.66
ϵ=.61
ϵ=.56
ϵ=.50
ϵ=.40

figure 73

Diagram demonstrating 'quasi limiting currents' in a fluidised bed at high bed expansions. ($\epsilon > 0.5$)

Packed bed height: 2 cm
Solution: 0.001M $CuSO_4$ + 0.5M H_2SO_4

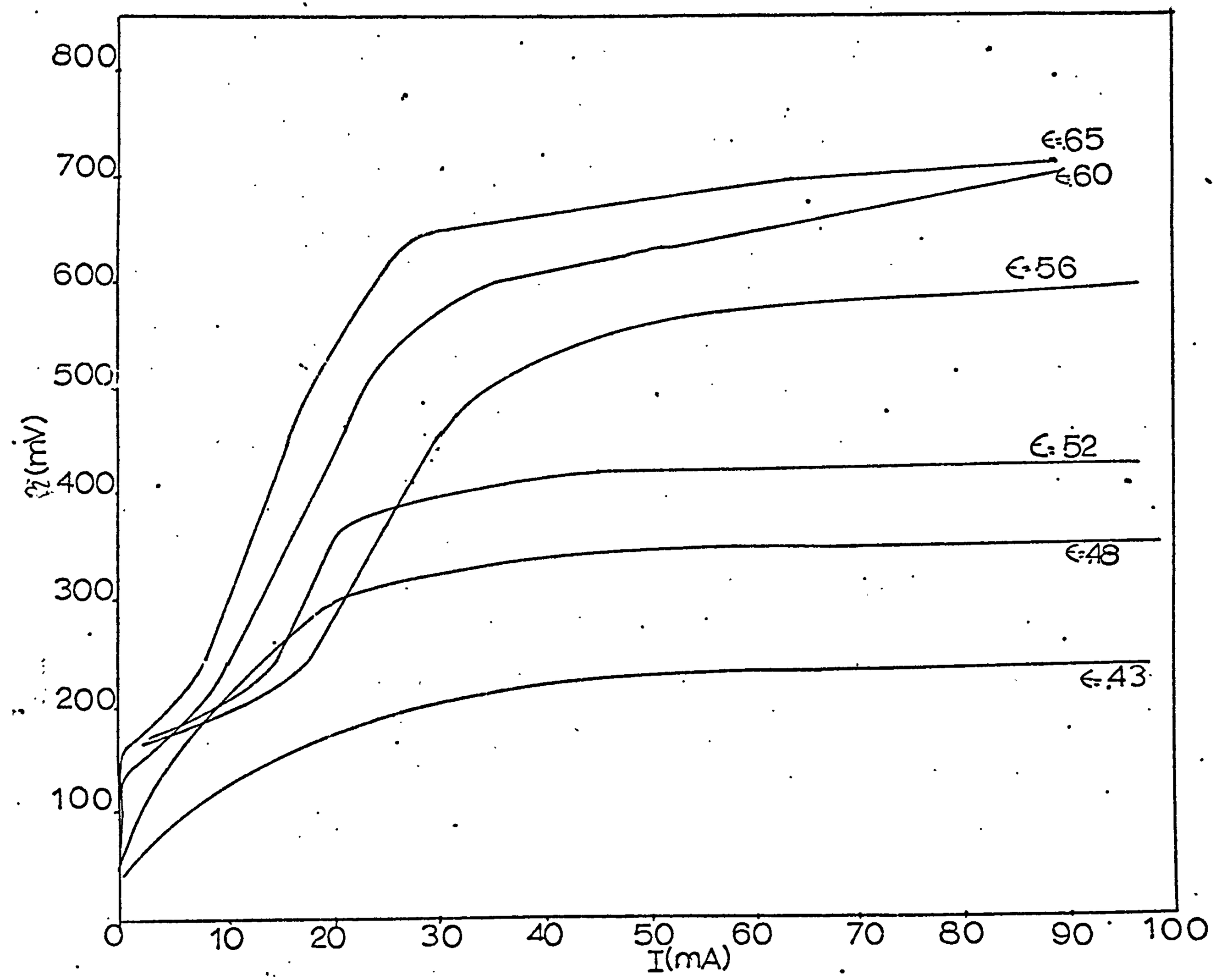
800
700
600
500
400
300
200
100
V(mV)
0
10
20
30
40
50
60
70
80
90
100
I(mA)
ϵ=65
ϵ=60
ϵ=56
ϵ=52
ϵ=48
ϵ=43

figure 74

Diagram demonstrating 'quasi limiting currents' in a fluidised bed at high bed expansions. ($\epsilon \geqslant 0.47$)

Packed bed height: 3 cm.
Solution: 0.001M $CuSO_4$ + 0.5M H_2SO_4

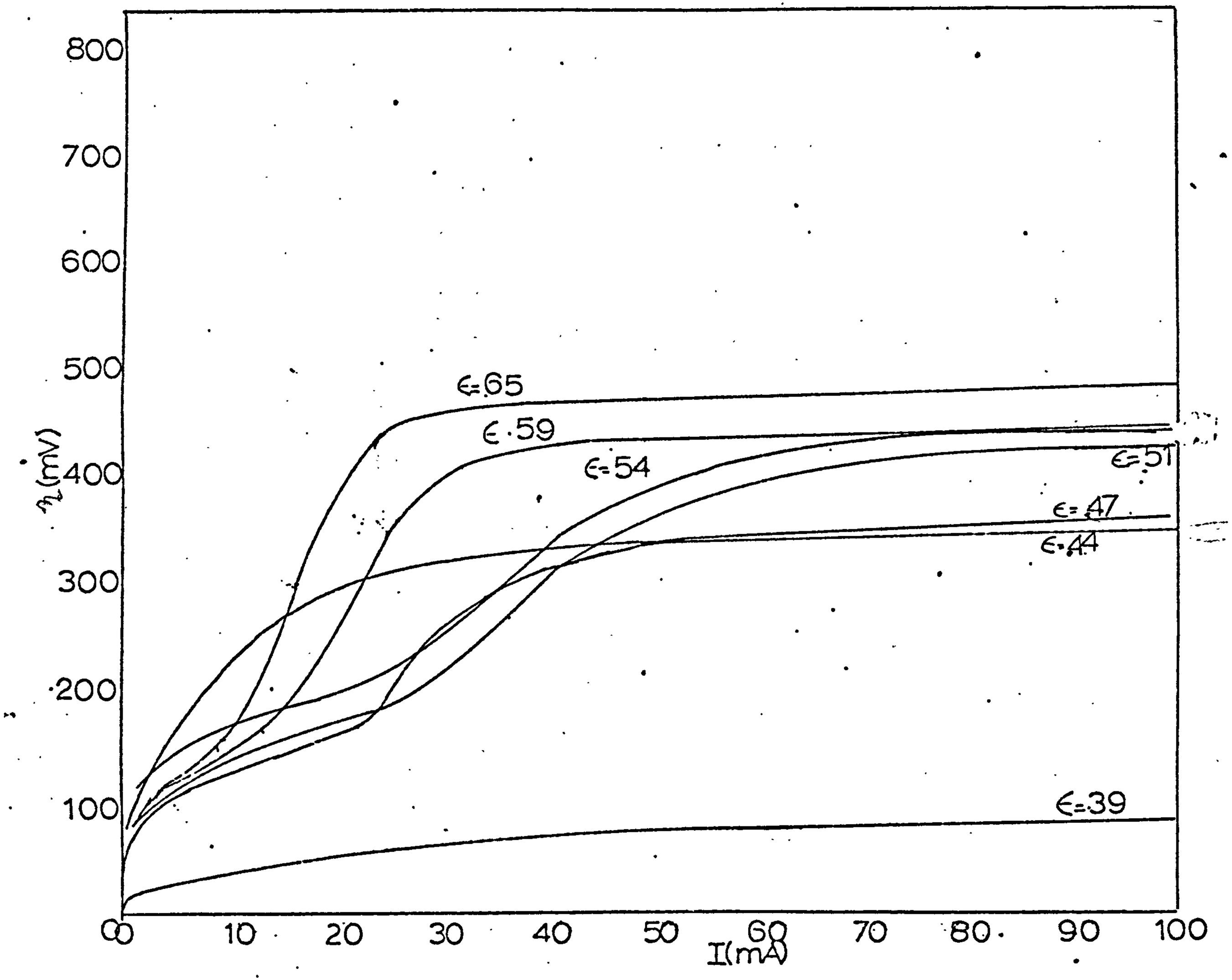
800
700
600
500
400
300
200
100
η(mV)
00
10
20
30
40
50
60
70
80
90
100
I(mA)
ϵ=65
ϵ·59
ϵ=54
ϵ=51
ϵ=47
ϵ·44
ϵ=39

figure 75 (ref. 120)

Performance of mechanically stirred reactors.

1. Rotating disc, radius 3cm
2. Rotating disc, radius 30cm
3. Rotating cylinder, radius 3cm
4. Solution pumped through cell.

L, laminar flow: t, turbulent flow
Power for electrolysis: a* electrowinning of Cu
b* electrorefining of Cu

Solution: 0.6M $CuSO_4$ + 1.7M H_2SO_4

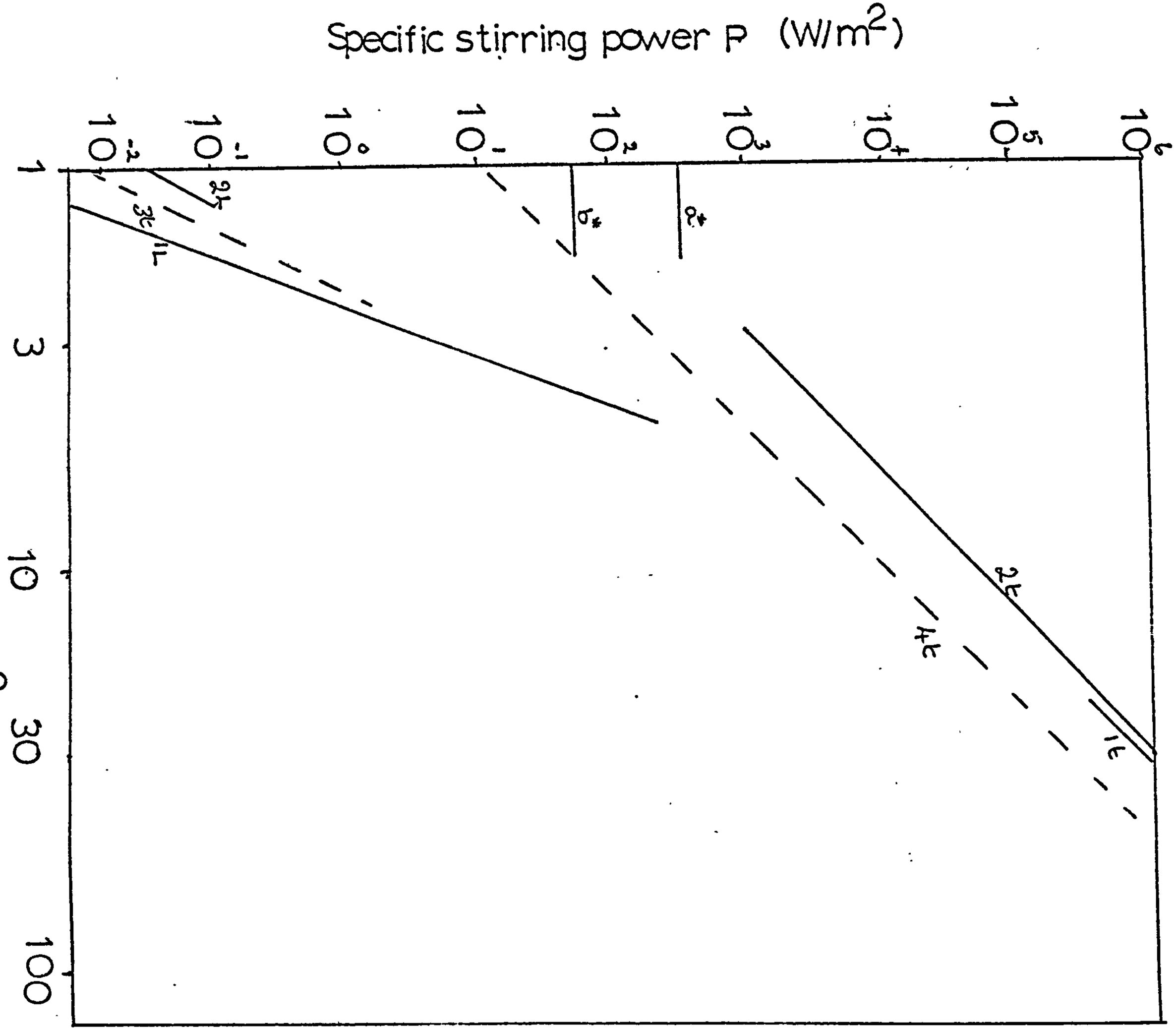
Specific stirring power P (W/m²)
10⁻²
10⁻¹
10⁰
10¹
10²
10³
10⁴
10⁵
10⁶
δ*
δ+
3c
1L
2c
4c
1c
1
3
10
30
100
iL(KA/m²)

figure 76

Experimental data for mass transfer to vertical cylinders 11mm long x 6.25mm dia. in flowing electrolyte

20°C
• 0·015M $CuSO_4$
■ 0·005M "
▼ 0·07M "

40°C
○ 0·015M $CuSO_4$
□ 0·005M "
▽ 0·07M "

$Sh = 2.25\,Re^{0.32}\,Sc^{1/3}$

$\log_{10}(Sh \cdot Sc^{-1/3})$

1·4
1·3
1·2
1·1
1·0
0·9
0·8
0·7
0·6

0·5
1·0
1·5
2·0
2·5
3·0

Log Re $U.d_e/\nu$

PLATE 1

The experimental apparatus

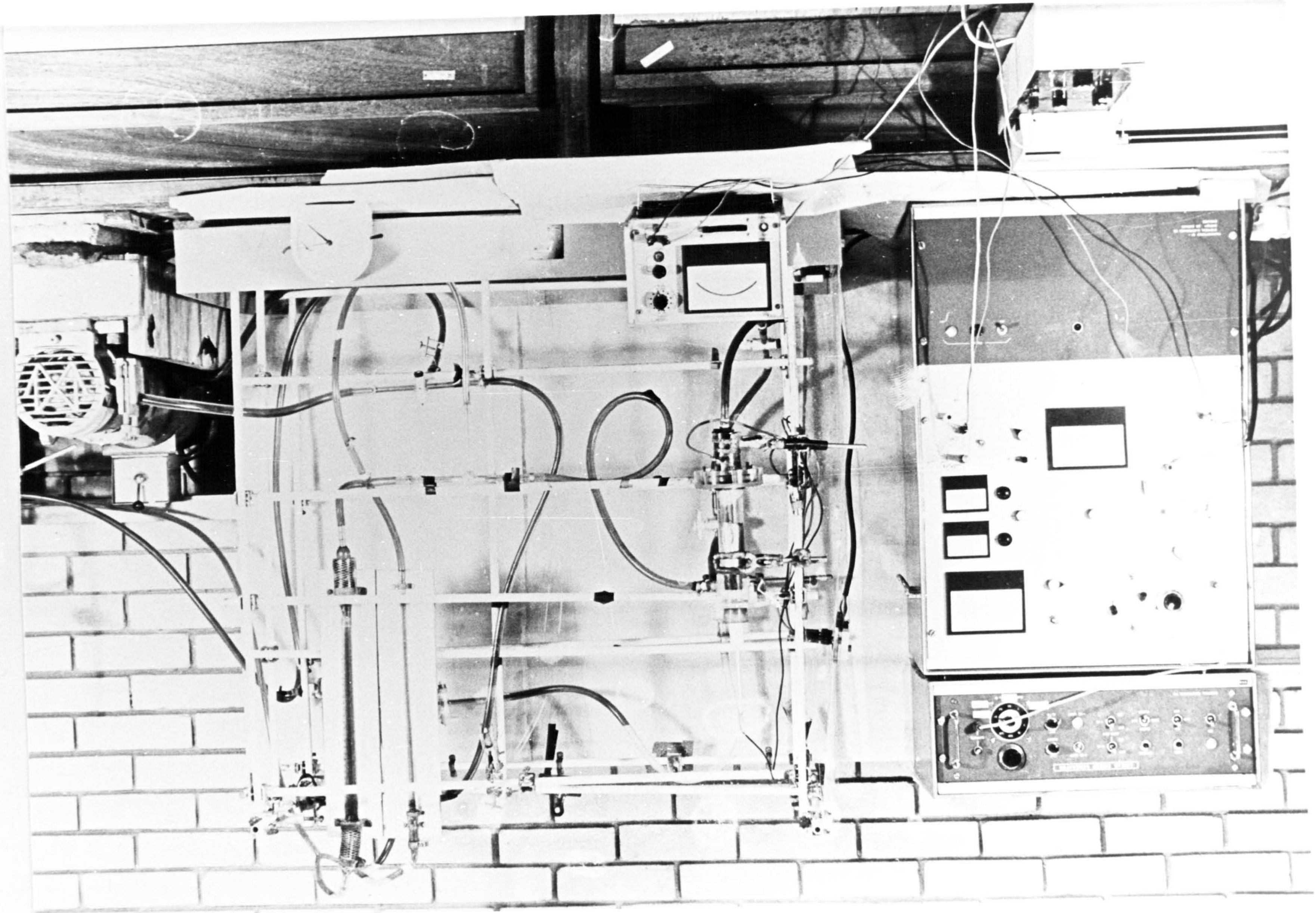

PLATE 2

Cracking of the perspex cell after long term experimental use in sulphuric acid.

PLATE 3

The effect of a cleaning solution on the surface of a copper particle.
x 1000

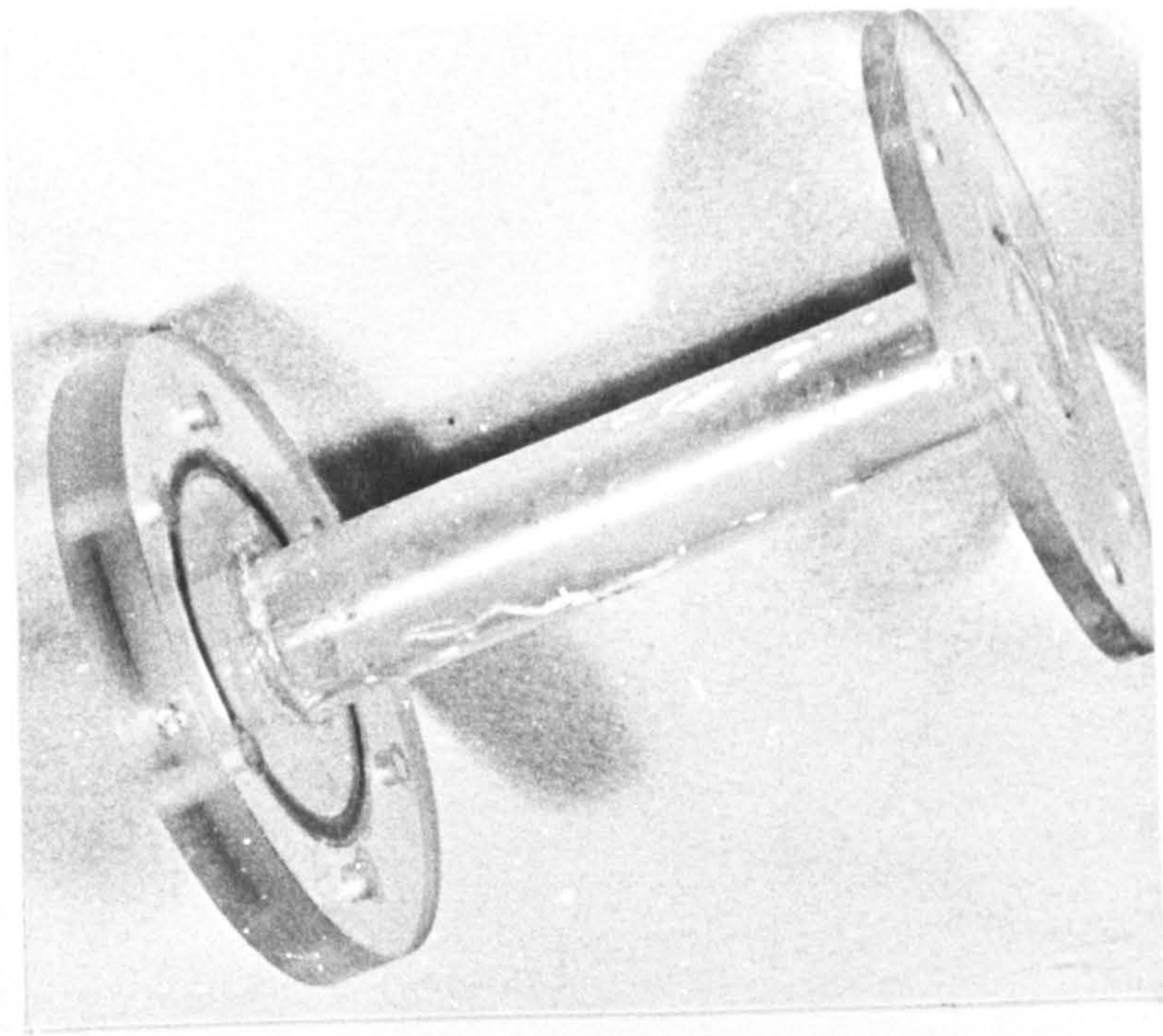

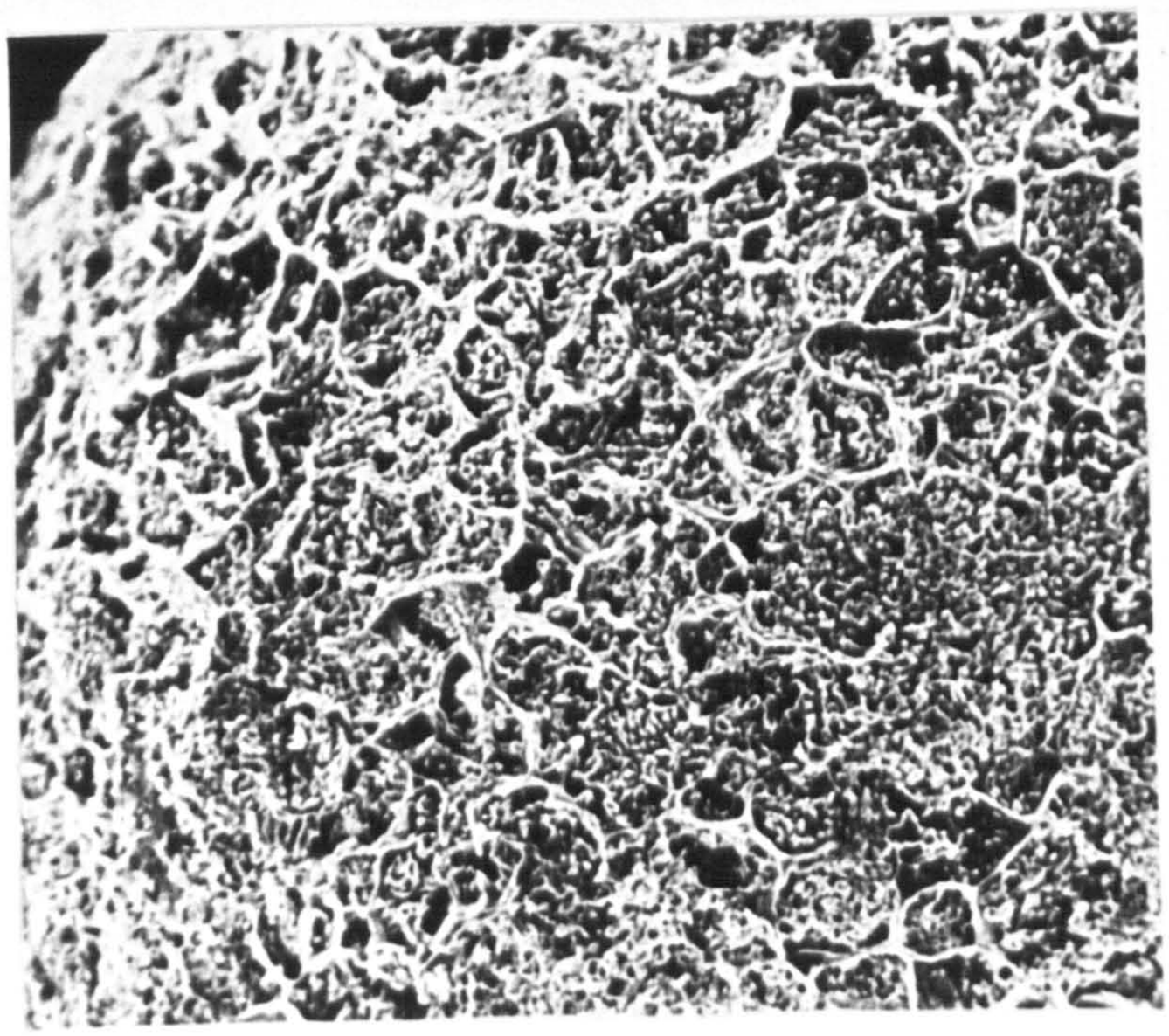

PLATES 4 and 5

As received copper powder.

X400 (175μ PARTICLE)

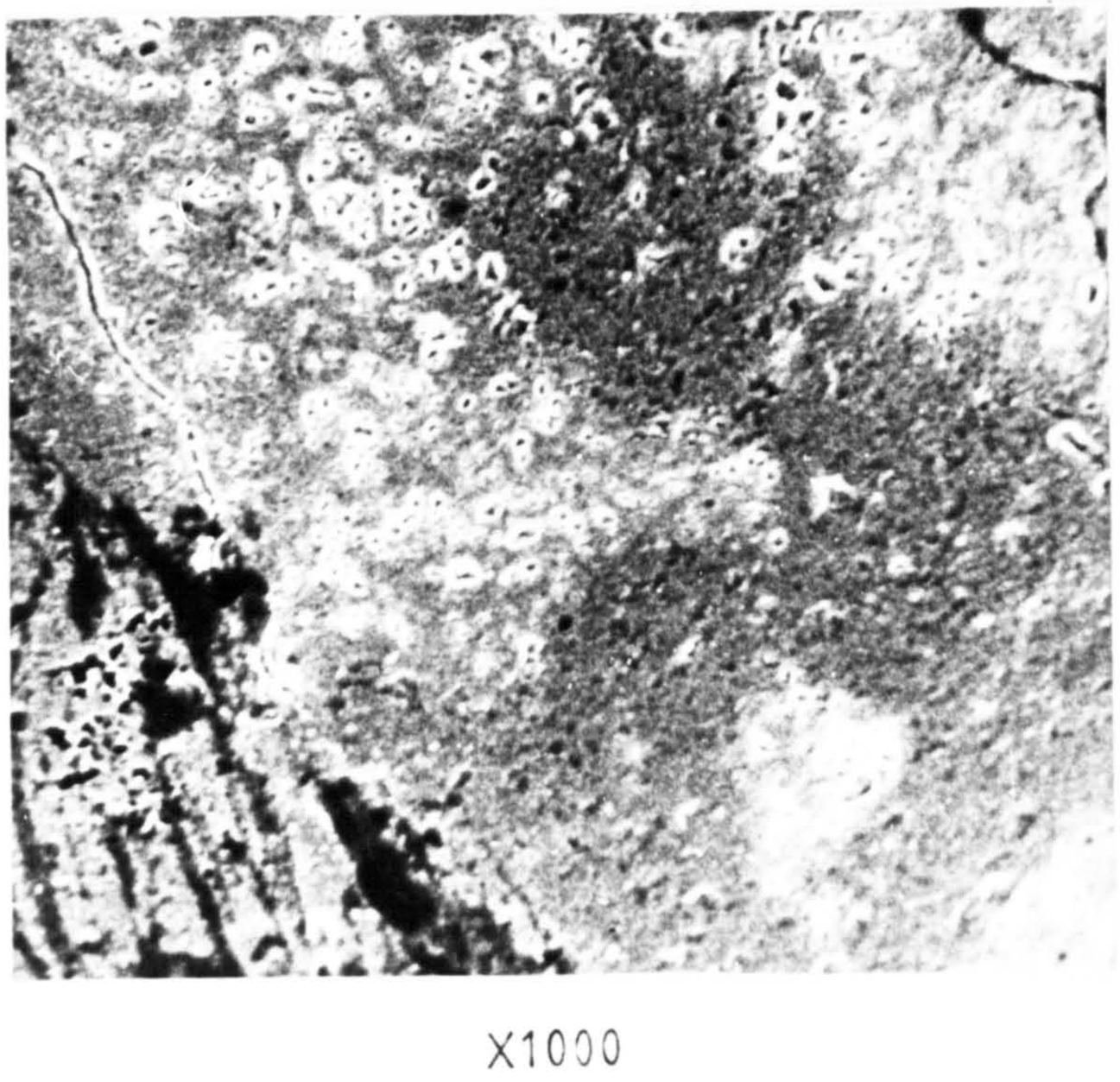

X1000

PLATES 6, 7, and 8

Growth of copper particles during constant potential/time experiments.

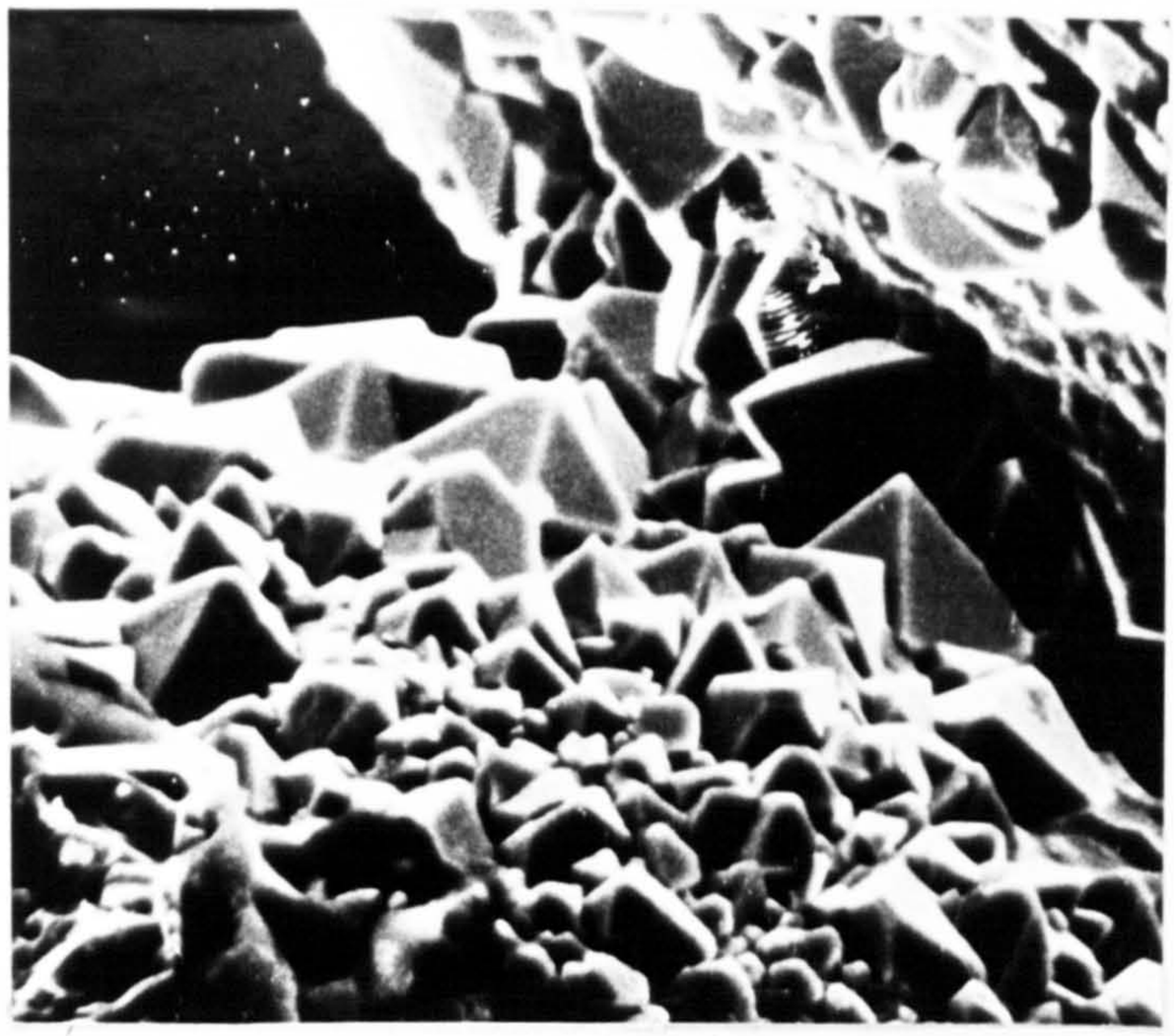

X 4.7K, η_p =120 mV, t=100 mins

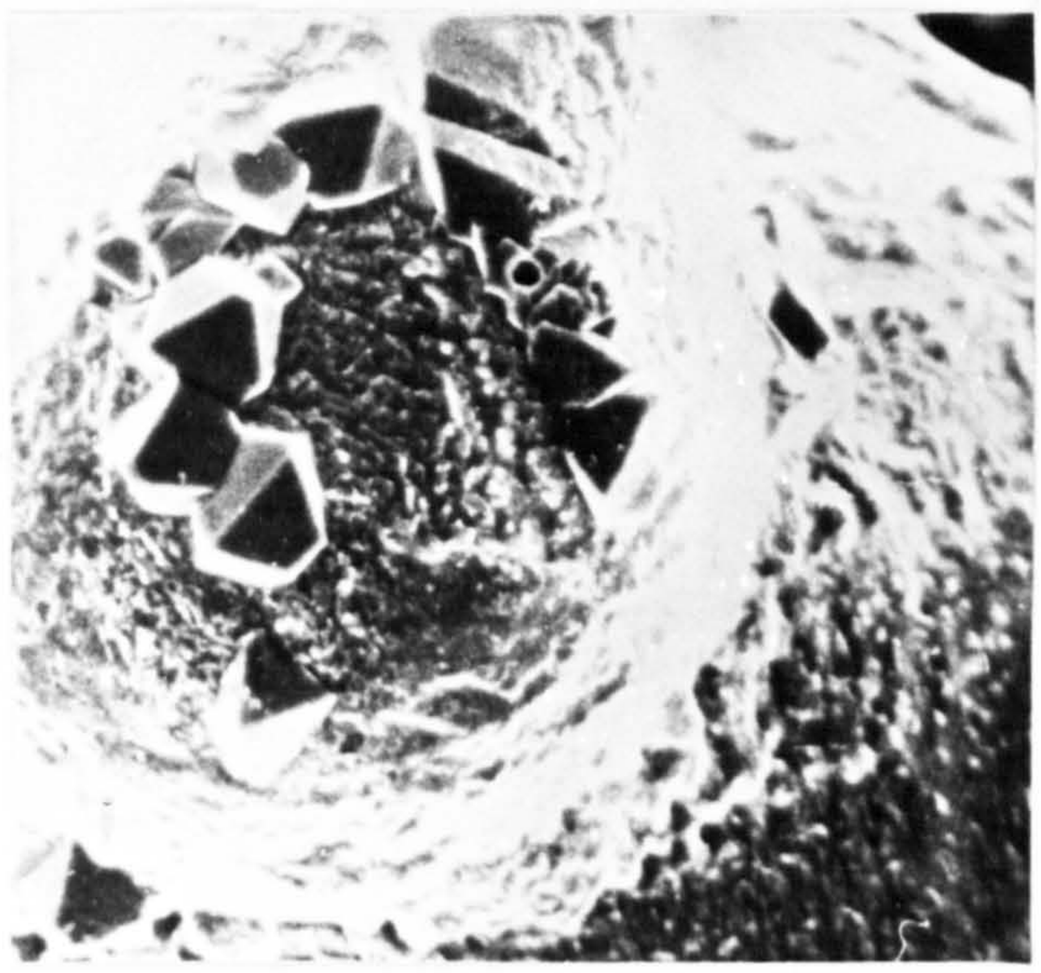

X5.0K, η_p =180 mV, t=100 mins

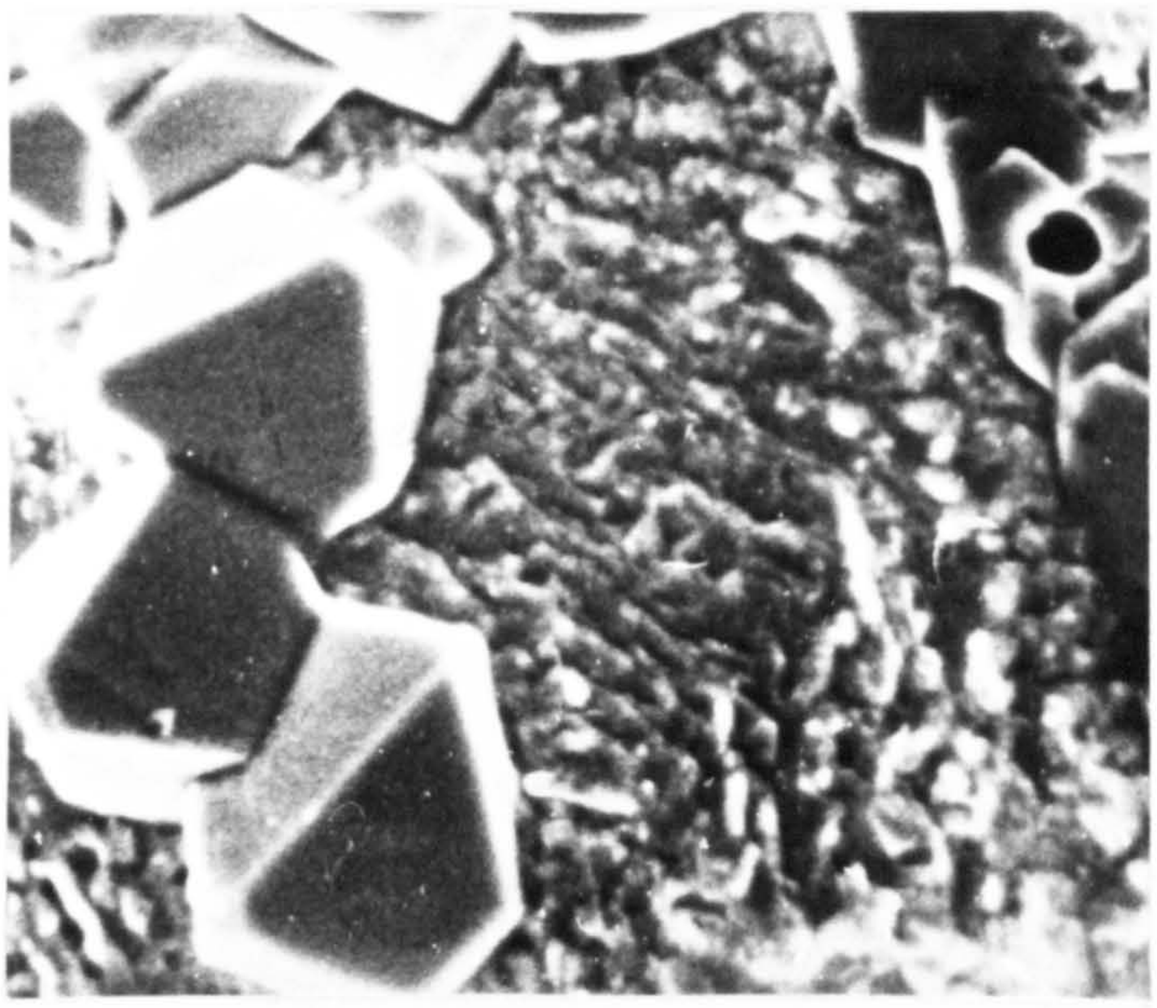

X10K, η_p =180 mV, t=100 mins

PLATES 9, 10, and 11

Growth of copper particles during constant potential/time experiments.

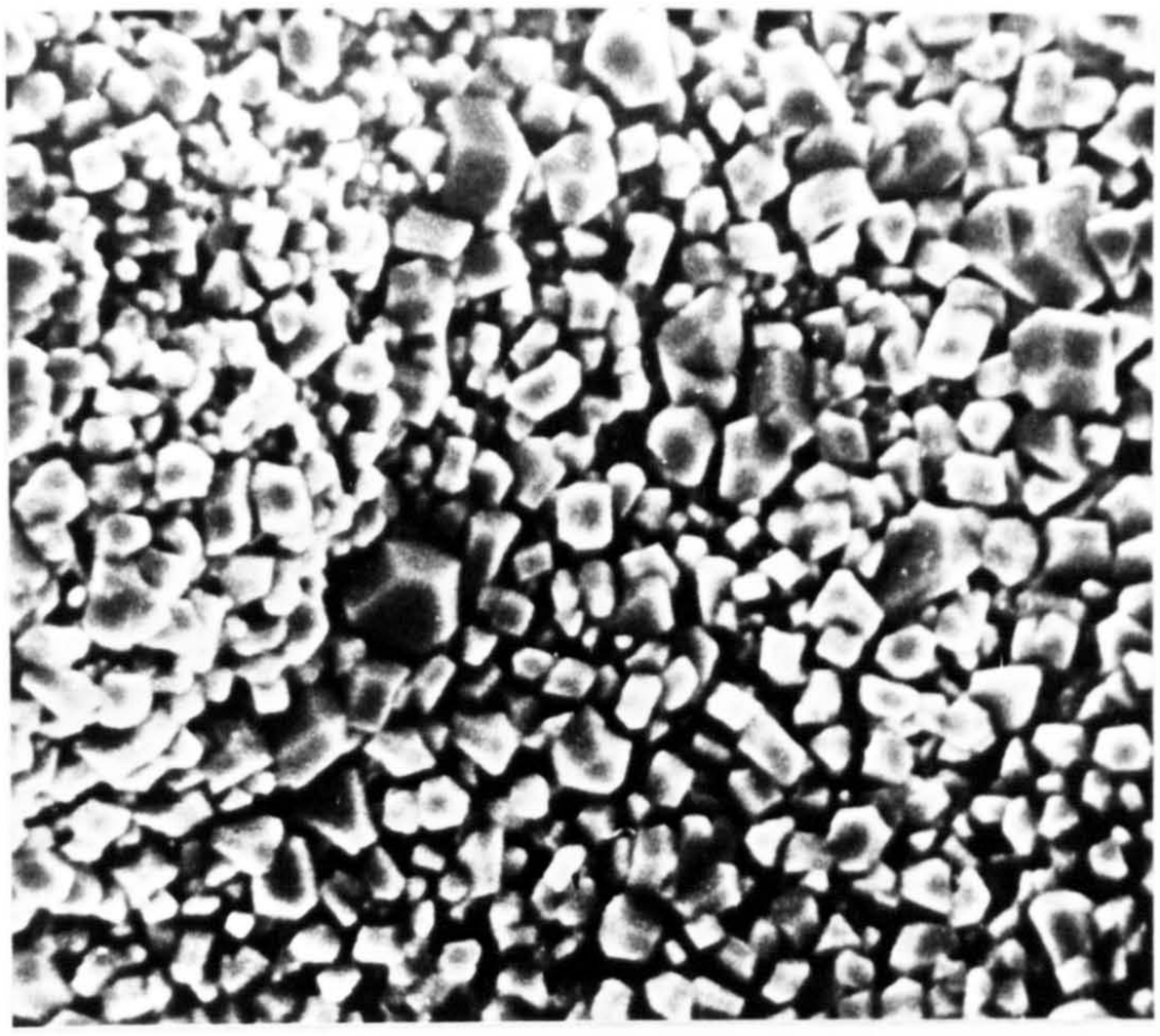

X5.0K, η_p = 240mV, t = 60mins

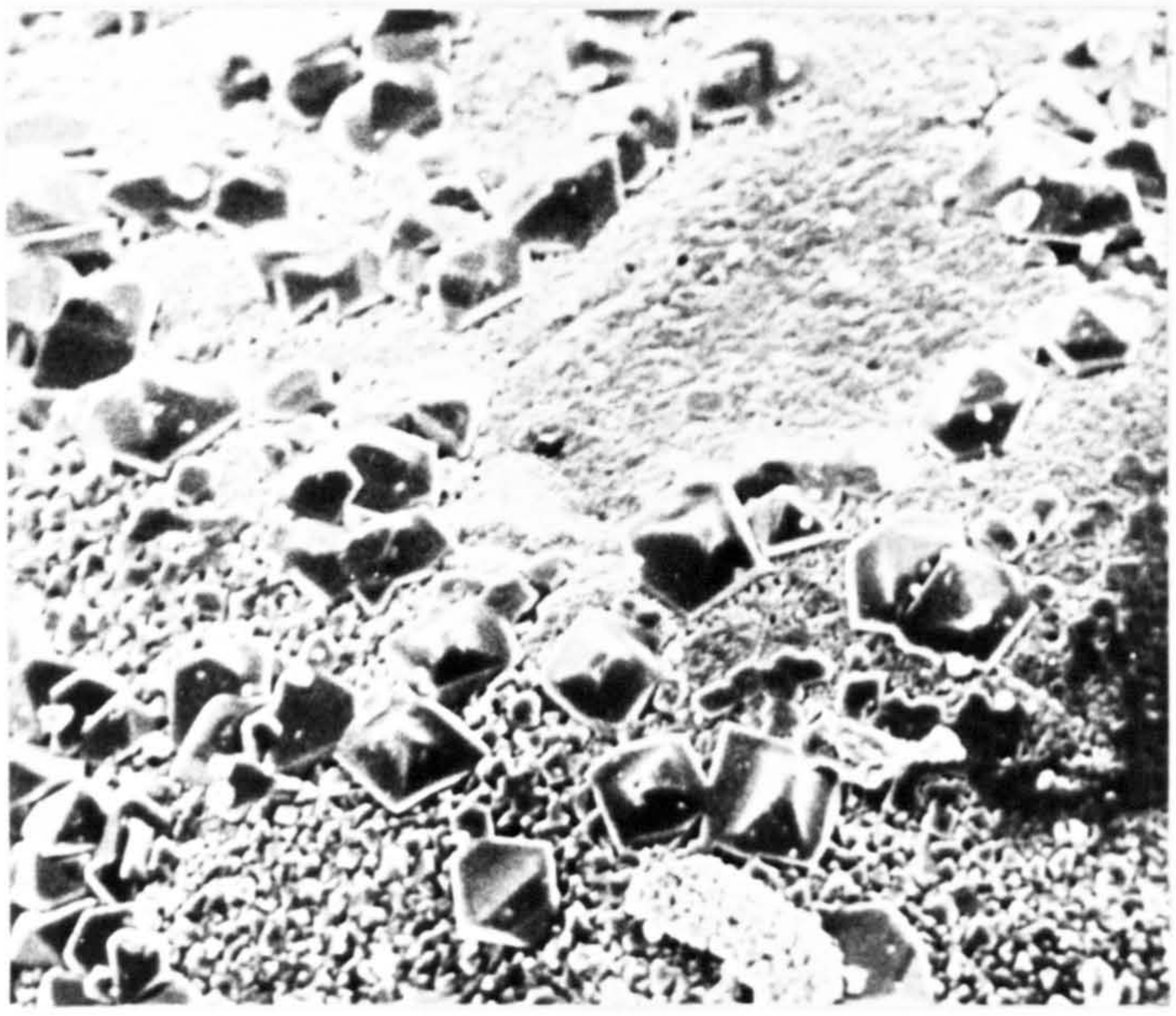

X2.0K, η_p = 360mV, t = 50mins

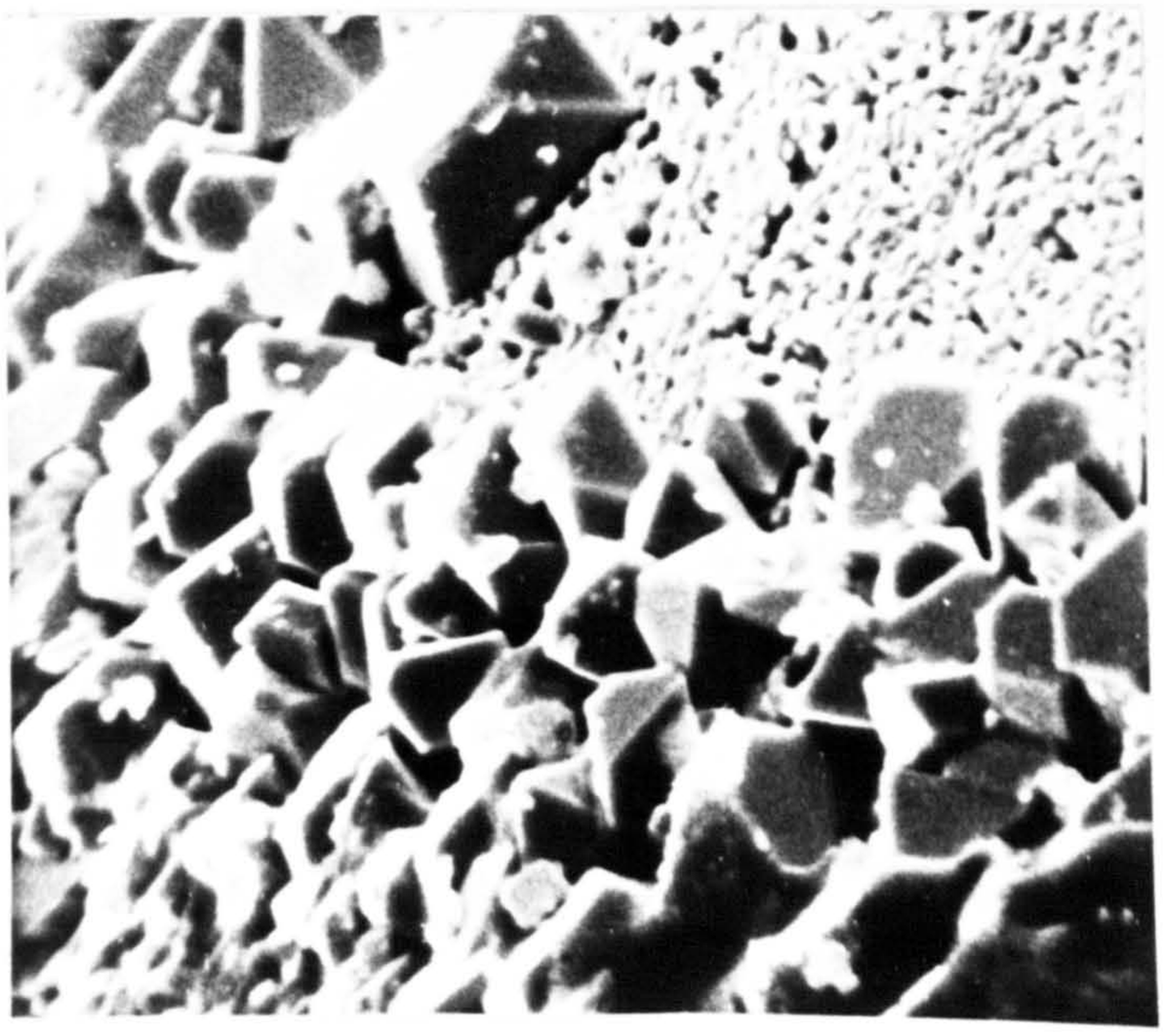

X5.0K, η_p = 360mV, t = 50mins

PLATES 12 and 13

Copper particles which agglomerated together in the fluidised bed during potential/time growth experiments

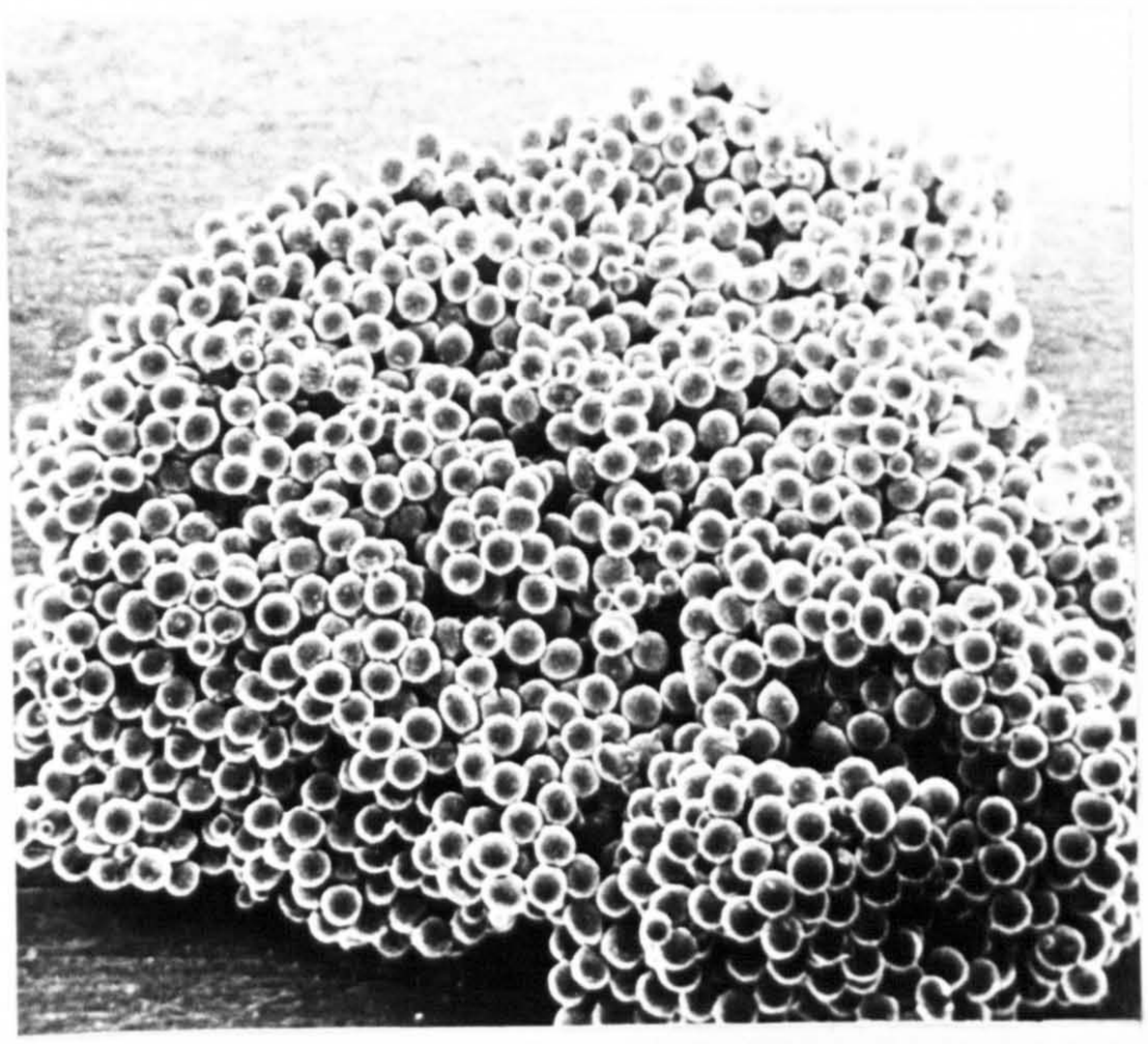

X20 . η_p = 360 mV . t = 50 mins

X90 . η_p = 360 mV . t = 50 mins

PLATES14 .—. 16

The growth of copper in particles which had agglomerated together in the fluidised bed during potential/time growth experiments.

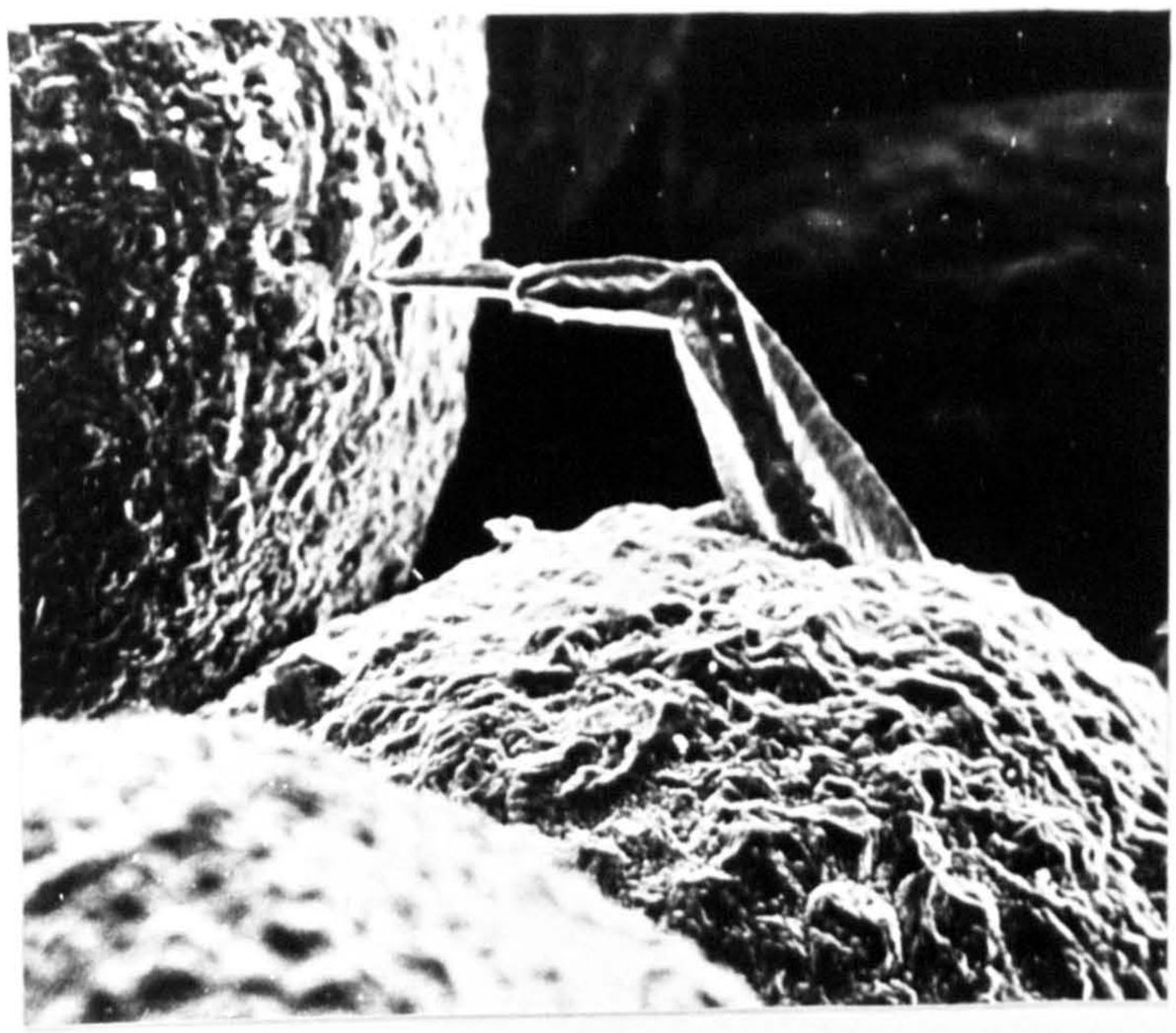

X 1.2K, η_p = 360 mV, t = 50 mins

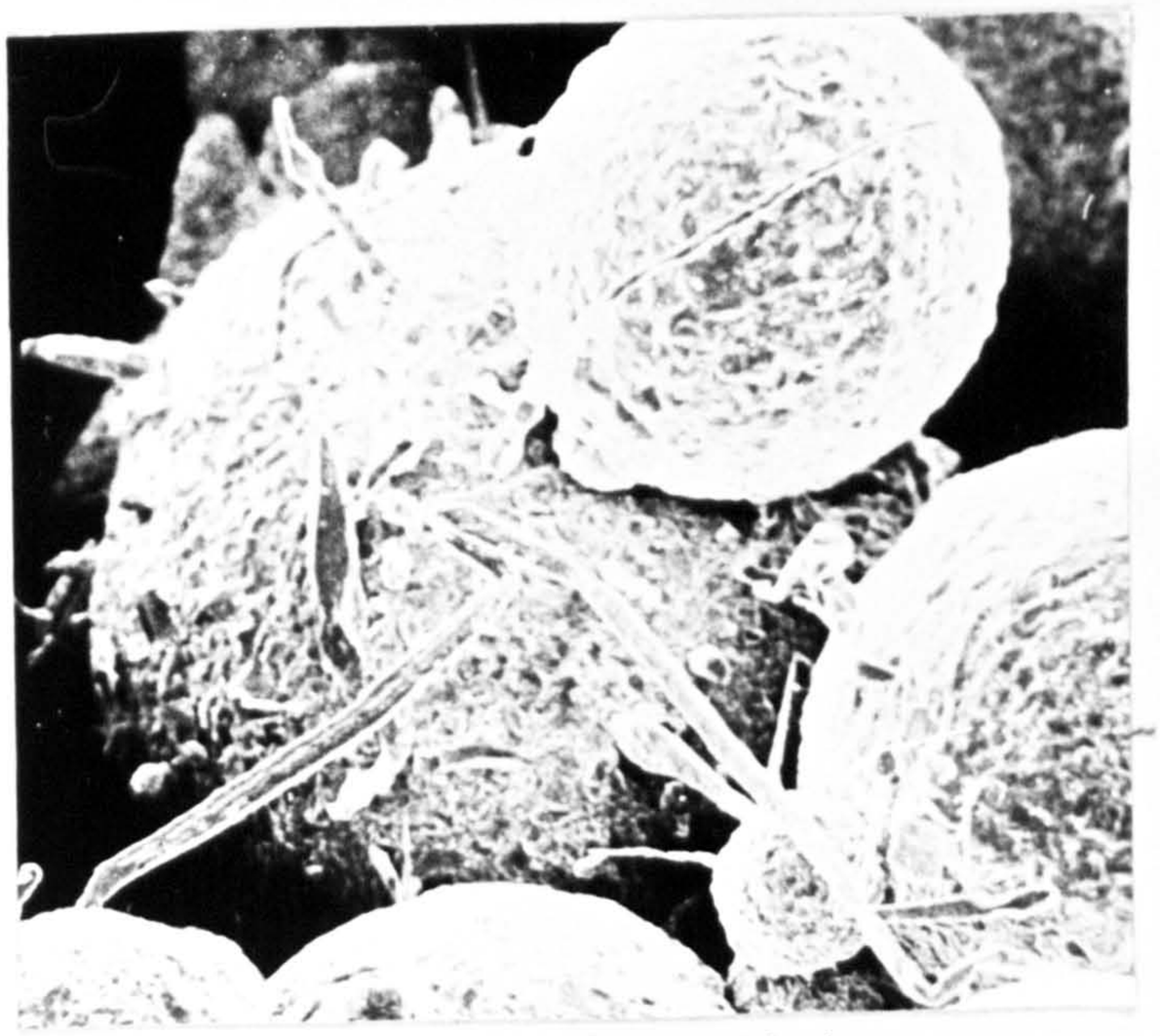

X500, η_p = 420 mV, t = 50 mins

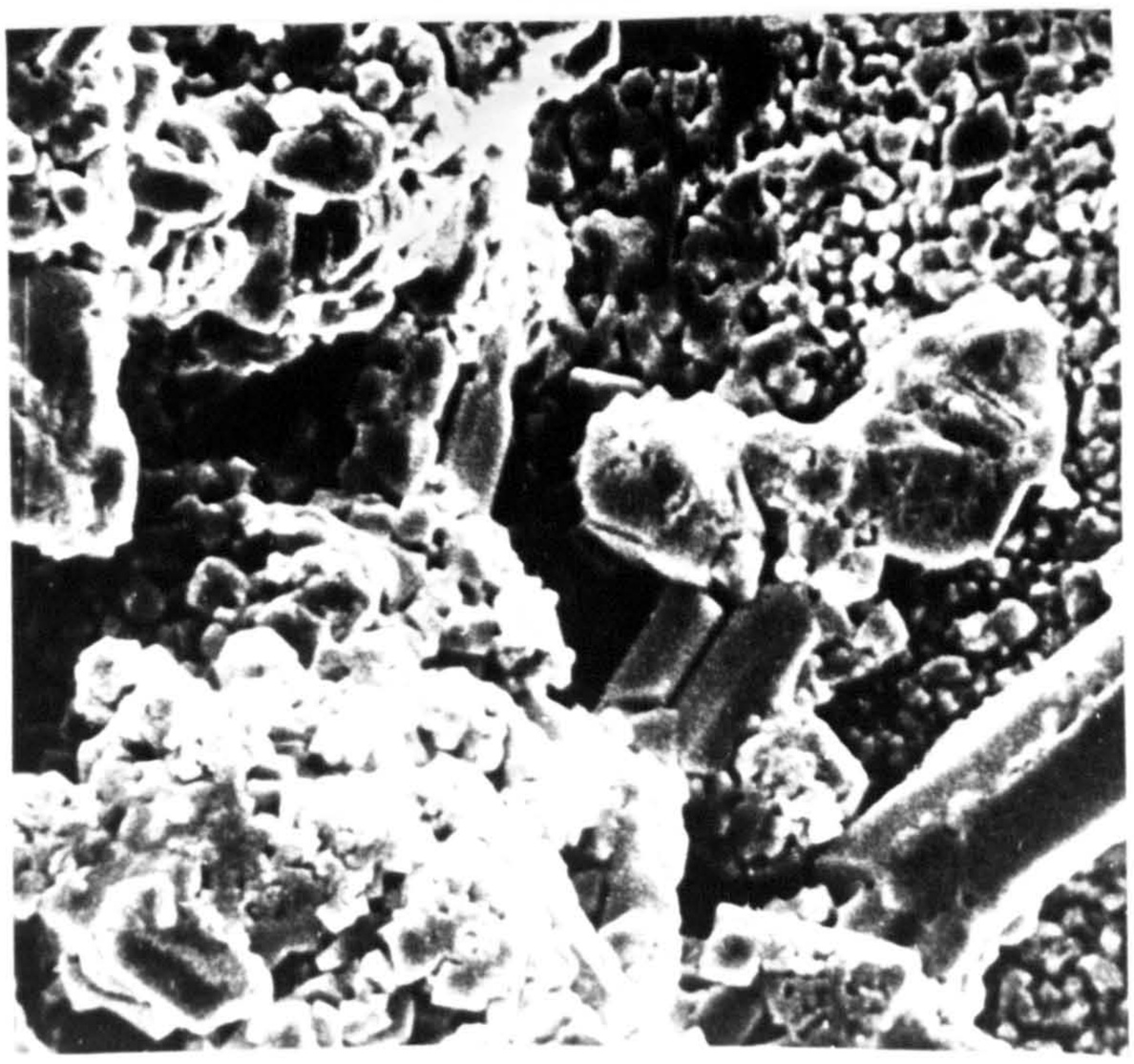

X 4.7K, η_p = 420 mV, t = 50 mins

AUTHOR INDEX

Firms Index

Product		
Atomised Copper Powder	J.J Makin Ltd	Kingsway, Rochdale.
Chart Recorders	Bryans Ltd	Mitcham, London
Chemicals	Fisons Ltd	Loughborough, Leics.
Climpex Tubing	Fisons Ltd	Loughborough, Leics.
Conductivity Bridges	Pye-Unicam	Cambridge, Cambridgeshire.
Glassware	Jencons(Scientific) Ltd	Hemel Hemstead Herts.
Grinding Paper(SiC)	Vickers Ltd	York, N. Yorks.
pH Meters	E.I.L. Ltd	Chertsey, Surrey.
Peristaltic Pumps	Watson-Marlow Ltd.	Falmouth, Cornwall.
Porous Plastic	Porvair Ltd	Kings Lynn, Norfolk.
Potentiostats	Chemical Electronics Ltd	Washington, Tyne and Wear
Rotameter Flow Meters	Baird and Tatlock Ltd	Sandbach, Chesh.
Spectrophotometers	Pye-Unicam	Cambridge, Cambridgeshire.
	Rank Hilger Ltd	Westwood, Margate?
Stereoscan	Cambridge Instruments	Melbourn, Royston.
Temperature Control Units	Baird and Tatlock Ltd	Sandbach, Chesh.